CHARACTERIZATION, BIOAVAILABILITY AND HEALTH RISK ASSESSMENT OF MERCURY IN DUST IMPACTED BY GOLD MINING

Bongani Ndhlovu Yalala

A Thesis submitted to the Faculty of Science, University of the Witwatersrand, Johannesburg, in fulfilment of the requirements for the degree of Doctor of Philosophy

2015

DECLARATION

I declare that this thesis is my own, unaided work. It is being submitted for the Degree of Doctor of Philosophy at the University of the Witwatersrand, Johannesburg. It has not been submitted before for any degree or examination at any other University.

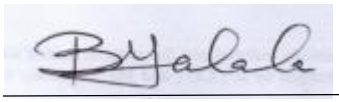

(Signature of candidate)

25th day of May 2015

ABSTRACT

Gold mining in South Africa has been the backbone of the economy for many years. With it came economic well-being, the growth and development of satellite towns, cities and metropolitan cities, e.g. Johannesburg-a place of gold. Unfortunately, it also came with adverse effects, most of which are now evident, after a century of mining, with little or no regard for pollution prevention or any form of remediation. Of interest, in this study, is the presence of tailings storage facilities (TSFs) found within the residential areas, in close proximity to commercial district and industry, having been built around them.

Currently, some 270 TSFs lie dormant, pregnant with vast number of toxic heavy metals from the initially low efficient but selective gold processing techniques. This led to the deposition of the sand dumps, with high sulphur, iron, chromium, cadmium, arsenic, and mercury amongst other toxic metals. Exposure to oxygen, and water, the pyrites were oxidized and formed acid mine drainage (AMD), which resulted in the leaching out all toxic heavy metals into ground water and surface water causing serious water pollution and environmental degradation. Due to the low efficient gold processing technique, some gold amount was discarded together with the tailings materials. The reprocessing of these dumps led to the generation of dust, which is easily distributed over large areas of land. The unrehabilitated, semi-rehabilitated, and the abandoned TSFs contributed to all forms of pollution, majorly, windblown dust from unprotected tops and sides, AMD leaching toxic heavy metals.

In this study, mercury, one of the most toxic elements found within the vast TSFs was determined. This was carried out as part of a larger environmental impact assessment on the effects and scale of pollution from the gold mining in the Witwatersrand. The study area consisted of the greater Johannesburg area, covering commercial business district (CBD), the industrial areas (Aeroton, City Deep, Germiston, Selby, Springs), and the residential areas (Alberton, Boksburg, Centurion, Germiston, Greenside, Sandton, Springs). Dust samples were collected from paved surfaces in the streets, and accessible buildings, were sieved into three

sieved into three fractions (PM_{100}, PM_{50}, PM_{25}), and most of the work focused on the smallest size fraction (PM_{25}) in order to study impact of inhalable and respirable dust. Three sequential extraction procedures (modified BCR-the European Community Bureau of Reference, selective sequential procedure (SSE), and novel sequential extraction procedure (n-SEP)) were applied for partitioning and evaluating the mobility, availability and persistence of mercury in urban dusts. Bioavailability of mercury was assessed by leaching dust with artificial gastric and lung fluids which mimicked body conditions. Contamination levels were assessed based on the enrichment factor (*EF*), contamination factor (C_f) and geoaccumulation index (I_{geo}) were calculated to further assess the environmental risk and provide a preliminary estimate of the main sources of mercury in street dust. Non-carcinogenic effects and carcinogenic effects due to exposure to urban street dusts were assessed for both children and adults.

The total mercury (Hg_{TOT}) ranged from 269 to 1350 µg kg^{-1}. In the PM_{25} size fraction, mercury exhibited the following decreasing order of Hg_{TOT}: industrial area > CBD > residential area. This order shows that the Hg_{TOT} concentration in the street dust decreased with increased distance from the TSFs. The highlight was that the highest Hg_{TOT} was reported in industrial areas next to the TSFs, tailings reprocessing areas, and tailings footprints. Furthermore, in residential areas grossly affected by TSFs and tailings reprocessing, reported high Hg_{TOT} values similar to those reported for industrial samples. These results indicated that the presence of TSFs were largely responsible for the mercury found in the dust. The results from the characterization of the dust showed a large concentration of fine particulate matter, with the characteristically high quartz (74 – 98 wt. %), and minor minerals phases such as chloritoid, chlorite, K-feldspar, jarosite, mica, muscovite, pyrite, and pyrophyllite, all below 10 wt. %. These have been known to enrich trace metals, hence a high concentration of mercury.

The close proximity of the tailings to the communities led to the determination of bioavailability of mercury from dust. The bioaccessible Hg extracted by lung fluid (up to 3% of Hg_{TOT}) was higher than that of gastric fluid (up to 1% of Hg_{TOT}) and

was related to the mobile pool of Hg in dust. This suggests that human exposure to Hg in dust via inhalation is greater than that via the gastric tract. These values were very similar to the values obtained from water soluble phase in the sequential extraction procedure (average 1.4% of Hg_{TOT}). This indicated that these fluids were able to extract the most bioavailable fraction of Hg, which is responsible for most of the transformation reactions involving mercury.

Contamination assessment factor was carried out to classify the pollution levels and indicate whether they are from natural or anthropogenic sources. Based on the EF, C_f, and I_{geo}, 70, 82, and 84% of the street dust samples were classified as heavily enriched, very highly contaminated, and strongly polluted by mercury, respectively, indicating that they are of anthropogenic origin.

The human health risk model was useful in identifying the areas of health risks from exposure to mercury pollution. It showed that children were more vulnerable than adults when exposed to mercury in dust via ingestion. The cancer risk for exposure to As, Cd, and Cr by both children and adults was significantly high for oral ingestion of dust. Cr (VI) was the highest contributor followed by As and lastly Cd. For inhalation pathway, the possibility of developing cancer after a lifetime exposure was low and below the acceptable limits (10^{-6}).

To my family:

Lindiwe Zulu, Thandolwenkosi, and Thabiso

ACKNOWLEDGEMENTS

Firstly, I would to thank my supervisor, Prof. Ewa M. Cukrowska, for affording me this chance to do my doctoral studies under her supervision, for her untiring effort, valuable advice, guidance, and supportand during these studies.

Secondly, I would like to thank Prof. Luke Chimuka, Dr. H. Tutu, Dr. J. Lusilao-Makiese, for their roles in making this work achievable, their encouraging words, being a constant source of information, and making the sampling trips enjoyable.

The Environmental Analytical Group (EACH), they made me feel at home, were always there for support, for constructive criticism, and would like to mention particularly for the lighter moments we shared. It made the difficult times bearable.

Without the financial support of THRIP/EEPP grant (Isabel Weiersbye) and Post Graduate Merit Award (PMA) from University of the Witwatersrand, this work could not have been possible. I therefore, sincerely, thank these institutions for their critical help.

To my family, particularly Mr. C. N. Yalala & the late Mrs. G. Yalala, who sow the seed of perseverance, dedication, determination, and hard work. To my siblings (Ntando, Nonhlanhla, Phumuzile and their families), for their constant support, encouraging words and their belief in me. They never failed me, even though there were not here physically, their love and their constant expression of love and desire for my success was heartfelt. Lastly, but not least, Mageba, Sithulisika Ndaba, Mntwana, Ndlela Zimnhlophe, Lindiwe Zulu for being by my side, for your love, and being a pillar of strength, and thank you for the blessings of our two sons, Thando and Thabiso.

TABLE OF CONTENTS

LIST OF FIGURES

LIST OF TABLES

LIST OF ABBREVIATIONS

ABS	Dermal absorption factor (chemical specific)
ADL:	Absolute Detection Limit
AFS	Atomic Fluorescence Spectrometry
AGA	AngloGold Ashanti Limited
AGF	Artificial gastric fluid
ALF	Artificial lung fluid
AMD	Acid Mine Drainage
ASGM	Artisanal small scale gold miners
AAS	Atomic Absorption Spectrometry
BW	Average body weight
c	mean concentration of mercury
CBD	Central business district
CDI	Chronic daily intake
C_f	Contamination factor
CF	Conversion factor
CR	Cancer risk
DRD	Durban Roodepoort Deep
ED	Exposure duration
EF	Enrichment factor
EF	Exposure frequency
ESP	Electrostatic precipitator
ET	Exposure time
FGS	Flue-gas desulphurization
FIMS 400	Flow injection mercury system
GEM	Gaseous elemental mercury
GOM	Gaseous oxidized mercury

Hg_{TOT}	Total mercury concentration
HI	Hazard index
HQ	Hazard quotient
Igeo	Geoaccumulation index
PEF	Particle emission factor
PM	Particulate matter
RfD	Reference dose
R_{ing}	Ingestion rate
R_{inh}	Inhalation rate
SA	Surface area of the skin that contacts the dust
SEM EDX	Scanning electron microscopy energy dispersive X-ray detector
SL	Skin adherence factor for dust
TSF	Tailings storage facilities
UNEP	United Nations Environmental Programme
USEPA	United States Environmental Protection Agency
XRD	X-Ray Diffraction
XRF	X-ray fluorescence

Chapter 1

Introduction

Gold mining activities on the Witwatersrand, with emphasis on the environmental impacts of tailings storage facilities are discussed with regards to windblown dust erosion. The problem statement of the study is presented.

1.1 Introduction

Gold mining started in the Central Rand in the Witwatersrand Basin in 1886. The exploitation of the auriferous conglomerates led to the development of the most advanced economy in Africa, from which nearly 50 000 tons of gold was produced (Mineral resources, South Africa Yearbook 2012/13; Robb and Robb, 1998). South Africa (SA) was considered to be the world's largest gold producer until 2007, when it was surpassed by China as the world's leading gold producer (Mineral resources, South Africa Yearbook 2012/13; Hartnady, 2009). However, in 2013, SA is now placed fifth, coming after China, Australia, United States of America (USA) and Russia (U. S. Geological Survey, 2013). According to a report published by the United States Geological Survey (USGS, 2013), SA is placed second in the world's gold reserves, with an estimated 6000 tons, coming after Australia, with about 7400 tons, respectively. 95% of SA's gold mines are underground operations and 98% of the gold that has been mined came from the Witwatersrand goldfields. In the 1970s, gold production reached record levels of 1000 tons and a yield of 13.11 grams per tons (g t^{-1}) (Janisch, 1986). It has since steadily declined over the years to an annual average of 250 tons, with a yield of 4.27 g t^{-1} (Amey, 2002). The steady decline over the years has been attributed to the increasing cost of mining due to deep shaft mining at depths of 4 km and below, the low-grade quality of the ore resulting in the low gold yields (g t^{-1}), rising operational and labour costs, the fluctuating gold prices, the closure of many gold mines, the introduction and implementation of new safety procedures and environmental laws. Currently the functional gold mines are in the West Rand, i.e., South Deep, Western areas, Carletonville, Klerksdorp and Welkom (Hayward *et al*., 2005).

The Witwatersrand gold ore bodies' occurred in conglomerate beds (reefs) containing a matrix of quartz and fine-grained phyllosilicates consisting mainly of sericite, chlorite, with minor amounts of muscovite, pyrophyllite and chloritoid (Hallbauer & Barton, 1987; Janisch, 1986; Hallbauer & Von Gehlen, 1983). This matrix also contained detrital heavy metals consisting of largely pyrite, zircon ($ZrSiO_4$), rutile (TiO_2), chromite ($FeCr_2O_4$), uraninite (UO_2), arsenopyrite (FeAsS), cobaltite (CoAsS) and rare platinum-group metals (Janisch, 1986; Hallbauer and

Barton, 1987). Other minerals phases found within the matrix included galena (PbS), pyrrhotite (FeS), gersdofite (NiAsS), chalcopyrite ($CuFeS_2$), sphalerite [(Zn,Fe)S], pentlandite [$(Fe,Ni)_9S_8$] and brannerite (UTi_2O_6) (Hallbauer and Barton, 1987).

In South Africa, mercury (Hg) occurs in a number of deposit types, commonly as cinnabar (HgS) in metal sulphide deposits and pyrite in coal (Yudovich and Ketris, 2005), and occurs together with gold (Au) in the placer deposits found in the Witwatersrand (Davies & Mundalamo, 2010). The major sources of Hg emissions were thought to be anthropogenic, with coal combustion in power generation, large-scale and artisanal gold production being the biggest contributors (Pacyna *et al*., 2002). Schroder *et al*., (1982) found that gold ores in Witwatersrand reef contained on average 1.38% Hg, with some ores containing as much as 2.23%. Erasmus *et al*., (1982), on the other hand, found that Hg concentration in the gold ores varied between 1.2 and 4.6% while Hallbauer & Barton's (1987) found Hg concentration in the gold ores to be between 0.54 – 4.5%. Schroder *et al*., (1982) went further and measured Hg emissions from gold extraction and refining process and estimated the total Hg emissions to be 193 kg yr^{-1} based on a total annual gold production of 706 tonnes. The Witwatersrand gold grains contain highly variable silver (Ag) and Hg contents (Hayward *et al*., 2005).

Initially, the poorly-controlled mercury amalgamation was used as the method for gold recovery. It resulted in the release of mercury into the river systems and emission into the atmosphere during the process, leading to wide spread environmental contamination and in the human mercury exposure (Lacerda, 2003; Telmer *et al*., 2006). Unfortunately, this method is still being practised by artisanal gold miners (popularly known as zama zamas or illegal miners) in South Africa. The mineral waste produced from this type of gold recovery was dumped in heaps called sand dumps (Naicker *et al.,* 2003). As mining became deeper, sulphidic ores were encountered and the amalgamation method became less efficient (mercury reacts with sulphur, making it less selective for gold) and as a result, cyanidation was introduced as a replacement method. This process required finer milled ore and

the mineral waste produced was deposited in slimes or tailings storage facilities (TSFs) or tailings dams. These processes were selective to mostly gold and to lesser extent sulphides and uranium. Therefore, all the other minerals and heavy metals were unaffected by the extraction process and found their way into the TSFs.

The development and growth of the gold mining industry gave way to the development and growth of the industry in the Witwatersrand basin. This gave rise to the development of Johannesburg town, which later grew into a vast metropolitan city, which today accommodates tens of millions of people (Forstner and Wittmann, 1976; McCarthy & Venter, 2006, Naicker *et al.*, 2003). Townships were established along the length of the outcrop to accommodate the growing number of mine workforce (McCarthy and Venter, 2006). However, black townships and informal settlements were located even closer and within the prescribed exclusion zones surrounding dominant and active tailing sites. In some cases, they encroached on mine reserves, and informal settlements were built on tailings footprint. Residents living near TSFs and from the informal settlements were exposed to the hazards posed by the tailings deposits.

Mine tailings are the single most important anthropogenic source of environmental pollution especially in arid and semi-arid regions. These tailings generally included sand dumps, slimes dams, tailing impoundments and rock dumps. Their impacts resulted from acid mine drainage (low pH ranging from 2.5 – 3.5) caused by the oxidation of pyrites, the high incidence of wind and water driven erosion events, and the sterilization of vast appreciable tracts of land partly as a result of shallow undermining (Tutu, 2006; Blight, 1991).

To date, approximately 270 tailings dams covering an area of 181 km^2 have been identified in South Africa (Aucamp & Van Schalkwyk, 2003; Rösner *et al*., 1998; Funke, 1990). They are, generally, situated close to major highways, important water courses and wetlands, residential and industrial areas. Most of the tailings dams were established poorly during a time when there was little environmental legislation in place, which required mining companies to rehabilitate and manage

their dams (Wates, Strayton and Brown, 1997). Therefore limited rehabilitation was undertaken and this has led to the current environmental problems being experienced. The Central Rand area, south of Johannesburg is one of the area's directly affected by the impact of mine tailings mainly due to their age, high population densities and commercial developments in their vicinities as well as the presence of numerous streams of the upper Klip River catchment area.

The previous metallurgical processes did not completely recover all the gold and therefore, small quantities remained in the tailings. Approximately 70 tailings dams were reclaimed in the Gauteng province, resulting in about 13 km^2 of land becoming available for potential development (Rösner *et al*., 1998). On the Central Rand, slimes dams with an average of 0.4 g Au ton^{-1} and sand dumps averaging about 0.6 g Au ton^{-1} were recovered (Viljoen, 2009; Rösner *et al*., 1998). However, tailings dams with low gold-grade (i.e., < 0.4 g Au ton^{-1}) remained on the surface and continued to be a source of acid generation and contaminant remobilization. Most of these tailings dams were incompletely reclaimed leaving behind significant variable quantities of residual tailings material. The resultant bare soils were characterized by low pH, lacked normal levels of soil nutrients and did not develop normal soil structure hence could not support the establishment of plant cover (Sutton and Dick, 1984). During the reprocessing of tailings dams, extensive dust and water pollution problems were reactivated (Viljoen, 2009). The milled TSFs have a greater fraction of finer material than older tailings dumps. It also contains a higher fraction of respirable and inhalable particle size fractions (Maseki, 2013; Ojelede *et al*., 2012). The vegetation was removed and exposed surfaces were subjected to wind erosion and oxidation.

The establishment of large and steep sand dumps and slimes dams from mining operation, without the necessary precautions, created optimal conditions for wind erosion. Factors such as the height of the sand dumps and slimes dams, the texture of the slimes dams' material (fine, powdery particles) and the alignment of the sand dumps and slimes dams with the prevailing winds increased the susceptibility of the sand dumps and slimes dams to wind erosion. Wind speed increased with height

therefore activities which were done in the locations well above the ground level were more susceptible to dust effect. The resurgence of dust pollution and dust fallout from active dumps was of particular concern to the communities living close to tailings dams. This was excessibated by the prevailing winds, north-westerly winds, which were dominant in the dry late-winter and early summer months when the surface of the mine dumps were still dry. The effect of prevailing winds in redistribution of contaminants played a significant role in the soil accumulation of metals and metalloids a distance away from the source (Van Alphen, 1999; Sterckeman *et al*., 2000; Stafilov *et al*., 2010; Fernandez-Camacho *et al*., 2010; Taylor *et al*., 2010; Sanchez de la Campa *et al*., 2011). People living downwind of mine tailings were exposed to the potentially inhalable trace metal/metalloid-bearing particles. Active dams rarely had dust problems compared to dominant dams.

Wind erosion can transport environmental contaminants such as metals and metalloids, pesticides, and biological pathogens, all of which are typically associated with finer atmospheric particles and tropospheric aerosols (Pope *et al*., 1996; Griffin *et al*., 2001; Csavina *et al*., 2011). Particles emitted from mine tailings due to wind erosion were usually in the coarse range (2 – 100 µm) (Csavina *et al*., 2011) while anthropogenic sources (combustion processes) are finer (<2 µm) (Charlesworth *et al*., 2011). However, they potentially can have a wide size distribution as well as a range of metal and metalloid concentrations. In particular, efflorescent deposits, generated by evaporating water that flows to the surface of the tailings by capillarity action, may contain metal and metalloid concentrations that are much higher than the surrounding tailings topsoil due to the presence of crystallized soluble contaminant salts (Meza-Figueroa *et al*., 2009; Hayes *et al*., 2012). Dry, efflorescent particles are particularly susceptible to wind erosion. Occupational studies have been published for mine-related dust and aerosol. However, little work has been done on the impacts of TSFs. Both Csavina *et al*. (2011) and Spear *et al*., (1998) showed that the majority of atmospheric metals and metalloids around smelting operations are in the fine to ultrafine size fraction (< 2 µm).

Dust and aerosol emissions associated with mining operations and TSFs were commonly associated with significantly elevated levels of one or more of these contaminants, Hg, Pb, As, and Cr, which accumulated in soils, natural waters and vegetation (Meza-Figueroa *et al*., 2009; Brotons *et al*., 2010; Csavina *et al*., 2011; Corriveau *et al*., 2011). As, Cd, Cr, Hg, Mn, Ni, Pb, and V, trace metals were found in association with finer particulates (Charlesworth *et al*., 2011). Meza-Figueroa *et al*., (2009) analyzed soils in Sonora, Mexico around the Pilares mine Nacozari tailings site for metal and metalloid content, and it showed that contaminant dispersion took place primarily by surface run-off, but enrichment factors for Hg, Cu, As, Zn and Pb in residential soils arose from wind erosion. According to Ravi *et al*., (2011) contaminants commonly associated with particulates from mining operations were usually mostly concentrated in the finer particle fraction, which travelled greater distances in the environment. Re-suspension of the dust and fine soil fraction can contribute a significant amount to the inhalable trace element load of urban aerosol (Zhao *et al*., 2006), or it can be washed-out where it can become an important component of suspended and dissolved solids in street run-off (Vermette *et al*., 1991).

Fine particles have high specific area that retains high amounts of metals (Wang *et al*., 2006). In addition, small particles are soluble and are more likely to traverse the gastric mucosa and be more efficiently adsorbed in human tissues than coarse fractions (Hemphill *et al*., 1991; Lin *et al*., 1998). Particle size affected dust deposition efficiency in the human respiratory system upon inhalation. The finer particles were deposited deep into the lungs where they can be transported directly to the blood stream (Krombach *et al*., 1997 Park and Wexler, 2008; Valiulis *et al*., 2008) whilst coarse particles were deposited in the upper respiratory system where they were either coughed and spat out or were swallowed into the digestive system where contaminants may be absorbed, depending on their bioavailability (Csavina *et al*., 2012). These finer particles made up of high surface areas with heavy metals bound to them were a great risk to human health since they appeared to be able to evade the body's natural defence mechanisms, with a consequence of redistribution

into other sites of the body, causing systematic health effects. It is well known that air pollution, in the form of particles of varying composition and size range, had an impact on the respiratory health of humans (Brunekreef and Forsberg, 2005; Gauderman *et al*., 2004; Roemer *et al*., 2000). These particles included trace metals, consisting of metal compounds or in their metallic form, depended on the prevailing exposure situation (Fang *et al*., 2005; Harrison and Yin, 2000; Karlsson *et al*., 2005; Konarski *et al*., 2004). Large size particles of dusts fallout in urban regions have been reported to be the major cause of prevalence of asthma (occur at upper nasal area) compared to association of fine particulates with inner respiratory disorders (Sax and Richard, 1984; Roosli, 2000; Wieringa *et al*., 1997.; USEPA, 2003).

Dust emanating from the mine tailings dams may have serious respiratory consequences for those working and living in the vicinity of tailings dams and those living on the tailings footprint (Terblance *et al*, 1994). Dust is one of the largest occupational hazards and it has been one of the largest occupational ‘‘killers” through the years. Exposure to any dust in excessive amounts created respiratory problems. Different dusts affected the body in different ways and caused harmful effects through skin or eye contact and ingestion, as well as by inhalation, depending upon the individual physical and chemical properties of dust (Health and Safety Executive, 1997). Dust has caused many diseases, the commonest of which associated with mining activities and individuals, were: asthma, chronic bronchitis and emphysema (irritation and inflammatory lung injuries), pulmonary tuberculosis (PTB), pneumoconiosis and in particular silicosis, asbestosis (lung damage) (Trade Union Congress, 2001; World Health Organization, 1999; (Choi *et al*., 2009; Crosby 1998).

Several cases of dust emanating from tailings dams were lodged against mining houses. The Meadowlands Community and Environmental Group lodged a court case based on the dust emission from the nearby slimes dams and the Riverlea community took two state departments and DRD Company to court over the resultant dust pollution from their reprocessing activities on the tailings dams. On windy days, material was observed billowing off the surface of the tailings and it

was impossible to see more than a few metres ahead. They had to keep their windows and doors closed and even found dust in their food. These problems have persisted for decades because of lack of proper remediation strategies to combat pollution from the tailings. The tailings sites have low pH and lack normal levels of soil nutrients, therefore these sites did not develop normal soil structure and cannot support the establishment of plant cover.

The Legal resources Centre (LRC) represented various individuals and organisations complaining about environmental pollution caused by gold mine tailings in the Witwatersrand basin. The complainants included Kagiso Environmental Awareness Forum, The Meadowland Environmental Group, Meadowlands Action Group, Fleurhof Community, South African Wildlife and Environmental Society, National association of Clean Air, Greater Booysens Reserve Anti-dust Association and Booysens Reserve Management Committee. Legislation on dust emissions from mines is not well established due to the limited information provided at present but also because dust impacts from mines were not properly estimated and evaluated.

One of the major reasons why these legal battles were unsuccessful was due to the fact that there was no information, on the adverse health effects suffered by the communities in question, linking with the levels of pollution encountered from the TSFs. Despite the vast available information on the different toxic heavy metals encountered in the tailings, these have not been monitored in the South African context. This has left the communities in question vulnerable to the continued exposure to pollution until such a time when these trace elements will be quantified and the responsible companies prosecuted. In this study, the focus is to determine the levels of mercury in the street dust in the gold mining environment, with emphasis on the windblown dust from the tailings.

The uptake of mercury, both through ingestion or inhalation, resulted in severe adverse health effects such as mercury intoxication and altered immune system effects. Exposure through inhalation of vaporized elemental mercury resulted in

high absorption into the blood stream and about 80% was retained (Clarkson *et al*., 2007). Groups associated with gold mining and its processing were, generally, exposed to elemental mercury and were diagnosed with chronic mercury intoxication (Bose-O'Reilly *et al*. 2010). However, even less exposed groups, mineral processors and the general population living near mining sites, were also found to have high levels of mercury exposure (Bose-O'Reilly *et al*., 2008). Women and children fall into the most vulnerable population groups to mercury exposure, children and foetuses are particularly at risk of suffering developmental problems and neurological damage, respectively. Children exposed to mercury poisoning exhibit typical symptoms such as ataxia, coordination problems, discolouration of gums and excessive salivation (Bose-O'Reilly *et al*., 2008). Akagi *et al*., (2000) reported on under height, underweight, gum discolouration and skin abnormalities found in school children in areas of heavy mercury amalgamation activities in the Philippines.

Consumption of fish with higher concentration levels of methylmercury resulted in severe chronic effects of mercury. Methylmercury is lipophic, therefore it is very well absorbed from the gastrointestinal tract, where it easily entered the bloodstream, distributed throughout the body, readily crossed the placenta and blood-brain barrier and accumulated in the brain (Kerper *et al*., 1992). It has its most devastating effect on the developing brain, the developmental effects includes hyperactive reflexes, deafness, blindness, cerebral palsy, mental retardation and general paralysis.

1.2 Problem statement

Currently, there are insufficient studies on the health effects associated with windblown dust from tailings deposits in South Africa. The effect on human health due to exposure by inhalation of dust containing metals and metalloids including mercury and ingestion of the same dust is at present relatively unclear. There is lack of exposure information on children residing in neighbourhoods adjacent to mine tailings and residential areas built on tailings footprint. Of particular concern, is the type, composition, size and deposition of particulate matter onto the soil in the residential areas and urban playgrounds where children spend significant amount of time. Generally, the ingestion of dust and soil is widely regarded as one of the key pathways by which children are exposed to heavy metals and metalloids from a variety of sources (De Miguel *et al*., 1997, Rasmussen *et al*., 2001; Madrid *et al*., 2002).

Particular attention has been focused on the urban dust in the greater Johannesburg area; an area heavily impacted by mineral dust pollution from the gold mining TSFs. Of interest is the fact that Johannesburg, the city, built on tailings footprints and adjacent to TSFs, has had very few studies on the impact of the fugitive dust generated from tailings dams on both the environment and human beings being studied. To our knowledge, mercury binding forms and speciation in urban dust in arid or semi-arid areas, impacted by gold mining, has not been reported. The lack of data currently makes it difficult to quantify risk associated with living in proximity to TSFs. There is a need to carry out a detailed assessment of mercury levels in urban dust in Johannesburg, and to evaluate the potential impact of dust on human health, the surrounding terrestrial, and aquatic systems. Furthermore, carry out a detailed assessment of the bioavailability and bioaccessibility of mercury in human beings exposed primarily through ingestion and inhalation of particulate matter/dust.

Chapter 2

Literature review

Sources of mercury in the environment, and biogeochemical cycle of mercury are discussed with special emphasis on point sources of mercury in South Africa. Special focus is given to human health risk assessment with respect to mercury in the mining environment. Analytical protocol used to determine and assess bioaccessibility, fractionation and human health risk assessment is discussed.

2.1 Sources of mercury in the environment

Mercury is a naturally occurring element, found throughout the world. It occurs in the earth's crust, in association with many minerals, in the form of sulphides of copper (Cu), iron (Fe), zinc (Zn) and other metals including cinnabar (HgS) (Rytuba, 2003). It's also present in trace amount as an impurity in precious minerals (gold and silver) (Schroder *et al*., 1982, Erasmus *et al*., 1982) and valuable minerals (0.2 and 0.3 ppm of Witbank and Highveld coalfields) (Leaner, 2009; Wagner, 2005; Lusilao-Makiese *et al*., 2012), respectively. Mercury from the natural sources has been responsible for the background environmental levels since pre-industrial age.

2.1.1 Natural sources

Natural sources of mercury were responsible for about 10% of the estimated 5500 – 8900 tons of mercury emitted and re-emitted to the atmosphere from all sources in 2010 (UNEP, 2013). These sources are defined as mercury released via natural processes such as volcanoes or geothermal processes or evasion from natural surfaces (soils, oceans, rivers, lakes) geologically enriched in mercury (Gustin *et al*., 2008; Rytuba, 2005; Nriagu and Becker, 2003; Friedli *et al*., 2001; Ferrara *et al*., 1998; Rasmussen *et al*., 1998). However, the majority of the mercury emission sources are actually re-emissions of mercury historically deposited from anthropogenic sources (Ebinghaus *et al*., 1999; Fitzgerald *et al*., 1998). Current estimate of mercury emissions from both natural and re-emission sources is 5207 Mg yr^{-1} (Table 2.1) (Pirrone *et al*., 2010; Mason, 2009).

2.1.2 Anthropogenic sources

Anthropogenic sources of mercury emissions account for about 30% of the total amount of mercury entering the atmosphere each year (UNEP, 2013), and approximately 75% came from Africa, Asia, and Europe (as shown in Figure 2.1). 40% of total global anthropogenic mercury emissions came from East and Southeast Asia, with 75% of the mercury from this region coming from China, and South Asia accounting for approximately 8%. This is attributed to the major increase in

industrialisation and economic growth of China, where huge quantities of coal are mined and used for power generation, industrial heating, and large scale gold production together with large scale artisanal gold mining occurring, as well.

Table 2.14: Total mercury emissions from natural and re-emission sources for 2008 (Pirrone *et al*., 2010; Mason, 2009).

Region	**Hg Emission ($Mg\ yr^{-1}$)**	**Contribution (%)**
Oceans	2682	51
Lakes	96	2
Forest	342	7
Tundra/Grassland/Savannah/Prairie/Chaparral	448	9
Desert/Metalliferrous/Non vegetated Zones	546	10
Agricultural areas	128	2
Evasion after mercury depletion events	200	4
Biomass burning	675	13
Volcanoes and geothermal areas	90	2
Total	**5207**	**100**

Anthropogenic sources are classified into two categories, namely: (1) primary anthropogenic sources, and (2) secondary anthropogenic sources (Pacyna *et al*., 2010). In the former, mercury of geological origin was mobilised and released to the environment. Mining, metallurgical processes including primary aluminium production, ferrous and non-ferrous processes, burning of fossil fuels, natural gas, and oil refining are the main sources in this category (UNEP, 2013) (Figure 2.2). However, in the latter, emissions occur from the intentional use of mercury, e.g.in artisanal gold mining to recover gold, electric products (light bulbs), measuring devices (thermometer, barometer), dental amalgam for filling teeth, production of non-ferrous metals and cement production (UNEP, 2013; Pacyna *et al*., 2006; Streets *et al*., 2005) . Table 2.2 shows the variation in the anthropogenic sources of mercury emission from 2005 - 2010.

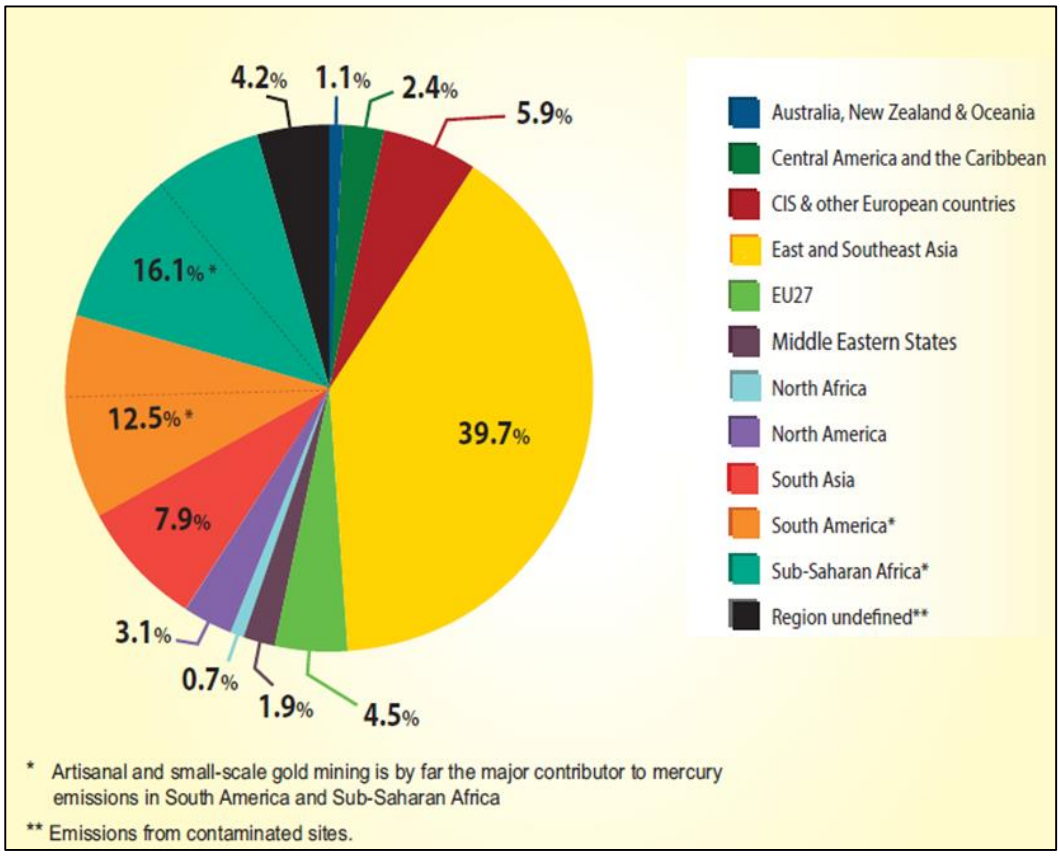

Figure 2.1: Global distribution of anthropogenic mercury emissions in 2010, showing contribution of anthropogenic emissions from different regions of the world (UNEP, 2013).

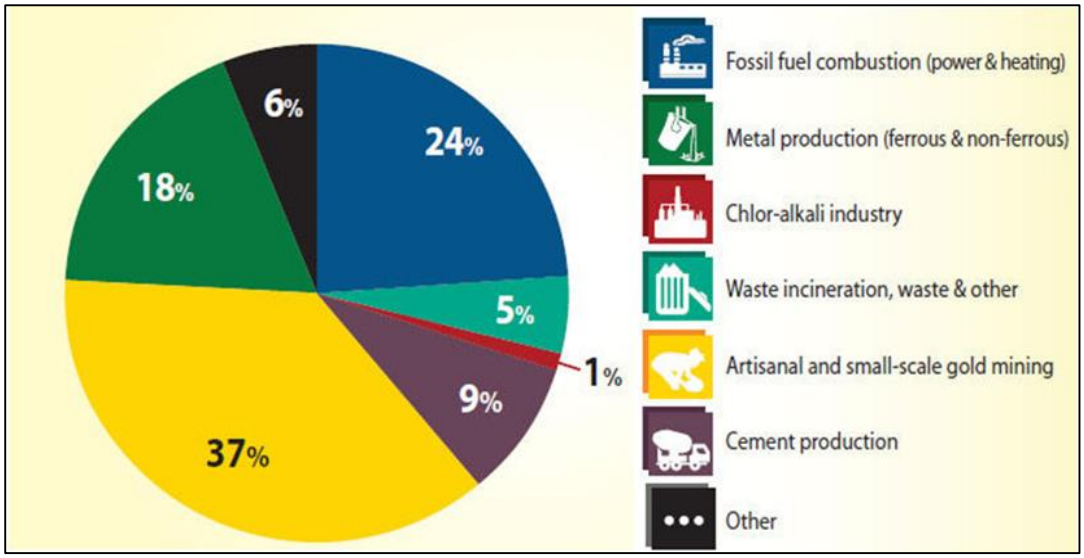

Figure 2.2: Global anthropogenic mercury emissions in 2010 from various sectors (UNEP, 2013).

Table 2.2: Estimated global anthropogenic emissions of mercury to the atmosphere in 2005 and 2010 from various sectors (UNEP, 2013; Pacyna *et al*., 2010).

Sector	**Emissions (Tonnes)**			
	2005	**%**	**2010**	**%**
Unintentional emissions				
Fossil fuels burning				
Coal burning (all uses)	878.0	46	474.0	24
Oil and natural gas burning			9.9	1
Mining, smelting, & production of metals				
Primary production of ferrous metals	200.0	10	45.5	2
Primary production of nonferrous metals (Al, Cu, Pb, Zn)			193.0	10
Large-scale gold production	111.0	6	97.3	5
Mine production of mercury			11.7	<1
Cement production	189.0	10	173.0	9
Oil refining			16.0	1
Contaminated sites			82.5	4
Intentional uses				
Artisanal and small-scale gold mining	351.0	18	727.0	37
Chlor-alkali industry	46.8	2	28.0	1
Consumer product waste	125.0	7	96.0	5
Cremation (dental amalgam)	25.7	1	3.6	<1
Grand Total	**1930**		**196.0**	

2.1.2.1 By-product or unintentional emissions

Non-ferrous ore processing and **metal production** is a source of atmospheric mercury because the ores of zinc, copper, lead and nickel contain significant amounts of mercury including the fossil fuels used to process them (Streets *et al*., 2011; Telmer & Vega, 2009). The volumes of the ores and metals produced resulted in large mercury emissions, which were released into the environment. However, due to the little and/or lack of information on the average concentration of mercury in the metal ores, uncertainties in the mercury emissions figures are introduced by estimating the mercury

concentration in the ores and fuels. Currently it's at about ± 25% (Swain *et al*., 2007; Pacyna *et al.* 2009; Streets *et al*., 2009).

Coal and oil combustion, are a major anthropogenic source of mercury to the atmosphere. Coal accounts for approximately 43% of total fuel used worldwide in electricity generation. Generally, mercury concentration in coal varies widely, however, it is considered to be low in coal (Table 2.3). The combination of the large volumes of coal burned and a trace amount of mercury present in coal results in significantly large emissions from this sector. According to Meij *et al*., (2002), mercury emitted from coal is gaseous elemental mercury (Hg^0) and 75% of Hg^0 is removed by the high efficient flue-gas desulphurization (FGD) system in combination with electrostatic precipitator (ESP) system. The remaining 25% is released into the atmosphere. Ever since the introduction of the air pollution control devices, including mercury emission control equipment, there has been a major reduction in the mercury emissions to the atmosphere (as shown in Table 2.2, where emissions from coal burning were reduced by almost 50% from 878 tons in 2005 to 494 tons in 2010).

From 1990 to 2005, emissions from coal fired-power stations remained stable, decreases from Europe and North America were offset by increases from Asia due to a sharp increase in energy production (UNEP, 2013; Sprovieri *et al*., 2010). In 2010, North America experienced a 50% (53 to 27 tons) reduction in the emissions from coal fired power plants. This has been attributed to implementation of mercury emission controls together with sulphur and particulate matter controls which result in the reduction of mercury emissions. The same technology was applied to the power stations in China, this could explain why the potential significance of the increased mercury emissions are not reflected in long-term measurements of Hg^0 (Sprovieri *et al*., 2010).

Table 2.3: Mercury concentration in coals from selected countries.

Country	Coal Type	Ave Hg (mg kg^{-1})	Reference
Argentina	Bituminous	0.10	Pirrone *et al*., 2009
Australia		0.10	Yudovich & Ketris, 2005
Botswana	Bituminous	0.09	Pirrone *et al*., 2009
China	Anthracite-Bituminous	0.15	Belkin *et al*., 2006
Colombia	Subbituminous	0.04	Pirrone *et al*., 2009
Egypt	Bituminous	0.10	Pirrone *et al*., 2009
Japan	Bituminous	0.05	Mukherjee *et al*., 2008
Peru	Anthracite-Bituminous	0.27	Pirrone *et al*., 2009
Philippines	Subbituminous	0.04	Pirrone *et al*., 2009
Romania	Lignite-Subbituminous	0.21	Pirrone *et al*., 2009
Slovak Rep.	Bituminous	0.08	Pirrone *et al*., 2009
South Africa	**Anthracite-Bituminous**	**0.20**	**Wagner & Hlatshwayo, 2005**
South Korea	Anthracite	0.30	Pirrone *et al*., 2009
Taiwan	Anthracite-Bituminous	0.67	Pirrone *et al*., 2009
Tanzania	Bituminous	0.12	Pirrone *et al*., 2009
Turkey	Lignite	0.11	Pirrone *et al*., 2009
Uk		0.28	Goetz *et al*., 1981
US	All types	0.17	Finkelman, 1993
Vietnam	Anthracite-Bituminous	0.28	Pirrone *et al*., 2009
Zambia	Bituminous	0.60	Pirrone *et al*., 2009
Zimbabwe	Bituminous	0.08	Pirrone *et al*., 2009
World	All types	0.30	Weiss, 2005; Llorens *et al*., 2000

Petroleum and natural gas production and processing are also known to release mercury to the environment, primarily via solid waste streams (Wilhelm, 2001). Oil deposits are known to contain mercury in trace amounts and occurs naturally (Pirrone *et al*., 2009). During the refining of the crude oil, mercury is removed from petroleum products and natural gas through solid waste and is deposed off in landfills. Consequently, emissions from combustion of the oils and its products are relatively

low as compared to coal. The emission values generally range from 0.007 to 30 g Mg^{-1} (Pirrone *et al*., 2006: Mukherjee *et al*., 2008) with expectation of higher mercury concentration in the residual oils than in the distillate oils.

Natural gas contains small amounts of mercury, however, it is removed during the removal of hydrogen sulphide. Mercury emission during the combustion of natural gas are considered to be insignificant (Pirrone *et al*., 1996; 1998).

Mercury mining emits and releases mercury from mercury bearing ores in which mercury is the primary and often only ore metal constituent (Rytuba, 2003 & 2000). These ores are found in the Almaden, silica-carbonate and hot-spring type mineral deposits where cinnabar is the main ore mineral in each of the three mercury deposits. There has been a steady decrease in the production of mercury from mercury deposits from the early 1980, mainly due to increased awareness of environmental problems associated with the use and release of mercury from industrial and mining processes, lower demand, and price. However, mercury continues to be produced as a by-product from sulphide deposits.

The processing of mercury ores generates fine-grained secondary phases which are concentrated in mine wastes such as calcines, condenser soot, and contaminated soils. Mercury is then released and transported from mine sites as mercury-enriched particles and colloids (Rytuba, 2003). The secondary phases in mine wastes are more soluble than the primary ore minerals and when released in aquatic environments, mercury-enriched particles can release inorganic mercury that can be methylated into methylmercury, the most toxic form of mercury, which bioaccumulates and is bioconcentrated in the food chain.

2.1.2.2 Intentional uses of mercury

The practice of **artisanal and small-scale gold mining (ASGM)** has been increasing worldwide owing to the rising price of gold, the privatization and proliferation of larger

mines, widespread poverty, improved, and better data from many countries and regions. This led to increases in mercury emissions from ASGM from 351 tons in 2005 to 727 tons in 2010 (Table 2.2). It is the world's largest source of mercury pollution from intentional use, contributing 37% of total anthropogenic mercury emission in 2010, and surpassing coal combustion in both industrial and power station burning (UNEP, 2013). Largely, this activity is unregulated, illegal, and thus, official data is still hard to obtain. There is a huge reliance on emission estimation, which unfortunately involves a great deal of uncertainty. Therefore a lot of work must be done to confirm and verify the emissions estimates from this sector, including field measurements around the ASGM sites to better establish the amounts and fate of the mercury used. This activity is concentrated in developing countries and countries with economies in transition (the Amazon region in South America, China in Southeast Asia, Indonesia, some African countries, and possibly Australia, and North America).

Artisanal and small-scale gold mining encompasses small, medium, informal, legal and illegal miners who use rudimentary techniques to extract gold (Veiga *et al*., 2006). This activity is characterised and influenced by the conditions on-site, cultural beliefs and economic significance. The use of mercury amalgamation method in the extraction of gold, particularly in developing countries, was influenced by the fact that mercury is: (i) easy to use and works quickly, (ii) available, (iii) cheaper than most alternative techniques, (iv) effectively extracts gold in most field conditions, (v) able to permit custom processing of small individual ore batches, and (vi) miners are not aware of, or choose to ignore, the health risks (Schmidt, 2012; Telmer and Veiga 2009; Veiga *et al*., 2006).

Approximately 10 to 15 million people are involved in artisanal and small-scale gold mining (Cordy *et al*., 2011; Swain *et al*., 2007) with operations in more than 70 countries, producing in the range of 350 tonnes of gold annually (Telmer and Veiga, 2009; Kasper *et al*., 2013). More than 200 000 Ghanaians are estimated to work in small-scale mining operations (Hilson *et al*., 2007; Hilson and Pardie, 2006), between

15 000 and 30 000 artisanal gold miners exist in Colombia (Cordy *et al*., 2011), and between 200 000 and 300 000 are found in Tanzania (van Straaten, 2000; Ikingura *et al*., 1997).

Seccatore, (2012), in a recent study, reported production from ASGM to be about 392 tonnes yr^{-1}, supporting the production figure suggested by Telmer (2009). According to Lacerda, Swain and others, (Swain *et al*., 2007, Lacerda, 1997), artisanal gold miners, worldwide, are the main consumers of mercury, and its losses, released to the environment, were placed at 1000, 1400 and 1608 tonnes giving an average of 1336 tonnes yr^{-1} (Swain *et al*., 2007; UNEP, 2013; Koekkoek, 2013) or more than 30% of all mercury annually used by different industrial applications. China is the predominant source of ASGM mercury emissions of 200 - 250 tonne yr^{-1}. Indonesia releases 100 - 150 tonne yr^{-1}, while Brazil, Bolivia, Colombia, Peru, Philippines, Venezuela and Zimbabwe each releases from 10-30 tonnes of mercury per year. Between 1.0 – 3.5 tons of mercury is lost to 1 ton of gold produced (Veiga *et al*., 2006; Veiga and Baker, 2004; van Straaten, 2000; Lacerda, 1997; Pfeiffer and Lacerda, 1988).

The amalgamation of the whole ore is the cause of environmental problems (Spiegel and Veiga, 2010). This technique results in the greatest loss of mercury, which ends up in the tailings, and amalgams generally contain 60% Au - 40% Hg ratio (Veiga *et al*., 2014 and 2006). The resulting amalgam is refined to varying degrees by burning using a blow torch at 450°C to produce a gold doré containing 2 - 5% mercury (Veiga and Hinton, 2002; Veiga *et al*., 2006). High amounts of gaseous elemental mercury are released directly into the atmosphere, resulting in tremendous exposure of miners and surrounding communities to mercury vapour. The distribution of mercury losses is as follows: 70% by volatilization during amalgam distillation, 20% dragged with amalgamation tailings, soils, water, and 10% volatilized in gold shop (Lacerda, 2003; van Straaten, 2000; Meech *et al*., 1998).

Significant releases of mercury are associated with inefficient whole ore amalgamation techniques with 26% extraction efficiency as compared to more than 90% extraction

efficiency of cyanidation (Veiga *et al*., 2009 and 2006). In most cases, miners work in unsafe areas, without any protective gear and their activities impact negatively both on the environment (result in the contamination of water systems, sediments and soils caused washing of the gold-mercury amalgam mixture) and human health (caused by inhalation of mercury vapours directly and/or indirectly). The extent to which illegal gold mining activities have contaminated local landscapes and areas of residents, with mercury is not known.

Volatile Hg contributes to the global atmospheric pool, which has been demonstrated to impact ecosystems remote from any mercury source. Leachable mercury can contaminate local drainages where it can be methylated and bioaccumulated in food webs (Lodenius and Malm, 1998).

One of the major problems with the worldwide databases on mercury emission is that mercury emission from gold mining is significantly underestimated. For example, Laperdina *et al*., (1999) reported Hg losses of about 9 tons yr^{-1}, while Yagolnitzer and other (1996) reported 56 – 98 tons yr^{-1}, figures that are six times higher than those of Laperdina, for the former Soviet Union. This suggested that the former Soviet Union figures were probably underestimated (Lacerda, 2003). A similar situation was observed in Zimbabwe, where an estimated 200 000 or more artisanal miners produced 5 tons Au yr^{-1}, a figure severely underestimated (Maponga, 1997). In some cases, countries maybe using mercury amalgamation in gold mining, however, inventory information is very scarce. Mercury emission figures are estimated using gold production figures and emission factors. Gold production figures are difficult to estimate because of smuggling, legally not registered enterprises, and the fact that artisanal miners do not tell the truth about their production figures. Therefore, the accuracy of mercury emission figures becomes highly questionable. Yet, mercury emission from gold mining is very significant and seems to be on the increase, especially in developing countries.

2.1.3 Re-emission sources

Re-emissions processes represent secondary sources of historically deposited mercury over natural surfaces (Driscoll *et al*., 2013). They have been placed separately mainly due to the fact that they cannot be conclusively or specifically classified under either anthropogenic or natural sources. However, their contribution has been proven to be significant to the global mercury emission inventory to the atmosphere. Sources mainly include the release of mercury previously deposited on vegetation, land and/or water surfaces. Another major contribution of mercury to the atmosphere, is made from accidental wildfires or intentional burning of forests clearing for agricultural purposes (Veiga *et al*., 1994). According to Pirrone *et al*., (2001; 1996), Corbitt *et al*., (2011), and UNEP, (2013), re-emission sources are the major contributors of mercury emissions to the global atmospheric mercury, with about 60% of the total mercury emissions.

Mercury in vegetation is due to uptake from the atmosphere, atmospheric deposition on to foliage and uptake from roots (Rea *et al*., 2002). However, the close proximity of the vegetation to point sources or contaminated sites increases its mercury content (Lodenius *et al*., 2003; Carballeira and Fernandez, 2002; Lodenius, 1998). According to Bailey and Gray (1997), inorganic mercury species predominated in mercury-enriched plants that have grown in contaminated soils in the mercury mineral belt. Both willow and alder vegetation samples accumulated higher levels of total mercury and MeHg, however, willow samples accumulated the highest total mercury and MeHg concentration (Bailey *et al*., 2002; Bailey and Gray, 1997). The vegetation samples collected from mercury mining sites contained total mercury concentration as high as 970 ng g^{-1} in the leaves, 210 ng g^{-1} in stems, and 370 ng g^{-1} in flowering parts (Bailey *et al*., 2002). MeHg was determined to be in the range of 0.45 to 2.8 ng g^{-1} and the leaf samples contained the highest concentration while the stem samples had the highest percentage of MeHg, respectively. Generally, mercury concentrations were highest for samples collected from tailings and around the mining sites as compared to the background sample sites. Due to the mercury content in vegetation, mercury emission

from biomass burning is significant (Pirrone *et al*., 2005; Sigler *et al*., 2003; Friedli *et al*., 2001; 2003; Roulet *et al*., 1999; Carvalho *et al*., 1998; Veiga *et al*., 1994). This release from vegetation is subjected to mercury concentration in foliage, the forest combustion efficiency, the efficiency of mercury release to the atmosphere, light intensity and temperature (Zehner and Gustin, 2002; Engle *et al*., 2001; Ferrara *et al*., 1997). Vegetation is an effective indicator of the impact of contamination source in its vicinity because plants have the capacity to accumulate these pollutants, therefore their concentrations are much higher than those in the air.

Mercury evasion from land surfaces is about 2430 Mg yr^{-1}, while that from water (oceans and lakes) surfaces is about 2780 Mg yr^{-1} (Pirrone *et al*., 2010; 2009). Evasion from ocean surfaces accounts for about 60% of the total mercury emissions (Corbitt *et al*., 2011; Soerensen *et al*., 2010; Mason, 2009; Mason and Sheu, 2002). In the ocean, mercury is present as elemental mercury (Hg^0), methylmercury (MeHg), dimethylmercury (Me_2Hg), aqueous divalent mercury (Hg^{2+}), colloidal mercury and particulate mercury (Mason *et al*., 2012). Mercury concentration in ocean surfaces and its distribution are variable and changing at different rates in response to fluctuations in atmospheric inputs.

2.2 Biogeochemical cycle of mercury

The mercury cycling and reaction pathways in different environmental compartments is influenced by environmental parameters, and the concentration of different mercury species available (Figure 2.3). Solubility, mobility, bioavailability, bioconcentration, biomagnification, and bioaccumulation are processes that occur in the biogeochemical cycle of mercury and these processes, among other factors, influence the transformation and transportation of mercury.

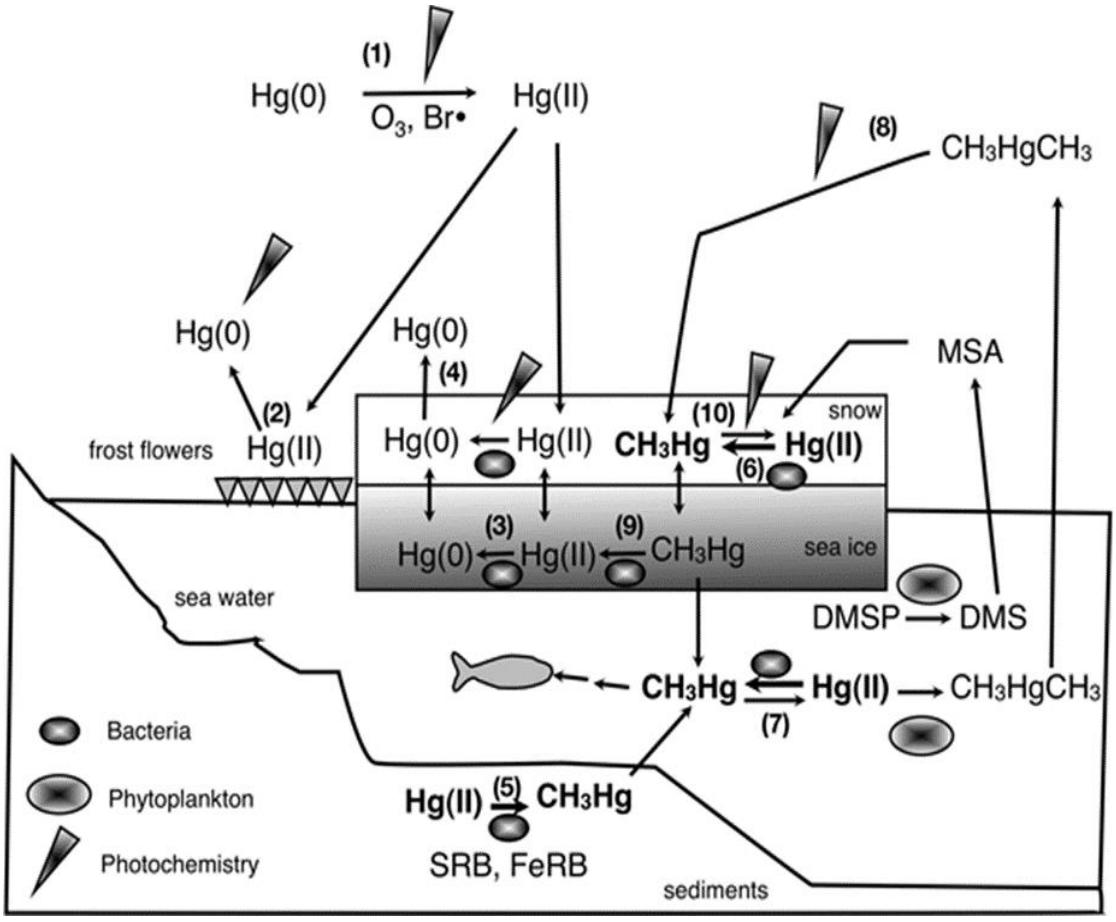

Figure 2.3: Major reactions and transport pathways of mercury in the biogeochemical cycle: (1) atmospheric oxidation of Hg(0) to Hg(II); (2) photoreduction of newly deposited Hg(II) to Hg(0); (3) biological reduction of Hg(II) to Hg(0); (4) evasion of Hg(0) to the atmosphere; (5) methylation of Hg(II) to CH_3Hg by sulfate-reducing bacteria (SRB) and iron-reducing bacteria (FeRB); (6) methylation of Hg(II) to CH_3Hg by aerobic pathway and/or by photomethylation in snow; (7) methylation of Hg(II) to CH_3Hg by algae and phytoplankton in the water column; (8) photochemical degradation of Me_2Hg in the atmosphere; (9) biological demethylation of CH_3Hg to Hg(II); and (10) photochemical demethylation of CH_3Hg in snow (Barkey *et al*., 2011).

2.2.1 Atmospheric mercury and transformation processes

Mercury in the atmosphere is dominated by gaseous elemental mercury (GEM or Hg^0) contributing, approximately 90-99% of atmospheric mercury and the remainder, occurs as gaseous oxidized mercury (GOM or reactive gaseous mercury, RGM or Hg^{2+}) and particle-bound mercury (Hg_P) (Pirrone *et al*., 2010; Steffen *et al*., 2007; Schroeder and

Munthe, 1998; Schroeder *et al*., 1991; Slemr *et al*., 1985). Hg^0 is relatively inert to chemical reactions, is sparingly soluble in water and has a lifetime of approximately 1-2 year (Lindqvist and Rodhe, 1985; Slemr *et al*., 1985), hence its redistribution globally, is made easy in the atmosphere (Durnford *et al*., 2010; Fitzgerald *et al*., 1998). Its current background concentration in the northern and southern hemisphere is considered to be in the range of 1.5 – 1.7 ng m^{-3}, and 1.1 – 1.3 ng m^{-3}, respectively (Lindberg *et al*., 2007; Lindqvist and Rodhe, 1985; Slemr *et al*., 1981).

In contrast, both Hg^{2+} and Hg_p have much shorter lifetimes, in the order of a few days to a week (Lindqvist and Rodhe, 1985; Slemr *et al*., 1981) (Table 2.4). However, they are both rapidly deposited from the atmosphere. Hg^{2+} is removed by both wet (rain and snow) and dry (aerosols) deposition processes while Hg_p is washed out (Lindberg and Stratton, 1998). Wet deposition involves the removal of Hg^{2+} from gas-phase and aerosol-phase while dry deposition involves surface uptake of both Hg^0 and Hg^{2+} (Zhang *et al*., 2009). Hg_p is released directly from emission sources (Keeler *et al*., 1995) but may also form when gas-phase mercury binds to particles (Pirrone *et al*., 2000; Forlano *et al*., 2000).

Table 2.4: Basic information of airborne mercury species (Valente *et al*., 2007).

Order	Mercury species	Abbreviation	Occurrence in air (%	Atmospheric life span	Reactivity
1	Gaseous elemental mercury	GEM, Hg^0, or Hg(0)	>95	1 month-1.5 yrs	Inert
2	Reactive gaseous mercury	RGM or Hg(II)	<1	1 day-1 week	Highly reactive
3	Particle-bound mercury	Hg_p	<1	1 day-1 week	Reactive
4	Organic mercury	MeHg	<3 of TGM		Reactive

60% of mercury deposition occurs over land and only 40% over water (oceans, seas, lakes, rivers, etc.) (Mason *et al*., 1994). This is achieved by the oxidation of Hg^0 into the disposable Hg^{2+} (Ariya *et al*., 2008; Brooks *et al*., 2006; Lindberg *et al*., 2002), which possibly occurs in the clouds (Lin and Pehkonen, 1997). This reaction may take place in the gas phase, and aqueous phase (in cloud and fog droplets and deliquesced aerosol particles), and heterogeneous reactions (partitioning of elemental and oxidised Hg species between the gas and solid phases, and the solid and aqueous phases for insoluble particle matter scavenged by fog or cloud droplets). Table 2.5 lists, and Figure 2.4 shows the most important reactions occurring in the atmosphere.

Table 2.5: Atmospheric mercury and transformation processes.

Type of Reaction	Reaction	References
Oxidation in the gas phase	$Hg^0(g) + O_3 \rightarrow HgO(g,s) + O_2$	Hall, 1995
	$Hg^0(g) + NO_3^* \rightarrow HgO(g,s) + NO_2(g)$	Sommar *et al*., 1997
	$Hg^0(g) + Cl_2(g) \rightarrow HgCl_2(g)$	Stein *et al*., 1996
	$Hg^0(g) + H_2O_2(g) \rightarrow Hg(OH)_2(g,s)$	Tokos *et al*., 1998
	$Hg^0(aq) + {}^*OH(g) \rightarrow {}^*HgOH(g)$	Sommar *et al*., 2001
	${}^*HgOH(g) + O_2(g) \rightarrow HgO(g,s) + HO_2^*(g)$	
Oxidation in the liquid phase	$Hg^0(aq) + O_3(aq) + H_2O \rightarrow Hg^{2+}(aq) + 2OH^-(aq) + O_2(aq)$	Iverfeldt & Lindqvist, 1986
	$Hg^0(aq) + H_2O_2(aq) + 2H^+ \rightarrow Hg^{2+}(aq) + 2H_2O$	Iverfeldt & Lindqvist, 1986
	$Hg^0(aq) + O_3(aq) + H^+ \rightarrow Hg^{2+}(aq) + OH^-(aq) + O_2(aq)$	Munthe, 1992
	$Hg^0(aq) + {}^*OH(aq) \rightarrow Hg^+(aq) + OH^-(aq)$	Lin & Pehkonen, 1997
	$Hg^+(aq) + {}^*OH(aq) \rightarrow Hg^{2+}(aq) + OH^-(aq)$	
	$Hg^0(aq) + HOCl(aq) \rightarrow Hg^{2+}(aq) + OH^-(aq) + Cl^-(aq)$	Lin & Pehkonen, 1999
Reduction in the liquid phase	$Hg^{2+}(aq) + SO_3^{2-}(aq) \rightarrow HgSO_3(aq)$ $HgSO_3(aq) \rightarrow Hg^0(aq) + Products$	Pleijel & Munthe, 1995
	$Hg^{2+}(aq) + HO_2^*(aq) \rightarrow Hg^+(aq) + O_2(aq) + H^+(aq)$	Pehkonen & Lin, 1998
	$Hg^+(aq) + HO_2^*(aq) \rightarrow Hg^0(aq) + O_2(aq) + H^+(aq)$	
Photoreduction in the liquid phase	$Hg(OH)_2(aq) \rightarrow Hg^0(aq) + Products$	Xiao *et al*., 1998
Equilibrium	$Hg^{2+} + 2Cl^- \leftrightarrow HgCl_2$	Lin & Pehkonen, 1999
	$Hg^{2+} + 4Cl^- \leftrightarrow [HgCl_4]^{2-}$	Lin & Pehkonen, 1999
	$Hg^{2+} + 2OH^- \leftrightarrow Hg(OH)_2$	Lin & Pehkonen, 1999
	$Hg^{2+} + SO_3^{2-} \leftrightarrow HgSO_3$	Lin & Pehkonen, 1999
	$Hg_2^{2+} \leftrightarrow Hg^0 + Hg^{2+}$	Munthe & McElroy, 1992

In the gaseous phase, oxidants and radicals are responsible for oxidizing Hg^0 to Hg^{2+} and they include: ozone (O_3), hydrogen peroxide (H_2O_2), NO_2, and nitrate radicals (NO^*_3), hydroxyl radicals (*OH & HO^*_2), organoperoxyl radicals (RO^*_2), respectively. The O_3 and *OH radicals may be the most important oxidants in the oxidation of Hg^0 resulting in the higher concentration of Hg(II) in the aqueous phase (47% of total Hg^0 oxidation is by O_3, Lin and Pehkonen, 1998a) and occurs during the day time. Halogens (Br_2, BrO, Cl_2, HOCl, and Cl*) represent an important type of oxidants in the marine boundary layer (Hedgecock and Pirrone, 2001; Lin *et al*., 2006) and in the Arctic environment (Lindberg *et al*., 2002). It is can be volatilized from sea-salt aerosol produced from oceans surfaces (Keene *et al*., 1996), or aqueous sea-salt particles (Oum *et al*., 1998), and produced from the photolysis of ozone. This reaction occurs at night-time, reaching its peak concentration just before sunrise (Impey *et al*., 1997).

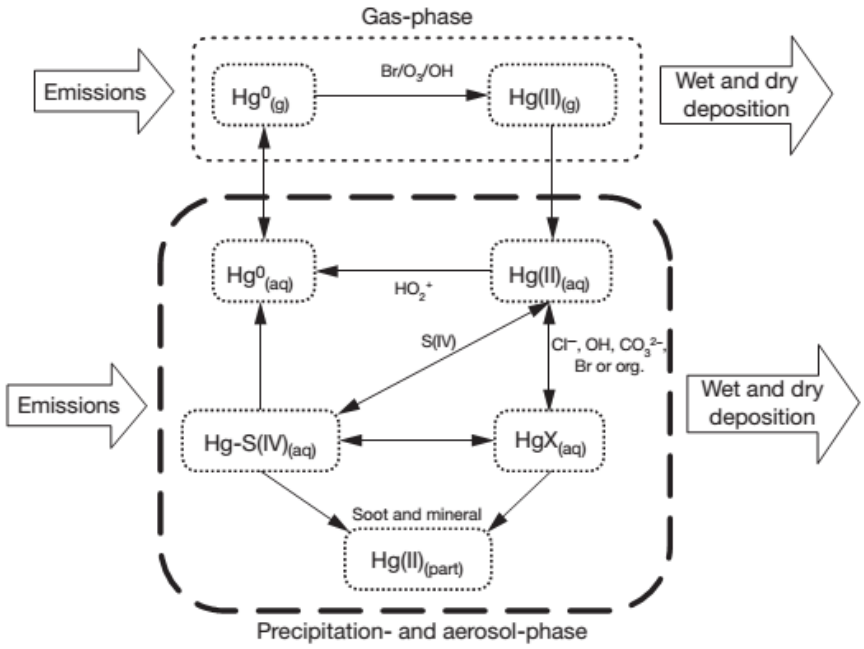

Figure 2.4: Schematic diagram of the most important transformation processes of mercury in the atmosphere (Travnikov and Ryaboshapko, 2002).

Aqueous-phase chemistry is associated with particle and droplet chemistry (rainwater, cloud water or fog water) (Seigneur *et al*., 1994). Oxidation of gaseous Hg^0 and reduction of Hg^{2+} take place simultaneously in the atmospheric aqueous phase. The important oxidants are O_3, H_2O_2 (Iverfeldt and Lindqvist, 1986; Munthe, 1992), *OH radicals (Lin and Pehkonen, 1997) and HOCl (Lin and Pehkonen, 1999) (Table 2.5). These reactions are dependent on their individual concentrations, their solubility, the pH, and the temperature of the water phase. For instance, lowering concentration of Cl_2 or increasing pH can cause considerable oxidation due to the great increase in chlorine solubility in water (Lin and Pehkonen, 1998). Chlorine becomes dominant during the night when the concentration of both the ozone and hydroxyl radicals are decreased due to the absence of the sun light (Lin and Pehkonen, 1999a). In the daytime, marine and terrestrial atmosphere, O_3 is the most predominant oxidant for Hg^0 due to an increase in the concentration of ozone radicals (Lin and Pehkonen, 1999b; Seigneur *et al*., 1994). Halogen and its compounds (Cl_2, Br_2, I_2 or BrO/ClO) act as alternative oxidants for Hg^0 (Ariya *et al*., 2009).

Hg^{2+} in fog and raindrops is removed by adsorption onto particulate matter, particularly, if the particulate matter is rich in elemental carbon (soot) as the adsorption coefficient for Hg on soot is high and due to the great amount of soot in the atmosphere (Petersen *et al*., 1998; Pirrone *et al*., 2000). Therefore, deposition of Hg^{2+} is by both dry and wet processes. Particulate-bound Hg undergo similar reactions to those of gas-phase Hg compounds.

However, Hg^{2+} in the aqueous phase, may also be removed by reduction to Hg^0 by SO_3^{2-} and HO^*_2 (Table 2.5) (Pleijel and Munthe, 1995). SO_3^{2-} exists in the atmosphere due to the elution of the emitted pollutant, SO_2. However, because of the short residence time of SO_3^{2-} in clouds or fog, the contribution of SO_3^{2-} to the Hg^0 production is generally low, lasting only for a few hours. HO^*_2 is generated from photo-chemical processes in the atmosphere and these radicals are non-specific in their reactions. Photoreduction of a variety of halide- and organo- Hg^{2+} complexes may result in the

formation of Hg^0. The photoreduction Hg^{2+} complexes showed that their pathways were not significant. However, sulphite, on the other hand, is the predominant reductant for aqueous Hg^{2+} when pH and aqueous sulphite concentration are optimal to maximise $HgSO_3$ formation. Otherwise HO^*_2 is the dominant reductant (Lin and Pehkonen, 1998).

According to Slemr *et al*., (2011) there has been a steady decrease in the tropospheric mercury concentration within both hemispheres from 1995 to 2009. This could be attributed to a shift in the biogeochemical cycle of mercury being possibly influenced by the following reasons: (a) the decrease of anthropogenic emissions, (b) the acceleration of the oxidation of mercury in the atmosphere, (c) the decrease of emissions from the legacy of historical mercury use and emissions, and (d) changing emissions from the oceans and soils to global change. However, the decreasing emissions from historical mercury use and emissions appears to be the most plausible explanation for the observed trend (Slemr *et al*., 2011).

2.2.2 Soil and sediments

Soils are known to be sinks for pollutants. The residence time of mercury in soils is estimated to be 80-100 yr (Fitzgerald and Lamborg, 2003; Smith-Downey *et al*., 2010). Natural emissions and re-emissions account for 35-70% of total mercury deposition in most regions (UNEP, 2013), while 5-60% of the deposited mercury is re-emitted within a few days (UNEP, 2013; Amyot *et al*. 2004; Hintelmann *et al*. 2002). Mercury that is not re-emitted, is associated with vegetation, i.e., mercury in the vegetation comes from atmosphere while mercury in the roots comes from the soil (Obrist, 2007). Mercury is absorbed through the gaseous exchange at the stomata of vegetation (Lindberg *et al*., 1992). It is recirculated and incorporated into soil pool via throughfall and literfall of vegetation (Grigal, 2002). Adsorbed mercury remains in the soil, slowly decaying and contributes to large soil mercury reservoir, which turns over slowly. This pool is responsible for the historical mercury emissions, which recycle mercury to the atmosphere over a long period of time (Driscoll *et al*., 2013). Studies of sediment, peat

and ice core suggest that mercury deposition peaked between 1950 and 1990 in most sites (Schuster *et al*., 2002; Biester *et al*., 2007; Muir *et al*., 2009; Mast *et al*., 2010).

Mercury is largely adsorbed onto the soil organic matter (top 4 inches of soil profile) by binding to reduced sulphur functional groups (Kim *et al*., 1997). Organic matter (fulvic and humic acids) complexes with mercury compounds and affects the transportation of mercury (Johansson *et al*., 1991; Johansson and Iverfeldt, 1994). Deposited Hg (>90%) in terrestrial ecosystems largely accumulates in soil organic matter (Skyllberg *et al*., 2003). On the soil surfaces, approximately 1–2% of total mercury is in the methylated form and is usually bound largely to organic matter (Kabata-Pendias and Mukherjee, 2007; Ravichandran, 2004). The remaining 98-99% of total soil mercury can be attributed to Hg^{2+} complexes (Mason *et al*., 1994), though a small fraction of this will be Hg^0 (Revis *et al*., 1989). Hg^{2+} has a strong tendency to form complexes with Cl^-, OH^-, S^{2-}, S containing functional groups of organic ligands and NH_3. Hg^{2+} forms stable complexes, due to its high reactivity with dissolved ligands and high water solubility. Inorganic sulphide binds mercury very strongly and plays an important role in the speciation of Hg in anoxic environments (Ravichandran, 2004). The predominant mercury form in acidic soils is $HgCl_2$ while in the basic to neutral soils is $Hg(OH)_2$ (Kim *et al*., 1997).

A small fraction of soil Hg, in association with dissolved or particulate organic matter, can be transported by riverine fluxes to reducing (anoxic) zones where methylmercury (MeHg) production is high. These zones include wetlands, riparian zones and surface water sediments. Factors such as temperature, hydrology, and hydrologic perturbations (i.e., changes in discharge, hydroperiod, and reservoir management), the supply of Hg^{2+} in a bioavailable form, labile organic carbon, and reducing conditions affect the methylation process (Munthe *et al*., 2007). This process is largely a microbial process, mediated by sulphate-reducing bacteria and to a lesser extent, mediated by iron-reducing bacteria (Fleming *et al*., 2006; Kerin *et al*., 2006; Gilmour and Henry, 1991). As is known, mercury has an extremely high affinity for organic matter, humic

substances (HS) and sulphur-containing ligands (Wallschläger *et al*., 1996; Hintelmann *et al*., 1995). Some mercury is absorbed onto dissolvable organic ligands and other forms of dissolved organic carbon (DOC). These often form stable complexes and thus this fraction of mercury has lower mobility and toxicity. Within the DOC, humic substances contribute to the vast majority of the binding capacity for mercury. Complexation with DOC generally limits the amount of Hg^{2+} available for uptake by methylating bacteria. Mercury associates with iron oxides under oxidizing conditions while organic matter and sulphides under more reducing conditions (Skyllberg *et al*., 2000; Heyes *et al*., 2004). Organic matter interacts with iron oxides and sulphides, thus oxidation-reduction cycles of iron that impact organic matter will also impact associated mercury (Krabbenhoft *et al*., 2005).

The recycling of mercury from soil to the atmosphere is aided by reduction of Hg^{2+} to Hg^{0}. This process is achieved via abiotic processes, although recent research has shown that biotic processes play a crucial role, as well (Fritsche *et al*., 2008; Gabriel and Williamson, 2004). Temperature (Kim *et al*., 1995; Lindberg *et al*., 1995) and solar radiation (Carpi and Lindberg, 1998; Gustin *et al*., 2002) enhance this process. In dry ecosystems, the presence of moisture in the soil from precipitation, promotes volatilization of soil mercury (Gustin and Stamenkovic, 2005).

2.2.3 Aquatic

Atmospheric mercury enters water environment through (i) direct deposition (wet and dry) of Hg^{2+} and methylmercury from atmosphere, (ii) runoff of Hg^{2+} and methylmercury bound to suspended soil/organic matter or attached to dissolved organic carbon, and (iii) leaching of Hg^{2+} and methylmercury into groundwater and surface waters (Figure 2.5). In aquatic systems, Hg^{2+} can be reduced to Hg^{0}, which is then emitted to the atmosphere (Engstrom, 2007) or can be methylated to methylmercury by microorganisms, such as sulphate-reducing bacteria (Compeau and Bertha, 1985; Watras *et al*., 1995) (Figure 2.5). In surface waters, mercury occurs as dissolved gaseous mercury (Hg^{0}), Hg^{2+}, and small fraction of MeHg (Sunderland *et al*., 2010;

Sunderland and Mason, 2007). Hg^{2+} exists both in the dissolved phase and attached to particulate matter, both living (phytoplankton, zooplankton) and detritus (Mason, 2009). The oxidation of Hg^0 and reduction of Hg^{2+} is controlled by both abiotic (photochemical reactions) and biotic processes. These processes occur simultaneously, establishing an equilibrium (Whaling *et al*., 2007; Mason *et al*., 2001). In the biotic processes, reduction of Hg^{2+} to Hg^0 occurs in the presence of algae, bacteria (Mason *et al*., 1995), and organic matter (Costa and Liss, 1999). Approximately 70% of the deposited mercury in aquatic environments is re-emitted to the atmosphere as Hg^0 (Corbitt *et al*., 2011; Soerensen *et al*., 2010; Mason and Sheu, 2002).

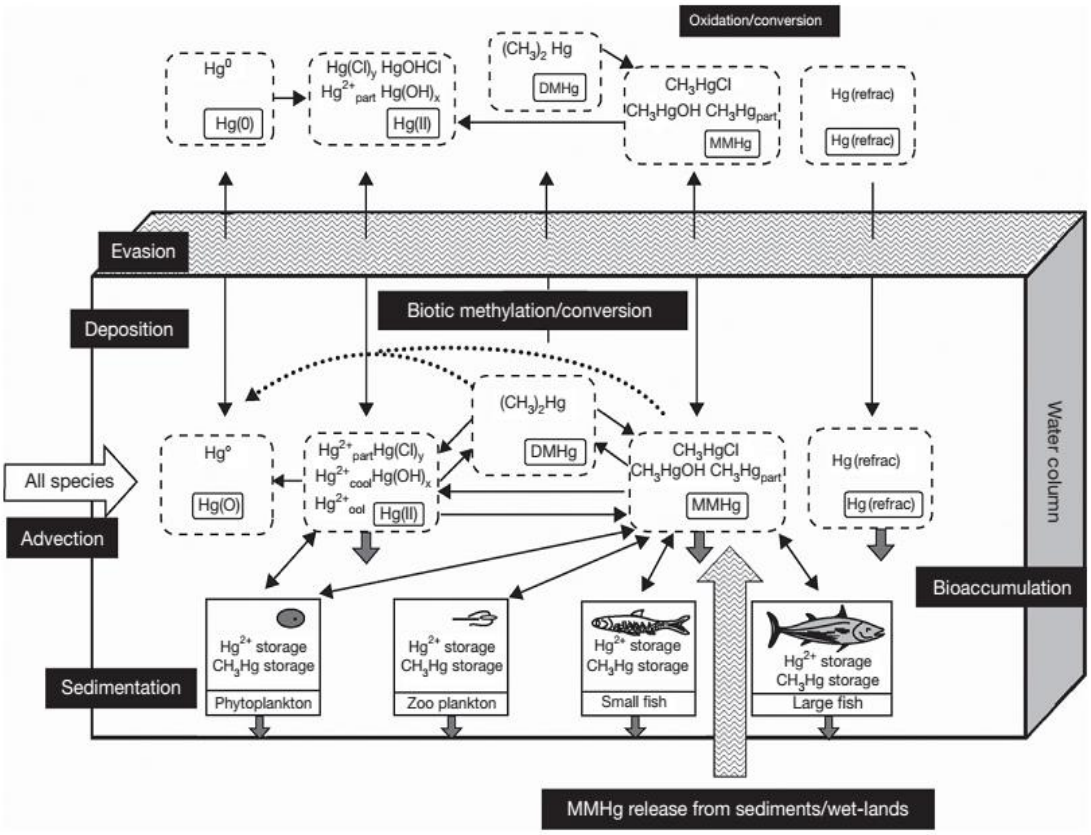

Figure 2.5: Generalised view of mercury biogeochemistry in the aquatic environment. (Hudson *et al*., 1994)

Wetlands (Rudd, 1995) and lake sediments (Gilmour *et al*., 1992) are important environments where methylation occurs. Speciation of mercury in the water column of the riparian systems is of great environmental importance, since it can be used as a tool

to monitor and control the ultimate transfer of mercury to wetlands and also the capacity of water bodies to accumulate large amounts of mercury in their sediments (Ulrich *et al*., 2007). Three sources of MeHg identified in freshwater ecosystem are terrestrial runoff, direct atmospheric deposition onto the lake surface and MeHg produced in the sediments, the water column and in the intestinal contents of fish (Rudd, 1995). However, in ocean waters, it can be concluded that the source of MeHg is different from the freshwater and coastal ecosystems, as proven by the presence of dimethyl mercury (Me_2Hg), suggesting that the organisms responsible are different. In open-ocean surface waters, the total MeHg is low as compared to the intermediate layers, where enhanced net methylation occurs. In these mixed layers (>1000 m), particulate matter is being degraded (Sunderland *et al*., 2009), it's a region of low oxygen (Stramma *et al*., 2008), and changes in the microbial structure in the ocean water column (Heimburger *et al*., 2010).

Methylation is the primary pathway by which mercury enters the food chain (Sorenson *et al*., 1990). Once in the food chain, the levels of mercury in aquatic organisms increased as larger organisms consumed smaller ones thus it bioaccumulated and was biomagnified to toxic levels such that when consumed by human beings it resulted in mercury poisoning. Both Hg^{2+} and MeHg can be removed from the water column bound to particulate matter into sediments (Fitzgerald *et al*., 1991) or evasion to the atmosphere (Mason and Benoit, 2003). The MeHg level is dependent on both the methylation and demethylation processes occurring in the bottom sediment (Winfrey and Rudd, 1990). Due to the photochemical reactions, demethylation and reduction of Hg^{2+} can take place thus preventing bioaccumulation of MeHg in fish. Winfrey and Rudd (1990) and Driscoll *et al*., (1994) have shown that a correlation exist between MeHg levels in fish and the lake pH. A decrease in pH, results in higher concentration of MeHg in fish tissue. This is attributed to increased amount of H^+ (aq) displacing Hg^{2+} from the binding sites and thus leads to methylation of Hg^{2+}.

Boudou *et al*., (2005) has clearly demonstrated that the presence of anoxic zones as created within the Petit-Saut reservoir facilitates mercury methylation and downstream bioaccumulation in fish species, via the direct and/or trophic transfer routes. The formation of neutral HgS complex, which was suggested to be a critical step for the uptake of mercury by methylating bacteria, was dominant at low concentrations of sulphide (Benoit *et al*., 1999). However, at low sulphide levels, thiols may then become competitive for mercury binding due to the fact that thiols have very strong binding constants and will dominate the Hg^{2+} species distribution under most environmental conditions (Haitzer *et al*, 2002). In oxic natural waters, the most important inorganic ligands are Cl^- and OH^- while DOC is the most important organic ligand. The predominance of DOC regulating Hg^{2+} speciation in aerobic freshwaters is now widely accepted, however, under brackish to marine conditions where Cl^- concentrations are high, mercury speciation is less certain.

2.3 Major anthropogenic sources in South Africa

2.3.1 Mercury emissions from coal mining and usage

Coal mining activities in South African are located in the Free State, Gauteng, KwaZulu-Natal, Limpopo, Mpumalanga, and the North West provinces, which hosts 19 coalfields (Figure 2.6). They are concentrated in the Vryheid Formation of the Ecca Group of the Karoo Sequence. Generally the carbon content of the coals increases eastwards while the number of seams and their thickness decrease. Thus, Mpumalanga and Limpopo Province coals are usually classified as bituminous, occurring in seams up to several meters thick, while KwaZulu-Natal coals are often anthracitic and are found in relatively thin seams.

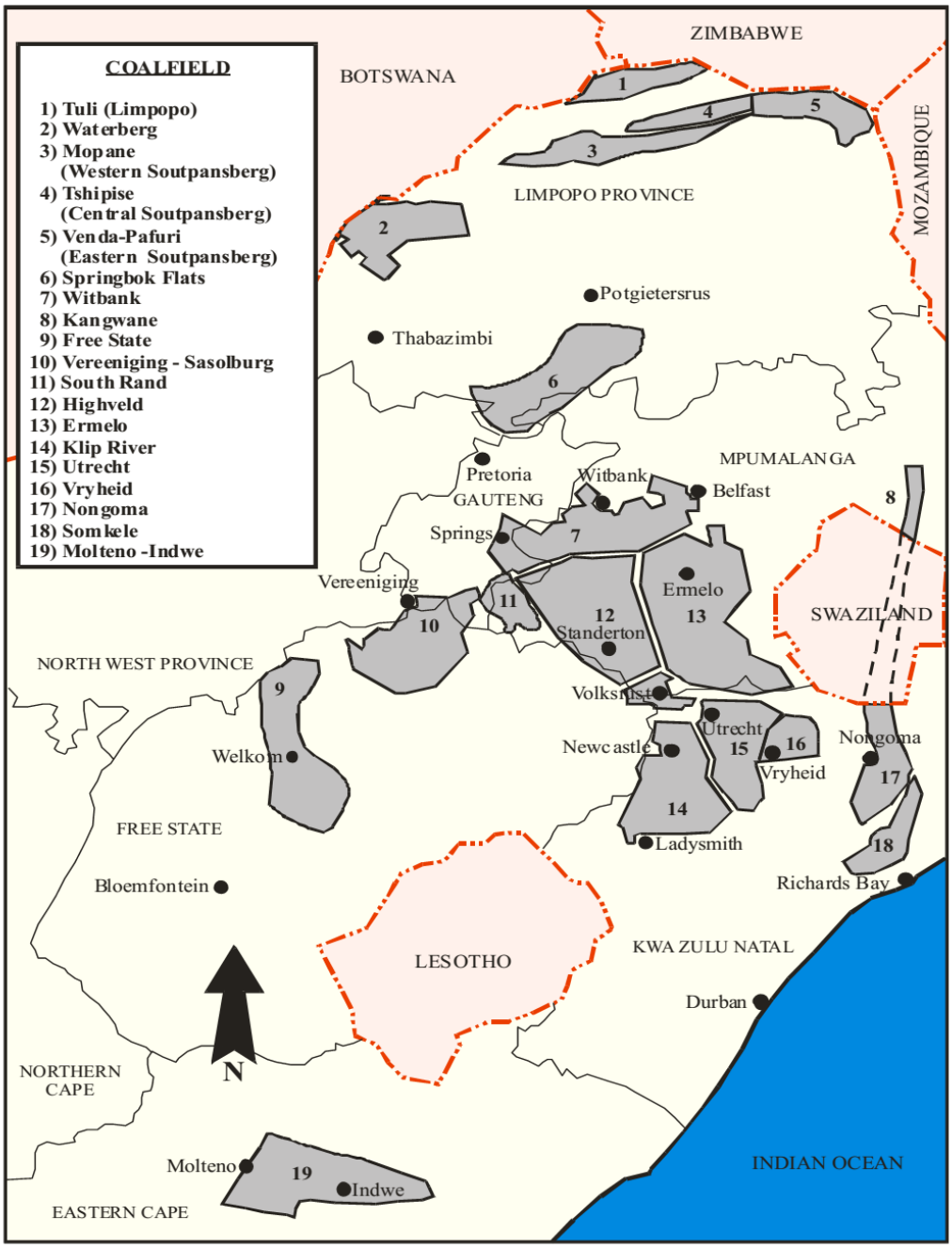

Figure 2.6: Coalfields of South Africa (Pinheiro, 2000).

South Africa is 7th world's largest coal producer, with 72% of total coal produced used for the country's primary energy needs, and 28% is exported internationally, making South Africa the fourth largest coal exporting country. Locally, 53% is used for

electricity generation, 33% for Sasol's synthetic fuel production, 12% for metallurgical industries (Arcelor-Mittal), and 2% for domestic heating and cooking. 95% of the country's electricity is generated from coal-fired power stations (Jeffrey, 2005). Approximately 96% of South African coal is bituminous thermal grade, 2% is anthracite, and 1.6% is metallurgical quality (coking) (Chamber of mines South Africa, Department of energy and minerals, 2007). 96% of the coal reserves are less than 200 m below the surface and over half the reserves are contained in seams thicker than 4 m (Cadle et al., 1993).

South Africa's estimated total remaining recoverable coal reserves is about 51 billion tons (Jeffrey, 2005), a 200 year supply at the current production rate. More than 70% of the estimated total reserves is contained in the Waterberg, Highveld and Witbank coalfields (Jeffrey, 2005). Witbank coalfields are the most important in South Africa, producing about 55% of South Africa's saleable coal (Hancox and Gotz, 2014; Jeffery, 2005). It's currently nearing depletion, and the likely replacement is the Waterberg coalfields, sitting with an estimated recoverable resource of 15000 Mt of in-situ bituminous coal (Dreyer, 2006; Jeffrey, 2005). Other important coalfields include, the Highveld in Mpumalanga, Sasolburg-Vereeniging in the Free State/Gauteng, and small operations in the KwaZulu-Natal province. The Highveld coalfields are largely responsible for supplying coal-fired power plants, Sasol's Synthetic Fuels (SSF), and Sasol Chemical Industries (SCI). Sasolburg-Vereeniging coalfields also supply SSF and SCI, as well as Lethabo power station while the remaining coal reserves of the Free State are low-grade bituminous coal suitable for power generation.

Coal is classified into four main types/ranks based on the amounts, types of carbon it contains, and on the amount of heat energy it can produce. These types are lignite, subbituminous, bituminous, and anthracite. The higher ranks of coal contain more heat-producing energy (EIA, 2008; Kroschwitz and Grant, 1993).

Lignite and sub-bituminous coals are the low rank coals characterised by high moisture levels, low carbon content (25-35% and 35-45%, respectively), and hence and low

energy content. These deposits tend to be relatively young and were not subjected to extreme heat or pressure, and are typically softer, friable materials with dull, earthy appearance. They are used almost exclusively for electricity generation, however, subbituminous coal is an important source of light aromatic hydrocarbons for the chemical synthesis industry.

Anthracite and bituminous coals are higher rank coals, characterised by higher carbon, higher energy, and lower level of moisture content (< 1% and 1-5% for anthracite and bituminous coals, respectively, Kolker *et al*., 2006). They both were formed under intense heat and pressure, and differ by their carbon content, i.e. 86-98% and 45-86% carbon content for anthracite and bituminous coals, respectively. Both are used for steam electric power generation, coke production for metallurgical processes, cement making and to provide heat and steam in industry. South African coals, are generally categorized as low rank bituminous with a moderate to high ash content, 20-30% (Table 2.6) (Wagner and Hlatshwayo, 2005).

2.3.1.1 Mercury concentration in South African coal

Mercury is a natural constituent of coal, occurring in trace amounts. In South Africa, mercury in coal lies in the range of 0.1 to 0.4 mg kg^{-1}, with an average mercury concentration of 0.327 mg kg^{-1} in Highveld coalfields and 0.2 mg kg^{-1} in Witbank coalfields (Watling and Watling, 1982; Lusilao-Makiese *et al*., 2012). Lusilao-Makiese *et al.* (2012) studied the Highveld and Witbank coals of South African and determined the average mercury concentration to be 0.199 ± 0.03 mg kg^{-1}, a value higher than the global average of 0.120 mg kg^{-1} (Zhang *et al*. 2004). The average mercury concentration in Highveld coals (0.219, 0.183, and 160 mg kg^{-1}) obtained by Lusilao-Makiese *et al*., (2012); Wagner and Hlatshwayo (2005); and Kolker, Twalt and Finkelman (2011) were comparable, even though they were determined in

Table 2.6: Estimated remaining recoverable reserves and coal type at the end of 2000 (Jeffery, 2005).

Coalfields	Reserves (Mt)	Coal Type	Uses
1. Tuli (Limpopo)	107.00	Bituminous	Coking
2. Waterberg	15103.00	Bituminous	Coking, steam
3.Mopane (Western Soutpansberg	260.89	Bituminous	Coking
4. Tshipise (Central Soutpansberg			
5.Venda-Pafuri (Eastern Soutpansberg			
6. Springbok Flats	1700.00		Coking, steam
7. Witbank	10139.77	Bituminous	Coking, steam
8. Kangwane	146.04	Anthracite	Coking
9. Free State	4918.78	Bituminous (low grade)	Steam
10. Vereeniging-Sasolburg	1898.09	Bituminous (low grade)	Steam; SSF, SCI
11. South Rand	707.97	Bituminous (low grade)	Steam
12. Highveld	10006.51	Bituminous	Steam
13. Ermelo	4596.89	Bituminous	Coking, steam
14. Klip River	569.74	Anthracite	Coking, steam
15. Utrecht	584.53	Anthracite	Coking, steam
16. Vryheid	122.20	Anthracite	Coking, steam
17. Nongoma	82.82	Anthracite	Coking, steam
18. Somkele			
19. Molteno-Indew		Bituminous (low grade)	Steam

different years and different seasons, respectively. The average mercury concentration for Waterberg coals was 1.63 mg kg^{-1} (Wagner and Tlotleng, 2012),
approximately 5 times higher than the average concentration of mercury found in the Highveld and Witbank coals, and was above the maximum value of 1 mg kg^{-1} indicated by Swaine (1994). The mercury concentration was determined for the Highveld, Witbank, and Waterberg coals, mainly to due to the fact that more than 70% of total coal produced comes from these coalfields. For the estimation of mercury emission from South African coal, an average concentration value of 0.2 mg Hg kg^{-1} was used.

One consequence of the mining and combustion of coal is the mobilization of trace elements, especially mercury, which has environmental and human health significance. Although mercury is present in trace amounts in coal, it can contribute significantly to the mercury load, as large amount of coal are used in the coal-fired power stations for generation of electricity, and also the fact that coal is the primary source of energy in South Africa. With an increase in the demand for electricity, the commissioning of two new coal-fired power stations, and de-mothballing three existing coal-fired power station, inevitably, mercury emissions will increase, unless strict emission control strategies are implemented.

2.3.1.2 Mode of occurrence

The occurrence of mercury in coal is due to natural geological processes, and its concentration in coals is influenced by parameters such as moisture, carbon content, sulphur, ash yield, etc., amongst other parameters (Mukherjee *et al*., 2008; Yudovich and Ketris, 2005). Mercury is a chalcophile element (with great affinity to sulphur-containing components in coal), and a coalphile element (associated with organic and inorganic matter in coal) (Yudovich and Ketris, 2005). Sulphur in coals can be divided into three categories: pyritic sulphur, sulphur in sulphate minerals, and organic sulphur (Alvarez *et al*., 1997). Mercury, generally, is bound to organic sulphur or sulphide (pyritic) mineral matter. These two forms of mercury phases are dominant, and their occurrence control the mercury distribution in coal. It is generally incorporated in pyrite and the proportion varies with mineral paragenesis (Kolkar *et al*., 2006). According to the Yudovich and Ketris (2005a) the mercury-sulphide association dominates in coal, generally. This was indirectly confirmed by the (a) highly positive correlation (R=0.97 and 0.99) between mercury and mineral sulphide content observed for two sets of 10 density fractions, and (b) sequential leaching analysis of 32 USA bituminous coals using oxalic acid, hydrochloric acid, hydrofluoric acid, nitric acid, showed that mercury was associated with sulphide minerals. The mercury–pyrite association accounts for 65–70% of the mercury in some coals. Some mercury could

be associated with the organic sulphur compounds present in coal (Diehl *et al*., 2004). This was shown by a positive correlation between mercury and organic sulphur (Yudovich and Ketris, 2005; Diehl *et al*, 2004; Toole-O'Neil *et al*., 1999). High sulphur coals usually contain higher amounts of mercury, associated with pyrite. In low-sulphur coals, mercury exist in low concentration, and the dominant phases are organic and sulphide minerals. In coal cleaning, substantial amounts of mercury, associated with coarse–grained pyrite, can be removed (Finkelman, 1994). As a result 50% to 60% of the mercury remaining in the cleaned coal product is associated with organic sulphur and inorganic sulphide, and the rest is disseminated in tails, sludges, and middlings.

South African coals are considered to contain low mercury levels and low sulphur content (Wagner and Hlatshwayo, 2005). These coals are associated with pyrite, followed by the organic fraction, and then carbonate (Wagner and Hlatshwayo, 2005). Coals from Vereeniging-Sasolburg coalfields are also associated with the sulphide or carbonate minerals while coals from the Witbank No. 4 seam (South Africa) showed that most of the trace elements determined had a chemical affinity for sulphide minerals, specifically pyrite (Bergh *et al*., 2011).

2.3.1.3 Mercury from power generation

Of the 17 fully operational coal-fired power plants in South Africa, 10 are state-owned (NERSA, 2005), while the remaining seven are either owned by municipalities or private companies. Eight of the operational coal-fired power stations are located in the Mpumalanga Province, a Highveld Priority Area due to the coal related pollutants from Eskom's power stations (Table 2.7) (Scorgie, 2012).

Table 2.7: Mercury emissions from coal-fired power plants of South Africa in 2006 (Masekoameng *et al*., 2010).

Power Plant	Emission Control Device	Emission Reduction Factor	Coal Combusted (M tonnes y^{-1})	Hg in coal (mg kg^{-1})	Hg emissions (Tonnes)
Arnot	FF	0.5	8.06	0.17	**0.69**
Duvha	ESP&FGC	0.5	15.91	0.23	**1.83**
Hendrina	FF	0.5	8.75	0.21	**0.92**
Kendal	ESP&FGC	0.1	20.12	0.44	**7.97**
Kriel	ESP&FGC	0.1	11.72	0.34	**3.59**
Lethabo	ESP&FGC	0.1	22.79	0.36	**7.38**
Majuba	FF	0.5	11.83	0.29	**1.72**
Matimba	CS-ESP	0.1	18.08	0.45	**7.32**
Matla	ESP&FGC	0.1	16.87	0.29	**4.40**
Tutuka	CS-ESP	0.1	11.65	0.29	**3.04**
TOTAL					**38.86**

ESP – Electrostatic precipitators; FF – Fabric filters; FGC – Flue-gas Conditioning.

In 2001, South African's total mercury emission was estimated to be 9.75 Mg, based on mercury concentration in coal of 0.15 mg kg^{-1} (Dabrowski *et al*., 2008). With the introduction of the three mothballed power stations and two new coal-fired power stations planned to be commissioned in 2015 and 2017, mercury emission will inevitably increase, worsening the impact of pollution on the environment and human beings, making Mpumalanga and surrounding areas a mercury emissions potential hotspot.

2.3.1.4 Mercury emissions from coal gasification

South Africa's oil-from-coal industry (SASOL) is second major coal user, in which low-grade coal (ash of about 20 - 30%) is used to produce viable alternative fuels and chemicals. Synthetic fuels are produced by conversion of low-grade coal into petroleum products while gasification of coal via the Fischer-Tropsch process produces synthesis gas, rich in hydrogen and carbon dioxide (van Dyk *et al*., 2006). Sasol plants, (17 and 80 fixed bed dry bottom gasifiers at Sasolburg and Secunda, respectively)

processed in excess of 35 million ton of bituminous coal to produce synthesis gas, which is converted into some 2.5 million ton of liquid fuels, and large quantity and variety of petrochemicals (Leaner *et al*., 2009). 70% of the coal used is gasified, and 30% is used for steam generation (Wagner *et al*., 2008).

The mercury content in the coals ranged from 0.009 to 0.24 mg kg^{-1}, with an average content of 0.15 ppm (Wagner *et al*., 2008). During the gasification of coal, mercury partitions between the crude syngas stream exiting the gasification process and the gasification ash. As much as, 2.5-20% Hg reports to the ash, and small proportion or less in the liquid hydrocarbon co-products fraction (Wagner *et al*., 2008). In the crude syngas, mercury exist as Hg^0 (Bunt and Waanders, 2008), due to its high volatility, and its removal together with other volatile elements (As, Se) is by the gas cleaning process, known as the rectisol process. Mercury is discarded off as per requirements of mercury containing waste during maintenance cleaning. This process contributes more to mercury-containing general waste than to atmospheric mercury emissions. In 2006, 4.2 tonnes Hg was released to the general waste from the coal gasification while 2.0 tonnes were released as atmospheric mercury emission (Masekoameng *et al*., 2010). Mercury emissions are expected to increase mainly due to Sasol's intention to increase the coal gasification process capacity by 2015 (Sasol, 2008). Of the 30% coal utilised for steam and electricity generation, an estimated 80% of the mercury associated with coal is emitted into the atmosphere (Wagner *et al*., 2008). Wagner and Hlatshwayo (2008) concluded that the gasification process is a more efficient coal utilisation process in terms of limited or zero Hg emissions from coal when compared to the combustion process.

2.3.2 Mercury emissions from gold mining

Mercury, naturally, occurs together with gold in the Witwatersrand goldfields and initially, was used to recover gold in the amalgamation process. However, its use has led to mercury pollution in the environment. During the reprocessing of the old tailings

dumps, it was remobilised resulting in its release and eventual re-contamination of the environment.

2.3.2.1 Mode of occurrence

Gold was discovered in 1886, in Langlaagte, central rand in the Witwatersrand goldfields (Frimmel & Minter, 2002). More than 50 000 tons of gold have been produced from seven major goldfields distributed in the Witwatersrand (Robb & Robb 1998) (Figure 2.7).

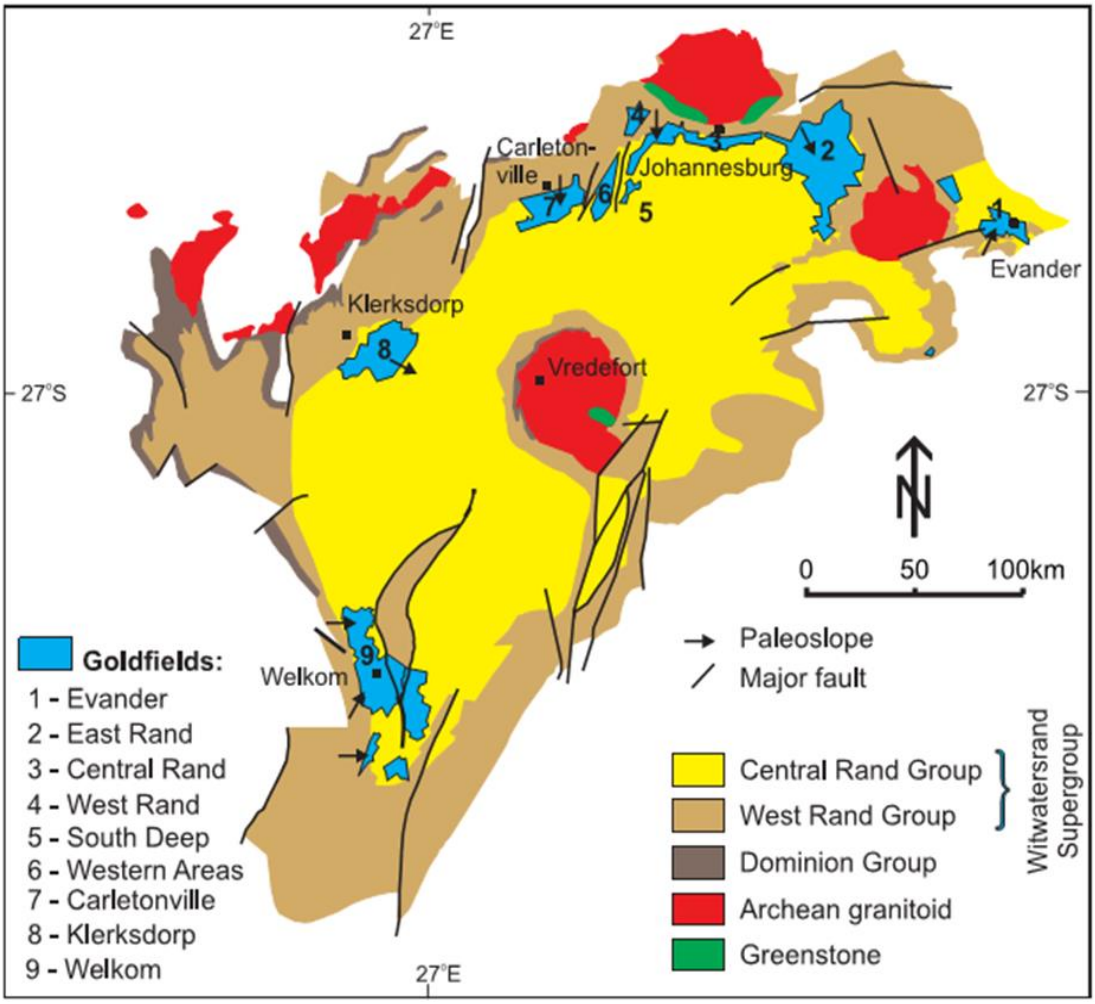

Figure 2.7: Map of the Witwatersrand basin to show major gold fields (Viljoen and Reimold, 1999).

Most of the gold is located within conglomeratic units, known locally as reefs (Hayward *et al*., 2012). In these beds, it's associated with rounded pyrite and uraninite and is embedded in a fine grained, hard quartzitic matrix (Frimmel, 1997; Reid, 1988; Hallbauer & Barton, 1987; Janisch, 1986; Hallbauer & Von Gehlen, 1983). Within the matrix, the gold, pyrite, and uraninite occur together with minerals, such as zircon, rutile, chromite, uraninite, arsenopyrite, cobaltite, and rare platinum-group metals (Feather & Koen, 1975).

Also minor elements such as silver, mercury and smaller amounts of bismuth, selenium, rhenium and osmium are found in the matrix (Kirk *et al*., 2003; 2001). The silicate minerals are the most abundant minerals in the conglomerate and include quartz, muscovite, pyrophyllite, chloritoid, biotite and chlorite (Frimmel & Minter, 2002; Phillips, 1987). Pyrites are the second most abundant minerals, making up 3 – 5% of the Witwatersrand conglomerates (Hallbauer, 1986). These included arsenopyrite, chalcopyrite, cobaltite, gersdorffite, sphalerite, galena and pyrrhotite (England *et al*., 2002; Hallbauer, 1986). Other minerals included in the conglomerate are feldspar, calcite, corundum, spessartine, and bismuthinite (England *et al*., 2002). The mineral composition of the gold-bearing conglomerate mined in the Witwatersrand basin is summarised in Table 2.8. (Forstner, 1976; Janisch, 1986, Hayward, *et al*.; 2005):

Table 2.8: Mineral composition of a typical Witwatersrand gold reef (Feather and Koen, 1975).

Mineral	Abundance
Quartz (SiO_2), primary and secondary	70 – 90%
Muscovite and other phyllosilicates	10 – 30%
Pyrites	3 - 4%
Other sulphides	1 – 2%
Grains of primary minerals	1 – 2%
Uraniferous Kerogen	1%
gold	~45 ppm in the Vaal Reef

According Hayward *et al*., (2012), the Witwatersrand gold grains contain highly variable silver (Ag) and mercury (Hg) contents, varying from 0.8 – 5 wt% for Ag and 0.25 - 3 wt% for mercury, respectively. Frimmel & Gartz, (1997) and Hallbauer & Els, (1986) reported ranges of 70 – 100 wt% for Au, 0 – 30 wt% for Ag and 0.6 – 5.8 wt% for Hg, respectively, of concentrations in gold particles. Von Gehlen (1983) studied the Hg content of gold grains, which range from 0.3% Hg in Barberton to 3% Hg in VCR (Ventersdorp Contact Reef, Western Deep).

2.3.2.2 Informal, artisanal and small-scale gold mining

In addition to the formal mining sector, informal gold mining takes place in those areas of the country where there are old mine workings or tailings dams, for example in the vicinity of Nigel in Gauteng, and Barberton and Sabie in Mpumalanga Province. This informal sector is distinct from the illegal operations in which mine output is stolen from the formal mining sector either at the mines or from the smelters. At present in South Africa, the informal mining operations in abandoned mines and the reworking of tailings is also on the increase. Most of these operations include sand and clay mining, as well as diamond and gold mining. Zama-Zama are considered to be illegal under the state and customary law. They fall outside the existing legislative framework as legitimate stakeholders and work outside of customary structures as well (Nhlengetwa, 2014).

According to the CSIR, it was estimated that in 1998 there were at least 1 250 informal gold miners active in South Africa. Since then, no other figures have been collated. Collectively, these miners are thought to produce less than 1 ton of gold annually, much of which is believed to be traded mainly with their suppliers of mercury based in Swaziland and Mozambique. According to Mutemeri and Petersen (2002), 20 000 is the number of artisanal to small-scale miners active in South Africa. Their crude and inefficient methods, to concentrate gold, employ Hg for the final extraction and are practiced on open pit to primitive underground excavations, old mine workings and mine dumps.

In terms of artisanal gold mining, Veiga *et al*. (2005) reported that as much as 50% of Hg vapours produced during artisanal gold mining practices are emitted into the air. These are subsequently deposited via wet and dry deposition onto land and into aquatic ecosystems. Furthermore, mercury wastes from artisanal gold mining can remain in the soil and sediment for several years (Ramirez *et al*., 2003) with long-term deposition and bioaccumulation of mercury-contaminated soil and sediment posing an environmental threat. The impacts of artisanal gold mining activities in the Inkomati WMA could be sustained in the cycling and mobilization of mercury-contaminated sediments in the water column. Therefore, this lack of information or limited available information on the actual mercury measurements and/or mercury concentration levels in the gold mining environment in South Africa signals the need to evaluate the major mercury sources in the gold mining sector and its impacts environmentally and effects on human beings.

2.3.2.3 Mineralogical composition of gold ores

Schroder *et al*. (1982) measured Hg emissions from gold extraction and refining processes and estimated total Hg emissions to be 193 kg yr^{-1} based on a total annual gold production of 706 tonnes. This Hg originates as trace level contaminant of the gold ore that is released to the atmosphere during gold processing and refining. This is the only South African study where an emission estimate is based on measured data. According Hayward *et al*., (2012), the Witwatersrand gold grains contain highly variable Ag and Hg contents, varying from 0.8 wt. % Ag and 0.25 wt. % to 5 wt. % for Ag and 3 wt. % for Hg within West Wits goldfields. Von Gehlen studied the Hg content of gold grains, which range from 0.3% Hg in Barberton to 3% Hg in VCR (Western Deep) (van Gehlen, 1983). Amalgamation of gold concentrates are still effectively employed on a manual basis, despite possible objections, since the procedure offers little scope for mechanisation. Consumption of mercury fluctuates between 10 and 40 mg per ton of milled rock whilst mercury losses during retorting normally do not exceed 0.02 g per ton milled. Approximately 43% of the total South African gold output is still attained by amalgamation (Forstner *et al*., 1976).

2.3.3 Mercury emissions from mine waste

Mining operations pose the greatest threat to human health and the environment due to the fact that they generate large quantities of wastes, and contain potentially toxic contaminants (Csavina *et al*., 2011; Brotons *et al*., 2010; Neuman *et al*., 2009; Petavratzi *et al*., 2005). Mineral dust and aerosol, generated from mining operations and tailings storage facilities (anthropogenic origin), are associated with higher levels of chemical contaminants (Vega *et al*., 2001), while mineral dust of natural origin is associated with lower levels of chemical contaminants (Reheis *et al*., 2009). Artisanal gold mining, smelting and processing, industrial mining and uranium mining were identified as four of the world's top ten pollution problems (Ericson *et al*., 2008). As, Cd, Cr, Hg, Mn, Ni, Pb, and V are associated with ultrafine particulates and have been suspected of causing sinusitis, asthma, and chronic bronchitis, pneumonia, lung haemorrhage, lung cancer and brain haemorrhage (Choi *et al*., 2009). Particle size of particulate matter plays a major role in the distribution of dust, and determines the depth of penetration and deposition in the respiratory system, where trace metal absorption efficiency ranges from 60-80% resulting in impairing the physiological function of the lung based on bioavailability of toxic metals (Espinosa *et al*., 2001; Infante and Acosta, 1991). Based on their potential to cause adverse health effects, particles are defined into 3 categories, namely: (1) ultrafine particles, <0.1 µm, (2) fine particles, <1 µm, and coarse particles, >1µm (as shown in Figure. 2.8 and 2.9) (Kampa *et al*., 2008).). They are also categorised as: (1) respirable fraction, <2.5 µm ($PM_{2.5}$), (2) inhalable fraction, <10 µm (PM_{10}) (Charlesworth *et al*., 2011), while according to European Committee for Standardization and British Standard Institute (1993) classification, particulate matter is classified as inhalable (<100 µm); thoracic (10 - 25 µm) and respirable particulates (0 - 10 µm).

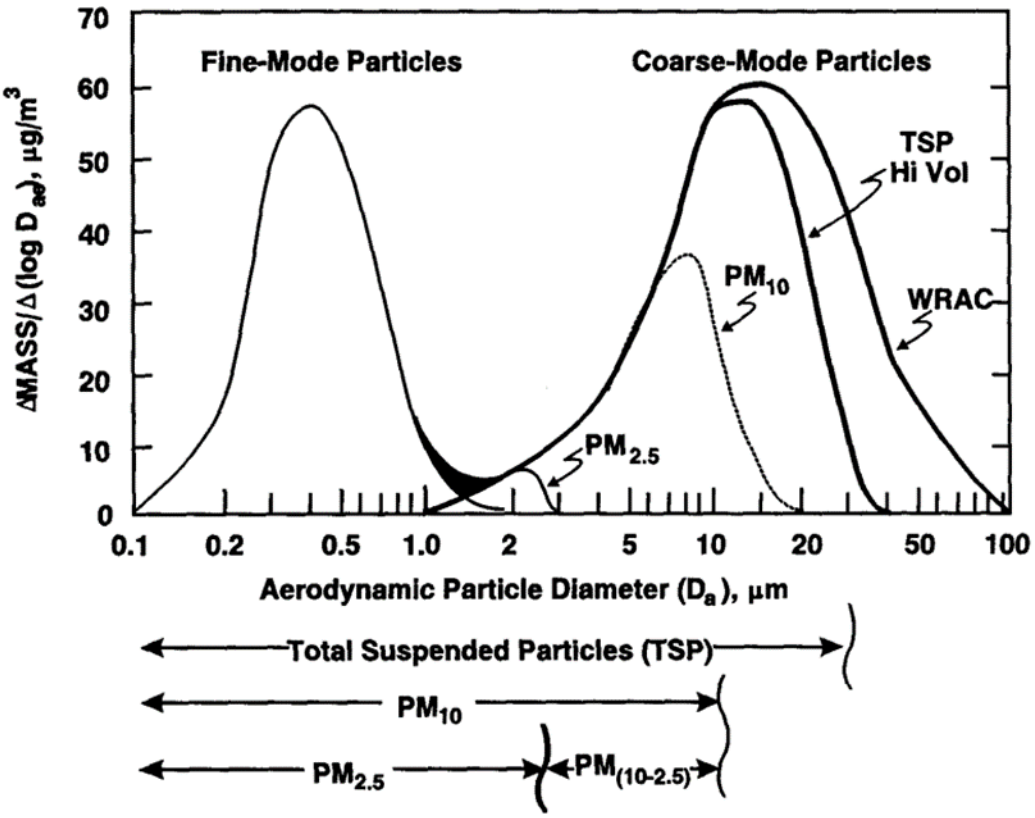

Figure 2.8: Schematic representation of the size distribution of particulate matter in ambient air (USEPA, 1996).

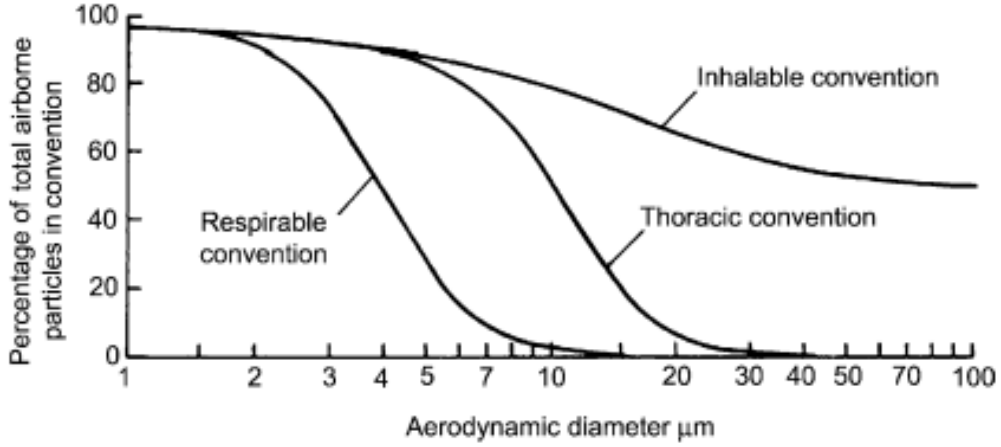

Figure 2.9: The inhalable, thoracic and respirable convention as percentage of total airborne particles (European Committee for Standardization and British Standard Institute, 1993).

Gold mining activities in the Witwatersrand basin has generated six billion tonnes of mine waste since the beginning of mining in 1886 (GDARD, 2011; Sutton and Weiersbye, 2007; Robb and Robb, 1998). This has led to the development of approximately 270 tailings storage facilities (TSFs), covering an area of about 180km^2 (Rösner *et al*., 2001). According to Sutton (2008), 88% of the mine residues deposits (MRD) are found within 1000 m of formal residential areas, with 71% within 500 m. In some cases, informal settlements and industries (Selby) have been built on tailings footprints, TSFs have been used as playgrounds (Sutton, 2008), and this has led to the population being exposed to the dust heavily laden with toxic metals and metalloids. The immediate environment surrounding the TSFs is susceptible to pollution emanating from these sources. Heavy metals (As, Cr, Co, Cu, Cd, Fe, Hg, Mn, Ni, Pb, Zn), metalloids, alkali earth elements, and radionuclides have been found in the TSFs environment (Da Pelo *et al*., 2009; Wade and Coetzee, 2008; Aucamp and Van Schalkwyk, 2003). Tutu (2005) determined the total metal concentration of tailings in the Witwatersrand to be in the range from 2.00 - 17 340 mg kg^{-1} with toxic metals contributing as follows: As (9 - 30 mg kg^{-1}), Co (0.3 - 18 mg kg^{-1}), Cr (79 - 254 mg kg^{-1}), Cu (16 - 34 mg kg^{-1}), Fe (11200 - 18980 mg kg^{-1}), Mn (49 - 106 mg kg^{-1}), Ni (0.5 - 20 mg kg^{-1}), Pb (19 - 49 mg kg^{-1}), and Zn (6 - 47 mg kg^{-1}).

Majority of the TSFs in the central rand lie in close proximity to the river systems, wetlands, and dams (Mphephu, 2001). Both tailings and mobilised metals are transported by streams into the dams. The dams thus act as sinks for sediments. In a study conducted by Ndasi (2007), he determined the concentration of mercury in the Russel stream sediments. It ranged from 100 to 13 700 µg kg^{-1}. The highest concentration of mercury was found in the clay type sediments (5 500 – 13 700 µg kg^{-1}). Most of the sediments came from the Crown mine tailings dumps placed a few kilometers upstream. During rainfall, water run-off erodes the tailings dams together with efflorescence formed which are transported into nearby streams and rivers (Rösner

and van Schalkwyk, 2000; Rösner *et al*., 2001). Clay minerals are more easily washed away by water.

Dust from tailings dams is a major contributor to poor quality ambient air in the Witwatersrand, especially from abandoned mine tailings (Annegarn, 2011; Annegarn *et al*., 1990). Dust pollution peaks are experienced during the months of late July to early October, where wind speeds in excess of 7 m s^{-1} are experienced (Ojelede *et al*., 2012). Cumulative dust concentration in excess of 5000 mg m^{-2} day^{-1} have been reported for tailings that have not been rehabilitated (Scorgie, 2006; Annegarn and Sithole, 2002). Due to the increase in the incidences of wind erosion from tailings dams, the Department of Environmental Affairs developed a draft set of regulations for dustfall (Table 2.9). During the months of August to October (2007), two sites from the Durban Roodepoort Deep (DRD) tailings dams recorded dust fall above the ALERT level of 2 400 mg m^{-2} day^{-1} and several more sites exceeded the ACTION level of 1 200 mg m^{-2} day^{-1} (Annegarn, 2007). During this period, wind speeds ranging between 6-8 m s^{-1} were experienced. This highlights the levels of air pollution coming from the tailings dams, and the dispersion and distribution of toxic metals and metalloids contained within the dust over great distances.

Table 2.9: South African national dust fall out standard (Department of Environmental Affairs (2012).

Restriction Areas	**Dustfall rate, *D* (mg m^{-2} day^{-1}, 30-day average)**	**Permitted frequency of exceeding dust fall rate**
Residential areas	$D < 600$	Two within a year, not sequential months
Non-residential areas	$600 < D > 1\,200$	Two within a year, not sequential months

The occurrence of quartz in the dust from Witwatersrand gold mine tailings storage facilities has been studied (Annegarn *et al*., 1988, 1990; Belle, 2005). Studies have

proved the link between quartz (crystalline silica) and the occurrence of silicosis (Hnizdo *et al*., 1995, 1994, 1993).

During one of these periodical dust storms, it was observed that particulate matter (PM_{10}) concentration reached a daily maximum of 2160 µg m^{-3}, giving a weekly average of 508 µg m^{-3} for the 7 day sampling period (Ojelede *et al*., 2012). When compared to the Department of Environmental Affairs (DEA), daily ambient concentration of PM_{10} limit of 120 µg m^{-3}, it was considered to be very high, and the effects experienced during these storms included soiling, reduced visibility, irritation of the eyes, and ingestion of particulate matter (Bullock, 2006). This may lead to adverse health effects because $PM_{2.5}$ is a respirable fraction of particulate matter, which is easily deposited in the alveoli of the lungs, and it's usually associated with toxic heavy metals (Hg, As, Pb, etc), which can be dissolved in the lung fluids resulting in the distribution to the whole body. PM_{100} particles are retained in the nasal cavities, while $PM_{0.1}$ can penetrate deep into the respiratory system, alveoli, where they can be retained and absorbed (as expressed in Table 2.10).

Table 2.10: Effects of particle size of dust in lungs

Dust Penetration (µm)	Effects
10-100	Retained in the nasal cavities.
5-10	Penetrates trachea, bronchial tubes, bronchioles or can be spat out or swallowed in the oesophagus. If the dust is too high, then dust particles may reach the alveoli of the lungs.
0.5	Very thin dust forms a deposit in the alveoli of the lungs. Under 0.5 µm, the dust particles behave like gas inside the body and align with the breathing cells.

One of the major problems in Gauteng is the increasing development of settlements (both formal and informal) beyond the buffer zones (mine reserves), and adjacent to the tailings (Annegarn, 2006; Aucamp and van Schalkwyk, 2003). This has led to a

large growing population living within and around the tailings dams. It was made worse with the sprouting of squatter camps around the tailings dams' area and in some cases, appearing on tailings footprints. This situation created a socioeconomic problem for the government because of the potential adverse health problems associated with mineral dust (air pollution) from the tailings dams. Unfortunately, this problem has escalated out of control due to failure by government to implement and enforce existing legislation (maintaining buffer zones within the vicinity of the tailings dams, adherence to particulate matter emissions limits, complying with disposal limits, rehabilitation of tailings dams, etc. (Table 2.11).

Table 2.11: Comparison of air quality standards between South Africa, United States and WHO.

Pollutant	**Average Time**	**WHO[a] (µg m^{-3})**	**USA EPA[b] (µg m^{-3})**	**SA NAQS[c] (µg m^{-3})**
$PM_{2.5}$	Annual	10	12	**25**
	24 hr	25	35	**65**
PM_{10}	Annual	20	50	**60**
	24 hr	50	150	**180**

[a] *World Health Organisation (2005)*
[b] *U. S. Environmental Protection Agency (2011)*
[c] *Department of Environmental Affairs (2009)*

Ojelede *et al*., (2012), observed that both older and recent tailings dams are enriched in the respirable and thoracic fractions (PM_5 and PM_{10}) of the particulate matter, with slime tailings dams contributing greatly to the ambient particulate load than sand dumps. These tailings are responsible for the release of particulate matter (mineral or aeolian dust) laced with toxic pollutant metals during the dust storm periods of the year, due to wind erosion of the tailings, and reprocessing of old mine tailings for their residual gold content (Blight, 2007; Annegarn, 2006; Naicker *et al*., 2003). This process has resulted in the deterioration of ambient air quality, and fine dust particles being dispersed into the atmosphere, and transported over large distances. Of interest, is the fact that erosion occurs both in dry season (winter) and wet season (summer)

indicating that wind erosion is an important component of total annual erosion (Blight, 2007).

In a study conducted by Kaonga and Ebenso (2012), it showed that more particulate matter emission was recorded in Kanana (a township in a gold mining area in Klerksdorp) than for Phokeng (a township in a platinum mining area in Rustenburg). This implies that the gold mining area appears to be emitting more particulate matter into the atmosphere than platinum mining. This may be attributed to the improved processing techniques allowing for finer milling and efficient extraction of residual gold content resulting in finer grain sizes in the tailings. However, this phenomenon could not be concluded from this once off comparison. There could probably be many more activities in Kanana that generate more atmospheric aerosols than in Phokeng. Certainly detailed source point measurements could help determine the causes of the difference in atmospheric aerosols in these two areas. Further studies are on-going.

2.3.4 Mercury from point sources (industries)

Outside the two major mercury sources, coal combustion and gold mining, cement production, ferrous metals production, and waste incineration are equally important sources of mercury (UNEP, 2002).

2.3.4.1 Cement production

Sources of mercury in the cement production are mainly derived from the raw materials. Major sources are coal for firing cement kilns, fly-ashes, and gypsum from combustion of coal while minor sources are limestone and oil (based on the quantity used). Fly-ash and gypsum may significantly increase the total input of mercury to cement production, depending on materials. Mercury exist naturally and in trace levels in these raw materials, therefore an increase in production means increase in the mercury emissions. During cement production, mercury is released through emission into the atmosphere, to a lesser extent to the soil, through wastes and residues, and in the cement product.

The industry contributes about 10% emission to the total anthropogenic mercury emissions, globally (UNEP, 2013). In South Africa, estimated mercury emissions from cement production units was 3.9 tonnes and 0.4 tonnes to air and waste, respectively (Masekoameng *et al*., 2010), in 2006. A similar value of approximately 3.77 Mg in 2005, was obtained by Leaner *et al*. (2009). Emissions are expected to increase as the cement industry has proposed to implement the use of alternative sources of fuel, particularly hazardous waste materials such as tyres, sewage sludge, etc. These materials may contain various levels of mercury and produce toxic gaseous emissions. Unfortunately, in South Africa, this industry is not regulated for sulphur, nitrous compounds or any cancer causing chemicals such as volatile organic compounds or persistent organic pollutants such as dioxins and furans or heavy metals such as mercury. The industry is only regulated for dust or particulates. Due to lack of legislation, the communities surrounding these plants, and the environment at large are susceptible to pollution coming from cement plants. Projected government infrastructure development, construction of coal-fired power stations and private sector developments will increase the demand for cement, which will most likely result in an increase in mercury emissions.

2.3.4.2 Ferrous metal production-iron and steel

Coal is used as a source of fuel and for the production coke that used in the smelting of iron ore. The major source of mercury emissions is from the production of coke (Pacyna *et al*., 2006). Mercury emissions was estimated to be 2.7 tonnes yr^{-1} (Masekoameng *et al*., 2010). Coke production is responsible for about one-third of the mercury emitted while the two-thirds came from scrap metal smelting. A further 0.29 Mg Hg was estimated to be released from pig iron and steel processing.

In relation to the global mercury emission levels from the ferrous metal production, there was decrease in the emission levels from 200 tons in 2005 to 45.5 tons in 2010 (Table 2.2). This was attributed to the global recession, however, due to the rapid

industrial growth experienced largely by China, demand increased for the iron products and hence mercury emission increased as well. Currently mercury emissions are expected to increase as South Africa produces to fulfil its export quarter of iron ore and its products to the east, as well as fulfil the local market.

2.3.4.3 Non-ferrous metal production – primary products

Mercury emissions from the primary metal ores (especially copper, lead and zinc smelting) is depended on the various technology used to process the ores, the mercury content in the ores, and the type of control devices used during processing. This industry was responsible for an estimated average of 0.32 Mg Hg yr^{-1} in 2004 (Leaner *et al*., 2009).

2.3.4.4 Consumer products, waste deposition (landfills) and incineration

Various mercury-containing products (batteries, lamps, and electric switches) are either discarded as general waste in landfills or incinerated. In South Africa, mercury-containing fluorescent tubes are discarded together with general waste in the landfills. According literature, landfills release gas containing various amounts of heavy metals, including Hg (Nguyen *et al*., 2007; de la Rosa *et al*., 2006; Lindberg *et al*., 2005). However, in South Africa mercury levels in landfill gas have not yet been determined. An estimate of 0.46 kg Hg (0.0005 Mg Hg) was released from a total of 1 829 066 fluorescent tubes imported in 2004, with an estimated average Hg concentration of 10 mg per item (Leaner *et al*., 2009). This a conservative estimate and Hg emissions are expected to increase due to a drive towards using energy efficient fluorescent tubes (Kumar *et al*., 2003; ESKOM, 2002).

Medical waste in South Africa is expected to be separated before disposal or incineration. Although the preference is to have the potentially hazardous medical waste incinerated instead of land filled. In 2004, an estimate of 0.60 Mg Hg was released to the environment. Poorly maintained, malfunctioning and lack of working

incinerators, both in public and private sectors, coupled with illegal dumping of medical waste, are likely to increase Hg emissions to the environment.

2.4 Human health risk associated with mercury

2.4.1 Toxicology of mercury

Generally, human beings are exposed to mercury in a chronic, low dosage ways for long periods of time, and in high dosage ways for short periods of time. Inhalation of mercury vapour, ingestion of MeHg from fish, and dermal absorption of mercury from application of cosmetics are the most important routes of human exposure to mercury (WHO, 1991 & 1990). There are concerns about the health effects of mercury and the proportion of anthropogenic mercury in the environment. Table 2.12, summaries the natural and anthropogenic inputs into the environment.

Table 2.12: Summary of toxicity for three important mercury species (NRC, 2000).

MeHg	Hg(0)	Hg(II)
Exposure		
Fish, marine mammals, crustaceans, animals and poultry fed fish meal.	Dental amalgams, fossil fuels, occupational exposure, incinerators	Oxidation of elemental mercury or demethylation of MeHg; deliberate or accidental poisoning with $HgCl_2$
Absorption		
Inhalation: Vapours of MeHg absorbed	Inhalation: ≈80% of inhaled vapour Hg^0 dose readily absorbed in lungs	Inhalation: Aerosols of $HgCl_2$ absorbed
Oral: Approximately 95% of MeHg in fish readily absorbed from GI tract	Oral: GI absorption of metallic Hg is poor; any released vapour in GI tract converted to mercuric sulphide and excreted	Oral: 7-15% of ingested dose $HgCl_2$ absorbed from the GI tract; absorption proportional to water solubility of mercuric salt; uptake by neonates greater than adults
Dermal: in guinea pigs, 3-5% of applied dose absorbed in 5 hr	Dermal: Absorption of Hg^0 vapour through human skin is very low relative to inhalation absorption	Dermal: In guinea pigs, 2-3% of applied dose of $HgCl_2$ absorbed
Distribution		
Distributed throughout body since lipophilic; ≈1-10% of absorbed oral dose of MeHg distributed to blood; 90% of blood MeHg in red blood cells; readily crosses blood-brain and placental barriers	Rapidly distributed throughout the body since it is lipophilic. Readily crosses blood-brain and placental barriers	Highest accumulation I kidney; fraction of dose retained in kidney is dose dependent. Does not readily penetrate blood-brain or placental barriers
Metabolism		
Slowly demethylated to Hg^{2+}	Hg(0) is oxidized in tissue and blood to Hg^{2+}	Hg^{2+} not methylated in tissue, but process may proceed in GI tract mediated by gut microorganisms
Excretion		
About 1% of burden released, mostly via bile and feces	Excreted as Hg^0 in exhaled air, sweat, and saliva, and as mercuric Hg	Excreted in urine and feces; also excreted in saliva, bile, sweat, exhaled air, and breast milk

2.4.1.1 Elemental mercury

Hg^0 is the main form of mercury released into the air by both natural and anthropogenic processes. Inhalation is the major exposure route with 80% of inhaled Hg^0 retained (Clarkson, 2002) while ingested Hg^0 is poorly absorbed with a bioavailability of less than 0.01%, and limited dermal absorption of Hg^0 takes place (Park and Zheng, 2012). Hg^0 accumulates in red blood cells, distributed to all tissues, and easily penetrates biological membranes, including the blood–brain barrier and the placental barrier. Its ability to cross the placental barrier results in the exposure to developing foetus in pregnant woman's body. Infants may also be exposed to mercury from a nursing mother's milk. Hg^0 is oxidised to the Hg^{2+} in the red blood cells and tissues in a few minutes. However, even though it is rapidly oxidised to Hg^{2+}, it remains in the vapour form in the blood for a short time, long enough to penetrate blood-brain barrier before oxidation takes place. Hg^{2+} accumulates in the brain because Hg^{2+} will not effectively cross the blood–brain barrier (Park and Zheng, 2012). The blood plasma mercury decreases in two processes: short half-time of less than a day and a longer one of about 10 days, therefore blood mercury levels reflect recent exposure (Clarkson *et al*., 2002).

Hg^0 accumulates in the central nervous system while mercury molecules accumulate in the brain (Friberg and Mottet, 1989) and with increased time of exposure it's eventually found in the kidneys (Park and Zheng, 2012). Hg^0 can also be absorbed through the mucosa and connective tissue of the nasal cavity and transported to the brain via the nerve cells. Mercury from the dental amalgam reaches the brain through the same way pathway (i.e., nerve cells, olfactory pathway) (Henriksson and Tjälve, 1998). After exposure to Hg^0, it diffuses into the blood and distributed into all organs of the body. The main route of excretion is via the urine and feces. Urine represents the cumulative dose from the kidney, hence it's used a biological marker. The biological half-life of Hg is estimated to be approximately 30 to 60 days in the body (Dart RC, 2004). The half-life of mercury in the brain is not entirely clear, but is estimated to be approximately 20 years. Hg^0 is bound strongly to selenium or SH-groups after

oxidation in the brain, which may contribute to the accumulation in the brain for a long time (Friberg and Mottet, 1989).

Toxicity

Following exposure to inhalation of Hg^0, ingestion or dermal application of inorganic mercury-containing medicinal products, neurological and behavioural disorders in humans have been observed. Neurotoxic symptoms such as tremors, emotional liability, insomnia, memory loss, neuromuscular changes, headaches, polyneuropathy, and performance deficits in tests of cognitive and motor function have been associated with exposure to Hg^0. In children exposed to excessive levels of Hg^0 and/or Hg^{2+} leads to acrodynia and photophobia effects. Exposure to mercury results in variable effects being experienced.

Acute exposure to high levels of Hg^0 can lead to central nervous system damage, evidenced by the following symptoms such as tremors, paraesthesia, memory loss, hyperexcitability, erethism, and delayed reflex, which are commonly reversible (Liu *et al*., 2008), resulting in severe lung damage, and even death due to hypoxia (Park and Zheng, 2012). It occurs in three phases: initial, intermediate, and final phases. The initial phase presents flulike symptoms lasting 1-3 days, followed by the severe pulmonary toxicity, the intermediate phase, and finally gingivostomatitis, tremor, and erethism (memory loss, emotional lability, depression, insomnia, and shyness).

With chronic exposure to Hg^0, the central nervous system and kidneys are the targeted organs, and the clinical symptoms experienced were triad of tremors, psychological disturbances or erethism, and gingivitis (Clarkson and Magos, 2006; Research Triangle Institute, 1999). Tubular damage in the kidney results in proteinuria, and in severe cases, nephrotic syndrome can occur. Also abnormalities in sensory and peripheral nerve conduction occurs (Research Triangle Institute, 1999). The human immune system can be affected, resulting in a decreased resistance to infection, cancers, or immune dysregulation that can induce the development of allergy or autoimmunity

(Moszczyński, 1999). The principal mechanism of mercury toxicity is the non-specific inhibition of enzyme systems and cellular damage due to mercuric ions having a high affinity to the sulfhydryl groups of proteins in the cells and oxidative stress and autoimmune response (Clarkson and Magos, 2006; Choi *et al*., 1999).

A case study was done on the potential effect of mercury in dental amalgam fillings. The amalgam contains about 50% metallic mercury, and is either released as mercury vapour or Hg^{2+}. Approximately 2 - 5 µg d^{-1}, which is 25 – 50% of the total mercury from dental amalgam fillings is absorbed daily by an adult (Spencer, 2000). In the oral cavity, Hg^0 is absorbed through the respiratory system while Hg^{2+} are assimilated in the gastrointestinal tract. Both Hg^0 and/or Hg^{2+} are distributed by the blood to most of the organs in the body. The major source of Hg^0 in the general population has been attributed to the dental amalgam fillings. This has been confirmed by evidence from several studies, where mercury levels in the urine and blood were associated with dental amalgam fillings exposure (Ahlqwist *et al*., 1999; Kingman *et al*., 1998; Kostyniak, 1998). This was confirmed by the positive correlation between dental amalgam filling and urine mercury level in elementary school children (Jung *et al*., 2012). Once the amalgam fillings were removed, the amalgam-related symptoms (Melchart *et al*., 1998), and reduction of the mercury levels in blood and urine was observed (Sandborgh-Englund *et al*., 1998). However, there is an on-going debate about the severe adverse health effects caused by mercury absorbed from dental amalgam fillings. In spite of all this, World Health Organization expert group accepted dental amalgam as a principal source of Hg^0 in the general population (World Health Organization, 1991).

2.4.1.2 Inorganic mercury

Inorganic mercury compounds are non-volatile, water-soluble, and exposure is rarely through inhalation. Instead, it is generally absorbed through the gastrointestinal tract, with a bioavailability of 7 – 15% after ingestion, found to concentrate in the kidneys, and produce kidney damage, which is a major target organ of inorganic mercury (Liu

et al., 2008; Park and Zheng, 2012). Chan (2011) suggested that Hg^{2+} may be absorbed through the skin by the transport of Hg across the epidermis and via the sweat glands, sebaceous glands, and hair follicles. Hg^{2+} is insoluble in lipids and has a biological half-life of 60 days (Dart and Sulliva, 2004), and is therefore, excreted through the urine faeces.

Toxicity

High acute exposure to mercury salts occurs through oral exposure and approximately 1 to 4 g of $HgCl_2$ is fatal in adults (Von Burg, 1995). This results in the corrosive damage to the gastrointestinal tract, leading to the development of mercurial stomatitis and impaired kidney function. Mercury salts are generally irritants on the skin that cause dermatitis, discoloration of the nails and corrosion of oral mucous membranes, and may cause corrosive burns. Because of their generally solid and non-volatile state at room temperature, it's rare to be exposed to mercury salts through inhalation (Research Triangle Institute, 1999; Von Burg, 1995; World Health Organization, 1991).

Chronic exposure, from inorganic mercury leads to kidney damage, mainly in the proximal convoluted tubules (Park and Zheng, 2012), and the observed clinical symptoms are polyuria and proteinuria (Clarkson and Magos, 2006; World Health Organization, 1991). In children, inorganic mercury poisoning occurs in children who use teething powders containing mercury compounds. Symptoms include profuse sweating and erythematous rash of the palms and soles, anorexia, fatigue, irritability, apathy, photophobia and polydipsia (Park and Zheng, 2012). Hg^{2+} is responsible for the toxicity effects in the brain due to its strong affinity for selenium and selenoproteins. The long-term retention of Hg^{2+} in the brain as HgSe, results in the accumulation of mercury in the brain tissue for years, inducing or promoting neurodegenerative diseases (Clarkson, 2007; Friberg and Mottet, 1989).

Special attention has been paid to the skin enlightening creams and cosmetic products. Skin enlightening creams, cosmetic soaps, and ointments are being used, mainly in Africa, Asia, Europe and North America (United Nations Environment Programme, 2008). However, these products contain mercury and mercury salts such as ammoniated mercury, mercury iodide, mercurous chloride, mercurous oxide, and mercuric chloride. Hg^{2+} is absorbed through the skin by the transport of mercury across the epidermis and also via sweat glands, sebaceous glands, and hair follicles (Chan, 2011). Mercury salts inhibit melanin formation by competing with copper in tyrosinase (Engler, 2005), resulting in skin lightening. The use of skin lightening products containing mercury have led to mercury poisoning. In China, a 34-year-old woman developed nephritic syndrome after using a skin lightening cream, and her blood and urine mercury concentrations returned to normal after chelation therapy with D-penicillamine (Tang *et al*., 2006). In Mexico, the following symptoms developed on a 30-year-old woman after using a cosmetic cream for a 5 years; malar rash, erythema on the palms and soles, hypersalivation, intention tremor, emotional liability, weakness, and insomnia (Tlacuilo-Parra *et al*., 2001).

2.4.1.3 Methylmercury (MeHg)

Mercury released into the environment both as Hg^0 vapour from burning processes and as Hg^{2+} in aqueous phase contaminates water, sediments, and soil. It was observed that active transformation of Hg^{2+} to MeHg species takes place in water, sediments and soils. Methylmercury then bioaccumulates in the plankton, molluscs, and finally in the muscle tissues of fish predators and other fish eating marine mammals, leading to methylmercury poisoning of fish eating communities. Approximately 95% of MeHg in fish ingested by human was found to be absorbed from the gastrointestinal tract into the blood stream, and distributed to all tissues readily crossing most biological membranes (blood-brain and placenta barriers) with ease (Figure 2.10).

MeHg is able to achieve high mobility in the body, mainly due to the formation of small molecular weight thiol complexes, which are readily transported across cell

membranes. MeHg attaches itself to the sulphur atoms of thiol ligands in the amino acid cysteine forming a complex whose structure mimics that of the large neutral amino acid, methionine. This results in the methylmercury-cysteine complex acting as a neutral amino acid and enters cells on the amino acid carriers.

MeHg accumulates in the scalp hair. This is achieved through the accumulation of the methylmercury-cysteine complex together with other normal amino acids into the hair follicles. The synthesis of keratin proteins incorporates the methylmercury-cysteine complex, and it also contains a high content of cysteine residues providing a storage for the transported methylmercury (Yu *et al*., 1993).

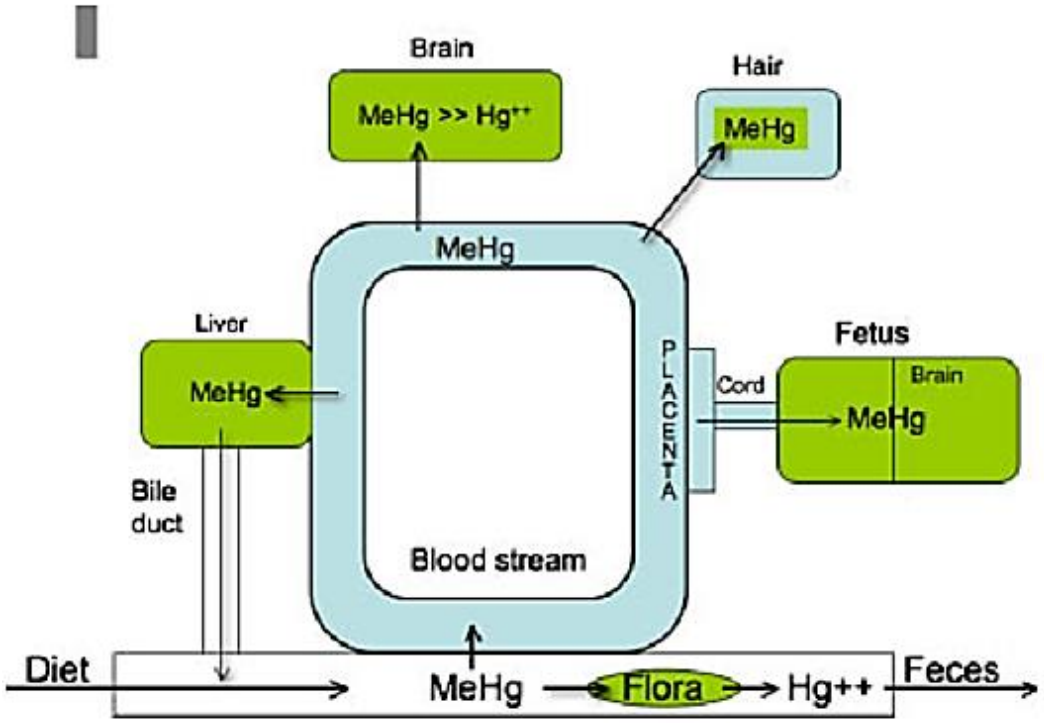

Figure 2.10: Schematic diagram showing the deposition and metabolism of methylmercury in a pregnant woman.

MeHg is largely found in the hair, the brain and in the red blood cells. In the hair, the hair to plasma ratio is about 2500 to 1, brain to plasma ration is about 50 to 1 and the red blood cells to plasma ration about 20 to 1 (Figure 2.11) (Clarkson *et al*., 2007). Some ingested MeHg is converted into Hg^{2+} in the gastrointestinal tract by microflora. However, Hg^{2+} formed, is poorly absorbed, therefore the major portion is eliminated through the fecal route (Clarkson, 2002). Hg^{2+} slowly accumulates and is found in the central nervous system. Clarkson (1990) states the World Health Organization tolerance limit to be 430 ng Hg/kg/d based on average body weights of different age groups or 50 µg L^{-1}, the minimum concentration before developing symptoms of Hg poisoning (Drake *et al*., 2001) and the reference dose of MeHg is 0.23 µg Hg per kg bodyweight per day. Consumption of fish with higher concentration levels above the daily intake limit will result in accumulation of MeHg hence severe chronic effects of mercury.

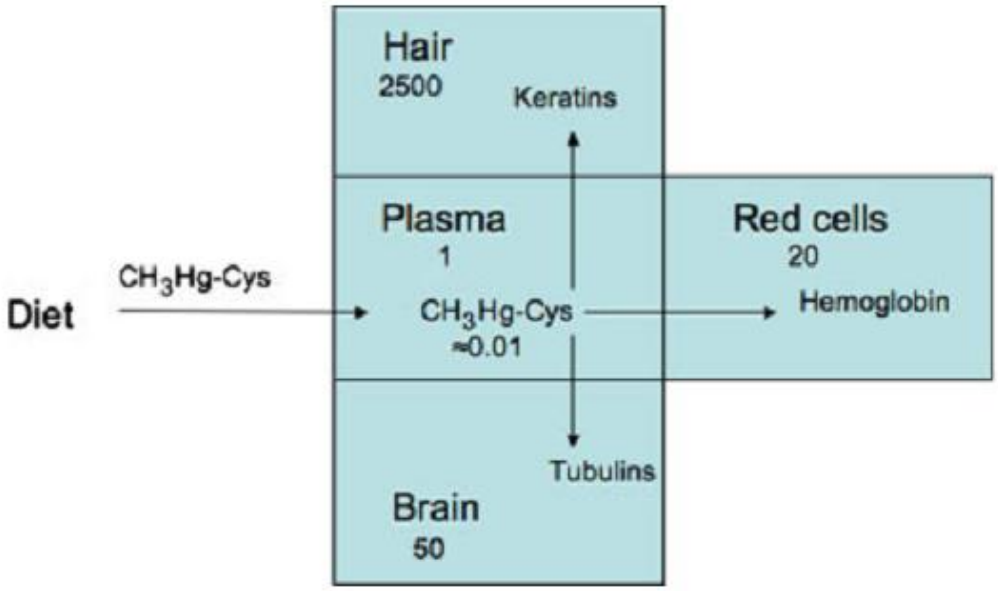

Figure 2.11: The speciation and transport of mercury from blood to hair and brain. The relative concentrations of methylmercury in each compartment have been standardized to the plasma level of unity.

Extremely high levels of mercury in urine, blood, and hair in the order of 175 µg L^{-1}, 39 µg L^{-1}, and 17 µg g^{-1}, respectively were observed in amalgam smelters in Talawaan, Indonesia (Bose-O'Reilly *et al.,* 2010). These workers are highly exposed to mercury contamination in the artisanal mining of gold. However, the mercury levels in blood, total mercury in hair, and organic mercury in hair came from the consumption of fish contaminated by MeHg (Bose O'Reilly *et al.,* 2010).

Toxicity

Major toxic effects of MeHg are on the central nervous system. In adults, MeHg poisoning is characterised by latent period between exposure and onset of symptoms. Paresthesia (a numbness or a pins and needles sensation) develops due to lowest dose. This is followed by ataxia, dysarthria, constriction of the visual fields, and loss of hearing. The presence of Hg^{2+} in the brain is responsible for brain damage. High prenatal exposure of MeHg to expectant mothers resulted in offspring with severe brain damage.

For short-term, high-level acute exposure to Hg^0 and Hg^{2+}, determination of blood mercury concentration is very useful. However, blood mercury does not correspond to the total body burden of mercury in the longer-term exposures because the level decrease within days of exposure (Risher, 2003).

For long-term, chronic exposure, urinary mercury is the best biomarker, and a good indicator of body burden for exposure to both Hg^0 and Hg^{2+}. This is due to the accumulation of mercury in the kidney tissues, which serves as the deposition site during chronic exposure (Clarkson and Magos, 2006). Also, hair mercury is very useful for assessing chronic exposure (Hursh *et al.,* 1985). Urinary mercury concentrations in an asymptomatic population would be <10 µg L^{-1} (ATSDR, 1999), and for blood mercury level in persons who do not eat fish is an estimated mean value of 2 µg L^{-1} considered to be background blood mercury level (Nordberg *et al*., 1992).

2.4.2 Mercury bioaccessibility

The terms ‘bioaccessibility’ and ‘bioavailability’ are commonly used in the field of human health and environmental risk assessment. Bioaccessibility defines a state in which a chemical can be dissolved by body fluids from soil into solution and is available for absorption, whilst bioavailability defines the process of absorption of leached chemicals via exposure routes and are transported to a target tissue (Ruby *et al*. 1999; Lioy, 1990; Hamel, 1998; Plumlee and Ziegler, 2007). Bioaccessibility is an in vitro measurement, whilst bioavailability is an in vivo determination.

Bioavailability of metals is generally assessed by the following methods: statistical methods, observational studies, experimental studies, epidemiological studies, and computer models. Particular attention was paid to the experimental studies, in this literature survey, as this formed an important component of this research, i.e., studying the bioavailability of mercury from urban dust samples Due to the difficulty associated with determination of bioavailability in gastric and lung systems in vivo methodology, synthetic digestive and lung fluids have been developed.

In vitro leaching procedures have become valuable tools in estimating the oral bioavailability of metals in soils (Ruby *et al*., 1993; Ruby *et al*., 1996). The fraction of metals dissolved in an in vitro leaching procedure is termed the bioaccessibility, which may be equated to the bioavailability by conservatively assuming that everything that is dissolved is taken up in systemic circulation (Ruby *et al*. 1999). To sum up, bioaccessibility encompasses what is actually bioavailable now plus what is potentially bioavailable. Figure 2.12 describes the bioavailability processes that determine the exposure to contaminants in both soil and sediment systems. The solid-bound contaminant (A) is released to a more accessible form (B), which is transported to a physiological membrane (C), uptake across the cellular membrane (D), and absorbed into the living system (E).

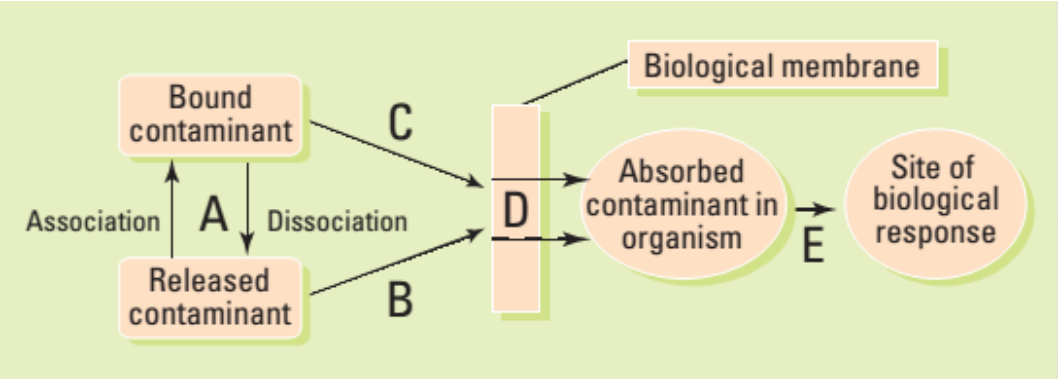

Figure 2.12: The bioavailability processes (A-D), where A, B, C, and D are processes governing bioaccessibility, while process D addresses bioavailability (Semple *et al*., 2004).

Metals have biological effects which can either be beneficial or harmful to the environment and human beings. Its harmful effects depend on exposure and bioavailability, i.e., how much metal enters and reaches the target organ(s) in the body. Therefore, in order to understand the bioavailability of a metal, its fate, transport and distribution in the environment, it needs to be assessed. Figure 2.13, illustrates the different exposure routes and the different types of body fluids that can be encountered by foreign materials during exposure. Table 2.13 gives an overview of the pathways for six important metals.

In-vitro extraction methods have been developed and applied to soils, sediments and dust samples in order to determine bioaccessibility of mercury in the gastrointestinal tract, and respiratory tract (Paustenbach *et al*., 1997; Zagury *et al*., 2009; Gray *et al*., 2010; Hu *et al*., 2011).

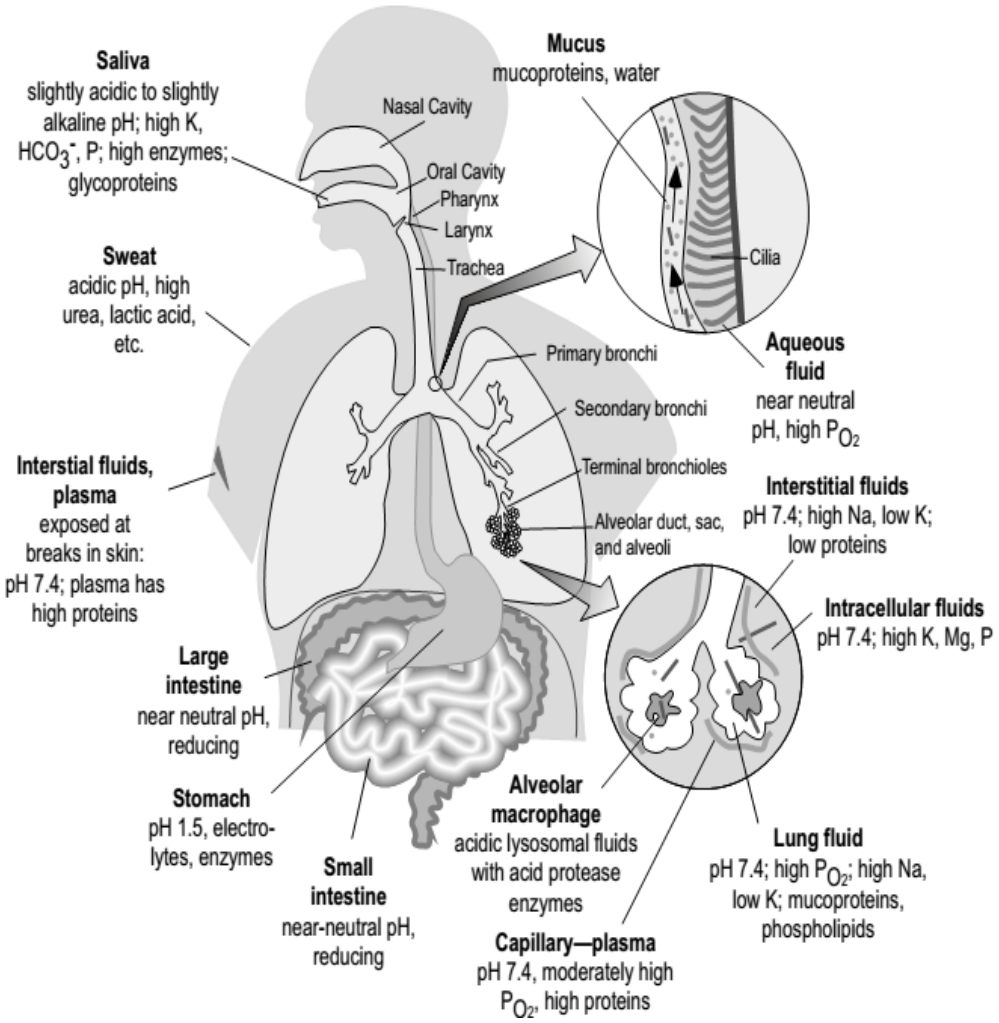

Figure 2.13: This schematic diagram illustrates the different exposure routes, the different types of body fluids and their composition encountered in the gastrointestinal and respiratory tract (Plumlee and Ziegler, 2006).

Table 2.13: Relevance of different media to metal exposures (Caussy *et al*., 2003)

	Air	Soil/Dust	Water	Biota/Food
Arsenic	+ Occupational Smelters	+ + Mining Smelting	+ + Natural	+ +
Mercury	+ **Occupational** **Cultural**	+ + + + 	+ + + + **Methylation** **in sediments**	+ + + + **Biomagnification** **MeHg in fish** [b]
Iron	+ + Occupational Mining	+ + Mining tailings	+ + Rust in pipes	+
Tin	+ Occupational Smelters	0	+	+ Organotin pesticides, TBT in fish [b]
Lead	+ + Occupational Smelters Leaded gasoline	+ + + Toddlers ingestion	+ + Lead pipes and solder	+ + + Leaded glazed and glass Paprika Wheat (Cairo)
Chromium	+ Occupational	+ +	+	+

[a] *+ + + + Highly relevant; + + + medium relevant; + + relevant; + less or infrequently relevant; 0 not relevant.*
[b] *MeHg, methylmercury; TBT, tributyltin.*

2.4.2.1 Gastrointestinal

Barnett *et al*. (2001), studied soil samples from EFPC floodplain and observed that the bioaccessible mercury was minimal at both pH 2.5 and 6.5, ranging from 0.3 to 14%, with an average of 3.2% total bioaccessible mercury in 19 soil samples in simulated stomach and intestinal environments, respectively. Only 4% of soil samples studies had greater than 5% bioaccessible mercury. These results were consistent with Ruby's findings (Ruby *et al*., 1999), which was that the bioaccessibility in the simulated stomach fluid was almost twice the corresponding value in the intestinal fluids. This suggests that bioavailability and uptake are greatly influenced by the dissolution of soil-bound metals in the stomach fluids. It was observed that Hg bioaccessibility in soils is seldom higher than 5% (Barnett and Turner, 2001). According to Zagury *et al*.

(2009), the average bioaccessibility of mercury in the studied soils (collected close to a chlor-alkali plant in eastern Canada and near a gold mine in Quebec) was <3.2%. However, bioaccessible mercury in the certified reference material (CRM) 025-050 sample (44.3% and 34.7% for gastric and intestinal phase, respectively) was more than 10 times higher than the soil samples. From calcines samples, bioaccessible mercury varied from 1.2% to 2.8% (Gray *et al*., 2010), and these results were comparable to previously published data of bioaccessible mercury in soils, with a range of 0.3 to 46% (Zagury *et al*., 2009, Barnett and Turner, 2001, Davis *et al*., 1997). Bioaccessible mercury ranged from 1.1 to 4.4% and 1.5 to 7.5% from gastric and gastrointestinal fluids, respectively, for children exposed to mercury contaminated soils (Guney *et al*., 2013). Bioaccessible mercury from simulated gastric fluid ranged from 0.013 to 0.28 mg kg^{-1}, 0.0062 to 0.044 mg kg^{-1}, and 0.0044 to 0.026 mg kg^{-1} in industrial, mining, and urban soils, respectively, from Portugal (Rodrigues *et al*., 2014). These results were comparable to bioaccessible mercury concentration by gastric juice from urban dust samples from Nanjing, China (Hu *et al*., 2011). The Portugal sample results of bioaccessible mercury expressed as a percentage of total mercury ranged from 0.1% to 0.7%, 0.1% to 1.2%, and 0.4% to 1.8% in industrial, mining and urban soils, respectively. Of interest, was the results of the mining soils from Iberian Pyrite Belt, South West of Portugal were comparable to mine-waste calcine samples from Almaden, Spain (Gray *et al*., 2010).

In Guangzhou, China, bioaccessible mercury from both road dust and household dust samples in the stomach phase was approximately 15%, respectively (Huang *et al*., 2014). However, in the intestinal phase, bioaccessible mercury was observed to have decreased slightly as compared to the stomach phase, with the greatest decrease experienced in the household AC filter dust samples (10%). Urban street dust from Nanjing, China contained an average of 0.045 mg kg^{-1} bioaccessible mercury from SBET protocol (Hu *et al* 2011), which expressed as a percentage of total mercury was 39.1%. This value was considerably high as compared to previous studies conducted in similar dust samples, highlighting high pollution levels.

2.4.2.2 Respiratory

Bioaccessible mercury from household dust ($PM_{2.5}$) samples, from China, was found to be 20.66% in the simulated lung serum (Huang *et al*., 2014), with high enrichment factor (7.02) due to extra indoor sources. In the soil samples obtained from industrial, mining, and urban areas in Portugal, bioaccessible mercury was 5.8%, 1.0 %, and 4.1%, respectively, from simulated lung fluid (Rodrigues *et al*., 2014).

2.4.3 Health risk assessment

Health risk assessment has been used to establish the probably of adverse health effects in humans exposed to hazardous chemicals in contaminated environments both national and international levels (Put *et al*., 2001; World Health Organisation, 2000). According to the World Health Organisation (2000) guidelines, health risk assessment focuses on health hazard characterisation and health impact assessment. The health characterisation process involves the identification and assessment of the hazard in the environment and its effects on the human health based on the evidence from epidemiology studies while health impact assessment involves the quantification of contaminants' (hazards) concentration and releases, the identification of exposed populations, the identification of potential exposure pathways and the estimation of contaminants intakes for each pathways for a range of scenarios and land uses.

Health risk assessment for each exposure pathway of mercury was measured and compared to the toxicological reference value (TRV) for each of the forms of mercury. TRV were based on the principal toxicological observed effect (Table 2.14). The importance of risk characterisation is to estimate the non-carcinogenic and carcinogenic effects.

Table 2.14: Toxicological reference values (TRV) for all mercury species according to exposure (Morisset *et al*., 2013).

Mercury species	Exposure	Toxicological effect	TRV	Source
Hg^0	Inhalation	Neurotoxicity	0.3 µg m^{-3}	US EPA, 1995
			0.2 µg m^{-3}	WHO, 2003
			0.2 µg m^{-3}	RIVM, 2001
IHg	Inhalation	Guideline value	1.0 µg m^{-3}	WHO, 2007
	Oral	Nephrotoxicity	4.0 µg kg^{-1} bw^{-1} $week^{-1}$	JECFA, 2011
			2.0 µg kg^{-1} bw^{-1} day^{-1}	RIVM, 2001
MeHg	Oral	Neurotoxicity	1.6 µg kg^{-1} bw^{-1} $week^{-1}$	JECFA, 2003
			0.1 µg kg^{-1} bw^{-1} day^{-1}	US EPA 2001
			0.3 µg kg^{-1} bw^{-1} day^{-1}	ATSDR, 1999

2.4.3.1 Non-cancer health risk

Non-cancer health risk is estimated using mathematical models developed by US EPA for chemicals with non-cancer risks (US Environmental Protection Agency 1989a, b). For non-cancer effect, in children, the inhalation of mercury vapour is the main route of exposure in all exposure pathways. The results were consistent with the observations obtained from the study conducted by Fang *et al*. (2011) and Meza-Figueroa *et al*. (2007). According to Sun *et al*. (2013), dust from the educational areas posed a high health risk of Hg on the children living in this area, as confirmed by the hazard indices of inhalation and direct ingestion.

2.4.3.2 Cancer health risk

The determination of cancer health risk is based on calculating the probability of developing cancer based on lifetime exposure, model and toxicity assumptions. Acceptable risk factors lie between 1.0E-06 and 1.0E-04, an acceptable value of one in

a million adopted in scientific literature remains without scientific evidence (US Environmental Protection Agency, 1991c).

2.5 Analytical methods used for In-vitro determination of bioavailability of metals/metalloids

Various simulated gastric juices and lung fluids have been used to study bioavailability of metals from different environment samples. Generally, these methods are grouped into two categories, namely: those with physiological components and those without physiological components. The mobility, bioavailability, and toxicity of trace elements in environmental media depends on chemical concentration of trace elements in environmental substrate (soils, sediments, dust, biota, etc.), substrate properties (pH, organic matter, chemical speciation of solids, surface area to volume ratio (particle size and particle composition), redox conditions, presences of anionic species etc.), and pH of the extraction solutions (Richardson *et al*., 2006; Krishnamurti and Naidu, 2003).

2.5.1 Ingestion

The following extraction protocols have been used to assess the bioavailability of metals through ingestion from different environmental media samples:

The SGDB (saliva, gastric juice, duodenum, and bile juice) method simulates the digestive system from the mouth, stomach, and intestine (Oomen *et al*., 2003). The leaching solutions were composed of different salts at varying pHs based on the different areas of the digestive system they represented.

Simplified bioaccessibility extraction test (SBET) has been used to simulate the stomach environment (Madrid *et al*., 2008; Kim *et al*., 2002). The leaching solution was made up of 0.4 M glycine adjusted to pH 1.5 with hydrochloric acid (HCl) and leached at 37°C. An intestinal phase was not used. This protocol was adapted from a procedure described by Ruby et al. (1996, 1993).

A modified version of European Standard Toy Safety Protocol EN-71 (European Committee for standardization, 1995) was composed of 0.07 M HCl, and leached at 37°C (Rasmussen *et al*., 2008).

In-Vitro Gastrointestinal method (IVG) was used to simulate the gastrointestinal environment. This solution contains physiological components such as porcine pepsin for the simulated gastric juice, while porcine bile extract, and porcine pancreatin are added to make up intestinal juice (Rodriguez *et al*., 1999).

CDM method (Barnett and Turner, 2001) was used to simulate a child gastrointestinal tract. It was made up of pH-adjusted deionized water (pH 2.5), with a low solid:liquid ratio (≈0.4 g in 0.5 L solution), and did not contain any physiological fluids.

From these methods, it was observed that bioaccessible mercury from simulated gastric juices was seldom higher than 5%.

2.5.2 Inhalation

Simulated lung fluids (SLF) have been used to evaluate human exposure to particulates from environmental emissions. Some of the most used SLF are outlined, in brief, below:

Artificial lung fluid (ALF) was used to simulate an acidic (pH 4.5) fluid found in the upper region of the lung, i.e., alveolar and interstitial macrophages in the lung.

Gamble's solution represents a neutral (pH 7.4) solution found deep in the interstitial areas of the lung.

Gray's solution was modified from gamble's solution and was designed to mimic extra cellular lung fluid. It was used to access bioaccessibility of mercury in human exposed to mercury through the inhalation of airborne calcine particles from mine waste (Gray *et al*., 2010; Eastes *et al*., 1995; Mattson *et al*., 1994).

2.5.3 Mercury fractionation

Recently, sequential extraction procedures (SEP) have been developed to quantitatively evaluate forms of mercury in sediments, soil, and tailings (Beldowski and Pempkowiak, 2007; Sanchez *et al*., 2005; Bloom *et al*., 2003; Biester and Scholz, 1997; Di Giulio and Ryan, 1987). The extraction steps of the SEPs for soils and sediments are critical mainly due to the challenges faced in obtaining adequate recovery by preventing losses, contamination or speciation changes, and limiting the interferences (Leermakers *et al*., 2005). Sequential extraction methods are advantageous because they are relatively easy to perform compared to other highly specialized analytical techniques. These extraction or leaching schemes have been used extensively to partially characterize the phase associations of metals in soils and sediments to identify the fraction or fractions of total metal that are or could become bioavailable (Tessier and Campbell, 1987; Campbell *et al*., 1988).

Soil samples obtained near chlor-alkali plants and gold mine tailings showed low mobility of mercury, with a total bioavailable mercury of <2.2% coming from the sum of water soluble, exchangeable, and organic matter fractions. A large percentage of mercury was found in the residual fraction (Zagury *et al*., 1999). Mercury bioaccessibility showed strong correlation with the sum of water soluble and exchangeable fractions, suggesting that these fractions are potentially good indicator of mercury bioaccessibility in soils. According Bloom *et al*. (2003), 9 out 11 varied mercury-contaminated samples from natural environment contained >50% of mercuric sulphide fraction, showing that the mercury in these samples has low mobility therefore low bioavailability due to the insolubility properties of mercuric sulphide. With this method, Bloom *et al*. (2003), was able to achieve detection limits of 0.1 - 5 ng g^{-1} for all fractions and identified that the F3 (organo-chelated) fraction was mostly strongly correlated with sediment methylation potential from contaminated natural samples. Fernandez-Martinez et al. (2005), working on soil samples collected from mercury mine processing sites showed highest concentration of mercury in the semi-mobile fraction (52 - 56% of the total Hg), while the non-mobile fraction contained about 40%. These samples exhibited high mobile mercury concentration of 6.5% probably due to

the fact that these samples were collected downstream from the chimney and were probably subjected to intense weathering processes and accumulation of leachates from the wastes near the chimney.

Sequential extraction protocols are designed for solubilising certain constituents (metals, metalloids, ions, etc.) in solid materials (rocks, soil, dust, sediments, biota). Specific solvents and solutions are used to target specific fractions, under specific conditions such as pH, reducing or oxidising conditions. This is called operational defined speciation. Different sequential extraction protocols are used for mercury and are listed as follows:

Novel sequential extraction procedure (n-SEP) used was a validated method used to study chlor-alkali contaminated soils (Neculita *et al*., 2005). The methodology of sequential extraction is described by Neculita *et al*. (2005).

Modified BCR (m-BCR) protocol, which was carried out according to Rauret *et al.* (1999) has been used to study the fractionation of potentially toxic metals in soils and sediments (Joksic *et al*., 2005; Brunori *et al*., 2004; Mossop and Davidson, 2003). The change from the original was made in increasing the concentration of hydroxylamine chloride from 0.1 to 0.5 M in the reducible phase.

A refined and extensively validated selective sequential extraction procedure (SSE) has been developed and implemented for the differentiation of mercury compounds into behavioural fractions (Bloom *et al*., 2003). It's a five step sequential extraction procedure with the following fractions: (i) water soluble (F1), (ii) "human stomach acid" soluble (F2), (iii) organo-chelated (F3), (iv) elemental Hg (F4), and (v) mercuric sulphide (F5).

2.6 Gaps in our current understanding of mercury sources in South Africa

The industries discussed in Section 2.3 are important in South Africa and a monitoring system must be developed to verify the initially reported mercury emission estimates from these sources. In addition, the contribution from artisanal gold mining must be determined in order to evaluate the impact this activity has on the human health and surrounding environmental ecosystems. The contribution from biomass burning as a potential source of mercury emission needs to established and well documented. All these activities need to be researched thoroughly and well documented in order to develop a working monitoring system that will be able to generate a mercury emission inventory in South Africa.

An area of interest that has yet to be explored, is the effect of toxic metals (i.e., mercury) in dust affecting the mining and surrounding communities. However, a lot of work has been done and documented on the effects of quartz (silica) in human respiratory system at an occupational level in South African gold miners (Hnizdo *et al*., 1993). Due to the improvement in the mining methods and the processing of the mineral ores, this has resulted in finer material waste dumped in the tailings dams, leading to the generation of mineral dust from unprotected tailings storage facilities. These finer particles (<25 μm), made up of high surface areas, with heavy metals bound to them, are a great risk to human health since they appear to be able to evade the body's natural defence mechanisms, and have a consequence of being redistributed into other sites of the body, causing systematic health effects.

As established in literature, it is worldly accepted that TSF are constant contributors to the aerosol of surrounding atmosphere. It is well established that the size of the particulate matter plays a major role in the deposition of the particulate matter in the respiratory tract. We have also established that the dust is laced with metals and/or metalloids (pollutants/contaminants). It was also established that during its seasonal variation, it exceeded the maximum concentration of airborne aerosols of South African Department of Environmental Affairs 24-hr limit value of 120 μg m^{-3}, it

reached an ambient concentration of 2160 µg m^{-3}. The missing link is the potential impact this dust has on human health and the environment. The data generated from this study seeks to address and understand the potential impact mercury has on the human health of individuals exposed to the dust by virtue of being surrounded by tailings dumps (i.e., living on, close to tailings dumps or living on tailings footprints or breathing the air heavily impacted by the minerals dust, in case of children being exposed to ingesting the soils impacted by mineral dust) and the potential impact on the environment, as mercury is not biodegradable.

Chapter 3

Aims and objectives

The aims, objectives, key questions, and the novelty of this work are discussed in the section.

3.1 Aim of the study

The aim of this study was to determine the levels of mercury, its bioavailability, and to determine the potential health risk assessment of mercury in inhaled and ingested street dust in Johannesburg, a metropolitan city negatively impacted by gold mining activities.

3.2 Motivation of the study

Mercury is a highly toxic trace metal, which is non-biodegradable. Historically, it was used for the processing of gold ores, and occurs together with gold in the gold ores in the Witwatersrand basin. After gold processing, it is deposited and has been accumulating in the tailings dams. Due to the large number of gold mine TSFs (approximately 270) in the Johannesburg city, neighbouring communities are exposed to huge amounts of dust generated by wind erosion of exposed surfaces of tailings storage facilities. The reprocessing and redeposition of older and dormant tailings has also contributed to the generation of dust, which has had a significant negative impact to the surrounding communities in the region (Annegarn *et al*., 2000; Annegarn, 2006). During the winter months, large amounts of dust (up to 2100 mg m^{-3} concentration per day) are generated, at high wind speeds of approximately 7 m s^{-1}, resulting in reduced visibility, irritation of the eyes, and ingestion of particulate matter. The dust generated normal contains large amounts of toxic metals and metalloids, which are dispersed and distributed over great distances. High exposure to mercury may result in the damage to the gastrointestinal tract, the nervous system, and the kidneys. Children and women fall into the most vulnerable population groups to mercury exposure, and are particularly at risk of suffering developmental problems and neurological damage, respectively. In this study, particular attention was focused on mercury due to its toxicity, persistence and non-biodegradability, bioaccumulation, bioconcentration, and bioavailability in the environment.

3.3 Objectives

To a gain thorough understanding of the mercury pollution in street dust in Johannesburg and its potential health risk, specific objectives have been formulated to address the aims and they are:

To determine the total mercury levels in street dust in Johannesburg.

To evaluate the particle size distribution and quantify mercury concentration in different particle size fractions i.e., PM_{100}, PM_{50}, and PM_{25}.

To analyse the mineralogy and elemental composition of the PM_{25} size fraction in the dust samples.

To assess bioavailability of mercury in PM_{25} size fraction in dust samples through inhalation and ingestion exposure pathways.

To evaluate mercury fractionation in PM_{25} size fraction in dust samples using sequential extraction procedures.

To assess the impact of long term pollution and seasonal changes on the spread of mercury in dust.

To assess human health risk for mercury in dust by modelling the mercury concentration data for inhalation and ingestion exposure pathways.

3.4 Hypothesis

It is hypothesised that the resulting dust due to wind erosion of gold mine tailings on the Witwatersrand basin poses significant health hazards to the surrounding communities, and causes severe damage to the environment, i.e., soil and water pollution. The dust generated contains toxic metals and metalloids, which are dispersed and distributed over great distances.

3.5 Key research questions

In order to achieve the aims and objectives of the study, specific questions were addressed:

What is the average mercury concentration in street dust in Johannesburg?

What is the impact of current and historic gold mining activities in relation to mercury pollution in Johannesburg?

What are the modes of occurrence of mercury in street dust in relation to its speciation?

What is the bioavailable mercury in urban dust from the inhalation and ingestion exposure pathways?

How do climatic and seasonal changes affect mercury in urban dust?

What are the quantified risks of communities exposed to mercury in street dust through ingestion and inhalation?

3.6 Novelty of the study

The original contribution of this study is the quantification of mercury levels in PM_{25} in urban dust, and its bioavailability in a negatively impacted gold mining metropolitan city, Johannesburg. It is also a contribution to the health risk assessment associated with ingestion and inhalation of dust contaminated with mercury. This information will be useful in developing national standards and/or limits of exposure of mercury in inhalable fraction of dust/particulate matter.

Chapter 4

Materials and methods

This chapter addresses the research approach used, namely: the collection, identification, handling and urban street dust, metal analysis and the experimental procedure followed by the bioavailability and sequential extraction studies.

4.1 Chemicals and reagents

Deionized water (DW) was produced by a commercial mixed-bed ion-exchange system Millipore (Millipore, Billerica, USA). All reagents used for sample extraction and digestion were analytical grade (Sigma Aldrich) except for acids (hydrochloric (HCl), hydrofluoric (HF), nitric (HNO_3), and sulphuric acid (H_2SO_4), used for the preparation of calibration and quality control standards, were suprapur grade for ultra-trace analysis (99.999% purity from Sigma Aldrich). Working standard solutions were prepared daily by serial dilutions of the 10 mg L^{-1} mercury standard solution (Ultraspec, from Merck, Dorset, UK). Tin (II) chloride solution ($SnCl_2$) was prepared daily by dissolving $SnCl_2$ ($\geq$ 98% trace metal analysis, Sigma Aldrich) in de-ionized water, and stabilizing it in 3% (v/v) HCl solution.

All digestion vessels, volumetric flaks, and other glassware used were pre-cleaned by detergent and rinsed with tap water. The vessels were soaked overnight in 10% HNO_3, rinsed with tap water, soaked in 10% HCl, finally rinsed with deionized water (18.2 MΩ cm, Milli-Q Plus, Millipore) and stored in cleaned zip lock polyethylene bags.

4.2 Instrumentation

Retsch sieves and AS200 Retsch Analytical Sieve Shaker (Haan, Germany) were used for all the separation procedures. Particle size distribution in the dust samples was determined by the Malvern MS-14 Particle Sizer (Malvern Instruments Ltd., Worcestershire, UK). Digestions of samples were carried out in a closed microwave system (Multiwave 3000, Anton Paar, Graz, Austria) (Figure 4.1). Totals (trace metals and metalloids concentration) were determined by inductively coupled plasma- optical emission spectrometer (Spectro Genesis ICP-OES, Kleve, Germany) designed for reliable analysis of environmental or industrial samples. Samples undergoing leaching experiments, were carried out at constant temperature of 37°C, shaken in a WiseCube Shaking Incubator (Seoul, Korea) and were centrifuged using Rotofix 32A (Hettich Zentrifugen, Germany).

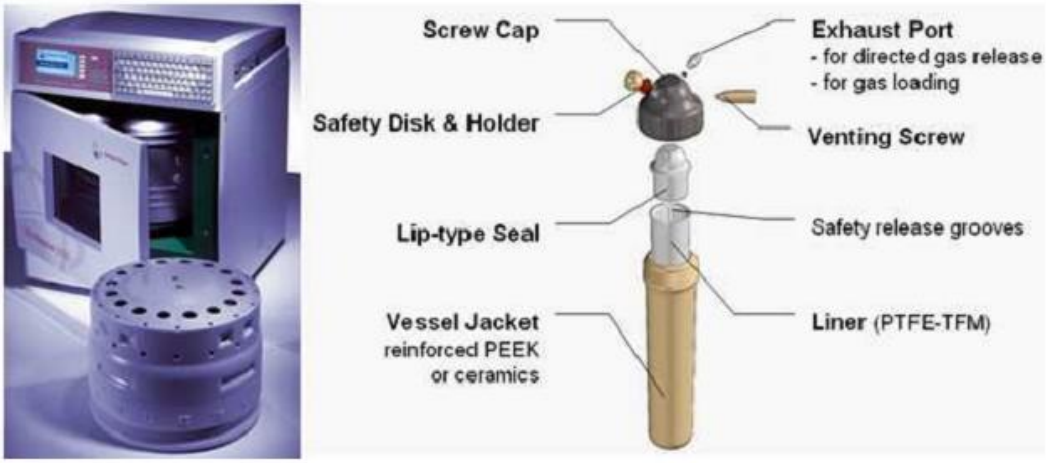

Figure 4.1: Anton Paar Multiwave 3000 microwave assisted extraction system (Multiwave 3000, Anton Paar, Graz, Austria).

Energy dispersive X-ray fluorescence spectrometry (ED XRF Bruker tracer SD III, Bruker-AXS Gmbh, Karlsruhe, Germany), D2 Phaser X-ray diffraction (D2 Phaser XRD, Bruker-AXS Gmbh, Karlsruhe, Germany), and scanning electron microscope (SEM, FEI Nova Nanolab 600 Dual beam FIB/SEM) equipped with an EDS X-ray detector were used to determine the elemental, chemical composition, and imaging of bulk and separated dust samples, respectively. The operating specifications are displayed in the Table 4.1

Table 4.1. Specifications of ED-XRF and XRD spectrometry

Description	ED-XRF	XRD
Geometry		Theta/theta
X-ray wavelengths	Rh X-ray source and Pd slits	Co, standard ceramic sealed tube
X-ray generation	Max: 30 µA at 40 kV; 55 µA at 15 kV	30 kV 10 mA^{-1}
Detectors	10 mm^2 – Flash detector	Scintillation counter, 1-dimensional LYNXEYE
Instrument type	Hand held	Portable desktop

A PerkinElmer Flow Injection Analysis-Mercury Hydride System (FIMS 400/FI-MH-AAS) (Perkin Elmer, Norwalk, Connecticut, USA) in conjunction with a PerkinElmer (Norwalk, CT, USA) AAnalyst 200 atomic absorption spectrometer provided with a quartz cell in an electrically heated mantle and an AS-91 auto sampler was used for mercury determination. Peak area was used for the measurement of the analytical signal. Instrumental details and operating conditions are summarized in Table 4.2

Table 4.2: Instrumental characteristics and settings for PerkinElmer FIMS 400**.**

Instrument	**PerkinElmer FIMS 400**
Spectrometer	
Technique	AA
Integration time (s)	20
Data processing	Peak Height, Smoothing: 0.5 sec or 19 points
Cell temperature	100°C
Lamp	HCL or EDL
EDL lamp current	190 mA
Measurement mode	Peak area
Slit width	0.7nm
Wavelength	253.7 nm
Cold Vapour Generation	
Reducing Agent	1.1 % (m/v) $SnCl_2$ in 3 % (v/v) HCl
Reductant flow rate	5.5 mL min^{-1}
Carrier solution	10.5 mL min^{-1}
Carrier gas (N_2) flow rate	50.0 mL min^{-1}
Sample loop volume	500 µL

4.3 Sampling sites and sampling protocol

4.3.1 Study area

Street dust samples were collected from the industrial sites, central business district (CBD) and residential areas of Johannesburg. Johannesburg is situated in the Witwatersrand basin, the major gold bearing deposit in South Africa. It hosts a population over 10 million and the growth of the city has encroached around the TSFs covering an area of 44 000 ha (Rösner and van Schalkwyk, 2000; Funke, 1990). Mine

tailings storage facilities are, generally, situated close to major highways, important water courses and wetlands, residential and industrial areas. They are characterized by elevated proportions of pyrite and other minor metallic sulfides. Numerous ore minerals and enhanced levels of toxic metals and metalloids, including mercury and cyanide were found in the gold mine tailings dams. These tailings are alkaline when they are deposited, however, due to the exposure to rain water and oxygen, this leads to the oxidation of pyrites resulting in the tailings becoming extremely acidic (pH 2.5-3.5), leaching of heavy metals, and low in plant nutrients (Moreno *et al*., 2007). Revegetation of such tailings, especially in semi-arid regions, presents a challenge due to erosion of the exposed bare tailings surfaces.

The study area is characterized by hot, wet summers (October to April) and cold winters (May to September). During this time, temperatures are usually mild to hot with average maximum daytime temperatures of 26-30 °C dropping to an average maximum of about 8-16 °C in July. The months of July to August are the coldest in winter with dominant wind direction of North to North Westerly and North Easterly with wind speeds of 7 ms^{-1} and the temperatures occasionally drop to below freezing point at night, causing frost (Ojelede, 2012). The mean annual rainfall is 750 mm, with the average annual evaporation varying between 1600 and 1700 mm. Figure 4.2 shows the sampling sites whilst Table 4.3 describes the sampling sites, the land use, and characteristics of the sampling locations.

For comparison and reference purposes, dust samples were also collected in the mining areas. The two mining sites chosen were; (i) Vaal River Complex, and (ii) West Wits mining complexes. The reasons why they were selected was mainly because they are active mining sites where pollution controls are poorly managed resulting in the emissions of dust from TSF, seepage of contaminated water from the TSF and waste rock dumps, trenches, and pollution control dams, uncontrolled release of process water from metallurgical plants, and finally, on-site secondary sources, and footprints (ores and mineral waste). These impacts led to severe contamination of land, surface

and ground water, and possible adverse health effects in the local population and surrounding communities.

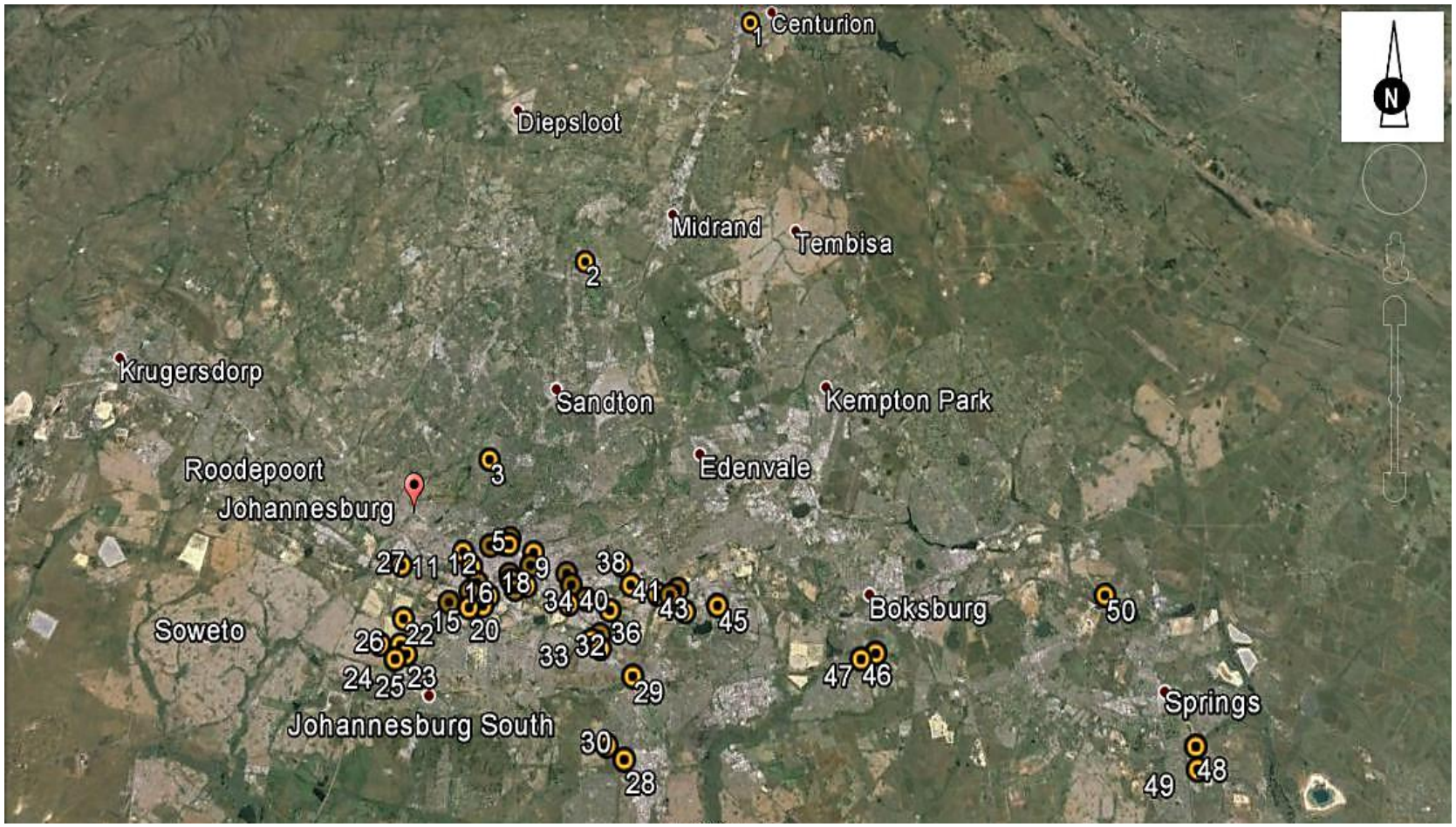

Figure 4.2: A map showing the location of the dust samples from the study sites in Johannesburg, South Africa.

Table 4.3: Description of sampling sites.

Site No.	Sampling sites	Land use	Longitude	Latitude
1	Res. Centurion, Pretoria	Residential area	25°52'10.03"S	28°10'31.06"E
2	Res. Sandton	Residential area	26° 1'53.91"S	28° 4'10.92"E
3	Res. Greenside	Residential area	26° 9'0.50"S	28° 1'7.53"E
4	CBD 1	Commercial area	26°11'33.26"S	28° 2'12.69"E
5	CBD 2	Commercial area	26°11'45.18"S	28° 2'11.22"E
6	CBD 3	Commercial area	26°11'43.73"S	28° 1'58.13"E
7	CBD 4	Commercial area	26°12'41.65"S	28° 2'18.44"E
8	CBD 5	Commercial area	26°12'23.16"S	28° 3'4.13"E
9	CBD 6	Commercial area	26°11'58.47"S	28° 3'8.69"E
10	CBD Cemetery	Commercial area	26°11'48.79"S	28° 1'29.02"E
11	Crown North 1	Residential area	26°12'3.22"S	28° 0'29.10"E
12	Crown North 2	Residential area	26°12'29.97"S	28° 0'52.07"E
13	Crown South 1	Commercial area	26°12'59.76"S	28° 1'7.92"E
14	Crown South 2	Commercial area	26°13'16.02"S	28° 0'53.52"E
15	Ophirton	Industrial area	26°13'42.28"S	28° 1'25.41"E
16	Cross	Industrial area	26°13'23.78"S	28° 1'36.48"E
17	Trump	Industrial area	26°12'52.61"S	28° 2'22.70"E
18	Rosettenville	Industrial area	26°13'1.77"S	28° 2'58.47"E
19	Loveday	Industrial area	26°13'9.33"S	28° 2'33.57"E
20	Booysen	Industrial area	26°13'46.86"S	28° 0'54.78"E
21	Crownwood	Industrial area	26°13'38.69"S	28° 0'8.76"E
22	Soccer City	Industrial area	26°14'12.66"S	27°58'31.39"E
23	Aeroton 1	Industrial area	26°15'16.82"S	27°58'46.28"E
24	Aeroton 2	Industrial area	26°15'26.42"S	27°58'22.94"E
25	Aeroton 3	Industrial area	26°15'0.71"S	27°58'31.32"E
26	Res. Diepkloof	Residential area	26°15'0.79"S	27°57'45.55"E
27	Res. Riverlea	Residential area	26°12'32.92"S	27°58'12.88"E
28	Res. Alberton 1	Residential area	26°18'5.05"S	28° 7'1.61"E
29	Res. Alberton 2	Residential area	26°15'37.80"S	28° 7'9.05"E
30	Res. Alberton 3	Residential area	26°17'42.08"S	28° 6'22.36"E
31	Steeldale 1	Industrial area	26°14'25.39"S	28° 5'50.98"E
32	Steeldale 2	Industrial area	26°14'50.35"S	28° 5'54.15"E
33	Steeldale 3	Industrial area	26°14'36.67"S	28° 5'33.61"E
34	City deep 1	Industrial area	26°13'31.81"S	28° 4'36.93"E
35	City deep 2	Industrial area	26°13'21.49"S	28° 5'14.30"E
36	City deep 3	Industrial area	26°13'39.87"S	28° 6'9.42"E
37	Benrose 1	Industrial area	26°12'35.07"S	28° 4'26.93"E
38	Benrose 2	Industrial area	26°12'14.80"S	28° 6'29.46"E

39	Benrose 3	Industrial area	26°12'56.27"S	28° 4'39.23"E
40	Heriotdale	Industrial area	26°12'50.83"S	28° 6'52.60"E
41	PPC Cement	Industrial area	26°13'5.87"S	28° 7'54.19"E
42	Germiston 1	Industrial area	26°13'6.46"S	28° 8'21.69"E
43	Germiston 2	Industrial area	26°13'36.03"S	28° 8'56.54"E
44	Germiston 3	Industrial area	26°12'55.28"S	28° 8'38.58"E
45	Res. Germiston	Residential area	26°13'21.81"S	28°10'09.01"E
46	Res. Boksburg 1	Residential area	26°14'47.80"S	28°15'30.56"E
47	Res. Boksburg 2	Residential area	26°14'36.01"S	28°16'2.93"E
48	Springs 1	Industrial area	26°16'54.19"S	28°27'36.57"E
49	Springs 2	Industrial area	26°17'34.08"S	28°27'36.88"E
50	Springs 3	Industrial area	26°12'28.34"S	28°24'36.57"E

The Vaal River mining operations is located near the Free State - North West border (Figure 4.3) about 170 km from Johannesburg, and includes Great Noligwa, Kopanang and Moab Khotsong mining. These three mines share a milling and treatment plant. The area is characterized by extensive shallow mining of the black reef and large spillages from old mine tailings facilities. Some old tailings facilities have been re-worked, however, reprocessing of old tailings is still being undertaken. There is overwhelming evidence of environmental degradation from the mining operations in the region, reports of artisanal mining activity using mercury amalgamation, and evidence of historical gold processing using mercury amalgamation from the sand dumps. Such activities have led to the long periods about 170 km from Johannesburg of contamination. All spillages, seepage, both ground and surface waters find their way into the Vaal River, situated in the south of the mining complex. This is influenced by the topography of the mining complex as it is sloped towards the Vaal River basin.

The West Wits operations are composed of Mponeng and Tau Tona, situated southwest of Johannesburg, on the border between Gauteng and North West Province. Due to lack of proper implementation of environmental protection laws, there was an accumulation different types of waste materials such as ash, iron oxide, pyrite, slag, mine residue spillage, mine waste rock, steel, rubber, scales from gold and uranium plants and domestic waste in borrow pits and mine property (AGA, 2009a). Currently,

there is remediation work being carried out and it involves the removal of all types of waste followed by backfilling and profiling with inert material, placement of soil cover the disturbed sites and rehabilitation with vegetation with a high capacity for absorption of heavy metals.

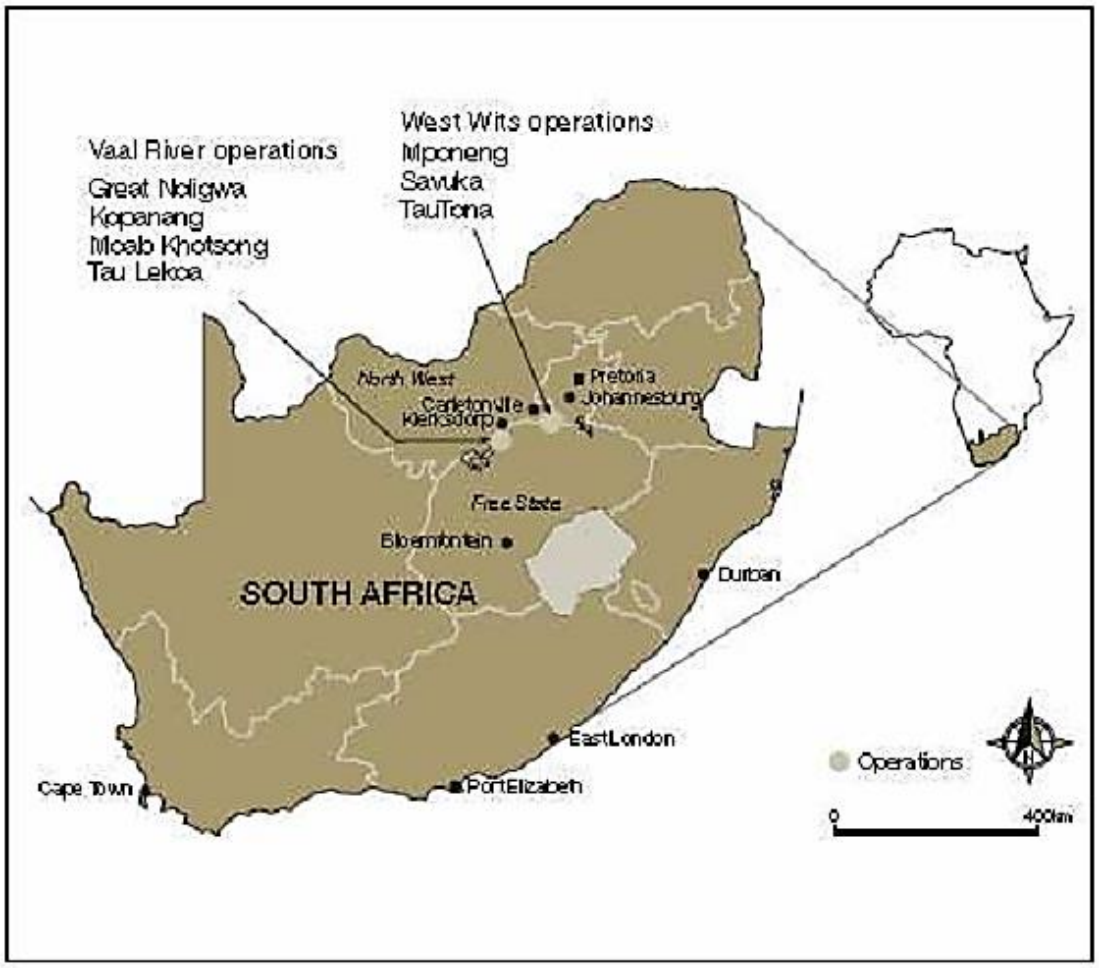

Figure 4.3: Vaal River and West Wits mining operations.

4.3.2 Sampling protocol

Dust samples were collected across the city using a plastic brush and dustpan, on impervious pavements along both sides of the road, transferred to zip lock polyethylene bags, and transported to the laboratory. The samples collected were distributed as follows: industrial area (28), CBD (9), and residential areas (13). Samples were

collected during the dry and sunny weather conditions. These samples were dried in an oven at 40°C for two days and then separated into three particle size fractions (PM_{25}; PM_{50}; PM_{100}). The size was chosen because finer fractions generally contain higher metal concentrations (Whicker *et al*., 1997) and particles below 25 µm are considered hazardous, as they easily adhere to children's hands (Duggan and Inskip, 1985) and furthermore are easily inhalable. After separation, the sieved samples were preserved in acid washed plastic containers in the refrigerator at 4°C until the bioaccessibility and extraction experiments began.

4.4. Analysis procedure

4.4.1 Elemental analysis

4.4.1.1 Total mercury determination

Dust samples were extracted using concentrated acids in a microwave system. Aliquots (0.25 g) of dust sample fractions PM_{25} were weighed out into digestion (PTFE) vessels and mixed with 13 mL of concentrated acids ($HCl:HNO_3:HF$ = 9:3:1 (v/v/v)). The mixture was then introduced into a closed microwave system at 800 W for 30 min, followed by 600 W for 20 min and finally cooled for 10 min (the program is displayed in Table 4.4). The concentrated HF was later neutralized with 4% (w/v) boric acid (H_3BO_3) and all samples were then made up to 50 mL with de-ionized water. Blanks were simultaneously processed with dust samples. The clear digested samples were stored in plastic bottles and kept in a refrigerator. Hg_{TOT} was determined by mercury analyser (FIMS 400 FIAS-AAS), and AS-91 auto sampler.

4.4.1.2 Total trace metal determination

Total trace metal concentration was determined in concentrated acid extracts from dust samples. These samples were extracted with concentrated acids in a closed microwave system (Aton Paar Multiwave 3000), as described above, in section 4.4.1.1. The clear digested solutions were made up to 50 mL with deionized water, stored in plastic bottles and kept in a refrigerator, prior to analysis on inductively coupled plasma-optical emission spectrometer (ICP-OES).

Table 4.45: Microwave assisted extraction program

Sample Type: Dust		**Mass:** 0.250 g		
Phase	**Power (W)**	**Ramp (min)**	**Hold (min)**	**Fan**
1	800	10	10	1
2	600	10	10	1
3	0	5	5	3

4.4.2 Characterization of dust

4.4.2.1 pH

The pH of dust was measured in a 1:2.5 (m/v) mixture using Knick Calimatic pH meter (Berlin, Germany) (Al-Khashman, 2007; Banerjee, 2003).

4.4.2.2 Particle size distribution

The particle size distribution of dust samples was determined using a Malvern Mastersizer S Particle Size Analyzer capable of analyzing particles between 0.05 and 1000 µm. The Malvern Mastersizer uses a laser to record the scattering pattern from a field of particles. It then uses an analytical procedure to determine the size of particles that created the scatter pattern.

4.4.2.3 Scanning electron microscopy

Morphological, mineralogical and chemical characterization was achieved by using a high vacuum SEM (FEI Nova Nanolab 600 Dual beam FIB/SEM) equipped with an EDS X-ray detector for single particle analysis, imaging, and quantification of elements in samples. Dust samples were prepared by mounting on stubs with a sticky carbon cover and then coated with carbon and gold/palladium prior to examination. Microscope conditions for backscatter imaging were accelerating voltage of 30 kV, working distance of 5 mm, and the beam spot size was 5.

4.4.2.4 XRD

X-ray diffraction (XRD) analysis of the PM_{25} dust samples was performed by packing samples into a plastic holder and using a D2 Phaser X-ray diffractometer equipped with unique choice of detectors, and a very easy to use software DIFFRAC EVA, which allows measurement and analysis right out of the box.

4.4.2.5 XRF

All samples were analyzed after sieving using Bruker Tracer III SD handheld XRF spectrometer equipped with a rhodium target X-ray tube and a silicon drift detector with a resolution of ca. 145 eV FWHM for 5.9 keV X-rays (at 200,000 counts per second) in an area 10 mm^2. The spot size on this specific instrument is less than 10mm diameter. Peak intensities for the Kα and Lα peaks were calculated as ratios to the Compton peak of rhodium and converted to parts-per-million (ppm) using Bruker's factory installed calibration.

4.4.2.6 CHNS

The CHNS analyser (Leco-932, USA) used in this study was calibrated with standards of Sulfamethazine and Corn Gluten (Leco) and the results are given in Table 4.5. A Sartorius CP2P micro balance (Gottingen, Germany) with a precision of 10^{-6} g was used to weigh samples. The samples were weighed into silver capsules and introduced into the oxidation furnace by means of a carousel.

Table 4.5: Standards calibration of the CHNS analyser

Standard	Carbon %	Hydrogen %	Nitrogen %	Sulphur %
Sulfamethazine	51.78	5.07	20.13	11.52
Measured (n=3)	**51.73 ± 0.22**	**5.03 ± 0.12**	**20.03 ± 0.10**	**11.52 ± 0.05**
Corn Gluten	52.29 ± 0.39	7.13 ± 0.07	11.35 ± 0.07	0.933 ± 0.04
Measured (n=3)	**52.23 ± 0.28**	**7.10 ± 0.12**	**11.38 ± 0.13**	**0.931 ± 0.11**

The above standards were chosen because their certified values are reported for all 4 elements (carbon, hydrogen, nitrogen and sulfur) although our components of interest for the study were only carbon and sulfur.

4.4.2.7 Contamination assessment factors

The enrichment factor (*EF*), contamination factor (C_f), and index of geo-accumulation (I_{geo}) were applied in order to evaluate and classify the level of pollution from dust.

Enrichment factor (EF)

Enrichment factors are generally used to characterize the magnitude of metal contamination in environmental samples (Tokalio *et al*., 2003; Voutsa *et al*., 2002; Lee *et al*., 1997). The enrichment factors were calculated with respect to Al (Aluminum) according to the following equation:

$$EF_{Hg} = \frac{(C_x/C_{Al})_{dust}}{(C_x/C_{Al})_{Earth's\ crust}} \quad (1)$$

Where $(C_x/C_{Al})_{dust}$ is the ratio of concentration of the metals being determined (C_{Hg}) to that of Al (C_{Al}) in the dust samples and $(C_x/C_{Al})_{Earth's\ crust}$ is the ratio in the reference Earth's crust (Atgin *et al*., 2000).Generally, EF values less than 10.0 are not considered significant, because such small enrichments may arise from differences in the composition of local soil material and reference soil used in EF calculations (Voutsa *et al*., 2002; Atgin *et al*., 2000).

Contamination factor (C_f)

The contamination factor was used to categorize the level of mercury contamination in dust samples by applying a modified contamination factor (Hakanson, 1980). The contamination factor (C_f^i) was defined as follows:

$$C_f^i = \frac{C_{0-1}^i}{C_n^i} \quad (2)$$

Where C_{0-1}^i is the mean concentration of mercury and C_n^i is the concentration of mercury at a relatively clean background site. In this study, the C_n^i value represented the background concentration value of metals in a natural environment away from the industrial and traffic zones. Contamination factor was evaluated by four classes (Loska *et al*., 2004; Hakanson, 1980), which are as follows: low ($C_f^i < 1$), moderate ($1 \leq C_f^i < 3$), considerate ($3 \leq C_f^i < 6$), and very high ($6 \leq C_f^i$) contamination.

Geoaccumulation index

Geoaccumulation index have been used to assess the heavy metal contamination levels in dust samples (Škrbić and Mladenovic, 2010; Amato *et al*., 2009; Faiz *et al*., 2009; Lu *et al*., 2009; Wei *et al*., 2009). Geoaccumulation index was calculated by the following equation (Škrbić and Mladenovic, 2010; Wei *et al*., 2010; Amato *et al*., 2009; Lu *et al*., 2009; Wei *et al*., 2009):

$$I_{geo} = \log_2\left(\frac{c_n}{1.5B_n}\right) \quad (3)$$

Where C_n represented the measured concentration of the metal n of interest and B_n was the geochemical background value. The constant 1.5 allowed us to analyze natural fluctuations in the content of a given substance in the environment and to detect very small anthropogenic influences (Wei *et al*., 2009). The Igeo was classified as: uncontaminated ($I_{geo} \leq 0$); uncontaminated to moderately contaminated ($0 < I_{geo} \leq 1$); moderately contaminated ($1 < I_{geo} \leq 2$); moderately to heavily contaminated ($2 < I_{geo} \leq 3$); heavily contaminated ($3 < I_{geo} \leq 4$); heavily to extremely contaminated ($4 < I_{geo} \leq 5$); extremely contaminated ($I_{geo} \geq 5$).

4.4.3 Bioaccessibility of mercury in gastrointestinal tract

Two different models were tested in this study. The first model involved use of the synthetic gastrointestinal solutions and the second involved the use of synthetic solutions in saliva-gastro-intestinal model.

For oral bioavailability, simulated gastric juices were prepared as listed in Table 4.6. Dust samples (~0.5 g) were accurately weighed, placed in a 50 mL vial, and 25 ml of appropriate simulated gastric juices were added. For the dilute HCl, the pH was adjusted to 1.5 whilst the artificial gastric juice was maintained at pH 2. The vials were sealed and placed in a Shaking Incubator, set at 37°C, shaken for 4 hrs at 150 rpm, mimicking the lung conditions. The vials were centrifuged at 1500 rpm for 15 minutes. The centrifuged samples were stored in clean sterile pyrex vials with teflon-lined cap and kept in a refrigerator prior cold vapour Hg_{TOT} determination by Hg analyzer (FIMS 400, PerkinElmer).

Table 4.6: Composition of simulated gastric solutions.

Salt	[a] **Artificial Gastric Juice (mg L^{-1})**	[b] **Dilute HCl (mL L^{-1})**
Calcium chloride dihydrate ($CaCl_2.2H_2O$)	200	
Hydrochloric acid (HCl)	1380	5.9
Potassium chloride (KCl)	820	
Sodium chloride (NaCl)	2750	
Sodium dihydrogen phosphate (NaH_2PO_4)	270	
Ammonium chloride (NH_4Cl)	305	
pH	**2.0**	**1.5**

[a] Adapted from Wittsiepe *et al*. 2001.
[b] Adapted from Stopford *et al*. 2003.

4.4.4 Bioaccessibility of mercury in respiratory tract

The bioavailability of mercury in dust samples were determined for the inhalable and oral fractions. For the inhalable fraction, three simulated lung fluids were used: Artificial lysosomal fluid (ALF), Gamble's and Gray's solution were used to simulate different interstitial conditions in the lung (Table 4.7). ALF is an acidic solution representing fluid present in the upper region of the lung, while Gray's was a modified Gamble's solution designed to model interactions of particles with extra-cellular lung fluid (Jurinski and Rumistidt, 2001; Eastes and Hadley, 1995; Mattson, 1994). Gamble's solution, a neutral solution presents the interstitial fluid deep within the lung. When preparing the simulated lung fluids, citrate was used instead of proteins to avoid foaming and acetate instead of organic acids. Gamble's and Gray's solution had a pH of 7.4, whereas ALF has a pH of 4.5 and has a much higher organic content than Gamble's solution (Barnett and Turner, 2001).

Dust samples (~0.2 g) were accurately weighed into 50 mL vials and 20 mL of the appropriate leaching solutions were added. The vials were sealed and placed in a Shaking Incubator, set at 37°C, shaken for 24 hrs at 150 rpm, mimicking the lung conditions. The vials were centrifuged at 1500 rpm for 15 minutes. The centrifuged samples were stored in clean sterile pyrex vials with teflon-lined cap and kept in a refrigerator prior cold vapour Hg_{TOT} determination by Hg analyzer (FIMS 400, PerkinElmer).

Table 4.7: Composition of simulated lung fluids

Salt	**(g L^{-1})**		
	Artificial lysosomal fluid	**Gamble's solution**	**Grays' solution**
Phosphoric acid	-	-	1.2000
Sodium chloride	3.2100	6.0193	6.8000
Ammonium chloride	-	-	5.3000
Sodium dihydrogen phosphate	-	-	1.7000
Potassium acid phthalate	-	-	0.2000
Calcium chloride dihydrate	0.1280	0.2771	0.2900
Sodium acetate trihydrate	-	0.9526	0.5800
Sodium hydrogen carbonate	-	2.6042	2.3000
Tri-sodium citrate dihydrate	0.0770	0.0970	0.5900
Sodium hydroxide	6.0000	-	-
Sodium carbonate	-	-	0.6300
Sulphuric acid	-	-	0.5100
Glycine	0.0590	-	0.4500
Citric acid	20.800	-	0.4200
Magnesium chloride hexahydrate	0.0500	0.2033	-
Potassium chloride	-	0.2982	-
di-sodium hydrogen phosphate	0.0710	0.1417	-
Sodium sulphate anhydrous	0.0390	0.0710	-
Sodium tartrate dihydrate	0.0900	-	-
Sodium lactate	0.0850	-	-
Sodium pyruvate	0.0860	-	-
Properties			
pH	**4.5**	**7.4**	**7.4**

4.4.5. Sequential extraction procedure (SEP)

Three different sequential extraction protocols were applied in the study for mercury fractionation. Two SEPs were specifically designed for mercury fractionation (Neculita *et al*., 2005; Bloom *et al*., 2003), whilst one (m-BCR) has been used for the

fractionation of metals in sediments (Rauret *et al.,* 1999). Brief details of these three methods are given in Table 4.8.

For an internal check on the procedure an additional step was applied. After the sequential extraction steps, the residual mercury content was determined by digestion with nitric, hydrochloric and hydrofluoric acid. The inclusion of the residual step in the procedures was for an internal check for quality control purposes, where the sum of steps 1 to 4 or 5 was compared with results of a separate acid digestion (Rauret *et al*., 2000). Extractions were performed using the reagents, and procedures given in Table 4.8. Samples were extracted for 18 hours and the solution were centrifuged and filtered. After each fraction the residue was rinsed with deionized water and added to the filtrate and diluted to volume (specified volume). This procedure was repeated for each extraction except for the last (aqua regia extraction step). All extracts (fractions) were stored in glass bottles with lined-teflon caps in refrigerator (4 °C) until analysis. The SSE protocol has an extra step worth mentioning, where the first three fractions were centrifuged and filtered through nitrocellulose filter units. Fractions F1, F2 and F4 were oxidized by adding 1.25 mL of 0.2 M BrCl solution per 125 mL solution before the rinse was added and the solution diluted to the required volume. The F3 fraction due to its high alkalinity value, was oxidized by adding 8.0 mL of 0.2 M BrCl solution per 100 mL solution.

Details of the experimental protocols are described in Table 4.8 (Neculita *et al*., 2005; Bloom *et al*., 2003; Rauret *et al*., 1999).

Table 4.8: Reagents and conditions employed for the three sequential extraction procedures.

STEP	FRACTION	SEQUENTIAL EXTRACTION PROCEDURE		
		[a] **novel sequential extraction procedure (n-SEP) (Neculita *et al*., 2005)**	[b] **Sequential selective extraction (SSE) (Bloom *et al*., 2003)**	[b] **Modified BCR (m-BCR) (Rauret *et al*., 1999)**
1	Water soluble **(F1)**	20 mL of deionized water 20 ± 2°C, 2 hrs, constant shaking	40 mL of deionized water Room temperature, 18 ± 4 hrs, constant shaking	40 mL of 0.11 mol L^{-1} CH_3COOH Room temperature, 16 hr, constant shaking
2	Exchangeable **(F2)**	20 mL of 1 M $CaCl_2$ (pH 5) 20 ± 2°C, 2 hrs, constant shaking	40 mL of 0.1 mol L^{-1} CH_3COOH + 0.01 mol L^{-1} HCl (pH 2)	
	Iron and manganese oxyhydroxides			40 mL of 0.5 mol L^{-1} $NH_2OH{\cdot}HCl$ (pH 1.5) Room temperature, 16 hr, constant shaking
3	Mercury bound with organic matter **(F3)**	20 mL of 0.2 M NaOH 20 mL of 4% (v/v) CH_3COOH 20 ± 2°C, 2 hrs, constant shaking	40 mL of 1 mol L^{-1} KOH	10 mL of 30% (w/v) H_2O_2 Room temp., 1hr, occasional agitation + 85°C 10 mL of 30% (w/v) H_2O_2 50 mL 1 mol L^{-1} NH_4Oac (pH 2)
4	Elemental Hg **(F4)**		40 mL of 12 mol L^{-1} HNO_3	
5	Residual mercury **(F5)**	$HCl/HNO_3/HF$ (9:3:1, v:v:v)	$HCl/HNO_3/HF$ (9:3:1, v:v:v)	$HCl/HNO_3/HF$ (9:3:1, v:v:v)

[a] For 2.00 ± 0.10 g sample; [b] for 1.00 ± 0.05 g sample

4.4.6 Health risk assessment of mercury in dust

4.4.6.1 Exposure assessment

In order to determine the average daily dose or chemical daily intake of mercury exposure to humans from dust, the United States Environmental Protection Agency (USEPA) model was used. This model was applied to three exposure routes, which are ingestion, inhalation, and dermal contact and were calculated using equations (4), (5), (6), and (7), respectively:

Ingestion dose:

$$CDI_{ing}(mg\ kg^{-1}\ day^{-1}) = C(mg\ kg^{-1}) \times \frac{R_{ing} \times CF \times EF \times ED}{BW \times AT} \quad (4)$$

Inhalation dose:

$$CDI_{inh}(mg\ kg^{-1} day^{-1}) = C(mg\ kg^{-1}) \times \frac{R_{inh} \times EF \times ED}{PEF \times BW \times AT} \quad (5)$$

Dermal contact dose:

$$CDI_{dermal}(mg\ kg^{-1} day^{-1}) = C(mg\ kg^{-1}) \times \frac{SA \times CF \times SL \times ABS \times EF \times ED}{BW \times AT} \quad (6)$$

Inhalation of vapours:

$$CDI_{vapour}(mg\ kg^{-1} day^{-1}) = C(mg\ kg^{-1}) \times \frac{R_{inh} \times EF \times ED}{V_F \times BW \times AT} \quad (7)$$

Where, CDI_{ing} is a daily exposure amount of mercury through ingestion (mg kg^{-1} day^{-1}); CDI_{inh} is a daily exposure amount of mercury through inhalation (mg kg^{-1} day^{-1}); CDI_{derm} is a daily exposure amount of mercury through the absorption via the skin (mg kg^{-1} day^{-1}); CDI_{vapour} is a daily exposure amount of elemental mercury through inhalation. The exposure factors for these models are displayed in Table 4.9.

Table 4.9: Exposure factors for dose models.

Factor	Definition	Units	Value	
			Children	Adult
c	Mean concentration of mercury	*mg kg^{-1}*		
[2]R_{ing}	Ingestion rate of soil	*mg day^{-1}*	200	100
[1]EF	Exposure frequency	*days year^{-1}*	350	350
[3]ED	Exposure duration	*years*	6	24
[1]BW	Average body weight	*kg*	15	55.9
[2]AT	Average time	*days*	365×ED	365×ED
CF	Conversion factor	*kg mg^{-1}*	1.00×10^{-6}	1.00×10^{-6}
[1]R_{inh}	Inhalation rate	*m^3 day^{-1}*	5	20
[1]PEF	Particle emission factor	*m^3 kg^{-1}*	1.32×10^{9}	1.32×10^{9}
[1]SA	Surface area of the skin that contacts the dust	*cm^2*	1800	5000
[1]SL	Skin adherence factor for dust	*mg cm^{-2}*	1	1
[1]ABS	Dermal absorption factor (chemical specific)		0.001	0.001
[1]V_F	Volatilization factor for elemental Hg	*m^3 kg^{-1}*	32675.6	32675.6
[x]RfD_{ing}			3.00×10^{-4}	
[y]RfD_{inh}			8.57×10^{-5}	
[z]RfD_{dermal}			2.10×10^{-5}	

[1] US Environmental Protection Agency, 2001
[2] US EPA, 1989.
[3] US EPA, 2001.

4.4.6.2 Risk characterization

Health risk assessment of exposure to dust was characterized into two categories, namely carcinogenic risk and non-carcinogenic risk. For the non-cancer risk, this was achieved by determining the hazard quotient (HQ) and hazard indices (HI) for enriched elements. The hazard quotient was determined by dividing the chronic daily intake (CDI) by a specific reference dose (RfD) as shown by eq. (8):

$$HQ_{ingestion} = \frac{ADD}{RfD} \quad (8)$$

$$HQ_{inhalation} = \frac{EC \times 0.001}{RfC} \quad (9)$$

Where, RfD is an estimation of maximum permissible risk on human population through daily exposure taking into consideration of sensitive group during a lifetime (mg kg^{-1} day^{-1}), RfC is reference concentration of inhaled material (mg m^{-3}), EC is exposure concentration (mg kg^{-1}), CDI is daily dose (mg kg^{-1} day^{-1}) In order to estimate the risk factor, the HQ value was assessed and when HQ ≤ 1, it indicated no adverse health effects while HQ > 1 indicated likelihood of adverse health effects (USEPA, 1986). The threshold value of RfD can also be used to estimate whether or not there are adverse health effects during a life time. This is achieved by comparing with the average daily dose (CDI) value to the reference dose. In cases were ADD was lower than the reference dose, it indicated no adverse health effects whereas if ADD was higher than the reference dose, it indicated a greater possibility of adverse health effects would be experienced (USEPA, 1993).

The determination of hazard index (HI) ascertains the cancer risk associated with various metals, and metalloids. Hazard index is calculated as shown in the eq. (10) (De Miguel *et al*., 2007; Lim *et al*., 2008; Zheng *et al*., 2010a, 2010b):

$$HI = \sum HQ_i \quad (10)$$

If HI < 1, there is no adverse health effects. If HI > 1, there is a greater chance of adverse health effects (Kong *et al*., 2011). Carcinogenic risk is the probability of an individual developing any type of cancer from lifetime exposure to carcinogenic hazards. The acceptable or tolerable risk for regulatory purposes is in the range of 10^{-6} – 10^{-4} (Ferreira-Baptista and De Miguel, 2005).

For carcinogenic risk (CR), the dose was multiplied by the corresponding slope factor (kg day mg^{-1}) to produce an estimate of cancer risk for the ingestion exposure pathway (U. S. Environmental protection Agency, 2011; Zheng *et al*., 2010a; Paustenbach, 2002; Kolluru *et al*., 1996), as shown by the eqn. (11):

$$CR = D \times SF_0 \quad (11)$$

For the health effects of inhalation of particulate matter, the excess lifetime cancer risk was calculated by the following eq. (12) (U. S. Environmental protection Agency, 2011):

$$CR = EC \times IURF \quad (12)$$

Where EC is chronic daily exposure concentration averaged over a 70 year lifetime for inhalation of particulate matter, IURF is inhalation unit risk factor (m^3 mg^{-1}).

Total risk was calculated using the following equation (13) (US EPA, 1989):

$$\sum Risk_{cancer} = CR_{inhalation} + CR_{ingestion} \quad (13)$$

The interpretation of the risk values was done with aid of list values in Table 4.10.

Table 4.10: Interpreting the risk numbers (Rendell and McGinty, 2007).

Risk	Risk in exponential	Risk in decimal	Read as a risk of …
1.0E-08	1×10^{-8}	0.00000001	1 in 100 million
1.0E-07	1×10^{-7}	0.0000001	1 in 10 million
1.0E-06	1×10^{-6}	0.000001	1 in 1 million
1.0E-05	1×10^{-5}	0.00001	1 in 100 000
1.0E-04	1×10^{-4}	0.0001	1 in 10 000
1.0E-03	1×10^{-3}	0.001	1 in 1 000
1.0E-02	1×10^{-2}	0.01	1 in 100
1.0E-01	1×10^{-1}	0.1	1 in 10

The total risk assessed was interpreted using U. S. Environmental Protection Agency benchmark as far as it applies to South African conditions. Acceptable risk factors are reported to lie between 1.0E-06 and 1.0E-04 (U. S. Environmental Protection Agency, 1991). The value of acceptable risk at one in a million (1.0E-06) has been widely accepted in scientific literature for various uses, however, it remains without scientific evidence and requires further investigations.

4.5 Quality Assurance/Quality Control (QA/QC)

The QA/QC program comprised of the analysis of procedure blanks, reagent blanks, and certified reference materials (CRM) (Table 4.11). The reagent blanks were made up of the batch solutions used in the leaching experiments whilst procedural blanks consisted of running an aliquot of the extraction fluids (acids added to digestion vessels with no samples) simultaneously with the field samples while River Sediment-Extractable Metals (LGC6187), Metals in Sediments (CRM015-050), and Estuarine sediment (CC580) were used as the reference material. Results were blank corrected. All samples were run in triplicate unless otherwise stated and standard QA/QC measures taken during analysis, including calibration using standards prepared in the same solution matrices as the extraction tests, blanks, and control samples, all of which were analyzed at frequencies sufficient to ensure acceptable QA/QC.

Table 4.11: Total mercury concentration in CRMs by FIMS 400/FI-MH-AAS.

CRM		Hg_{TOT} ± SD (n=5; mg kg^{-1})			
Type	**Name**	**Certified**	**Measured**	**RSD (%)**	**Recovery (%)**
Sediment	RTC015-050	0.221 ± 0.006	0.220 ± 0.048	11.76	99.50
Sediment	LGC6187	1.400 ± 0.100	1.441 ± 0.117	9.98	103.00
Sediment	ERM-CC580	132.000 ± 3.00	131.240 ± 4.90	3.70	99.00

The instrumental detection limit (LOD) was calculated using LOD = 3.00 × SD, where SD is the standard deviation of replicates of procedural blanks. Figure 4.4 illustrates the calibration curve for mercury at a specific wavelength (253.7 nm) from mercury analyzer (FIMS 400/FI-MH-AAS).

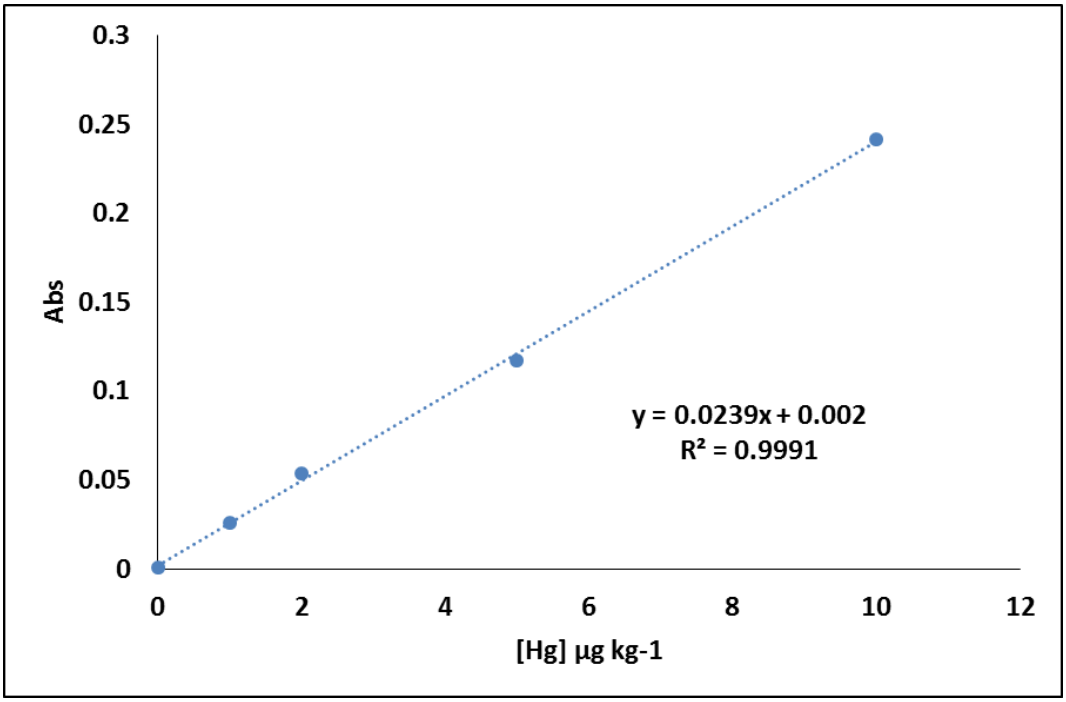

Figure 4.4: Typical calibration curve for mercury from FIMS 400/FI-MH-AAS.

Chapter 5

Determination of mercury in street dust

Spatial distribution, contamination assessment factors, and seasonal variation of total mercury concentration in Johannesburg street dust was determined. The pH of the dust, its particle size distribution and total elemental analysis were carried out to understand the interactions with mercury in the dust. The dust was characterised by the following techniques: ED-XRF, XRD, SEM-EDS.

5.1 Mineralogical characteristics of dust

ED-XRF results of some selected dust samples is presented in Table 5.1. Major elemental concentrations are: SiO_2 (30.5 - 86.3%), Al_2O_3 (13.5 – 19.8%) and Fe_2O_3 (3.7–7.1%). From this, quartz is the principal oxide in the dust samples with an average of 66.3%, followed by small concentrations of alumina, arsenic, calcium, chromium, copper, manganese, nickel, potassium, and titanium oxides. Note, however, that alumina was the lowest oxide available in the selected samples.

Mineralogy of the dust determined by XRD was dominated by quartz, and ranged from 74.3 to 97.6 wt. % with an average of 87.56 wt. % (Table 5.2). The rest of the mineral phases were below detection limit, and it ranged from 2 to 10 mg kg^{-1} depending on the metal of interest (Figure 5.1; Rösner *et al*., 1999), and the quartz considerably prevailed over the minor mineral phases. For tailings material, both from East and West rand, quartz was by far the most dominant mineral phase ranging from 65 to 81 wt. % and 70 to 93 wt. %, averaging 71 and 78 wt. % (Table 5.2). The presence of quartz in large quantities reflects the original type of rock present in this region. In comparison, dust had the highest amount of quartz as compared to the tailings materials. This could be attributed to the small particle sizes with a large surface area, which allows enrichment of different minerals and mineral phases to take place (Zverina *et al*., 2012; Duong and Lee, 2011; Luo *et al*., 2011; Zhao *et al*., 2011; Zhao *et al*., 2010; Duong and Lee, 2009; Madrid *et al*., 2008). The lack of pyrite in the tailings material can be attributed to the shallow sampling depth at the top of the tailings, within the oxidized zone, where the depletion of pyrite occurred due to years of oxygen exposure. The results of oxidation of pyrite led to the formation of secondary minerals such as gypsum ($CaSO_4$) and jarosite ($KFe_3(SO_4)(OH)_6$), and a low pH in the tailings pore water (AMD). Blight and Du Preez (1997) concluded that the top layer (1-1.5 m thick) of TSFs were characterized by high concentration of heavy metals and sulphates, and low pH due to oxygen exposure.

Table 5.1: ED-XRF mineral composition (wt. %) of PM_{25} dust.

Sample	Major Element (wt. %)												
	SiO_2	ZnO	MnO	Cr_2O_3	TiO_2	CaO	CuO	V_2O_5	K_2O	Fe_2O_3	Al_2O_3	NiO	As_2O_3
Res. Alberton 1	86.3	3.16	2.50	1.82	1.61	1.64	2.35	-	-	-	-	0.65	-
Res. Alberton 2	63.4	3.67	6.90	4.15	4.01	7.75	3.06	2.60	2.30	1.56	0.59	-	-
Res. Alberton 3	55.6	7.18	11.6	8.92	6.20	6.34	-	-	-	2.60	1.53	-	-
Res. Boksburg 1	66.0	4.00	5.15	4.12	5.14	2.95	4.55	3.55	2.15	1.55	0.86	-	-
Res. Boksburg 2	30.5	12.5	16.5	13.0	11.5	7.65	-	-	-	-	-	-	8.45
Res. Diepkloof	68.9	1.45	2.20	1.52	3.75	5.94	1.33	1.47	2.24	8.30	1.62	1.31	-
Res. Riverlea	77.4	-	2.81	2.03	3.78	8.75	-	-	2.00	2.60	0.64	-	-
Res. Sandton	62.0	4.17	5.74	4.68	5.29	4.51	4.40	3.62	3.35	1.43	0.79	-	-
CBD 1	64.4	4.61	5.28	4.16	4.44	8.01	4.17	-	2.51	1.64	0.81	-	-
CBD 2	66.1	6.21	7.23	-	5.92	7.80	-	-	3.12	2.39	1.18	-	-
CBD 3	81.0	6.78	1.69	1.41	1.58	1.48	2.06	-	-	-	-	-	3.99
CBD 4	63.6	4.33	5.56	4.59	4.61	4.70	4.16	3.42	2.38	1.84	0.85	-	-
CBD Cemetery	84.4	4.51	-	2.89	2.79	-	5.38	-	-	-	-	-	-
Soccer City	73.1	-	4.45	3.59	5.73	3.28	-	3.09	2.31	3.56	0.91		
Ophirton	70.4	4.21	5.17	3.96	4.18	4.70	-	3.02	2.32	1.32	0.74	-	-
Selby 1	71.8	3.76	3.64	3.34	3.76	5.84	3.60	-	1.98	1.74	0.54	-	-
City Deep	54.8	6.67	8.59	12.2	5.41	5.49	-	-	3.08	2.47	1.31	-	-
Crownwood	67.4	3.52	4.48	3.50	3.85	4.20	2.79	2.45	2.16	2.04	0.64	2.95	-
Heriotdale	54.5	4.23	6.78	4.96	4.22	14.1	4.46	-	3.11	2.65	1.00	-	-
PPC Cement	64.6	3.14	3.97	3.18	3.07	5.60	3.73	2.18	1.95	2.15	0.63	5.81	-
Detection limit	0.01		0.001	0.001	0.003	0.01	0.0003	0.001	0.005	0.02	0.01	0.001	

Table 5.26: Comparison of X-Ray Diffraction (XRD) mineralogical results of street dust, tailings dust, gold ore, and material from gold mine tailings expressed in weight %.

Sample	**Dust from this study**				**[a]Tailings material**	**[b]Pyrite bearing gold ore**	**[c]Gold Tailings**				
	Heriotdale	**City Deep**	**CBD 2**	**Boksburg 1**			**Site 1**	**Site 2**	**Site 3**	**Site 4**	**Site 5**
Quartz	94.4	90.8	90.8	74.3	78.0	74.0	80.5	70.3	69.3	64.7	71.0
Pyrophyllite	**bdl*	**bdl*	**bdl*	**bdl*	2.0	12.0	-	-	-	5.7	16.5
Pyrite	**bdl*	**bdl*	**bdl*	**bdl*	-	9.0	1.0	1.0	1.0	-	1.5
Kaolinite/Chlorite	**bdl*	**bdl*	**bdl*	**bdl*	-	2.0	7.3	8.3	6.7	5.0	3.0
Jarosite	**bdl*	**bdl*	**bdl*	**bdl*	3.0	1	2.7	2.7	1.0	1.0	1.5
Plagioclase	**bdl*	**bdl*	**bdl*	**bdl*	-	1	-	-	-	-	-
Mica	**bdl*	**bdl*	**bdl*	**bdl*	-	1	9.5	9.8	6.3	5.3	5.5
Chloritoid	**bdl*	**bdl*	**bdl*	**bdl*	6.0	-	-	9.5	15.0	19.7	2.3
K-Feldspar	**bdl*	**bdl*	**bdl*	**bdl*	-	-	1.0	1.0	1.0	1.0	-
Clay	**bdl*	**bdl*	**bdl*	**bdl*	-	-	-	-	1	-	-
Gypsum	**bdl*	**bdl*	**bdl*	**bdl*	0.1	-	12	-	-	-	-
Muscovite											

**bdl – below detection limit*

[a] Rösner, (1999)

[b] Tlowana *et al*., (2013)

[c] Nengovhela *et al*, (2006)

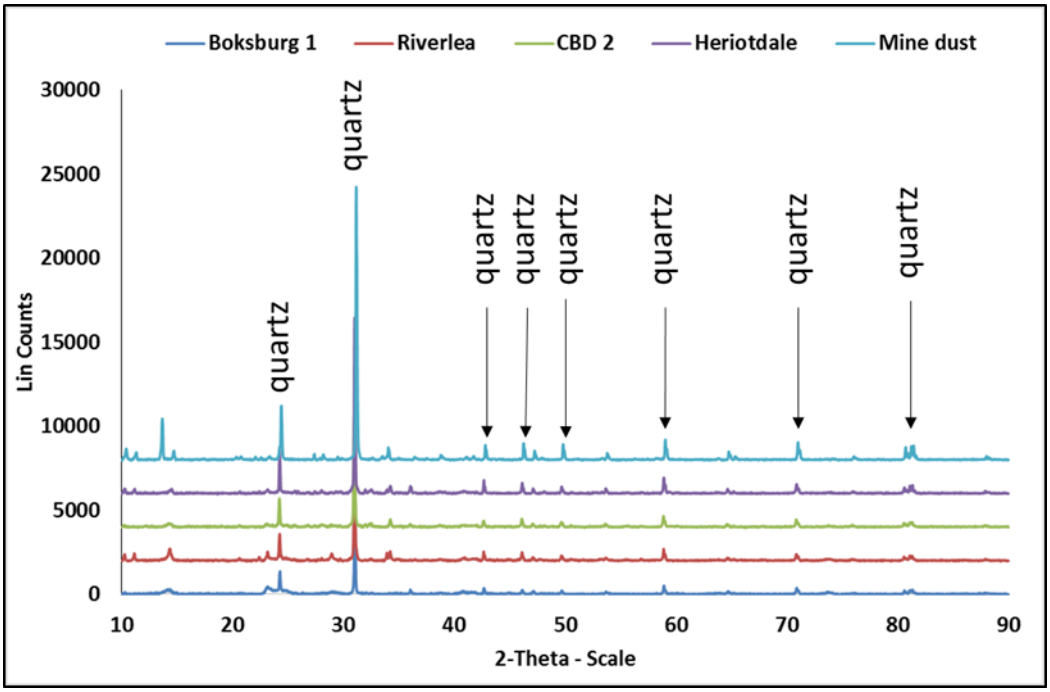

Figure 5.1: X-ray diffractograms showing quartz as the main mineral in urban dust from Johannesburg for selected samples (Boksburg 1, Riverlea, CBD 2, Heriotdale and mine dust). The rest of diffractograms are placed in appendix B.

This relationship between pyrite and oxygen was further confirmed by Nengovhela *et al*., (2006). The impact of the vegetation on the tailings in terms of the presence and consumption of oxygen was well described. The oxygen diffused deeper into the tailings due to the porosity caused by roots. This further accelerated pyrite oxidation leading to a continued AMD generation, and resulting in a prolonged pollution as long as the tailings exist. This highlighted the differences between the rehabilitated and unrehabilitated tailings. Unrehabilitated tailings were characterized by loosely bound fine particulate matter at the top, with high concentration of trace elements, with low pH (pH<3). The exposure of the tailings surface to oxygen resulted in the trace elements being leached out hence there were below detection limit from XRD (Table 5.2) on dust samples. Rehabilitated tailings had a greater depth of oxygenated zone, with low pH and the vegetation cover prevented any erosion talking place from the surfaces. However, precipitation of trace metals occured at outer toe walls of TSFs, and in surfaces where seepage discharge take places due to the evaporation of supersaturated solutions (AMD)

(Tutu *et al*., 2008; Naicker *et al*.,2003). Windblown dust from these tailings resulted in the distribution of dust laden with toxic trace metals**.**

The minor mineral elements determined were as follows: mica, chlorite, chloritoid, pyrophyllite, clay, gypsum, pyrite, jarosite, pyrite, rutile, hematite, clinochlore, muscovite, and k-feldspar (Tlowana *et al*., 2013; Ojelede, 2012; Nengovhela *et al*., 2006). Total elemental analysis determined the following trace elements: Al. As, Ca, Cd, Co, Cu, Cr, Fe, Hg, Ni, Mn, Mo, Si, Ti, Pb, S, U, V, and Zn (Table 5.2), and enrichment of Al, Ca, Fe, Mn, Ti, and Si was observed in the tailings material, street dust and windblown dust (PM_{10} and PM_5 fractions) (Tlowana *et al*., 2013; Ojelede, 2012; Nengovhela *et al.*, 2006). However, Al, Ca, Fe, Mn and Si elements are of geologic nature.

In comparison with other cities, Moreno *et al*. (2007) identified silica, kaolinite, alunite, jarosite, illite and iron oxides in PM_{10} particles in the vicinity of an ore processing plant near a gold mine in Southeastern Spain, while Querol *et al*. (2000) identified pyrite as the main component, together with clay, quartz, calcite, gypsum and plagioclase after a spill of mining heavy metals in the South western Spain.

The SEM was used to view the structure of particulate matter in the dust. A larger percentage of the particulate matter consisted of quartz with well define crystalline structures and at times coated with other elements such as sulphur, manganese etc. (Figure 5.2, 5.3, and 5.4).

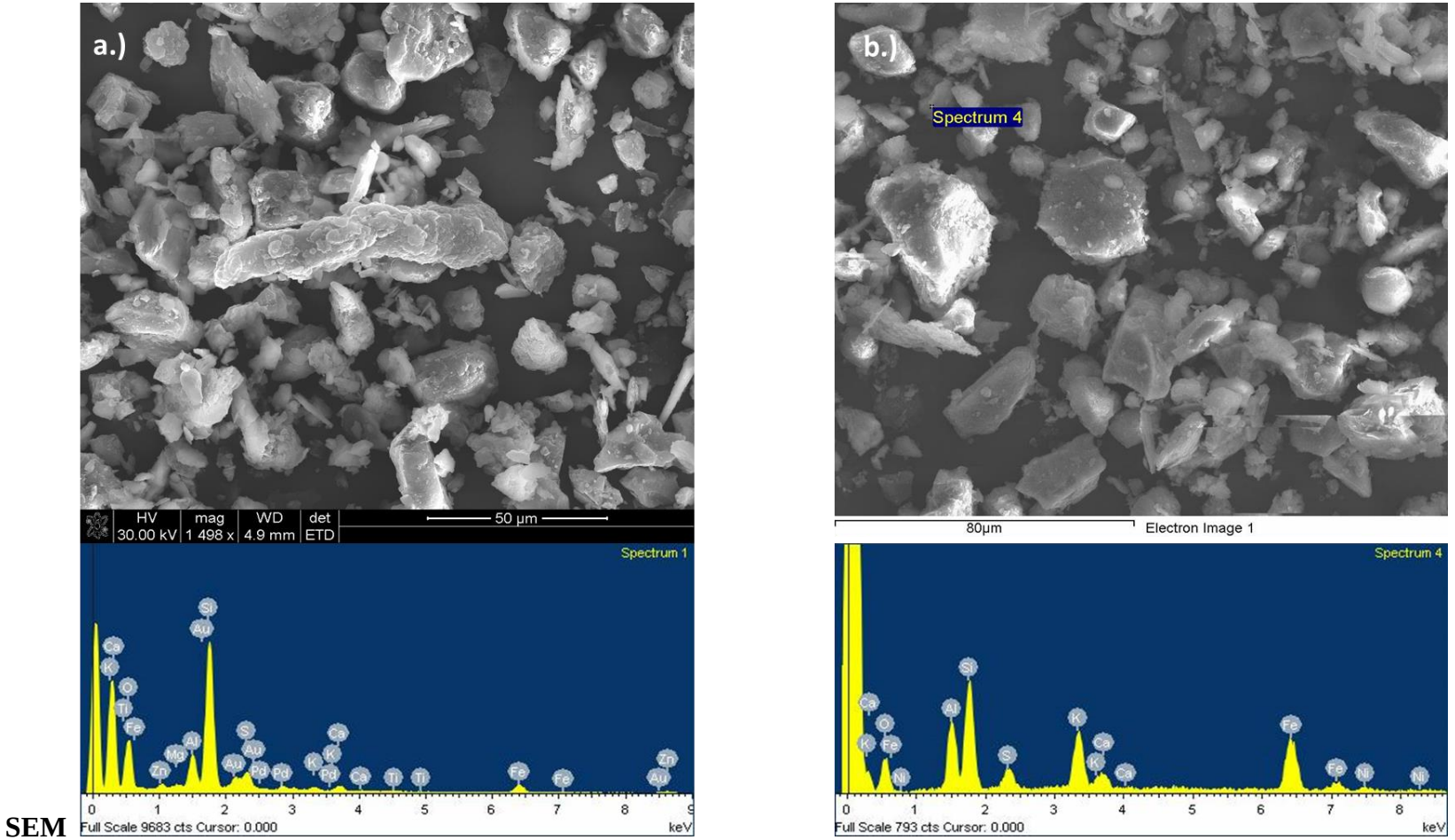

SEM

Figure 5.2: SEM images of Johannesburg dust and EDS spectra. (a.) Crownwood sample indicates the presence of Si, Al (dominant); Fe, Ca, Mg, Zn, K, Ti, and S. (b.) PPC Cement sample indicates the presence of Si, Al, Fe (dominant), S; K, Ca, Ni.

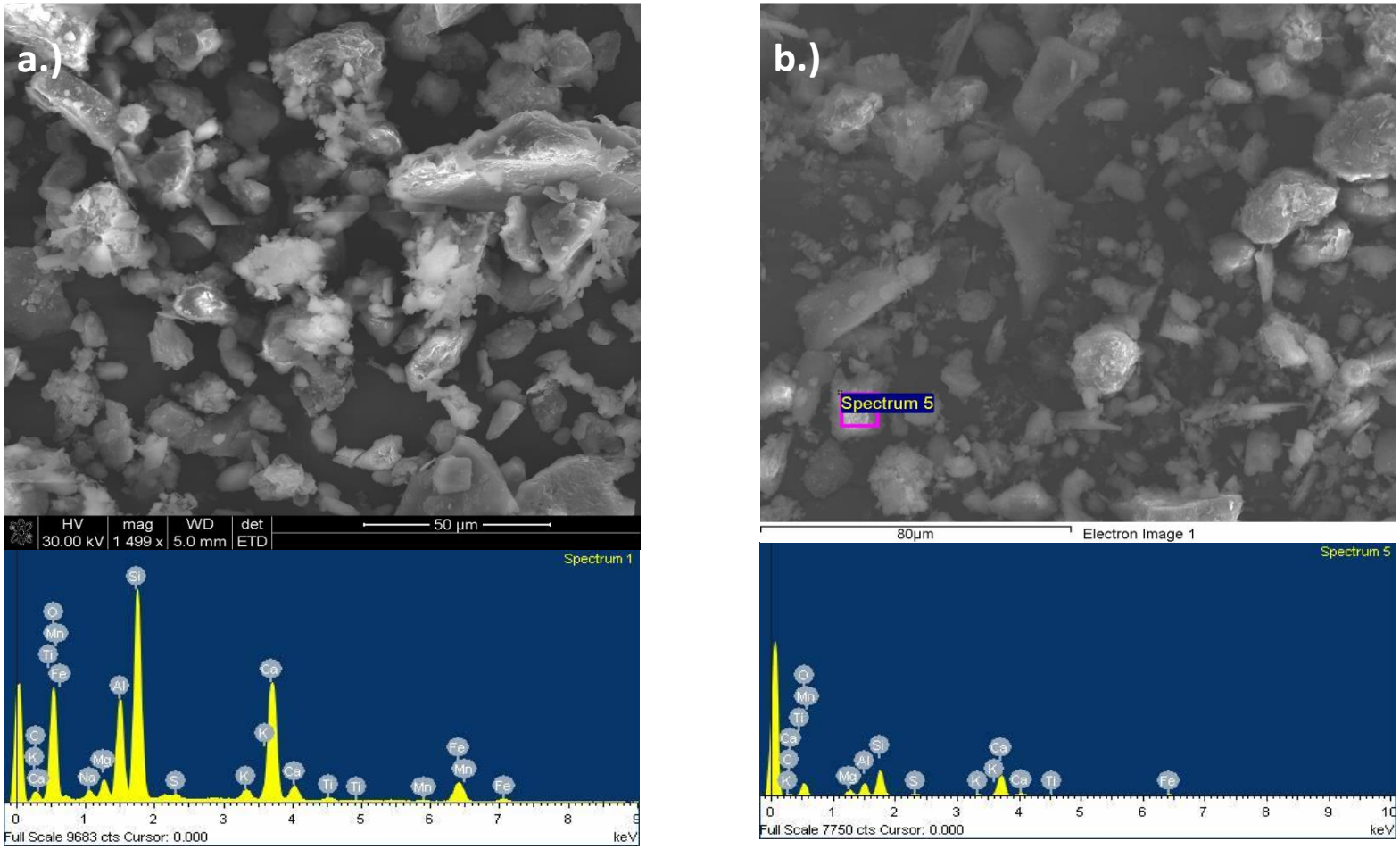

Figure 5.3: SEM images of Johannesburg dust and EDS spectra. (a.) Cemetery sample indicates the presence of Si, Al; Fe, Ca, Mg, Mn, Na, K, Ti, and S. (b.) Riverlea sample indicates the presence of Si, Al, Fe, S; K, Ca, Ti, Mn, Mg.

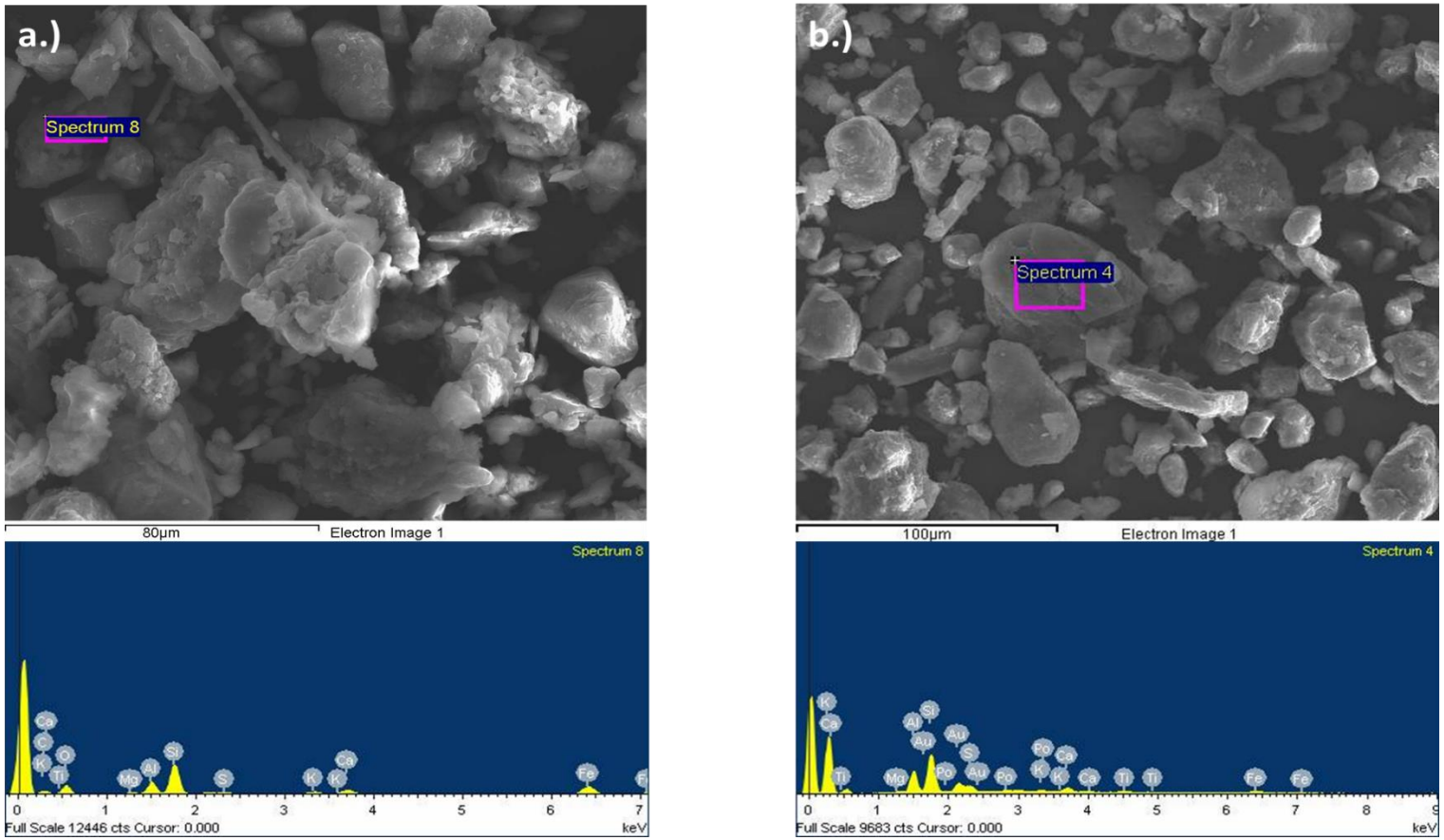

Figure 5.4: SEM images of Johannesburg dust and EDS spectra. (a.) CBD 4 sample indicates the presence of Si, Al; Fe, Ca, Mg, K, Ti, and S. (b.) Sandton sample indicates the presence of Si, Al, Fe, S; K, Ca, Ti, Mg.

5.2 Hg_{TOT} concentration in dust fractions

Results of Hg_{TOT} obtained from Johannesburg dust samples in 3 different particles size fractions are presented in Figure 5.5 (and in Table A.1 placed in appendix A) whilst the spatial distribution of Hg_{TOT} in PM_{25} fraction is shown in Figure 5.6. Hg_{TOT} in Johannesburg dust ranged from 80 to 243 (PM_{100}), 122 to 499 (PM_{50}), and 270 to 1349 (PM_{25}) µg kg^{-1}, with a mean of 151, 291, and 600 µg kg^{-1}, and are about 2, 3, and 7 times higher than the crustal value of Hg in soils (85 µg kg^{-1}) for PM_{100}, PM_{50}, and PM_{25}, respectively. The percentage relative standard deviation (%RSD) between replicates in all samples was not greater than 10%.

The highest $Hg_{TOT,}$ was observed in the samples collected from the industrial sites followed by samples from the Central Business District (CBD), and lastly samples from residential areas. This trend was evident in the three different particle size fractions. High Hg_{TOT} values were mostly obtained in the south-eastern and south-western parts of Johannesburg. This is mainly due to the presence of TSFs from historic gold mining activities in the area and clearly shows the impact of the prevailing wind direction on distribution of Hg_{TOT}. The dominant prevailing wind directions were north north-westerly, north westerly, northerly, and north north-easterly with 13.9%, 13.5%, 9.1%, and 8.9%, respectively (Figure 5.7). These winds bring the greatest concentration of Hg_{TOT}, indicating possible anthropogenic emission sources in these directions. Lastly, the highest Hg_{TOT} was found in PM_{25} whilst the lowest Hg_{TOT} was measured in PM_{100}, showing that Hg_{TOT} increased as particle size decreased.

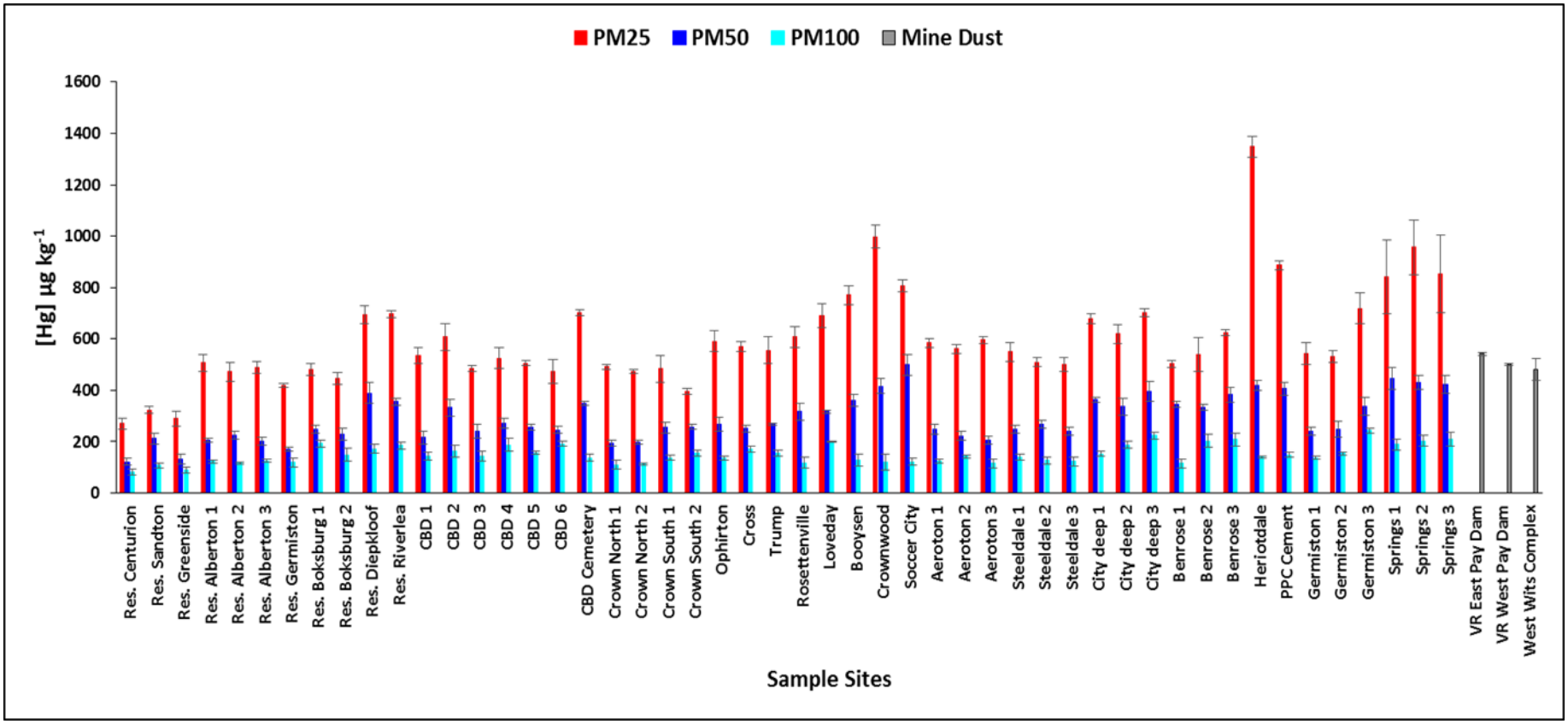

Figure 5.5: Comparison of mean Hg_{TOT} concentration in three different particle size fractions in dust samples. Error bars represent standard deviation of the mercury concentrations, (n=3).

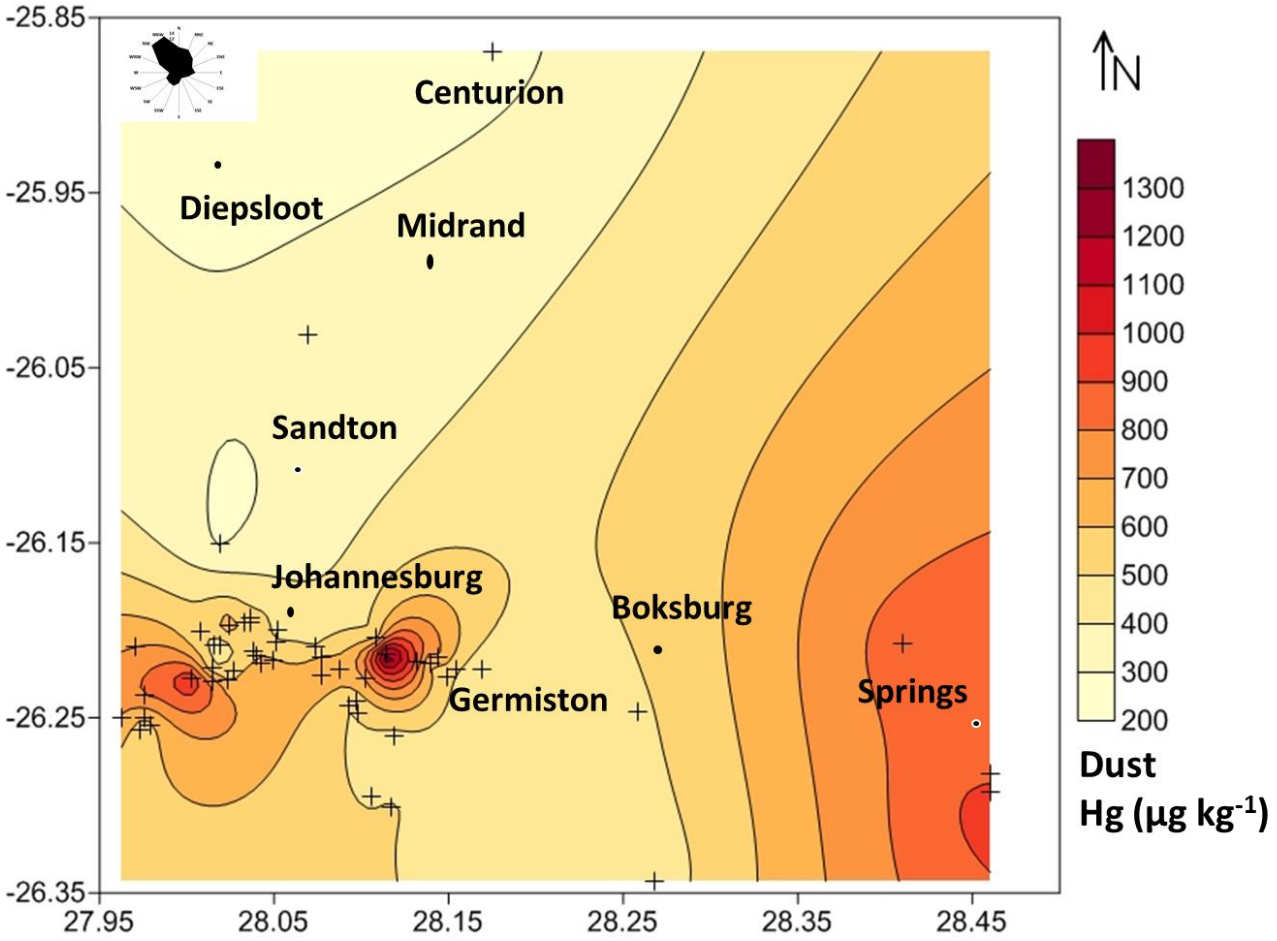

Figure 5.6: Spatial distribution of Hg_{TOT} in PM_{25} in dust samples from Johannesburg, South Africa.

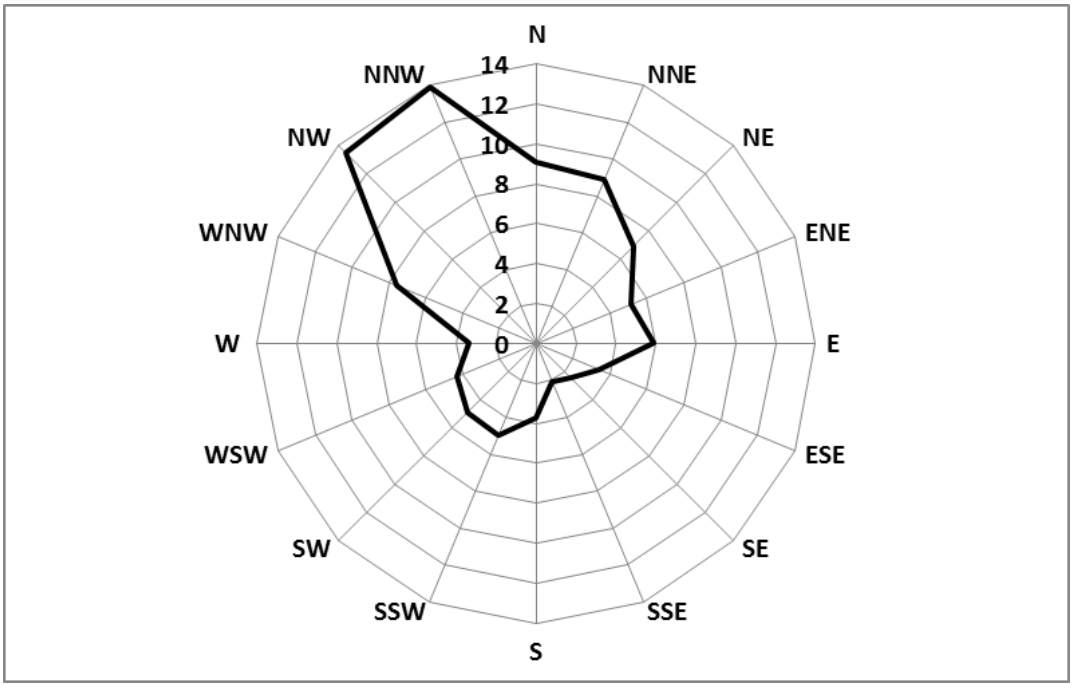

Figure 5.7: Dominant prevailing wind direction of Johannesburg, South Africa.

Hg_{TOT} in PM_{25} from industrial sites ranged from 500 to 1349 µg kg^{-1}, with an average of 687 µg kg^{-1}. The highest Hg_{TOT} was found in the TSF reprocessing area (Heriotdale), followed by industrial sites built on TSF footprints (Selby 1 & 2, Loveday, Rosettenville, and Trump), and lastly industrial sites built next to TSF (Aeroton, Benrose, Booysen, City Deep, Germiston, PPC, and Steeldale). Significant quantities of residual tailings materials are left behind due to incomplete reclamation processes resulting in exposure of toxic heavy metals. These metals are susceptible to distribution through leaching by rain water, re-emission and resuspension of dust through wind erosion, and seepage to ground water (Ojelede *et al*., 2012; Tutu *et al*., 2008; 2005; Naicker *et al*., 2003; Rösner and van Schalkwyk, 2000; Marsden, 1986). Hence elevated levels of mercury and other toxic heavy metals.

In the CBD, Hg_{TOT} concentration was found to range from 473 to 702 µg kg^{-1}, with an average of 548 µg kg^{-1}. The highest Hg_{TOT} concentration in the CBD area was found in the vicinity of the Braamfortein cemetery. During the cremation, mercury is released as elemental mercury (Hg^0), and is deposited in the surrounding areas of the crematorium (Mari and Domingo, 2010; Takaoka *et al*., 2010; Nieschmidt and

Kim, 1997; Yoshida *et al*., 1994). Meanwhile, the Hg_{TOT} gradually decreased as you move further away from the cemetery. Hg_{TOT} in PM_{25} dust samples from Braamfontein cemetery were greater than 490, 370, and 115 µg kg^{-1} reported from soils surrounding Purewa crematorium, Hamilton crematorium, and South crematorium, respectively, situated in Remuera, Auckland, New Zealand (Nieschmidt and Kim, 1997). This demonstrated that crematoria acted as a considerable source of Hg to its immediate environment. The presence of Hg in the emissions from the crematorium was attributed to the high Hg content (0.5g) in the dental amalgam fillings in the teeth, which is approximately 50% mercury (Mari and Domingo, 2010). Studies of occupational exposure of individuals working in crematories was carried out in the United Kingdom (UK) by measuring the mercury levels in hair. Only 3% of the crematoria workers were found to have Hg concentration higher than 6 µg g^{-1}, generally considered as a tolerable concentration for mercury in hair (Maloney *et al*., 1998). In countries such as Switzerland and UK, Hg emission calculations from crematories gave ranges of 0.61 to 1.53% of total Hg contamination produced by all waste incineration methods (Mari and Domingo, 2010), and 5.3 to 15.7% of UK mercury emissions to air in 2000 (DEFRA, 2003), respectively. Unfortunately, in the South African case, this kind of study has not been carried out, therefore contribution of Hg from the crematorium to the atmospheric Hg emission was not determined. Globally, atmospheric Hg emissions from crematoria were estimated to account for about 0.8% of the total anthropogenic Hg emissions (Nriagu, 1989; Nriagu and Pacyna, 1988).

In the residential areas, Hg_{TOT} ranged from 270 to 697 µg kg^{-1}, with an average of 462 µg kg^{-1}.The highest Hg_{TOT} of 697 and 693 µg kg^{-1} were determined in Riverlea and Diepkloof (Soweto), respectively. In Riverlea, an old sand dump was being reprocessed, whilst Diepkloof is surrounded by three Crown Gold Recoveries tailings dams (CGR) situated to the north of the township (Figure 5.8). Heavy dust storms in these areas have resulted in dust fallout from tailings in excess of 2 400 mg m^{-2} day^{-1} (Ojelede *et al*., 2012), and led to legal action being taken between communities and mining companies (Annegarn and Sithole, 2002; Annegarn *et al*.,

1991; Marsden, 1987; Blight, 1989; Blight and Caldwell, 1984). The excessive dust fallout caused visibility problems, increased chances of exposure through ingestion and inhalation of particulate matter, became a nuisance due to its deposition on surfaces, and contamination of exposed environments (Figure 5.9). Ojelede *et al*., (2012), reported high levels of PM_{10} and PM_5 (i.e. thoracic and respirable fractions) from TSFs surrounding Soweto, having a mean of 53% vol. and 37% vol., respectively. These results indicated that TSFs were rich in fine material, representing a higher risk factor during dust storm episodes. Literature has reported that respirable and thoracic fractions readily penetrate and are easily deposited in trachea-bronchial-alveoli region of the human respiratory track resulting in a host of respiratory problems (Pope III *et al*., 2004; Nemmar *et al*., 2002; Fernandez-Espinosa *et al*., 2001; Renwick *et al*., 2001). Elemental analysis and physical examination of dustfall material revealed TSFs as the dominant source of particulate matter collected on filters (Ojelede *et al*., 2012).

Figure 5.8: Sampling sites and Hg_{TOT} concentration results for Aeroton, Diepkloof, Riverlea townships, and Soccer City in relation to the tailings dams.

Figure 5.9: Dust storm episode associated DRD gold mine tailings in Soweto.

The lowest Hg_{TOT} (270 µg kg^{-1}) was determined in the suburb of Centurion in Pretoria. This residential area is far away from point sources of mercury emission. The presence of mercury and other metals and metalloids in dust in the residential areas was attributed to other anthropogenic sources, most likely traffic emissions (both exhaust and non-exhaust), as major highway passes through some suburbs. Elements such as Ba, Zn, and Pb found in fine/ultrafine and nano particles were attributed to road traffic emissions (Lin *et al*., 2005). While trace elements such as Cu, Zn, Ba, Sb, and Mn are characteristics of non-exhaust emissions (Kwon and Castaldi, 2012; Oliveira *et al*., 2011; Gietl *et al*., 2010; Amato *et al*., 2009; El Haddad *et al*., 2009). The volumes of the traffic increases during peak hours, increasing the emissions (Duong and Lee, 2011; Amato *et al*., 2011a, b; Omstedt *et al*., 2005).

The contribution of mercury from burning petroleum-based fuels is relatively low, however, the actual figures on the concentration and fate of the mercury in common fuels is lacking (Wilhelm and Bloom, 2000). The use of mercury in cars is primarily

in switches that operate convenience lights under the hood and trunk, and in anti-lock brake mechanisms (Lourie, 2003). Some of this mercury is released into the atmosphere during the wear and tear of the anti-lock braking mechanisms whilst most of this mercury is released during the recycling of the cars to make new steel (Lourie, 2003). In this case, the impact of traffic was observable, as the lowest Hg concentrations were determined in residential areas with low traffic intensity. Large traffic volumes were experienced on the highways situated next to the TSFs, and industrial areas. However, due to the large concentration of metals and metalloids in the tailings, the enrichment is believed to be from anthropogenic sources.

To completely understand the spatial distribution of Hg_{TOT} in gold mining environment, samples were also collected from two different active mining sites and their concentrations were as follows: 541, 500, and 480 µg kg^{-1} for Vaal River (VR) 1 and 2, and West Wits (WW) mining sites, respectively (Figure 5.10). Possible sources of the dust could be the dusty road surfaces, emissions from mining processes, and exposed TSFs' surfaces.

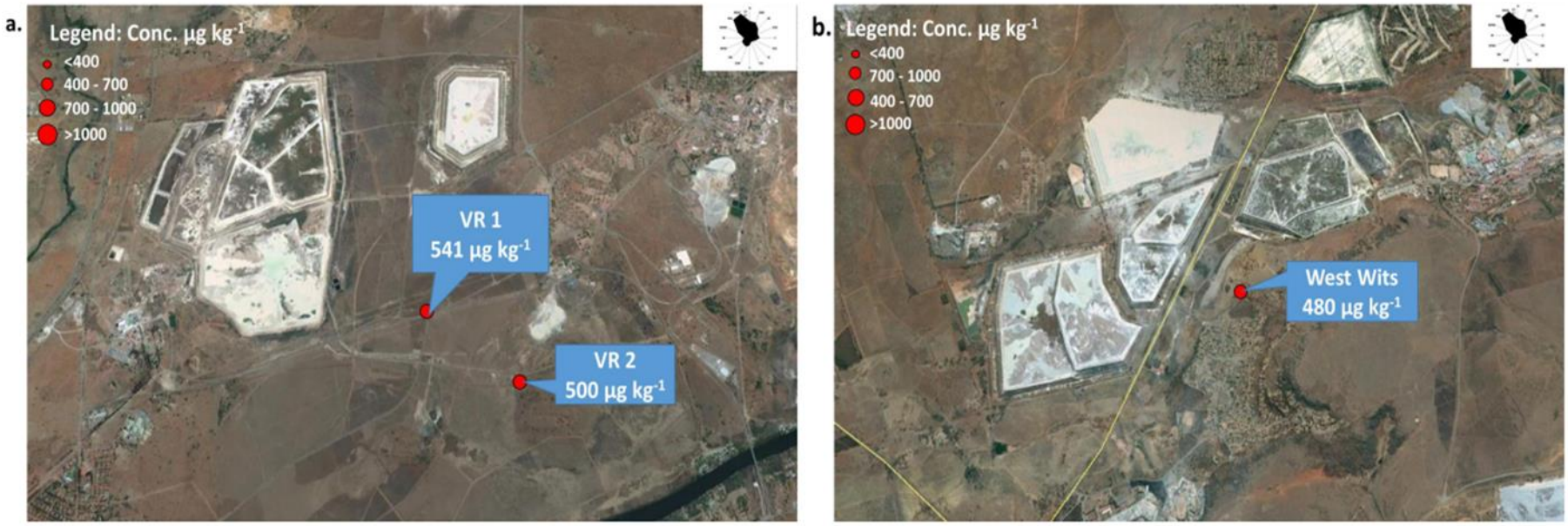

Figure 5.10: Sampling sites and results of Hg_{TOT} concentration of a.) Vaal River 1 and 2, and b.) West Wits mining areas, respectively.

Total mercury concentration in dust from the WW region was similar to the concentrations obtained in the VR region. These results were in agreement with the results obtained from old North tailings and sediments samples collected near the old North TSF (265 and 414 µg Hg kg^{-1}, respectively) in WW area (Lusilao, 2012). Based on the results, the following order was observed: HgDust > HgSediments > HgSoils. This is expected, as metal concentration in dust are greatly enriched due to high adsorption capacity of the small particle size fractions whilst in sediments metals are thought to be higher than in soils due to the accumulation (Ordonez *et al*., 2002). Lusilao (2012), reported that the source of mercury pollution in this area was the gold mining and its activities. This was demonstrated by the decrease of mercury levels away from the point source (mainly TSFs and pollution control dams), as it was observed in this study of dust in Johannesburg.

Of interest was the TSF deposits (both old and recent), where fine particulate matter (respirable and thoracic fractions) are enriched (Ojelede *et al*., 2012). According to Ojelede *et al*. (2012), PM_5 and PM_{10} in the recent slimes dams ranged from 14 to 24 vol.%, and 22 to 38 vol.%, respectively, while, in the older slimes dams and sand dumps, they ranged as follows: (6 to 17 vol.%; 11 to 26 vol.%), and (1 to 8 vol.%; 2 to 12 vol.%), respectively. This explained the impact of improved gold processing technique, where the recent TSFs are characterized by finer particulate matter mainly due to advances in technology, which have resulted in optimized processing techniques leading to finer milling and extraction of residual gold content, hence the reprocessing of old TSFs (Durand *et al*., 201). Ojelede *et al*. (2012), also highlighted that the presence of coarse mode (1.0 to 10 µm) and giant suspended particle (GSP) modes in the airborne suspended particles was a confirmation that their source were the tailings dams. They further showed that the level of coarse fraction dust was highest during the day, and lowest at night occurring at lower wind speeds. Under the influence of high wind speeds, the GSP mode displayed dominance over the coarse mode. Therefore, the release of dust from exposed surfaces of the TSFs resulted in the dispersion and distribution of toxic metals and metalloids including mercury over great distances, causing a health hazard to nearby residents (Maseki, 2013; Oguntoke *et al*., 2013; Ojelede *et al*., 2012). The

wind speed and direction influenced the dispersion and distribution of dust from the TSF (Ojelede *et al*., 2012). This was evidenced by the high Hg_{TOT} in the communities downwind of the tailings. Areas associated with the gold mining belt are grossly affected and they stretch from the Springs (East Rand) to Randfontein (West Rand), a distance of 95 km. The south eastern and south western part of Johannesburg exhibited high Hg_{TOT}, an indication of the prevailing wind direction (north easterly, north, north westerly, particularly in the windiest months of the year, July to September).

Therefore, anthropogenic sources from industry (gold mining and manufacturing) and traffic are thought to be the main cause of metal enrichment in the urban dust of Johannesburg. This is enhanced by the deposition of particles transported by air, which are subsequently a source of natural and anthropogenic elements in dust by means of re-suspension, re-emission, and particles washed-off urban surfaces which have been enriched anthropogenically.

Comparative study of Hg_{TOT} in dust was carried out between Johannesburg and various cities in the world and presented in Table 5.3. Hg_{TOT} from Johannesburg was two times greater than that reported from Manchester, UK, i.e., 600 µg kg^{-1} versus 368 µg kg^{-1}. In both dust samples, Hg was determined in the fine fraction (i.e., PM_{25} and PM_{38} for Johannesburg and Manchester, respectively).

Table 5.3: Hg_{TOT} concentrations in dust of other cities reported in the literature.

Sample Type	Location	Hg_{TOT} (mg kg^{-1})	Reference
Dust	**Johannesburg, South Africa**	**0.60**	**This study**
Street dust	**Manchester, UK**	**0.37**	**Unpublished data**
Household dust	Ottawa, Canada	0.03	Rasmussen *et al*., 2001
Street dust	Luanda, Angola	0.13	Ferreira-Baptista and De Miguel (2005)
Street dust	Kavala, Greece	0.20	Christoforidis and Stamatis, 2009
Street dust	Beijing, China	0.34	Zhang *et al*., 2006
Street dust	Hong Kong, China	0.60	Tanner *et al*., 2008
Topsoil	Palermo, Italy	0.68	Manta *et al*., 2002
Roadway dust	Baoji, China	1.11	Lu *et al*., 2009
Street dust	Glasgow, Scotland	1.20	Rodrigues *et al*., 2006
Street dust	Huludao, China	1.22	Zhen *et al*., 2010
Road dust	Calcutta, India	1.95	Chatterjee and Banerjee, 1999
Street dust	Avile's, Spain	2.56	Ordóñez *et al*. 2003
Attic dust	Idrija, Slovenia	129.00	Gosar *et al*., 2006

The presence of Hg was attributed to anthropogenic sources, The average Hg_{TOT} in PM_{25} dust of Johannesburg was greater than those in Ottawa, Kavala, Luanda, and Beijing cities (Christoforidis and Stamatis, 2009; Zhang *et al*., 2006; Ferreira-Baptista and De Miguel, 2005; Rasmussen *et al*., 2001). However, it was lower than those in Baoji, Glasgow, Huludao, Calcutta, and Aviles cities (Zhen *et al*., 2010; Rodrigues *et al*., 2006; Ordonez *et al*., 2003; Manta *et al*., 2002, Chatterjee and Banerjee, 1999). The high levels of Hg_{TOT} were from anthropogenic sources such as coal-fired power stations, coking plant, coal waste from coal usage for heat and power, and Hg/Pb/Zn smelting industries (Zhen *et al*., 2010; Rodrigues *et al*., 2006; Ordonez *et al*., 2003; Manta *et al*., 2002, Chatterjee and Banerjee, 1999). Samples from Hong Kong and Palermo were at the same level as those in Johannesburg.

The results from Chinese and other cities, showed a similar trend as the results obtained from the dust samples of Johannesburg, i.e., the highest mercury concentration was observed in the industrial areas, mainly near coal-fired power

station, coke oven plant, cement plant, and zinc smelting (Sun *et al*., 2013; Zhen *et al*., 2010; Lu *et al*., 2009; Ordonez *et al*., 2002). In China, coal consumption is very high, mainly due to the fact that coal is the main energy source, and Hg concentration in consumed raw coal averaged 260 ppb, which is higher than the average Hg concentration in the world (130 ppb) (Jiang *et al*., 2005). Extremely high Hg_{TOT} concentration from attic dust was observed from Idrija, Slovenia, where the anthropogenic source of pollution was the smokestack of the smelter (mercury processing) (Gosar *et al*., 2006). As such the distribution of the pollution was influenced by the local wind direction, and therefore, mercury was enriched in the finer particulate matter at great distances from the source of pollution as compared to the point source. Interestingly, the most bioavailable fraction, non-cinnabar bound Hg was found to be enriched in the finer grained material (dust) at a great distance from the source of pollution.

5.3 Total metal analysis in dust

The total elemental analysis in dust samples showed a similar trend as observed for Hg_{TOT} with higher concentrations of heavy metals in industrial areas and lower concentrations in the residential areas (Table 5.4). The gold, pyrite (Fe, As) and other sulphides occur together with minor elements such as Ag and Hg (Kirk *et al*., 2003; Kirk *et al*., 2001). Since these elements and gold occur together, they are found in the same areas. This relationship is further confirmed by high correlation coefficients between Fe and Hg (R^2 = 0.801), Fe and S (R^2 = 0.773), and Hg and S (R^2 = 0.789) (Table 5.5). The inter-dependence in the PM_{25} size fraction could indicate that these three elements come from the same source, possibly the TSFs (Table 5.2). It is believed that the presence of Cu could be from mining activity (Csavina *et al*., 2011). In the study carried out by Meza-Figueroa *et al*., (2009), the enrichment factors of Hg, Cu, As, Zn and Pb in residential soils was reported to be caused by the wind erosion from Nacozari tailings in Sonora, (Mexico).

Moreover, the uniform spatial distribution of elements like Ca, Cd, Co, Cu, Ni, Pb, V, and Zn across all the different land uses is proof that traffic emission is a

significant source (Omar *et al*., 2007; De Miguel *et al*., 1999; Salim Akhter and Madany, 1993). However, in some areas its contribution is overshadowed by the emission from the tailings. Studies of trace elements in ambient air have shown that traffic emissions could be a significant contributor to the atmosphere and hence accumulation in soils and dust (Martuzevicius *et al*., 2004; Gao *et al*., 2002; Espinosa *et al*., 2001; Janssen *et al*., 1997). The principal source of Co, Ni, and V is the combustion of fuel while Cd, Cu, Pb, Sb, and Zn are released from tire rubber abrasion and brakes (Adachi and Tainosho, 2004; Singh *et al*., 2002; Sternbeck *et al*., 2002; Pacyna, 1998). Huang *et al*. (1994), were able to show that Al, Fe, and Zn, were emitted from vehicles with catalytic converters. It has been proven that these elements increase in heavily impacted traffic regions as compared to lesser traffic impacted areas. Elements such as Ca, Al, Mn, Fe, and Sc are crustal elements and therefore their presence in the dust is an indication of the vehicle re-suspension of road dust.

Table 5.4: Total metal concentration in studied PM_{25} particle size fraction samples.

SAMPLE	METAL CONCENTRATION																			
	$10^3 \times mg\ kg^{-1}$														$mg\ kg^{-1}$					
	Al	As	Ba	Ca	Cr	Cu	Fe	K	Mg	Mn	S	Si	Ti	Zn	Cd	Co	Li	Ni	Pb	U	V
Sandton	44.7	0.3	5.1	15.8	0.8	0.3	**46.9**	55.3	4.7	13.6	**1.4**	16.8	5.9	0.6	35.0	29.0	152	0.0	0.0	118	133
Diepkloof	71.7	0.2	5.9	27.4	0.4	0.1	**66.0**	42.1	3.0	0.9	**1.5**	26.7	4.9	0.4	36.9	0.0	157	0.0	0.0	151	138
Riverlea	60.5	0.1	3.4	29.8	0.4	0.1	**66.1**	31.4	3.7	0.9	**3.6**	21.2	4.9	0.3	33.9	22.0	149	0.0	0.0	155	147
Boksburg 1	80.5	0.2	7.5	11.4	0.4	1.1	**85.4**	14.6	2.9	1.1	**1.5**	21.8	8.2	0.8	35.9	20.5	158	0.0	0.0	157	255
Boksburg 2	54.4	0.3	6.2	29.8	0.6	0.2	**52.7**	19.2	7.6	1.5	**3.6**	19.1	6.2	08	35.1	35.3	144	18.9	0.0	115	176
Alberton 1	50.2	0.2	5.9	28.7	2.1	0.6	**77.5**	17.4	7.5	2.8	**3.1**	23.7	5.2	0.8	34.6	57.0	135	23.4	98.7	352	190
Alberton 2	46.7	0.4	7.4	41.3	3.0	0.4	**62.4**	17.0	12.3	6.1	**3.8**	23.0	5.9	0.9	35.7	38.5	127	0.0	93.4	0.0	166
Alberton 3	47.9	0.3	8.1	39.1	4.4	0.4	**72.5**	16.8	9.4	9.0	**2.1**	21.8	4.4	1.6	365	47.2	141	16.6	162	132	187
CBD 1	44.9	0.2	3.1	38.1	0.8	0.6	**66.0**	25.6	7.7	1.5	**3.1**	14.9	4.6	1.1	32.1	41.2	136	22.0	0.0	204	131
CBD 2	55.9	0.3	5.5	45.3	0.7	0.6	**63.5**	22.9	7.1	1.5	**4.2**	14.6	4.7	1.1	34.2	32.4	144	41.9	0.0	96.6	129
CBD 3	49.1	0.2	4.2	24.0	1.0	0.6	**73.0**	18.1	58.6	1.5	**3.8**	17.2	4.8	1.5	33.8	37.5	137	19.6	275	147	146
CBD 4	55.3	0.2	7.0	30.1	0.9	0.5	**83.2**	15.3	7.5	2.1	**4.7**	16.9	4.6	1.2	31.1	53.2	137	25.1	1083	119	163
Cemetery	51.8	0.1	2.8	19.1	2.0	0.9	**84.2**	13.0	8.3	2.1	**33.6**	12.5	0.0	0.9	34.4	36.4	139	14.6	0.0	116	185
Soccer City	51.6	0.2	3.5	10.1	0.5	0.1	**48.1**	35.8	3.5	0.8	**2.4**	20.3	6.9	0.3	34.8	17.5	133	0.0	0.0	189	130
Ophirton	48.7	0.1	3.2	18.3	0.8	0.4	**75.4**	15.9	5.8	1.5	**5.7**	23.1	4.3	1.1	37.8	29.3	145	0.0	0.0	0.0	151
Selby 1	52.7	0.1	2.7	27.7	1.2	2.4	**82.8**	15.1	9.1	1.8	**5.3**	16.8	5.4	2.2	37.7	66.6	148	52.1	530	266	162
City Deep	50.9	0.3	6.6	24.2	4.8	1.4	**83.5**	13.9	7.1	3.2	**4.7**	17.7	4.4	6.0	34.3	422.0	150	193.0	277	63.1	182
Crownwood	52.1	0.2	3.7	20.9	1.6	0.3	**75.1**	13.3	8.3	2.0	**4.6**	24.9	0.0	1.1	35.8	24.5	145	52.3	0.0	142	163
Heriotdale	57.5	0.1	1.6	74.5	0.8	0.3	**59.5**	14.9	23.4	2.8	**7.4**	7.6	2.9	0.5	26.3	143	133	69.2	0.0	280	120
PPC Cement	45.7	0.3	0.2	36.7	1.7	3.1	**132**	11.6	14.0	2.4	**88.6**	11.4	0.0	0.9	0.0	0.81	121	7.97	0.0	224	173
VR 1	35.8	0.5	2.0	13.7	0.2	0.3	**60.8**	10.1	2.6	3.7	**18.1**	17.5	0.0	0.6	28.3	94.8	112	40.4	0.0	411	63.4
VR 2	24.0	0.1	1.60	4.67	0.1	0.1	**44.9**	4.40	1.7	8.3	**18.1**	14.7	0.0	0.6	25.3	23.0	105	0.0	0.0	240	75.4

Table 5.5: Pearson correlation between elements in PM_{25} dust samples from Johannesburg. The values in bold red indicate the strongest correlations (R>0.5)**.**

	Al	*As*	*Ba*	*Ca*	*Cd*	*Co*	*Cr*	*Cu*	*Fe*	*Hg*	*K*	*Li*	*Mg*	*Mn*	*Ni*	*Pb*	*S*	*Si*	*Ti*	*U*	*V*	*Zn*
Al	1.00																					
As	-0.15	1.00																				
Ba	0.28	**0.61**	1.00																			
Ca	-0.12	0.08	-0.17	1.00																		
Cd	-0.13	0.35	0.42	0.12	1.00																	
Co	-0.25	0.11	-0.40	0.18	-0.16	1.00																
Cr	-0.39	0.41	0.35	0.10	**0.53**	0.34	1.00															
Cu	-0.13	-0.16	-0.39	0.00	-0.16	**0.76**	0.23	1.00														
Fe	0.15	-0.34	-0.39	0.46	-0.02	0.31	0.09	0.25	1.00													
Hg	-0.04	-0.31	**-0.61**	0.46	-0.17	0.19	-0.11	-0.01	**0.80**	1.00												
K	0.05	0.13	0.06	-0.25	-0.07	-0.31	-0.38	-0.43	-0.48	-0.25	1.00											
Li	**0.61**	-0.10	0.37	-0.42	0.05	-0.42	-0.18	-0.22	-0.34	-0.42	0.36	1.00										
Mg	-0.28	-0.01	-0.38	**0.83**	0.02	0.39	0.22	0.25	**0.69**	**0.64**	-0.45	**-0.60**	1.00									
Mn	-0.33	**0.51**	0.43	0.36	**0.79**	0.09	**0.80**	0.00	0.13	-0.08	-0.32	-0.32	0.38	1.00								
Ni	-0.22	0.09	-0.49	0.12	-0.16	**0.89**	0.06	**0.72**	0.19	0.15	-0.21	**-0.50**	0.32	0.00	1.00							
Pb	-0.03	-0.09	0.27	0.01	-0.01	0.01	0.13	0.20	0.13	-0.17	-0.24	-0.06	0.03	0.10	-0.09	1.00						
S	0.05	-0.33	-0.43	**0.66**	-0.09	0.07	-0.06	-0.05	**0.77**	**0.79**	-0.24	-0.25	**0.79**	0.05	-0.02	-0.11	1.00					
Si	0.37	-0.10	0.28	**-0.58**	0.21	-0.33	-0.15	-0.29	-0.40	-0.34	0.24	**0.62**	**-0.70**	-0.22	-0.28	-0.09	**-0.50**	1.00				
Ti	-0.10	0.42	0.41	0.13	-0.03	-0.17	0.23	-0.16	-0.11	-0.24	0.00	-0.27	0.11	0.40	-0.16	0.06	-0.15	-0.43	1.00			
U	0.07	-0.39	-0.39	0.25	-0.08	0.14	-0.21	0.27	0.28	0.30	-0.03	-0.19	0.28	-0.16	0.20	-0.01	0.29	0.05	-0.40	1.00		
V	0.38	0.11	0.43	-0.37	0.19	0.13	0.33	0.32	0.00	-0.37	-0.49	0.21	-0.19	0.23	0.09	0.09	-0.25	0.21	0.06	-0.02	1.00	
Zn	-0.18	0.17	0.24	-0.05	0.09	0.38	**0.66**	0.35	0.07	-0.18	-0.30	0.17	-0.01	0.23	-0.02	0.30	-0.17	0.02	-0.04	-0.20	0.19	1.00

5.4 Seasonality variation of Hg_{TOT} in PM_{25} size fraction in Johannesburg street dust

In this part of the study, temporal trends of Hg_{TOT} were determined during the wet season (Figure 5.11).

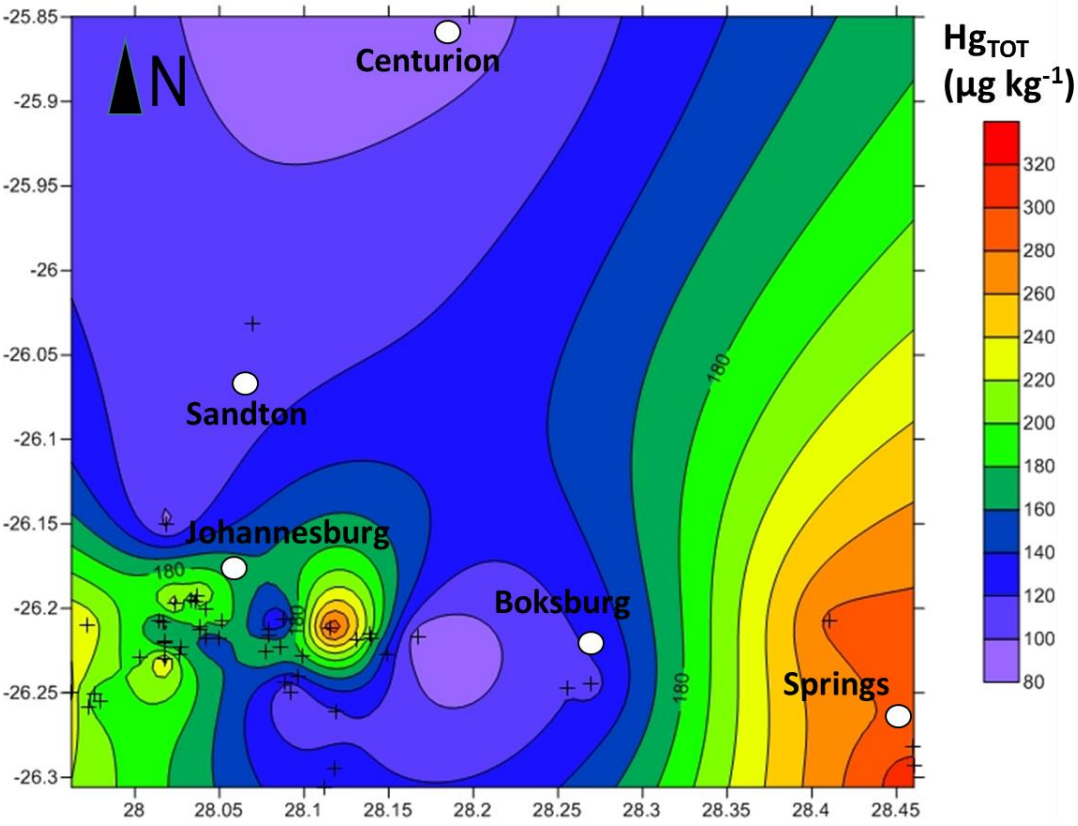

Figure 5.11: Spatial distribution of Hg_{TOT} in PM_{25} size fraction in Johannesburg street dust during the wet season.

Hg_{TOT} ranged from 91.00 to 318.00 µg kg^{-1} with an average of 177.2 µg kg^{-1}. According to the land usage, it ranged from 101.9 to 318.0 µg kg^{-1} with an average of 191.7 µg kg^{-1}; 182.0 to 220.5 µg kg^{-1} with an average of 195.1 µg kg^{-1}; and 91.5 to 232.0 µg kg^{-1} with an average of 130.2 µg kg^{-1} for industrial, CBD, and residential areas, respectively. The same trend observed in Hg_{TOT} in the dry season was observed in the Hg_{TOT} in the wet season, i.e. the highest Hg_{TOT} concentration was reported for samples

in the industrial area, followed by CBD, and lastly residential area. Of interest, in this case was that the average Hg_{TOT} of the CBD was slightly higher than the average of Hg_{TOT} in the industrial areas. This could be attributed to the presence of tall buildings, which acts as a wind break during the windy months (July to October) prior to the onset of rains. Therefore dust accumulates, thereby accumulating large amounts of mercury in the finer particulate matter. This period coincides with high dust period, i.e. spring season, in the Witwatersrand region. This period is usually characterized by high wind speeds, high erodibility of dust, humidity, and low rainfall (Oguntoke *et al*., 2013; Annegarn *et al*., 1991). During this period, huge amounts of dust are distributed over great distances while some dust being deposited locally.

Hg_{TOT} concentration values are far less than what was obtained during the dry season, where the dust is allowed to accumulate on the surfaces next to the roads due to prevailing weather and environmental conditions, which favour the deposition of dust. This points out that there is a lot of washing away of the dust during the wet season (Oguntoke *et al*., 2013). The on-set of rains comes with high relative moisture, and high rainfall. High moisture in the atmosphere provides water that binds dust particles thereby reducing dust erodibility by wind, and also reducing wind speed and erosivity (Smith and Lee, 2003; Lee *et al*., 1994). The accumulated road-deposited sediment (RDS-dust) constitutes washoff particles that leads to urban runoff pollution (Zhao *et al*., 2010a). Studies conducted by Lusilao (2012), reported that during the wet season, mercury concentration in the sediment surfaces near the TSFs decreased from about 950 to 320 µg kg^{-1}, while the Schoonspruit river sediments recorded an increase from 103 to 1004 µg kg^{-1}, indicating transportation and distribution of mercury along water courses, and receiving environments downstream.

5.5 pH of dust

The pH of the dust ranged from 5.3 to 10.3, with an average of 7.6 (Figure 5.12). Most of the investigated dust samples were neutral, with the exception of samples from the mining sites, and some from industrial sites. Samples from the mining sites were

slightly acidic and were as follows: 5.3, 5.4, and 5.4, for VR 1 and 2, and West Wits mining areas, respectively. These pH values were within the expected pH of the soil in the VR area and varied between 5.5 and 6.4 (AGA VR EMP, 2009). This could be evidence of acidification of the TSF due to pyrite oxidation, and exposure of the TSFs to the atmosphere. Characterization of pH of five different tailings dams carried out by Nengovhela *et al*. (2006), showed that the pH ranged from 2 to 4, an indication of the generation of the AMD by the tailings dams. The actual mobility of contaminants in the tailings is determined by the pH, redox conditions and the presence of other ions, dissolved organic matter and clays.

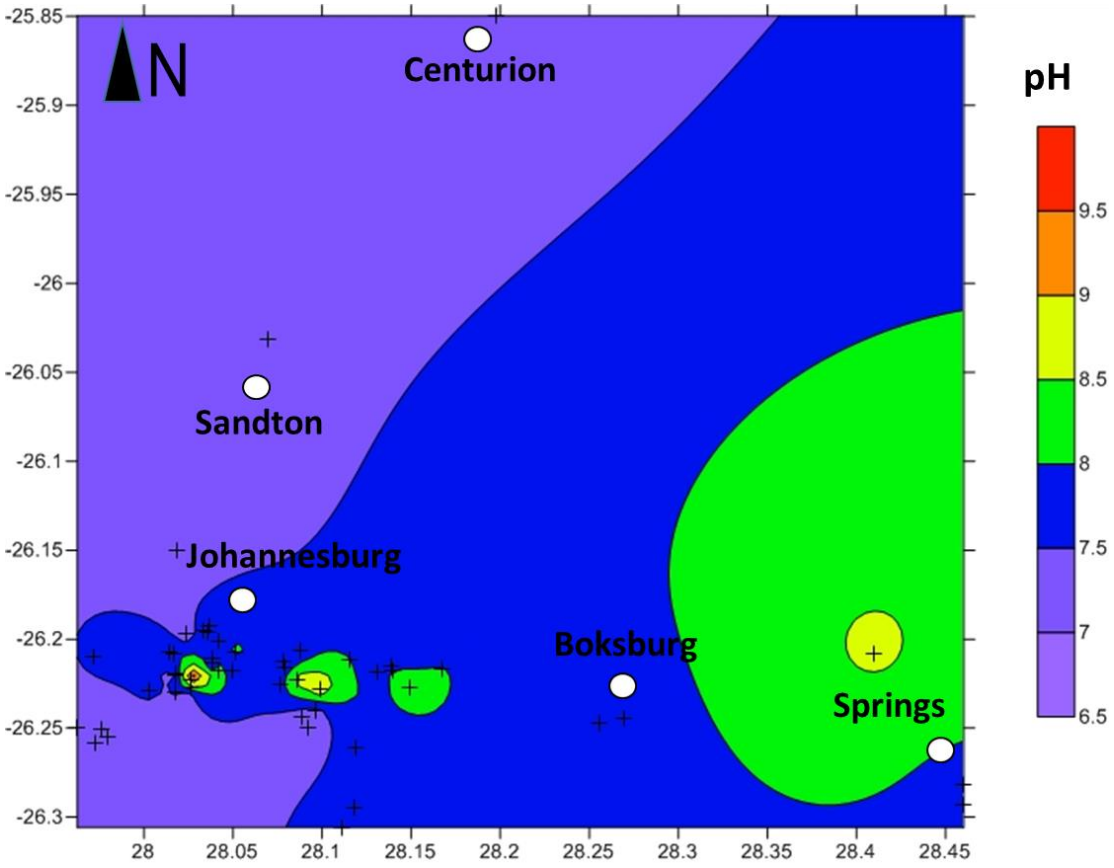

Figure 5.12: Spatial distribution of pH of the dust samples from Johannesburg, South Africa.

On the other hand some samples from the industrial sites were slightly alkaline to alkaline. These were City Deep 2 & 3, Loveday, Springs 3, and Cross with pH values 8.73, 8.86, 8.53, 8.60, and 10.26, respectively. The presence of trace carbonates and the liming of cyanide containing solution, added to control pH during gold ore processing, resulted in the tailings having a near-neutral pH (Naicker *et al*., 2003). The loss of material from the unoxidised dry slimes dams surfaces due to wind erosion leads to the distribution of dust characterized by near-neutral pH and laden with toxic metals and metalloids. Most of the TSFs were left undisturbed in the Johannesburg area for almost a century, and were left exposed to a combination of oxygen and rainwater. This resulted in the oxidation of the pyrite and other sulphides in the tailings material, which produced AMD (Marsden, 1986). The acidified waters leached out toxic heavy metals into ground water beneath the dumps and some found its way into rivers and streams on surface (Naicker *et al*., 2003; Jones *et al*., 1988).

5.6 Size distribution of dust samples

The particle size distributions of a few selected dust samples are illustrated in Figure 5.13. The distribution patterns of the dust samples were similar, characterized by unimodal distribution with most particles in the range from 100 to 400 µm. The PM_{25} fraction in dust samples ranged from 0.8 to 10.1 % volume from Sandton to Heriotdale, respectively, (Figure. 5.14).

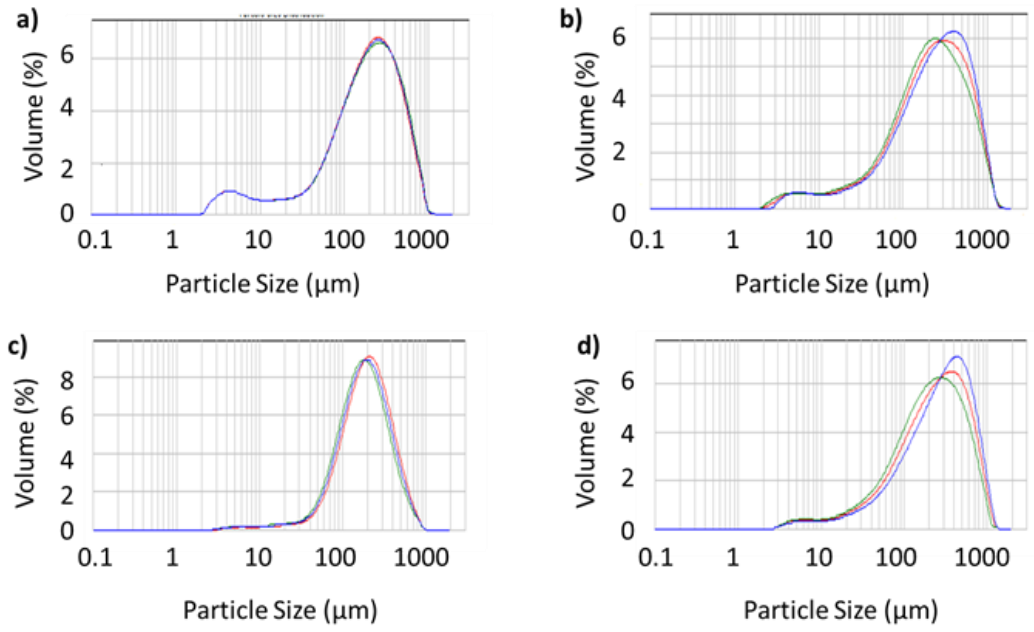

Figure 5.13: Particle size distribution of dust samples (a) Industrial area - Heriotdale. (b) Industrial Area – City Deep. (c) Residential Area – Sandton (d) CBD 2.

Particles smaller than 100 µm could easily be re-suspended under windy conditions resulting in adverse health effects on human beings, due to the dust entering the nose and mouth during normal breathing (Driver *et al.*, 1989). The thoracic dust (PM_{10}) and respirable dust ($PM_{2.5}$), both found within the PM_{25}, may remain suspended in the air for long periods of time (De Miguel *et al.*, 1997). PM_{10} passes through the nose and throat, reaching the lungs, whilst $PM_{2.5}$ will penetrate the alveoli, where gaseous exchange takes place in the lungs. High Hg_{TOT} in dust samples was associated with high % volume of PM_{25} fraction. The particle size analysis results showed that the contents of PM_{25}, PM_{50}, PM_{100}, and $>PM_{100}$ in the dust samples of Johannesburg ranged from 0.8 to 10.1, 0.6 to 7.4, 1.4 to 15.9 and 71.7 to 97.2% with averages of 4.6, 3.9, 12.0, and 79.4%, respectively (Figure 5.13). These results show that about 21% of dust could become suspended into the atmosphere, whereas about one twentieth (i.e. less than 0.1%) could enter the respiratory system.

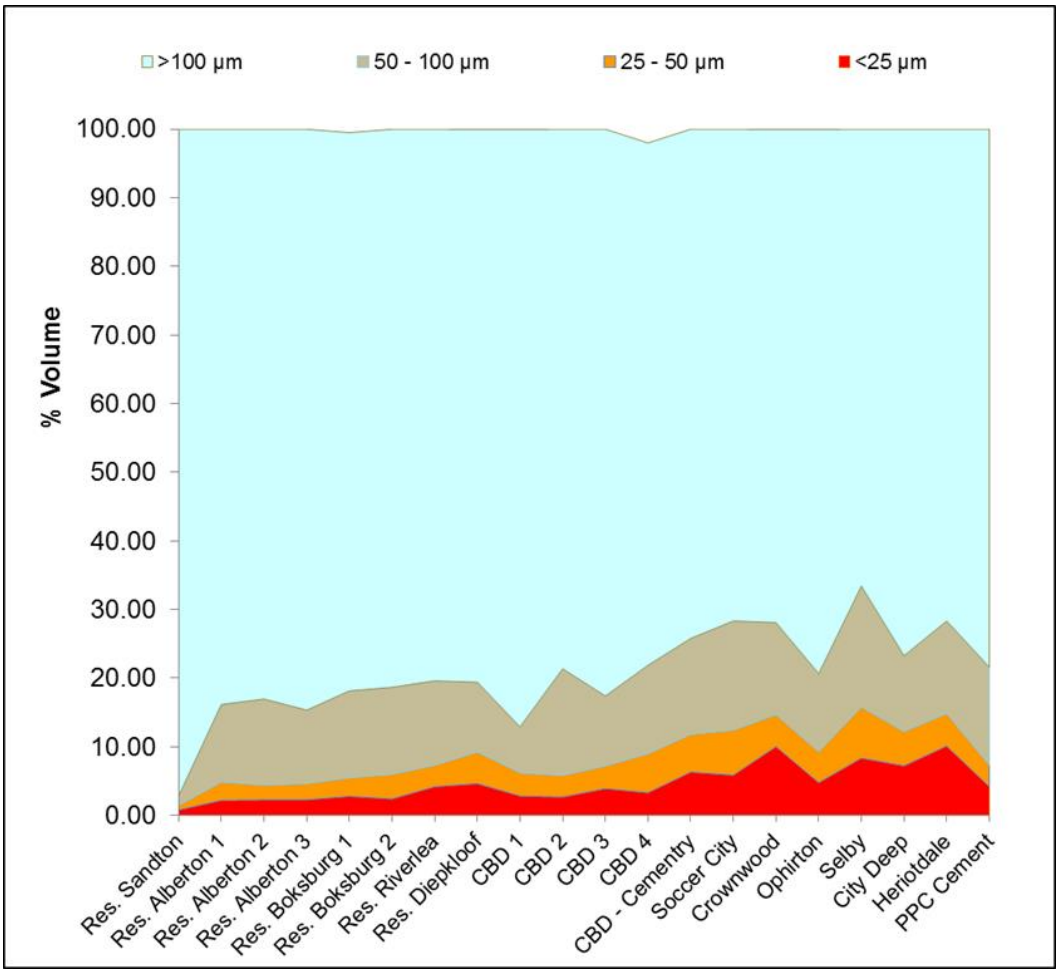

Figure 5.14: Particle size distribution in dust samples from Johannesburg, South Africa.

The highest % volume of PM_{25} fraction was recorded in industrial samples and were as follows: Heriotdale, 10.1%; Crownwood, 10.0%; Selby I, 8.4%; City Deep, 7.2%, and Ophirton, 4.8%. The least % volume of PM_{25} fraction was recorded in residential area of Sandton, which was 0.80%. Particles less than 25 µm from industrial areas made up a mean of 7.2% of the dust, which is about 2 times higher than the CBD's mean (3.8%), and 3 times higher than the residential area's mean (2.3%). The remaining particle size fractions (PM_{50} and PM_{100}) followed the same trend as PM_{25} with the following % volume order: industrial area > CBD > residential area. Therefore, dust from the industrial areas consisted of higher proportions of inhalable, thoracic and respirable particles with increased risk of adverse health effects to human beings.

The particle size distribution followed the same trend as for Hg_{TOT}. The samples that contained low Hg_{TOT} also had low % volume of PM_{25}, whilst samples with high Hg_{TOT} also had high % volume of PM_{25}. However, considering particle size distribution, the larger the particle size, the lower Hg_{TOT} whilst the smaller the particle size, the higher the Hg_{TOT}. It can be concluded that there is a negative correlation between the particle size fraction and Hg_{TOT} with a correlation coefficient of -0.77, as shown in Figure 5.15. In this study, correlation analysis also showed that mercury concentration positively correlated with the % volume of PM_{25} in dust samples (R^2 = 0.51), as shown in Figure 5.16. This may explain the significant decrease of mercury levels observed in dust samples moving away from the vicinity of the gold tailings dams (TSFs, tailings footprints, TSF reprocessing sites) to the residential areas and also confirmed that gold mining tailings are the main source of mercury pollution in the area.

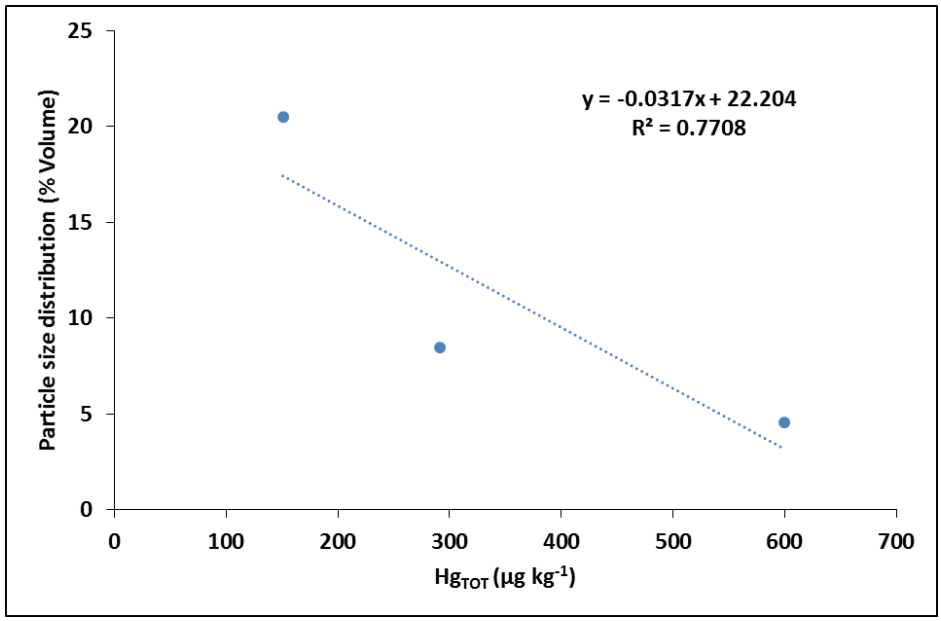

Figure 5.15 Correlation between Hg_{TOT} and particle size distribution in street dust from Johannesburg.

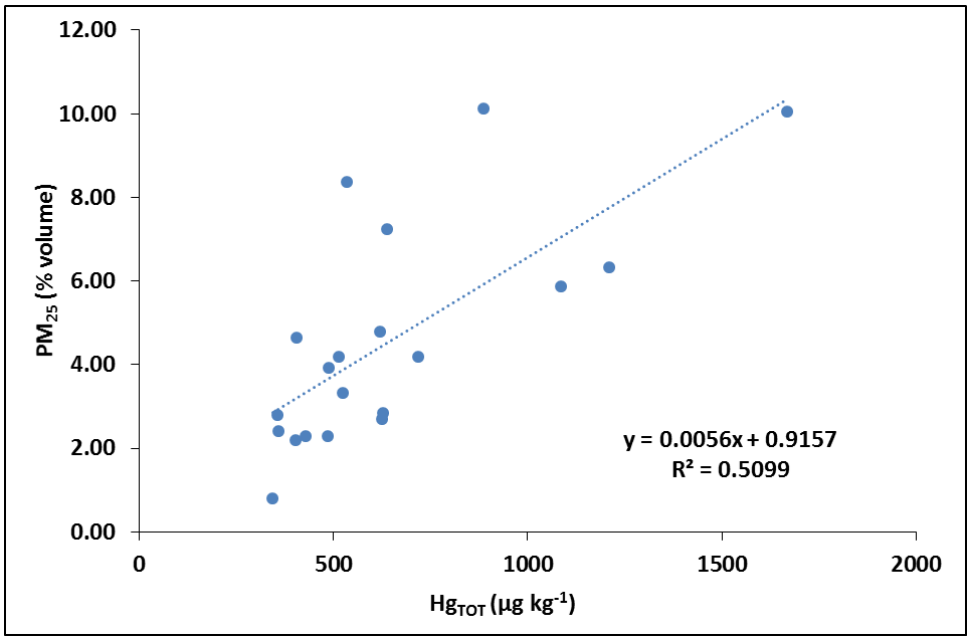

Figure 5.16: Correlation between Hg_{TOT} and % volume in PM_{25} street dust from Johannesburg.

Hg_{TOT} increased as particle size decreased in dust due to the presence of high specific surface area (Zverina *et al*., 2012; Duong and Lee, 2011; Luo *et al*., 2011; Zhao *et al*., 2011; Zhao *et al*., 2010; Duong and Lee, 2009; Madrid *et al*., 2008). Smaller particle sizes have high surface area per unit of mass, and are able to adsorb large quantities of heavy metals (Deletic and Orr, 2005). Therefore, the smaller the particle size, the higher the adsorption capacity for mercury and other metals/metalloids. In addition, industrial areas where TSFs are being re-processed, dust is generation. Therefore, there is an increase in the finer particulate matter resulting in the increase of Hg_{TOT} in the dust and leading to a greater potential of human health risk when people are exposed.

The presence of organic matter, clay and mineral phases, in the finer particle size fraction, generally have a tendency to exchange or replace cations in clays or adsorb ions on mineral and organic material surfaces (Duong and Lee, 2009). Clay minerals consist of plate-like sheets, have large specific surface area, and contain negatively charged surfaces. These surfaces are balanced by cations, which can be replaced or

exchanged by other cations with stronger affinities for the surfaces. This process describes an important property of clays known as *cation exchange capacity* (CEC), which is responsible for the use of clays in the remediation processes of contaminants.

Therefore, different studies have reported a higher concentration of Hg_{TOT} in the dust with the smaller particle size (Ajmone-Marsan *et al*., 2008; Wang and Qin, 2007; Beckwith *et al*., 1986). Similar observations were made by Londonio *et al*., (2012) and Moreno *et al*., (2005), where higher Hg_{TOT} were found in the finer fraction of the dust samples coming from industrial areas and were closest to the point sources, such as mining sites, coal-fired power stations, cement plant, and coking plant.

5.7 Contamination assessment factors

In order to assess the contamination assessment factors, enrichment factor (EF), contamination factor (C_f), and geoaccumulation index (I_{geo}) were calculated using equations 1 to 3 in Chapter 4, respectively. To calculate EF, aluminum was set as the reference element and its concentration in the crust was adopted as background value assuming that its anthropogenic contribution is minimal (Rashed, 2008). A value of EF close to 1 indicates the source as crustal origin, whereas values > 10 are considered to be a non-crustal (anthropogenic) source (Meza-Figueroa *et al*., 2007; Liu *et al*., 2003; Gilbert, 1987). EF can also assist in determining the degree of metal contamination. The mercury contamination of urban dust was also evaluated based on the contamination factor suggested by Hakanson (1980). In order to calculate I_{geo} of dust samples from Johannesburg, the average Hg content (0.080 mg kg^{-1}) in the earth crust was used as the background (Taylor, 1964) because there is no published data on the background level of Hg in soil and dust from Johannesburg or South Africa. This assessment was handy in making a clear distinction between natural and anthropogenic sources of mercury.

Table 5.6, lists the contamination assessment factors of mercury in PM_{25} dust samples. All samples from the industrial areas had elevated levels of Hg_{TOT} and this was mainly attributed to TSF sources. These contamination assessment factors generally decreased from industrial areas to residential areas.

Table 5.6: Contamination assessment factors for selected PM_{25} dust samples from Johannesburg.

Site No.	Sampling Sites	Enrichment Factor (*EF*)	Contamination Factor (C_f)	Geoaccumulation index (I_{geo})
1	Res. Alberton 1	**12.82**	5.98	1.99
2	Res. Alberton 2	**12.98**	5.55	1.89
3	Res. Alberton 3	6.90	5.75	1.94
4	Res. Boksburg 1	8.78	5.68	1.92
5	Res. Boksburg 2	7.93	5.25	1.81
6	Res. Diepkloof	9.34	5.44	2.44
7	Res. Riverlea	**11.12**	5.46	2.45
8	Res. Sandton	6.97	3.80	1.34
9	CBD 1	9.63	6.29	2.07
10	CBD 2	9.84	7.15	2.25
11	CBD 3	6.87	5.72	1.93
12	CBD 4	9.83	6.17	2.04
13	CBD Cemetery	8.43	8.26	2.46
14	Soccer City	**21.91**	9.48	2.66
15	Crownwood	**10.66**	11.74	2.97
16	Ophirton	**12.43**	6.96	2.21
17	Selby 1	**10.66**	6.54	2.13
18	City Deep	**18.50**	7.97	2.41
19	Heriotdale	**27.68**	15.87	3.40
20	PPC Cement	**18.08**	10.44	2.80

5.7.1 Enrichment factor (EF)

EF of mercury was from 7.3 to 29.4, with an average of 12.7 (Figure 5.17). Seventy percent of dust samples had EF of mercury above 10, indicating that the mercury pollution was predominantly from anthropogenic sources. All samples from industrial areas had EFs above 10 and ranged from 11.3 to 29.4 with an average of 18.2, indicating mercury sources are predominantly of anthropogenic sources (i.e., gold mine

TSFs as well as tailings reprocessing). On the other hand, 75% of samples from residential areas fell below the EF value of 10 and ranged from 7.33 to 13.79 with an average of 10.1 implying that the mercury source is natural. Exception were observed in the samples collected from Diepkloof and Riverlea residential areas, heavily impacted by TSFs and tailings reprocessing, respectively. Forty percent of samples from CBD were borderline, ranging from 7.3 to 10.5 with an average 9.5.

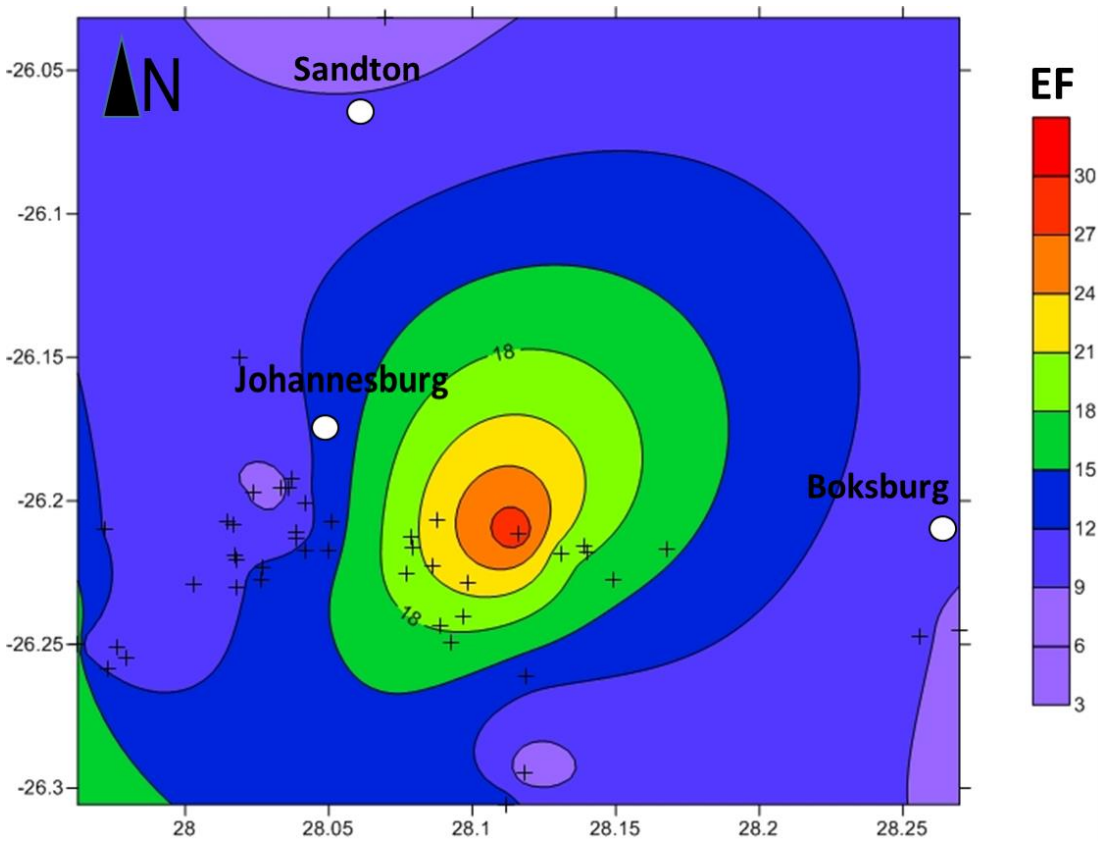

Figure 5.17: Spatial distribution of enrichment factor (EF) of mercury in PM_{25} size fraction in Johannesburg street dust.

EF of mercury in road dust samples from Baoji (China) was reported to range from 8.0 to 41.4, with an average of 20.7 (Lu *et al*., 2009). 94.7% samples had EF of mercury above 10, indicating that the source of mercury originated from anthropogenic activities, namely coal-fired industrial activities. In Taipei, EF of mercury in street dust

samples was of 189 indicating that the source was overwhelmingly anthropogenic, particularly from the incineration of municipal solid waste, and emissions from electronic, paper, and pharmaceutical industries (Zhang *et al*., 2014; Al-Khashman, 2007). Some Chinese cities such as Hangzhou and Xi'an reported EF values of 8.1 and 21.3 for street and urban dust (Zhang and Wang, 2009; Han *et al*., 2006). Their contamination status ranged from significant to very high enrichment. This was possible due to the various sources of pollution encountered in this region, coming from engineering, and textile industries.

5.7.2 Contamination factor (C_f)

The mercury contamination factor for PM_{25} urban dust samples from Johannesburg ranged from 4.0 to 16.9 with an average of 7.5, and was classified from moderate to very high contamination (Figure 5.18). The contamination factor (C_f) indicated very high contamination levels of mercury in industrial (Heriotdale; Crownwood, PPC Cement, Soccer City, City Deep, Ophirton, and Selby 1), and CBD areas (Cemetery, 1, 2, and 4), respectively. Samples from the residential areas were categorized as considerable contamination levels ($3 \leq C_f < 6$).

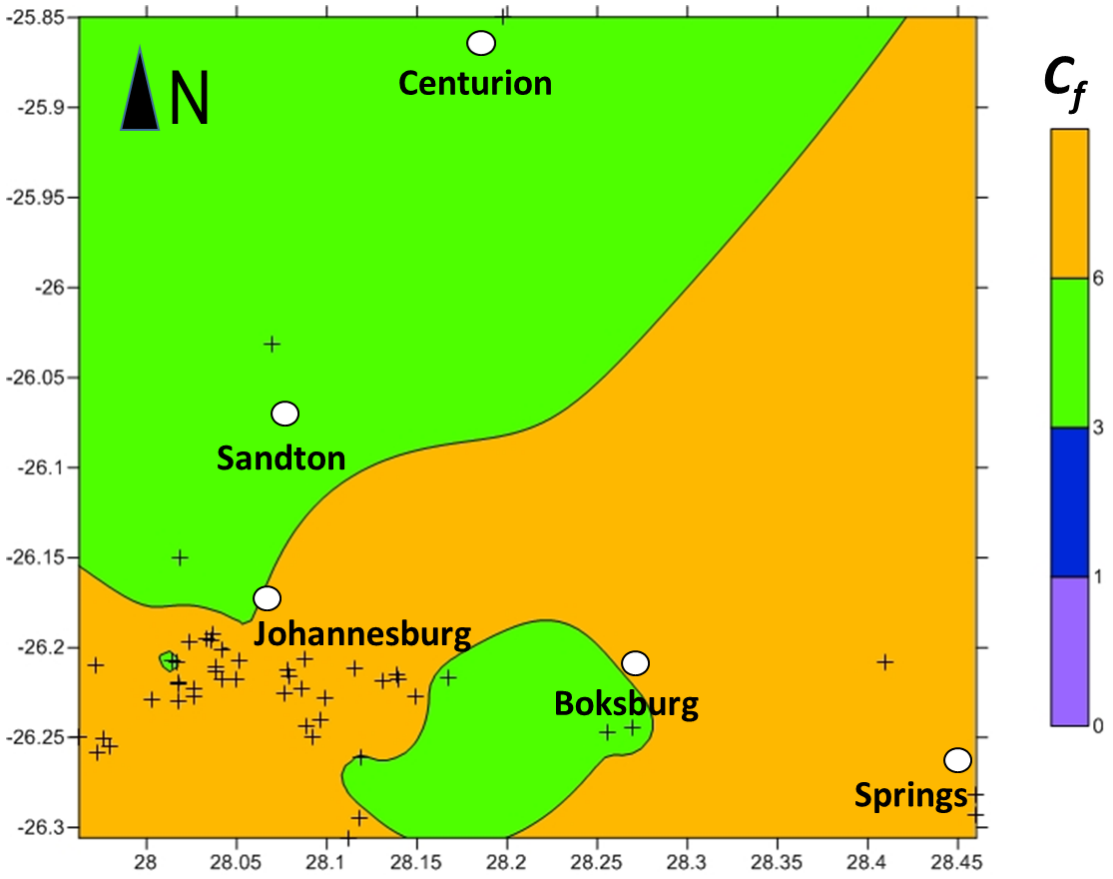

Figure 5.18: Spatial distribution of contamination factor (C_f) of mercury in PM_{25} size fraction in Johannesburg street dust.

5.7

.3 Geoaccumulation index (I_{geo})

The I_{geo} ranged from 1.2 to 3.5 with a median and a mean value of 2.2 and 2.3, respectively, indicating contamination to be from moderately to strongly polluted (refer to Table 5.7). The I_{geo} was between 2.1 to 3.5, 1.7 to 2.6, and 1.2 to 2.5 with averages of 2.3, 2.1, and 1.9 for samples from industrial, CBD, and residential areas, respectively (Figure 5.19). Categorically, contamination ranged from unpolluted to strongly polluted for samples from residential to industrial areas.

Table 5.77: Mercury contamination assessment of the dust samples from Johannesburg with I_{geo} (no unit).

Class	Value	Quality	# of sampling site
0	$I_{geo} < 0$	Practically unpolluted	-
1	$0 \leq I_{geo} < 1$	Unpolluted to moderate polluted	-
2	$1 \leq I_{geo} < 2$	Moderately polluted	1-5, 8, 11
3	$2 \leq I_{geo} < 3$	Moderately to strongly polluted	6-7, 9-10, 12-18, 20
4	$3 \leq I_{geo} < 4$	Strongly polluted	19

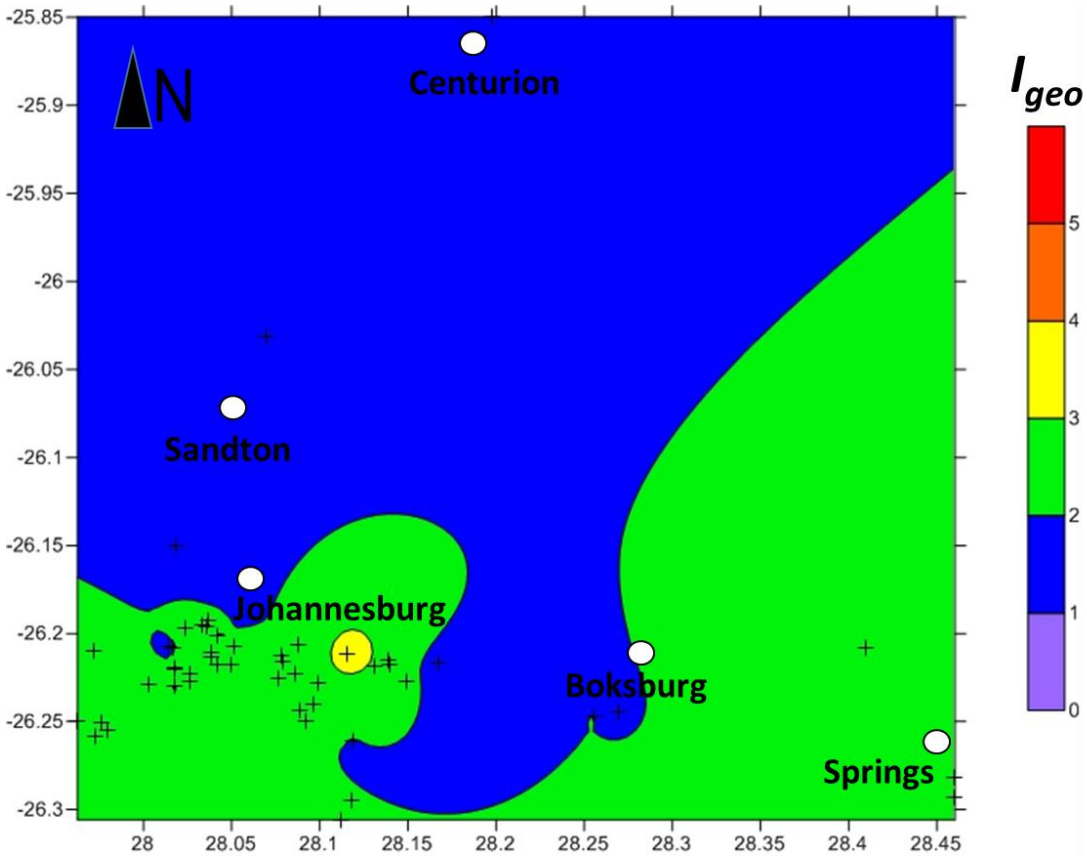

Figure 5.19: Spatial distribution of geo accumulation index (I_{geo}) of mercury in PM_{25} size fraction in Johannesburg street dust.

In comparison with other cities, Kong *et al.* (2011) obtained similar results of I_{geo} (-0.2 to 3.2) for road dust samples from Fushun (China), a coal based city. They identified

the anthropogenic source of mercury as coming from the combustion of coal. In Zhuzhou (China), a heavily industrialized city, characterized by metal production (Pb/Zn smelting operation being the largest operation) reported I_{geo} of mercury in the range from 0 to 2 for street dust samples, with contamination status from uncontaminated to moderate contaminated (Li *et al*., 2013). In Baoji (China), the studied road dust samples had a higher I_{geo} index than the Johannesburg dust. It ranged from 3.01 to 5.27, with an average of 4.13 (Lu *et al*., 2009), and was classified as strongly to extremely polluted. In agricultural soils, Chengdu and Guangzhou cities were moderately contaminated with Hg with I_{geo} values of 1.2 and 2.0 while Gansu, Kunshan, and Yangzhou appeared to be least contaminated with I_{geo} values of 0.4, 0.7, and 0.7. These I_{geo} values gave indication that the agricultural soils in these cities were moderately contaminated by Hg from an anthropogenic source (mining, fertilization, and pesticide application). Compared with the dust from Johannesburg, the agricultural soils were less contaminated, probably due to the practice of agriculture, where the soil is turned during the ploughing period, and the heavy metals are leached deeper into the soil due to the watering effect. On the other hand, dust consisting of fine particulate matter has a tendency of adsorbing huge amount of heavy metals, and tends to be left undisturbed for longer periods, unless it rains. Therefore, heavy metals accumulate resulting in huge concentration levels being reported in dust.

Samples from industrial areas were classified as strongly polluted by all the contamination assessment indices. This indicated that the source was predominantly anthropogenic. However, residential and CBD areas exhibited low to moderately polluted samples with sources being predominantly natural, with exception of residential areas affected by the presence of TSFs.

Chapter 6

Availability and bioaccessibility of mercury in dust

The results discussed in this chapter address issues of environmental mobility and bioavailability of mercury from dust samples. This was achieved by determining the bioaccessibility of mercury in the gastrointestinal tract and respiratory tract. Synthetic solutions mimicking the digestive and lung fluids were used in the determination of bioavailable mercury. A sequential extraction procedure (SEP) was carried out to determine the fractionation of mercury in the urban dust. These results were used to predict the potential health risk associated with human exposure to mercury through ingestion and inhalation of dust.

6.1 Determination of bioaccessibility of mercury in dust

The bioavailability of mercury, which is defined in this study, as the quantity of mercury that dissolves in the simulated gastric and lung fluids, was determined in the ingestion and inhalation fractions of the dust samples. The obtained results are presented in the Appendix B (Tables B.1 and B.2).

6.1.1 Bioaccessibility of mercury from ingestible fraction in dust samples

The fraction of mercury in dust samples extracted by the artificial gastric fluid (AGF) and dilute HCl (0.07M HCl) are shown in Figure 6.1.

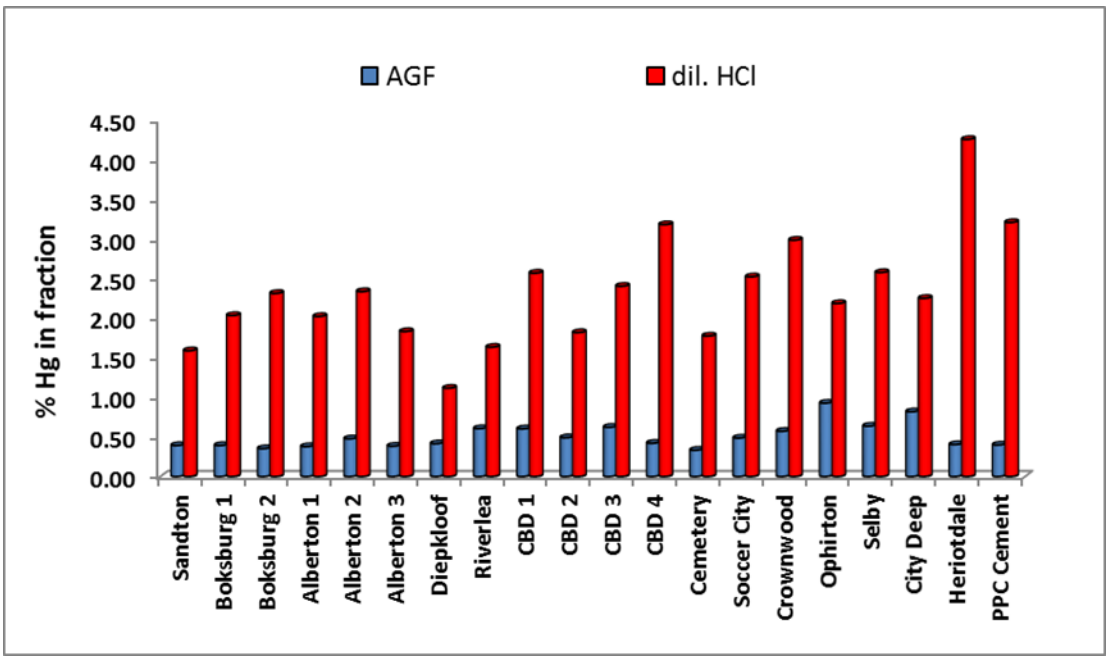

Figure 6.1: Comparison of Hg extracted by oral leachates (artificial gastric fluid, pH = 2.0 and dilute HCl, pH = 1.5) from dust samples from Johannesburg (*PM_{25} particle size fraction, n=3*).

Bioaccessibility was expressed as the percentage of mercury concentration extracted by AGF with respect to its independently determined total concentration in dust samples (25 µm particle size fraction). Mercury extracted by AGF ranged from 1.3 to

6.2 µg kg^{-1} with an average of 3.1 µg kg^{-1}. According to the different land uses, it ranged from 3.0 to 6.2 µg kg^{-1} (average 4.64 µg kg^{-1}) in industrial road dust; 2.1 to 3.3 µg kg^{-1} (average 2.9 µg kg^{-1}) in CBD road dust, and 1.3 to 3.6 µg kg^{-1} (average 1.56 µg kg^{-1}) in residential road dust (Appendix B). The relative gastric Hg bioaccessibility expressed as a percentage of Hg_{TOT} ranged from 0.33 to 0.93% with an average of 0.51%. According to the land use, it ranged from 0.40 to 0.93%, 0.33 to 0.60%, and from 0.39 to 0.67% with an average of 0.61, 0.49, and 0.42%, in industrial dust, CBD dust, and residential dust, respectively. Higher bioaccessible Hg concentration was observed in the dust samples from industrial areas, followed by samples from CBD and lastly samples from residential areas. These results show a similar trend and are comparable to those obtained by Hu *et al.* (2011) who reported an average bioaccessible mercury value 45 µg kg^{-1} in dust. However, Hg concentration extracted in this study was much lower and the extracting solution used was different. Recent leaching studies have shown that contaminant matrix will affect the availability of a contaminant (Luo *et al*., 2011). Bioavailable mercury from the AGF fraction did not exceed the probable mercury effect concentration of 1.06 µg g^{-1}, above which harmful effects are likely to be observed in sediment-dwelling organisms (MacDonald *et al*., 2000).

Mercury concentration extracted by dilute HCl (pH 1.5) solution ranged from 12.1 to 65.6 µg kg^{-1} (average 26.0 µg kg^{-1}) in industrial dust; 11.4 to 16.1 µg kg^{-1} (average 13.7 µg kg^{-1}) in CBD dust; and 5.5 to 9.7 µg kg^{-1} (average 7.6 µg kg^{-1}) in residential dust. The overall Hg concentration extracted ranged from 5.5 to 65.6 µg kg^{-1}, with an average of 15.6 µg kg^{-1}. In relation to Hg_{TOT} concentration, the percentage of Hg in the dilute HCl fraction remained below 5% in all dust samples, showing average values of 2.9%, 2.4% and 1.9% in industrial, CBD and residential dust, respectively. These values are comparable to previous studies, which showed that low percentages (0.1 to 3.5%) of Hg are soluble in dilute HCl solutions (Biester *et al*., 2002; Boszke *et al*., 2008; Issaro *et al*., 2009). In comparison with concentrated HCl, mercury extracted

was 10 times higher in concentrated HCl fraction than in the dilute HCl fraction (Figure 6.2).

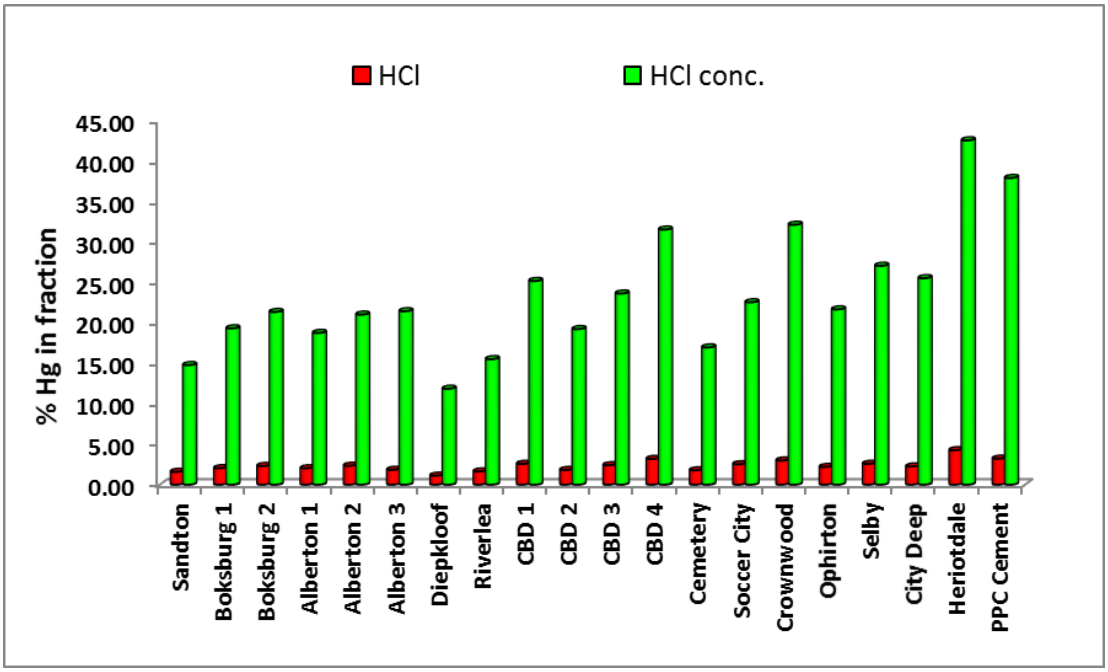

Figure 6.2: Comparison of oral leachates (concentrated HCl and dilute HCl) in the extraction of mercury from dust samples (*PM_{25} particle size fraction, n=5*).

The overall Hg extracted by concentrated HCl ranged from 50.9 to 655.2 µg kg^{-1}, with an average of 157.6 µg kg^{-1}. According to land usage, mercury concentrations extracted by concentrated HCl ranged from 123.8 to 655.2 µg kg^{-1} (average 253.1 µg kg^{-1}) in industrial dust, 144.4 to 159.7 µg kg^{-1} (average 135.4 µg kg^{-1}) in CBD dust, and 50.9 to 76.9 µg kg^{-1} (average 74.2 µg kg^{-1}) in residential dust. The percentage of mercury distribution was as follows: 21.7 to 42.6%, 17.0 to 31.5%, and 14.8 to 21.4% with averages of 29.1, 23.3, and 18.0% for industrial, CBD, and residential samples.

The mercury concentrations extracted by simulated gastric fluids (AGF, 0.07M HCl, and conc. HCl) demonstrated a strong correlation to the Hg_{TOT} in the dust samples with

correlation coefficients of 0.63, 0.87, and 0.85 (Figure 6.3, Figure 6.4, and Figure 6.5). These results indicates that the simulated gastric fluid extractable Hg is determined by Hg_{TOT} levels in the dust.

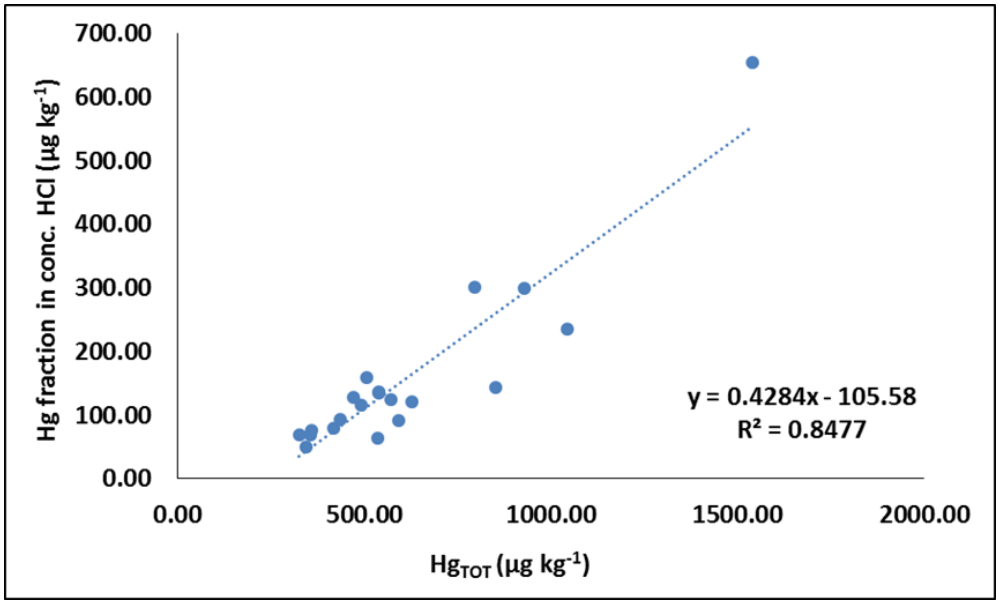

Figure 6.3: Correlation between Hg_{TOT} and conc. HCl in street dust from Johannesburg.

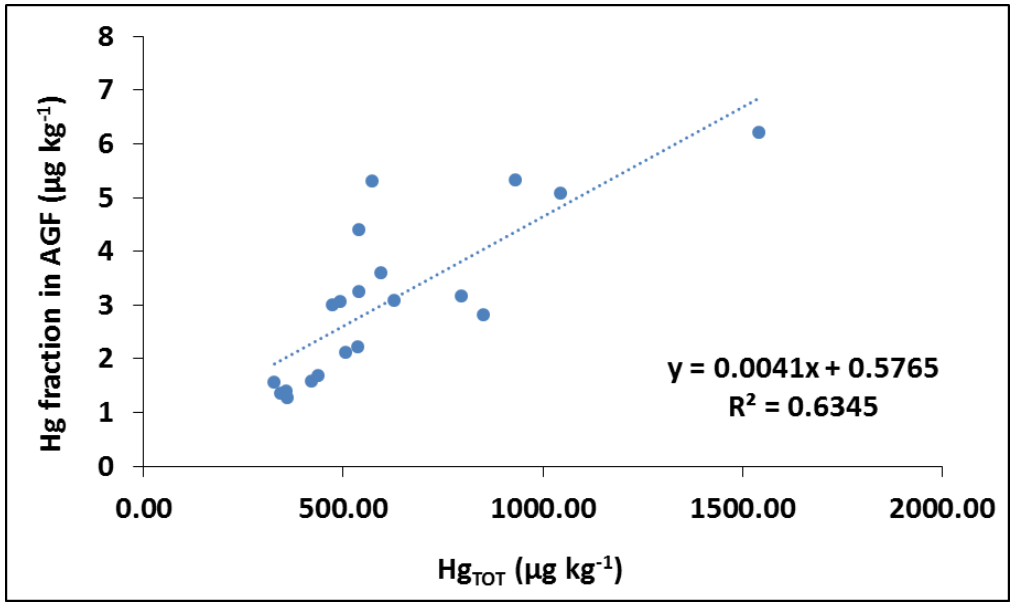

Figure 6.4: Scatterplot of correlation between Hg_{TOT} and ACF extractable Hg fraction in Johannesburg dust samples.

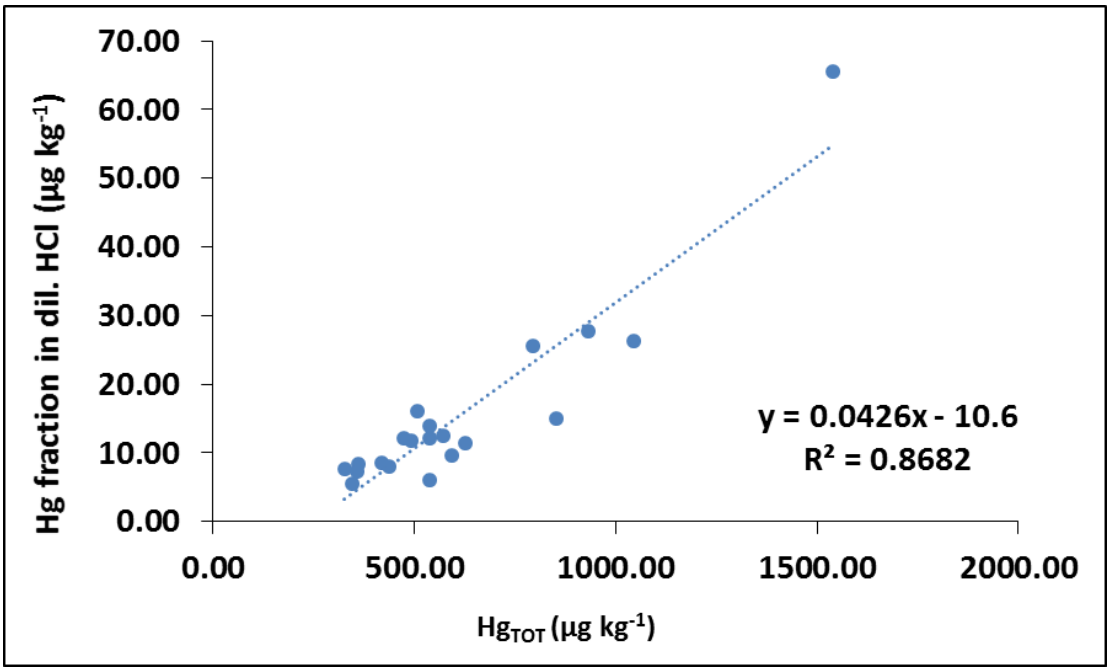

Figure 6.5: Scatterplot of correlation between Hg_{TOT} and dilute HCl extractable Hg fraction in Johannesburg dust samples.

Mercury concentrations extracted by gastric fluids showed the following order: industrial > CBD > residential dust, and the percentage of Hg extracted by simulated gastric fluids were as follows: conc. HCl > dil. HCl > AGF. These results suggest that conc. HCl was able to extract, not only the mobile fraction, but also part of the semi-mobile fraction (Hg bound to amorphous and crystalline iron and manganese oxides). Even though, the amount extracted by the gastric juices was very small (3.08 µg Hg kg^{-1}or 0.51% bioaccessible Hg), it's still a cause for concern as Hg is not biodegradable. Instead in the ecosystems, Hg can be converted from one form to another depending on the environmental conditions. The presence of sulphate reducing bacteria can convert elemental mercury to methyl mercury which accumulates in aquatic life forms. Hg can, therefore, biomagnify, bioconcentrates and bioaccumulates in the food chain leading to Hg poisoning in the human beings when they consume fish contaminated with Hg.

On the other hand, the implication of ingestion of dust, the exposure, solubilization and uptake of trace metals (including mercury) into the human system causes considerable adverse health effects in human beings. For instance, dust can be transferred to humans through hand to mouth ingestion or dermal contact, especially in children due to their outdoor activities (Bright *et al*., 2006). This activity is governed by the fineness of the particles (Siciliano *et al*., 2009; Yamamoto *et al*., 2006; Sheppard and Evenden, 1994). Furthermore, very fine clay particles (<2 µm) attach themselves onto the surface of the skin (through dermal absorption), because they are of the same scale of roughness as the surface of the skin, and become resistant to cleaning (Sheppard and Evenden, 1994). Moreover, the fine clay fraction is usually enriched with trace metals (including Hg) therefore its ingestion leads to a higher intake of toxic trace metals as compared to the coarse particulate matter. The increase in the Hg_{TOT} content with the decrease in particle size attests to the accumulation of Hg in finer particulate matter (Figure 5.5). This highlights the potential health risk associated with the ingestion and inhalation of finer particulate matter (dust). Furthermore, Hg_{TOT} in dust was significantly correlated ($R^2 = 0.51$) with % volume in the PM_{25} fraction in dust (Figure 5.8).

6.1.2 Bioaccessibility of mercury from inhalable fraction in dust samples

The results of the lung leaching from the inhalable fraction in the dust samples are shown in Figure 6.6.

The Hg concentration extracted by the artificial lysosomal fluid (ALF) (pH 4.5) is substantially higher than Hg found in Grays' (pH 7.4) and Gamble's (pH 7.4) solution, as expected at lower pH. Overall extraction by lung fluids ranged from 4.2 to 34.4 µg kg^{-1} and 0.4 to 3.6 µg kg^{-1} with an average of 11.1 and 1.71 µg kg^{-1} for ALF and Grays', respectively. ALF extracted Hg ranged from 8.3 to 34.4 µg kg^{-1} (average 17.5 µg kg^{-1}) in industrial dust; 6.7 to 15.9 µg kg^{-1} in CBD dust (average 10.4 µg kg^{-1}); and 4.2 to 8.1 µg kg^{-1} in residential dust (average 6.0 µg kg^{-1}).

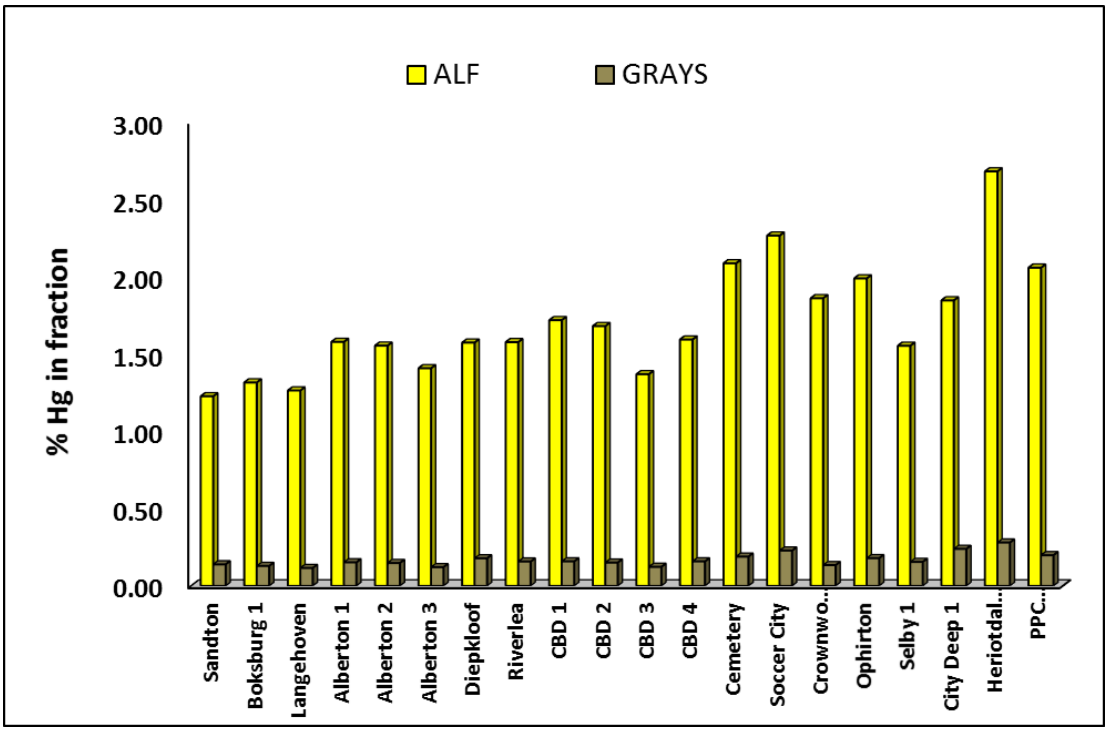

Figure 6.6: Comparison of Hg extracted by simulated lung fluids (ALF, pH =4.5 ± 0.1, and Grays, pH = 7.4 ± 0.1) from Johannesburg dust samples (PM_{25}, n=3).

Grays' extractable Hg varied from 0.8 to 3.6 µg kg^{-1} (average 1.7 µg kg^{-1}) in industrial dust; 0.8 to 1.4 µg kg^{-1} in CBD dust (average 1.0 µg kg^{-1}); and 0.4 to 0.8 µg kg^{-1} in residential dust (average 0.6 µg kg^{-1}). In terms of percentage of Hg extracted, ALF extractable Hg ranged from 1.6 to 2.7% (average 2.0%) in industrial dust; 1.4 to 2.1% in CBD dust (average 1.7%); and 1.2 to 1.6% in residential dust (average 1.4%). For Grays extractable Hg, it ranged from 0.1 to 0.3% (average 0.2%) in industrial dust; 0.1 to 0.2% in CBD dust (average 0.2%); and 0.1 to 0.2% in residential dust (average 0.1%).These results were lower than what has been previously published (Guney *et al*., 2013; Hu *et al*., 2011; Barnett and Turner, 2001; Davies *et al*., 1997). The concentration of Hg extracted by ALF showed the following order: Industrial areas > CBD > Residential areas. The same trend was observed for Hg concentration extracted by Grays' solution. However, Grays' extractable Hg was lower than in ALF leachates.

Gamble's solution extraction results were below the method detection limit of 0.028 µg Hg L^{-1}.

Less than 3% of Hg_{TOT} in dust could be dissolved in the lung fluids. This implies that mercury is most likely to be taken up in the upper region of the lung due to the acidic conditions whereas the bottom region would experience minimal uptake due to the neutral nature of the lung. The higher concentration of Hg extracted by ALF can be attributed to the higher organic content found in the ALF as compared to Grays' and Gamble's solution (Colombo *et al*., 2008). The percentage Hg extracted in both ALF and Grays' decreased as follows: industrial area > CBD > residential area, respectively. To understand the relationship between Hg_{TOT} and lung fluid extractable Hg fractions, correlation studies were carried out, as shown Figure 6.7 and Figure 6.8. The correlation coefficient values for ALF extractable Hg and Grays' extractable Hg fractions showed a strong correlation between Hg_{TOT} and lung extractable Hg fractions form Johannesburg dust samples (ALF: $r^2 = 0.97$, Grays': $r^2 = 0.90$). This suggests that the bioaccessible Hg fraction is influence by the Hg_{TOT} in the Johannesburg dust. Therefore, lung fluid extracted Hg fractions are directly proportional to $Hg_{TOT,}$ implying that an increase in the Hg_{TOT} results in an increase in the bioaccessible Hg fraction. This result is similar to the reported AGF extracted Hg fraction. However, in the latter, the Hg extracted was approximately 3 times greater than in AGF leachates.

Results from the in vitro tests showed that despite the elevated acidity of the simulated gastric solution (pH 1.5) compared to pH 4.5 in the simulated lung fluid, ALF was able to extract more Hg in the analyzed dust samples. The higher extraction efficiency was related to the higher concentration of organic chelators in simulated lung fluid (Barnett and Turner, 2001; Biester *et al*., 2002).

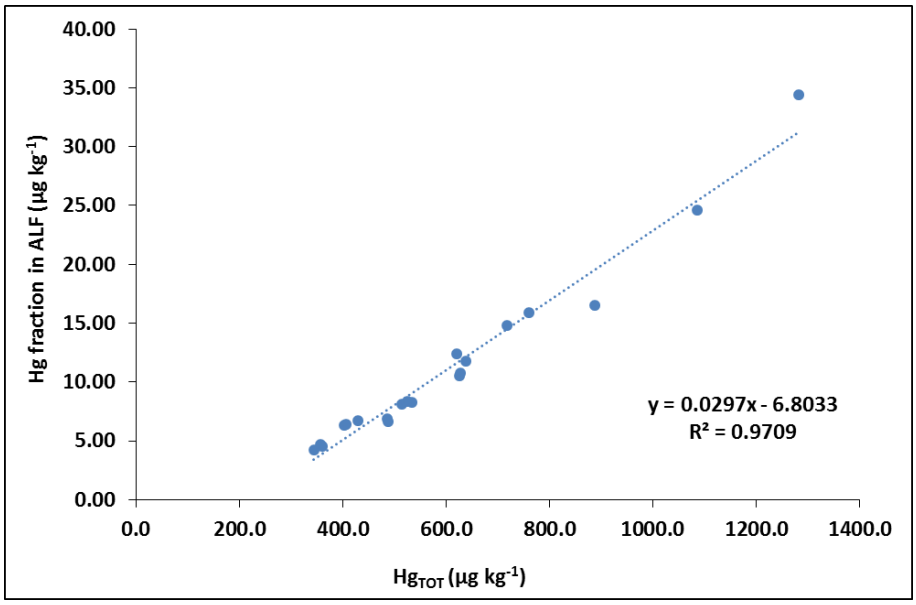

Figure 6.7: Scatterplot of correlation between Hg_{TOT} and ALF extractable Hg from Johannesburg dust samples.

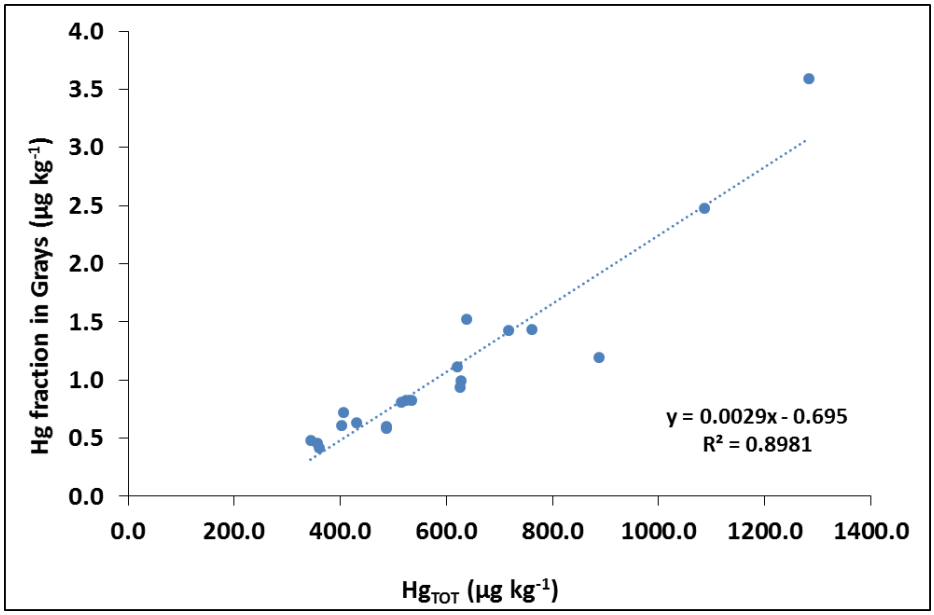

Figure 6.8: Scatterplot of correlation between Hg_{TOT} and Grays extractable Hg from Johannesburg dust samples.

6.2 Sequential extraction procedure (SEP) of mercury from dust

Three different SEPs were used to assess Hg fractionation in dust samples, namely: modified BCR (m-BCR), novel Sequential extraction procedure (n-SEP), and

Sequential Selective Extraction (SSE), respectively (Neculita *et al*., 2005, Bloom *et al*., 2003, Rauret *et al*., 2000). The obtained results for all three procedures are presented in Appendix C (Tables C.1, C.2, and C.3).

6.2.1 Sequential extraction of mercury using modified BCR (m-BCR)

Hg fractionation results are presented in Figure 6.9. The concentration of Hg in the water, exchangeable and acid-soluble fraction (F1) was very low for all the dust samples tested and represented less than 2.5% of Hg_{TOT} content. Mercury in F1 ranged from 0.1 to 2.5% with an average of 0.8%. This fraction highlights the most easily available Hg content under environmental weathering conditions (Bloom *et al*., 2003; Wallschläger *et al*., 1998). In some instances, the contribution of water soluble mercury species is very small and often below the detection limit (Kot and Matyuskina, 2002; Kot *et al*., 2002).

Hydroxylamine hydrochloride (F2), being a more aggressive solvent, extracted a little more Hg as compared to acetic acid (F1 fraction). In this fraction, percentage Hg extracted ranged from 0.3 to 3.8% with an average of 1.1%. This fraction targets Hg adsorbed onto amorphous Fe and Mn oxides and some Hg in the mineral matrix. Samples from the industrial areas leached out a higher percentage of Hg (1.0%) as compared to the residential area samples (0.7%). This was expected as the industrial area samples had a higher % volume of the PM_{25} size fraction, therefore a larger surface area for the adsorption of mercury and mineral oxides.

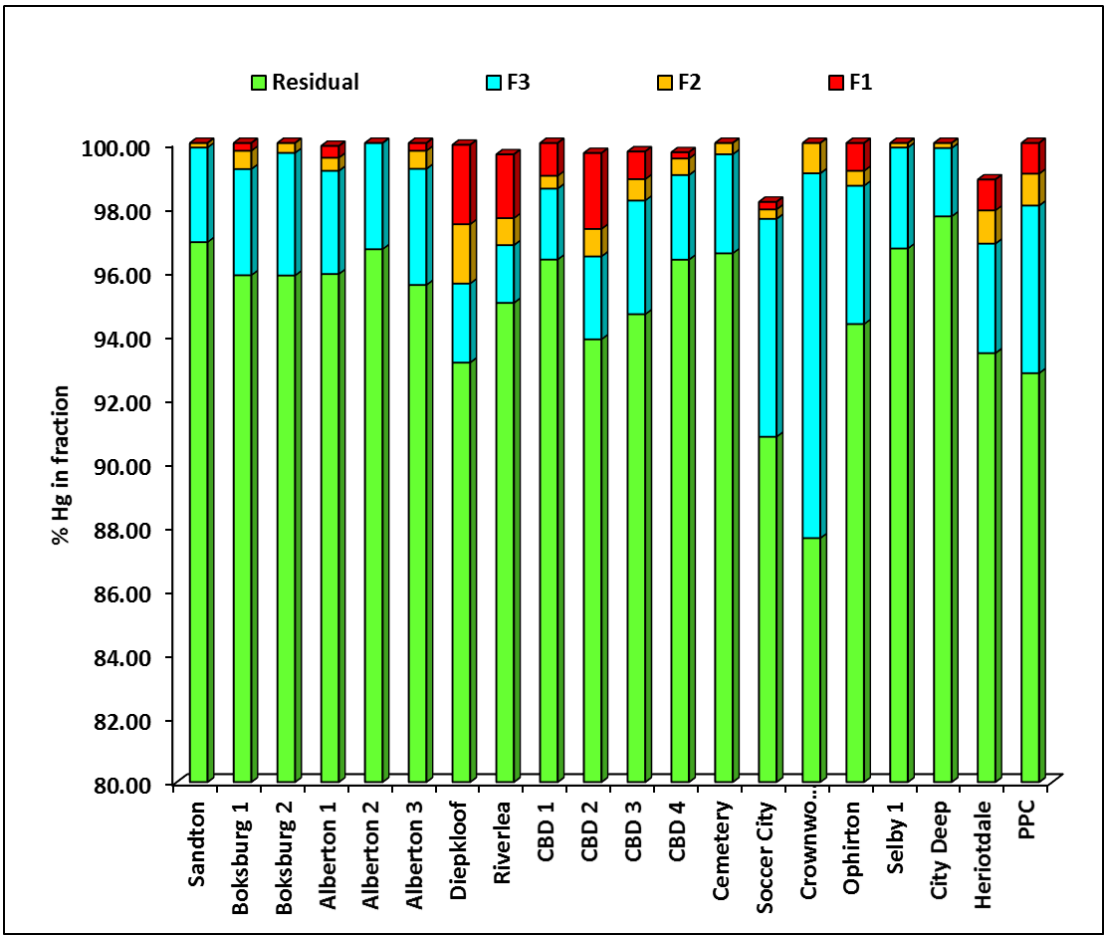

Figure 6.9: Hg fractionation using the modified BCR SEP in selected dust samples from Johannesburg (*PM_{25} size fraction, n=3*)**.**

The mercury fraction bound to amorphous and crystalline iron oxide and organic matter (F3) had the second highest contribution to the Hg_{TOT} content and ranged from 1.8 to 11.4% with an average of 3.8%. This fraction, known as the "oxidisable metals fraction," is extracted by ammonium acetate and hydrogen peroxide, which are more aggressive than hydroxylamine hydrochloride, and target both amorphous and crystalline iron oxides as well as organic matter. Although the oxidisable mercury compounds represent one of the least soluble fractions they are still a cause for concern as they can be leached out from dust particles under extreme environmental conditions such as those encountered in AMD imp acted areas. The fraction contributing the most to the Hg_{TOT} in the dust was mercury bound to sulphides (F4), which ranged from 88

to 97% with an average of 94.8%, representing mostly insoluble compounds of mercury such as cinnabar (HgS), metacinnabar (m-HgS), and mercury selenide (HgSe).

The average percentage of each Hg fraction extracted from dust samples had the following trend: residual (94.80%) > organic crystalline iron oxides (3.76%) >amorphous Fe-Mn oxides (1.11%) ≥ exchangeable (0.83%), which were similar to the findings of Sanchez *et al*., (2005), even though the substrate were different. For soils heavily contaminated with mercury from mercury mining, Sanchez *et al*., (2005), reported negligible mercury concentration in the water-soluble, exchangeable, and carbonate fraction (F1), 1.7% of Hg_{TOT} concentration in the reducible fraction (F2), 33% of Hg_{TOT} concentration in the oxidisable fraction (F3), and 54% of Hg_{TOT} concentration in the residual fraction.

Correlation studies between m-BCR fractions revealed positive correlation between them (Table 6.1). The following fractions: F1, F2, F3, and residual are influenced by Hg_{TOT}. On the other hand, the residual fraction affects F1, F2, and F3. However, F2 and F3 are mostly affected as compared to F1 because of percentage composition implying that an increase in the amount of the residual fraction leads to the decrease in the amounts of fractions F2 and F3. It's important to keep in mind that m-BCR is a non-selective SEP for mercury, and is an operationally defined procedure influenced by concentration of metals and metalloids and matrix.

Table 6.1: Correlation among different Hg fractions extracted using m-BCR.

	HgTOT Conc.	*F1*	*F2*	*F3*	*Residual*
HgTOT Conc.	1.00				
F1	0.36	1.00			
F2	0.64	0.20	1.00		
F3	0.69	0.06	0.80	1.00	
Residual	1.00	0.35	0.61	0.65	1.00

6.2.2 Sequential extraction of mercury using Bloom's SSE method

Mercury fractionation results for dust samples determined by Bloom's SSE procedure are shown in Figure 6.10.

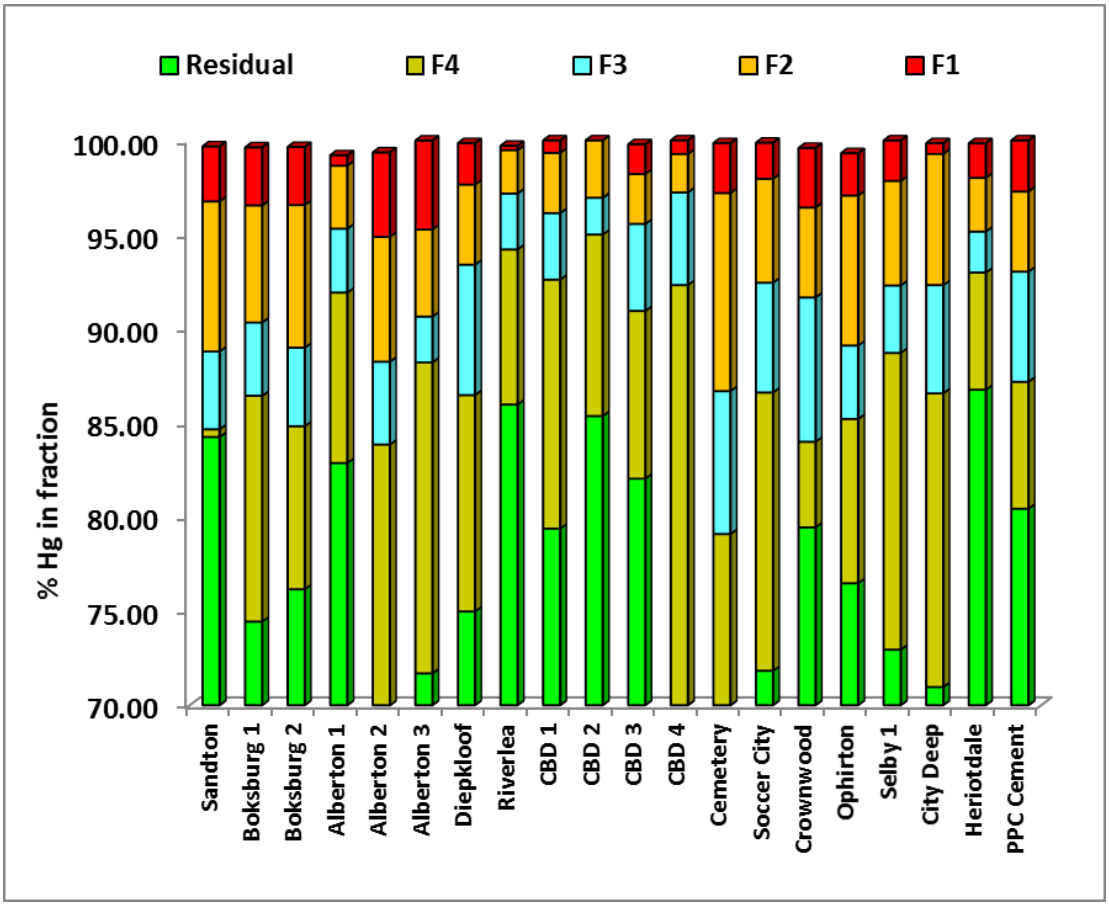

Figure 6.10: Hg fractionation using the SSE in selected dust samples from Johannesburg (*PM_{25} size fraction, n=3*).

The dust samples contained a small percentage of Hg in the water-soluble fraction (F1, 2.2%), whilst a significant percentage of Hg was present in highly insoluble form, cinnabar and metacinnabar, HgS (F5, 76.8%). This was in agreement with what was mentioned by Kocman *et al*., 2004 and Biester *et al*., 2000, 1999) who reported that up to 1% and 93% of total mercury was found in water soluble and residual fractions, respectively, and the residual fraction was characterized by a combination of cinnabar

and non-cinnabar mercury. The exchangeable Hg concentration in dust samples ranged from 10.7 to 73.9 µg kg^{-1} (average of 31.7 µg kg^{-1}) accounting for 2.0 to 10.5% with an average of 5.1% of Hg_{TOT}. A sum of F1 and F2 yielded 6.7%, which is still less than 10% of Hg_{TOT} concentration.

Organically bound Hg (F3), extracted from Johannesburg dust, contributed with an average of 29.4 µg kg^{-1}, and ranged from 11.9 to 76.6 µg kg^{-1} accounting for 2.3 to 10.5% averaging 4.5% of Hg_{TOT}. This result is expected as the total carbon content of selected dust samples averaged 5.4%. A similar result (7%) was reported by Bloom *et al*., (2003) for gold mine tailings and he also confirmed that F3 fraction selectivity extracted organo bound mercury (99%) and by leaching pure organo-Hg dispersed in kaolin powder. There is an expectation that mercury concentration in this fraction (F3) would be high in samples with high amounts of organic matter due to the fact that mercury is associated mostly with humic organic matter (Kocman *et al*., 2004). This is an important fraction as it is correlated with methylation potential (Bloom *et al*., 2003).

Elemental Hg and strongly complexed Hg species (F4) had a higher contribution than the organically bound Hg. It range from 1.3 to 125.7 µg kg^{-1} (average of 70.3 µg kg^{-1}), accounting for 0.4 to 22.4% with an average of 11.3%. A combination of F3 and F4 fractions yielded 16.4%. Bloom *et al*., (2003), reported from his studies that F4 fraction extracted > 95% elemental Hg from pure compound of Hg^0.

The mercury sulphide fraction and the residual fraction were combine to form one fraction (F5), and had the following percentage Hg extraction in the range of 61.2 to 86.8% with an average of 76.8%, and was in the HgS form. Using pure compounds of cinnabar (HgS), meta-cinnabar (m-HgS), and mercury selenide (HgSe), Bloom *et al*., (2003), was able to extract 100% Hg using aqua regia. This showed that the aqua regia was capable of extracting 100% Hg from HgS compounds therefore its use in the leaching of the HgS fraction (F5). F5 showed a strong positive correlation (r^2 = 0.95) with the Hg_{TOT} concentration (Figure 6.11). This indicated that F5 is influenced by the

sample concentration (Hg_{TOT}). On the other hand, correlation studies between the fractions within the dust samples revealed a moderate correlation between them (Table 6.2). This indicates that there exists a direct proportionality relationship between each of the following fractions: F1, F2, F3, and F4. An increase in any one fraction will lead to an increase in the remaining three fractions. However, an increase in the amount of fraction F5 resulted in the decreased amounts of fractions F1 to F4. This suggested that most chemical processes involved in mercury cycling in the soil/dust occur within the non-cinnabar mercury forms (F1–F4), as cinnabar (F5) is an insoluble form of mercury that does not enter in the mercury cycle.

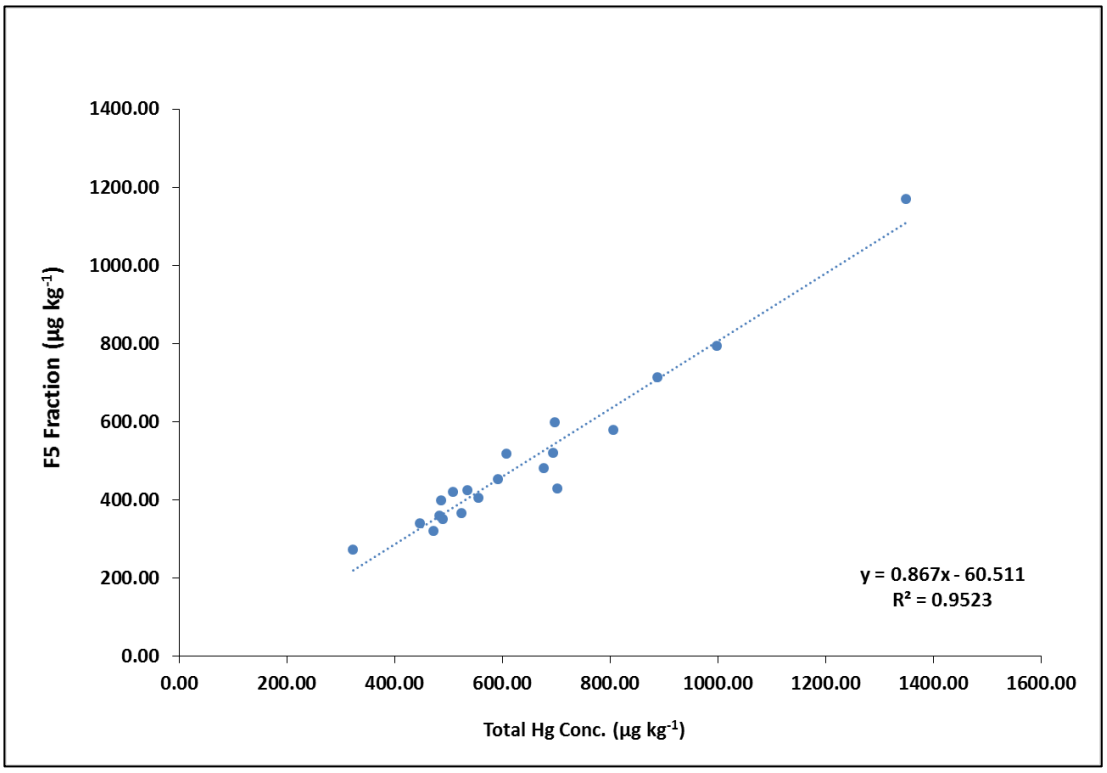

Figure 6.11 Hg_{TOT} correlated with the residual fraction (F5).

Table 6.2: Correlation among different Hg fractions using SSE.

	F1	*F2*	*F3*	*F4*	*Residual*
F1	1.00				
F2	0.52	1.00			
F3	0.56	0.65	1.00		
F4	0.08	0.36	0.31	1.00	
Residual	0.44	0.26	0.48	0.13	1.00

6.2.3 Sequential extraction of mercury using Neculita's (n-SEP) method

Neculita's SEP results for Hg are presented in Figure 6.12.

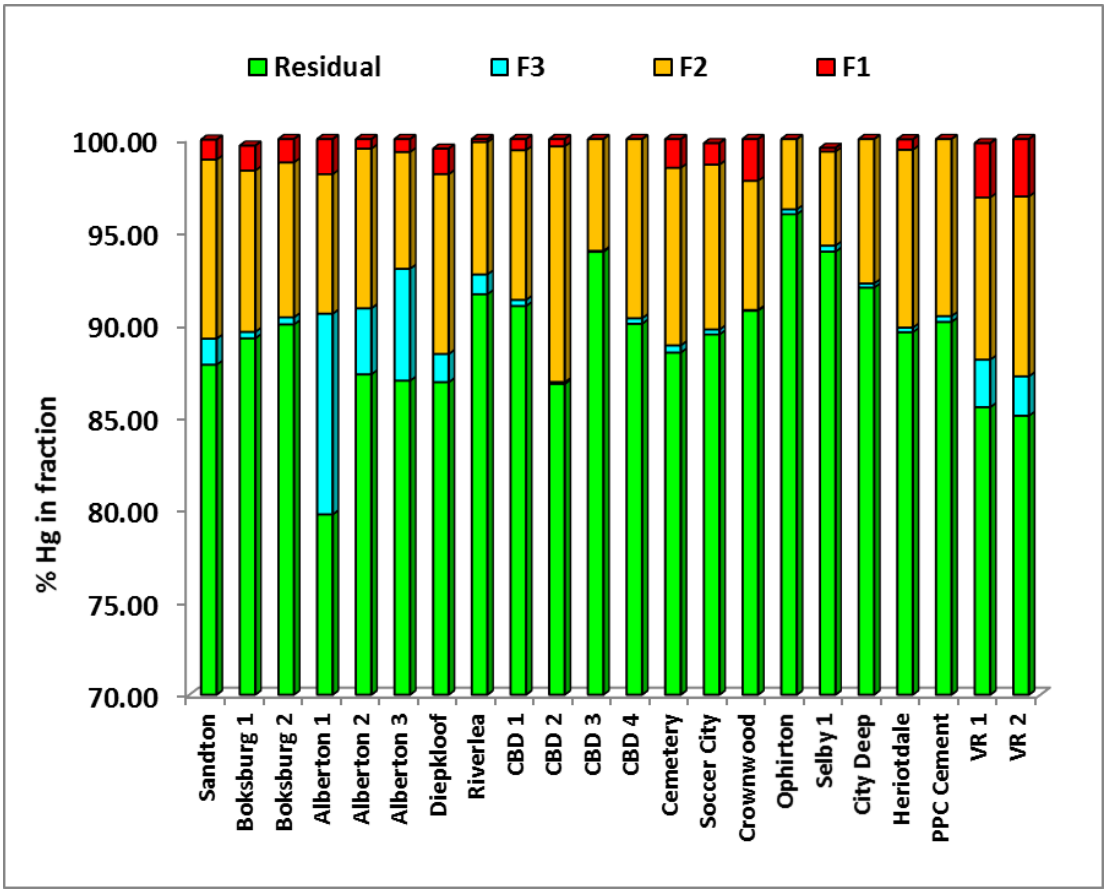

Figure 6.12: Hg fractionation using the n-SEP in selected dust samples from Johannesburg (*PM_{25} size fraction, n=3*).

The F1 (water-soluble), F2 (exchangeable), and F3 (organic) fractions represents low percentages of Hg extracted and they ranged from 0.0 to 3.2%, 4.1 to 12.7%, and 0.1 to 2.6% with averages of 1.1%, 8.3%, and 1.4%, respectively. The organic fraction (F3) was very low and these results were consistent with the low total carbon content (5.4%) of the dust samples. This phenomena was observed by Bloom *et al*., (2003).

In all dust samples, the largest Hg proportion was found within the residual fraction, and ranged from 85.1 to 93.9% of the Hg_{TOT}. Generally in naturally occurring conditions, the residual fraction represents the immobile form of Hg, based on the matrix of the substrate and source of contamination (Bloom *et al*., 2003; Wallschläger *et al*., 1998). In this study, there is a reason to believe that Hg^0 deposited was eventually converted to other Hg species that can be adsorbed by the sulphides, based on the presence of high concentration of sulphides, generally found within the tailings.

Correlation studies between the fractions within the dust samples revealed a moderate correlation between them (Table 6.3). This was confirmed by the high correlation coefficients between Hg_{TOT} and Residual (r^2 = 1.00), Hg_{TOT} and F2 (r^2 = 0.89), Hg_{TOT} and F1 (r^2 = 0.45), F1 and residual (r^2 = 0.43), F1 and F2 (r^2 = 0.38), and F2 and Residual (r^2 = 0.86). This indicates that there exists a direct proportionality relationship between each of the following fractions: F1, F2, residual and Hg_{TOT}.

Table 6.3: Correlation among different Hg fractions using n-SEP.

	Hg $_{TOT}$	***F1***	***F2***	***F3***	***Residual***
Hg_{TOT}	1.00				
F1	0.45	1.00			
F2	0.89	0.38	1.00		
F3	-0.28	0.00	-0.28	1.00	
Residual	1.00	0.43	0.86	-0.33	1.00

6.2.4 Discussion

Hg fractions have different mobility and potential bioavailability characteristics. Water-soluble and exchangeable fractions (n-SEP), exchangeable, water and acid-soluble fraction (m-BCR), and water soluble and human stomach acid soluble fraction (SSE) are the most active, mobile and bioavailable phases of Hg and probably the most important Hg classes in view of environmental concerns (Kot and Matyushkina, 2002). From all three SEPs, extractable Hg in F1 fraction was 0.5%, 1.1%, and 2.2% for m-BCR, n-SEP, and SSE, respectively. These result were similar to the results reported by Bloom *et al*., (2003) for gold mine tailings, with extractable Hg in F1 fraction of 3%. Kocman *et al*. (2004) reported extractable Hg in F1 fraction of up to 1% using SSE procedure determined in the soil from Idrija Hg-mine region, Slovenia. These results were comparable to the results obtained in this study. Despite the different substrates (soils, sediments, dust), Hg extracted in F1 fraction was less than 5%, this implied that mercury deposited was transformed into other Hg species depending on the environmental conditions. In several studies, it was demonstrated that Hg^0 transformations take place immediately after being deposited in the soil and slowly converted into Hg species present in the sediments (Hg associated with organic matter) (Bloom *et al*., 2003; Wang *et al*., 2003; Boening, 2000). However, the oxidation of Hg^0 to Hg^{2+} in soils is considered to be slow kinetically, therefore most of the Hg^0 might be re-emitted before oxidation takes place (Biester *et al*., 2002a). This was confirmed by studies carried out in areas of Hg, naturally enriched and highly contaminated, whereby high rates of gaseous Hg flux were observed (Gustin *et al*., 2000). The F1 extractable Hg fraction results were compared to the AGF extractable Hg and the F1 fraction (average of 1.4% of Hg_{TOT}) was three times more than the AGF extractable Hg (0.5% of Hg_{TOT}). This was attributed to the under estimation by gastric fluid. It was expected that, both bioaccessible Hg in F1 fraction and AGF extractable Hg would have similar results, since they both represent the mobile and bioavailable fraction.

The acid-soluble fraction is approximately equivalent to the sum of water-soluble and exchangeable fractions (Li *et al*., 2009). F2 fraction, simulating human stomach acid

soluble Hg species, was determined as the fraction of Hg in soil potentially available for absorption in the human digestive system. This kind of absorption through the gastrointestinal tract appears to be the most critical endpoint and exposure pathway for the human community around Hg contaminated soil sites (Barnett and Turner, 1995). A sum of the first three fractions yielded the following: 5.4%, 10.8%, and 11.9% for m-BCR, n-SEP, and SSE. This combination was made up of the mobile and semi-mobile fractions, and of interest, they are similar except for m-BCR, a non-selective SEP for Hg. The implication is that these two methods (n-SEP and SSE) extract the same Hg species from dust. Very low concentration of Hg was determined in the water-soluble (F1) and exchangeable (F2) fractions regardless of the different land use types. Even though the concentration of Hg extracted was very low, this is the bioavailable Hg fraction, which is converted into methylmercury either by biotic or abiotic processes in the environment resulting in the bioconcentration, biomagnification and bioaccumulation of Hg in the food chain (Covelli *et al*., 2009; Boszke *et al*., 2006; Piani *et al*., 2005; Biester *et al*., 2002b, 1999; Kim *et al*., 2000; Wallschläger *et al*., 1998; Barnett *et al*., 1997).

Amorphous or poorly crystalline or hydrous oxides of manganese and iron are extracted together and are well known sinks in the surface environment for heavy metals contaminants due to their large surface area and/or microporous structure (Trivedi and Axe, 2001). Secondary oxides deposited as coatings on mineral surfaces or as fine discrete particles, can occur by any or a combination of the following mechanisms: co-precipitation, adsorption, surface complex formation; ion exchange and penetration of the lattice (Hall *et al*., 1996). According to Jenne (1968) Fe and Mn oxides are the principal soil surface that control the mobility of metals in soils and natural water. They are able to achieve this by immobilizing metals by providing large surface areas for adsorption to take place. Initially, the amorphous oxyhydroxides of iron and manganese strongly sorb trace elements in exchangeable forms, however, as time goes by, they are transformed to less mobile, and specifically adsorbed forms. The use of acidified hydroxylamine hydrochloride 0.1 M releases metals mainly from

amorphous manganese oxide phases with little attack on iron oxide phases (Shuman, 1982). Increasing the hydroxylamine hydrochloride concentration to 0.5 M (Sahuquillo *et al*. 1999) and decreasing the pH from 2 to 1.5 (Chao 1972; Sahuquillo *et al*. 1999) provides effective attack on the iron oxide phases while still releasing metals from manganese oxide phases.

Organo-bound mercury (F3) in dust samples was reported as 3.8%, 1.4%, and 4.5% for m-BCR, n-SEP and SSE, respectively. These values indicate low total carbon content in the Johannesburg dust, this was attributed to the typically low organic material in mine wastes. The source of Hg possibly was the result of leaching of some sulphide minerals. Some of the extractants can dissolve sulphides with enhanced selectivity whilst silicates are attacked to some extent (Klock *et al*., 1986). Even though the organo –bound mercury was very low in concentration, it is still a cause for concern, as this is the most toxic form of Hg. It will biomagnify, bioaccumulate and bioconcentrates in the food chain resulting in exposure to humans.

Organic matter exhibit a high degree of selectivity for divalent trace metal ions as compared to monovalent ions and the order of binding strength being Hg > Cu > Pb > Zn > Ni > Co (Filgueiras *et al*., 2002). Mercury has a high affinity for soil organic matter, especially for reduced sulphur groups such as thiol ligands (Skyllberg *et al*., 2006; Khwaja *et al*., 2006; Skyllberg et al., 2000; Schuster, 1991). According to Kennedy *et al*., (1997), metallic pollutants in the oxidisable fraction are thought to remain immobilized in the soil/dust for longer periods. However, due to decomposition processes, they are mobilized. Maximum sorption onto soil organic surfaces occurs in the pH range of 3 to 5, however, an increase in pH leads to a decrease in sorption, mainly due to the increase in dissolved organic matter complexed with Hg (Yin *et al*., 1996). F3 (Hg bound to organic matter) was regarded as a stronger complex (Wallschläger *et al*., 1998a) due to its association with stable high molecular weight humic substances that release small amounts of metals in a slow manner (Filgueiras *et al*., 2002). Therefore they are considered as having limited mobility and bioavailability.

It also should be borne in mind that: (1) Hg bound to organic matter (F3) could include methylmercury species (mainly monomethylmercury) in spite of being a very small proportion in general (Bloom *et al*., 2003); (2) in addition to the organic matter concentration, redox potential, pH and Cl^-ions play a key role in the determination of Hg speciation in soil solution and the resultant chemical transformation that may occur (Ravichandran, 2004); (3) organochelated Hg (F3) was observed to be strongly correlated with methylation potential and thus seems to play an important role in the biogeochemical cycle of Hg in some cases (Bloom *et al*., 2003; Kocman *et al*., 2004); and (4) Hg fractionation (and speciation) in soil/sediment is dynamic (Wallschläger *et al*., 1998a, 1998b) and subject to shift with alteration of environmental conditions including physical, chemical factors, and especially microbial population and activities.

Residual fraction is generally thought to contain significant quantities of sulphides, which tend to act as one of the major sinks of Hg. Mercury sulphide (HgS) formed is an immobilized form of mercury due to its low solubility (10^{-54} mol dm^{-3}) (Barnett and Turner, 2001; Lechler *et al*., 1997). In all three sequential extraction procedures, the residual fraction had the following percentage Hg extraction: 87.6 to 97.7%, 85.1 to 93.9%, and 61.2 to 86.8% with averages of 94.8%, 89.6%, and 76.8% for m-BCR, n-SEP, and SSE, respectively. This indicated that most of the Hg in the dust was found in the residual form and inside the dust mineral matrix. Therefore the amount of Hg was distributed as follows: residual > inside mineral matrix > surficially adsorbed > water soluble and loosely adsorbed. One factor to be consider in the release of Hg from the residual fraction is the presence of pyrites. These have a tendency to increase the risk of Hg pollution because they are a significant acid mine drainage producing mineral and Hg compounds, particularly cinnabar and meta-cinnabar) are more soluble and reactive in acids (Bloom *et al*., 2003). It has been reported that the presumably non-soluble cinnabar appeared to become soluble and form aqueous complexes with sulfide if it accumulated to a high enough concentration (Ravichandran *et al*., 1998;

Jay *et al*., 2000) due to sulfate reduction mediated by sulfate reducing bacteria (SRB) (Mason and Benoit, 2003).

In comparison with other sequential extraction studies conducted on different substrates, various outcomes have been observed and in most cases there have been similarities with results obtained in this study (refer to Table 6.4). According to Bloom *et al*. (2003) and Bloom and Katon (2000), mercury species from the soils/sediments had the following ranges of: 0.4 to 1.3%; 0.8 to 1.2%; 0.5 to 1.0; 3.4 to 12.3%; and 85.9 to 93.1% for water-soluble, human stomach acid-soluble, humic/organic matter, elemental Hg and complex-compounds, and residual/mercuric sulphide, respectively. Most of the Hg determined in the mine and contaminated sites were found in the F4 and F5 fractions, indicating that this Hg is immobile and not bioavailable (Bloom and Katon, 2000). The use SSE of Hg has been useful in defining the different Hg species present in different substrates and the transformation they may undergo when introduced to different environments.

For example, floodplain soils contaminated 50 years ago by soluble $Hg(NO_3)_2$, most of the Hg determined was in the form of non-bioavailable cinnabar, having been transformed in to insoluble, non-bioavailable cinnabar (Bloom and Katon, 2000). Addition of mine tailings to sediments resulted in most of the Hg being converted to organo-mercury. This implies that all Hg from mine sources has the potential to increase methyl mercury production if transported to wetlands.

Application of SSE on sediments led to the following distribution of mercury released in each fraction: F1 and F2 were found to be almost negligible, contributing less than 5% of the Hg_{TOT} concentration, indicating low risk of Hg mobility in the sediments; F3 and F4 were the dominant phases representing nearly 80% of Hg_{TOT} in the sediments (Yu *et al*., 2012).

Table 6.4: Sequential extraction methods proposed by others to determine the mercury species in soils and/or sediments (Values presented in red are obtained in this study).

Reagents	**Compounds extracted**	**Bloom *et al* (2003) & Bloom and Katon, 2000**	**Neculita *et al* (2005)**	**Sánchez *et la*., 2003 (Modified BCR)**
Deionized water	Water soluble	0.4 – 1.3%, (2.2%)	<1.1%, (1.1%)	
HCl/CH_3COOH	Human stomach acid soluble	0.8 -1.2%, (5.1%)		
0.5M NH_4Ac-EDTA + $CaCl_2$	Exchangeable compounds		2.1 – 39.6%, (8.3%)	
0.11 mol L^{-1} CH_3COOH	Exchangeable, water soluble, and carbonate fractions bound Hg			0%, (0.9%)
0.2M NaOH + CH_3COOH (4% v/v)	Organic compounds		0.1 – 2%, (1.4%)	
0.5 mol L^{-1} NH_2OH/HCl (pH 1.5)	Reducible Hg			1.7%, (0.8%)
8.8 mol L^{-1} H_2O_2 (pH 1.5)/1 mol L^{-1} CH_3COONH_4 (pH 2)	Oxidisable Hg			3.3%, (3.8%)
KOH	Humic/Organic	0.5 – 1.0%, (4.5%)		
HNO_3	Complex compounds	3.4 – 12.3%, (11.3%)		
Aqua regia	Residual and HgS	85.9 – 93.1%, (76.8%)	65 – 116%, (89.6%)	54.0%, (94.8%)

According to Liu *et al*. (2006), the most abundant Hg fraction was the organically bound Hg (F3) with percentage higher than 50% of total Hg. The second highest fraction was F4 (20–30%), representing Hg^0 based on the fact that all free Hg^0 present in a sample could be dissolved in cold 12 M HNO_3 (Gerlach *et al*., 1995; Bloom *et al*., 2003). It should be noted that some other classes of Hg compounds such as Hg(I), Hg associated with amorphous organo-sulfur, Hg–Ag amalgams, and Hg associated with crystalline Fe/Mn oxide phases may be extracted into F4 fraction. Besides F3 and F4, the aqua regia soluble Hg fraction (F5), operationally termed as mercuric sulfide (HgS) including both cinnabar and metacinnabar and mercuric selenide (HgSe), also contributed an accountable portion to total Hg in the samples (about 10%).

In conclusion, the Hg extracted by the gastric juices, lung fluids and F1 and F2 of the sequential extraction procedures were in agreement. The SEP results complemented the oral and lung leaching results. In both cases, the concentration of Hg leached out was very low, approximately 2.5% for the highest Hg concentration leached out (oral and lung) and 2.2% for water-soluble fraction from the three sequential extraction. This means that there is a high concentration of the insoluble cinnabar Hg species in the dust samples. These result indicated that the highest concentration of Hg found in the residual fraction corresponds to a very stable Hg species (HgS), which is immobilized. The implications are that when the environmental conditions change to favour the leaching of the insoluble cinnabar Hg species, there will be a great deal of mercury released into the environment leading to greater contamination and exposure to humans.

Chapter 7

Health risk assessment model

Health risk assessment model was used to identify areas where potential health risks lie due to mercury pollution. It was also used to determine the exposure pathway which resulted in the highest levels of risk for humans exposed to road dust mercury.

7.1 Risk assessment

Risk assessment was carried out to estimate the potential health risk faced by human beings when exposed to toxic heavy metals in street dust. In this study, Hg, As, Cd, and Cr(IV) were identified as potential hazardous agents with respect to human health.. According to USEPA, (2011a), all these elements have toxicological health effects on humans, and some are carcinogenic (As, Cd, Cr) (WHO, 2011). The biggest concern about these chosen elements is the fact that they are released and dumped on TSFs during the gold mining activity becoming a health risk when humans are exposed to windblown dust from the TSFs, and exposed to AMD polluted waters, and sediments. In order to assess the exposure of humans (children and adults) to trace elements (Hg, As, Cd, and Cr(IV)) in street dust, a model developed by US Environmental Protection Agency (USEPA, 1996) was used. Equation (4) – (13), in Chapter 4, were used in the model to calculate the exposure of children and adults to trace metals in street dusts. Exposure of humans to trace elements in street dust can occur via three main pathways: (a) oral ingestion of dust particles; (b) inhalation of resuspended particulates through the mouth and nose; (c) dermal absorption of trace elements in particles adhered to exposed skin; and vapour inhalation, in the case of mercury. Both non-cancer and cancer risk of the exposure routes were considered.

7.1.1 Non-cancer Risk

The non-cancer health risk to children from exposure to mercury in street dust via different pathways are shown in Table 7.1. The hazard quotient (HQ) values for each of the pathways used in the model for the exposure of children to mercury in dust were as follows: 9.16E-04 to 1.76E00 for exposure by vapour inhalation; 9.06E-02 to 1.01E-01 exposure by oral ingestion; 9.11E-04 to 1.01E-03 for dermal contact; and 9.59E-07 to 1.19E-06 for exposure by inhalation of dust and suspended soil particles, respectively. These results indicate that greatest exposure of children to mercury was observed via the vapour inhalation and the least was observed in the inhalation of resuspended dust particulate matter.

Table 7.1 Non carcinogenic risk, chronic daily intake (CDI), Hazard quotient (HQ), and Hazard index (HI) for mercury in dust (PM_{25}) via ingestion, inhalation, dermal, and vapour exposure pathways for children.

SAMPLE SITES	[Hg_{TOT}] mg kg^{-1}	mg kg^{-1} day^{-1}				HQ_{ing}	HQ_{inh}	HQ_{dermal}	HQ_{vapour}	HI = ΣHQ_i
		CDI_{ing}	CDI_{inh}	CDI_{dermal}	CDI_{vapour}					
Sandton	0.32	4.13E-06	1.15E-10	1.16E-08	1.26E-04	4.82E-02	3.84E-07	5.50E-04	4.21E-01	0.47
Diepkloof	0.69	8.87E-06	2.48E-10	2.48E-08	2.71E-04	1.03E-01	8.26E-07	1.18E-03	9.04E-01	**1.01**
Riverlea	0.70	8.91E-06	2.49E-10	2.49E-08	2.73E-04	1.04E-01	8.30E-07	1.19E-04	9.09E-01	**1.01**
Boksburg 1	0.48	6.17E-06	1.72E-10	1.73E-08	1.89E-04	7.20E-02	5.75E-07	8.23E-04	6.29E-01	0.70
Boksburg 2	0.45	5.71E-06	1.60E-10	1.60E-08	1.75E-04	6.66E-02	5.32E-07	7.61E-04	5.82E-01	0.65
Alberton 1	0.51	6.49E-06	1.81E-10	1.82E-08	1.99E-04	7.58E-02	6.05E-07	8.66E-04	6.62E-01	0.74
Alberton 2	0.47	6.04E-06	1.69E-10	1.69E-08	1.85E-04	7.04E-02	5.62E-07	8.05E-04	6.16E-01	0.69
Alberton 3	0.49	6.25E-06	1.75E-10	1.75E-08	1.91E-04	7.29E-02	5.82E-07	8.33E-04	6.38E-01	0.71
CBD 1	0.53	6.83E-06	1.91E-10	1.91E-08	2.09E-04	7.97E-02	6.36E-07	9.11E-04	6.97E-01	0.78
CBD 2	0.61	7.77E-06	2.17E-10	2.18E-08	2.38E-04	9.06E-02	7.24E-07	1.04E-03	7.92E-01	0.88
CBD 3	0.49	6.21E-06	1.74E-10	1.74E-08	1.90E-04	7.25E-02	5.79E-07	8.29E-04	6.34E-01	0.71
CBD 4	0.53	6.71E-06	1.87E-10	1.88E-08	2.05E-04	7.82E-02	6.25E-07	8.94E-04	6.84E-01	0.76
Cemetery	0.70	8.98E-06	2.51E-10	2.51E-08	2.75E-04	1.04E-01	8.36E-07	1.20E-03	9.16E-01	**1.02**
Soccer City	0.81	1.03E-05	2.88E-10	2.88E-08	3.15E-04	1.20E-01	9.59E-07	1.37E-03	1.05E+00	**1.17**
Ophirton	0.59	7.56E-06	2.11E-10	2.12E-08	2.31E-04	8.82E-02	7.04E-07	1.01E-03	7.71E-01	0.86
Selby 1	0.56	7.11E-06	1.99E-10	1.99E-08	2.18E-04	8.29E-02	6.62E-07	9.48E-04	7.25E-01	0.81
City Deep	0.68	8.66E-06	2.42E-10	2.43E-08	2.65E-04	1.01E-01	8.07E-07	1.15E-03	8.84E-01	0.99
Crownwood	1.00	1.28E-05	3.57E-10	3.57E-08	3.91E-04	1.49E-01	1.19E-06	1.70E-03	1.30E+00	**1.45**
Heriotdale	1.35	1.72E-05	4.82E-10	4.83E-08	5.28E-04	2.01E-01	1.61E-06	2.30E-03	1.76E+00	**1.96**
PPC Cement	0.89	1.13E-05	3.17E-10	3.18E-08	3.47E-04	1.32E-01	1.06E-06	1.51E-03	1.16E+00	**1.29**

HQ value through inhalation of dust particles is 3 to 6 orders of magnitude lower than the other three exposure pathways (vapour inhalation, ingestion and dermal contact), and therefore inhalation of resuspended particles through the mouth and nose is almost negligible compared to the other routes of exposure. Considering the non-cancer hazard index (HI) for the exposure of children to mercury in dust, some sites were higher than the threshold value of 1, indicating greater adverse health risks. These sites included Cemetery, Crownwood, Heriotdale, PPC Cement, and Soccer City, (industrial areas, grossly affected by mine tailings and reprocessing of tailings dams, and presence of tailings footprint), Diepkloof and Riverlea (residential areas surrounded by mine tailings) (Figure 7.1).

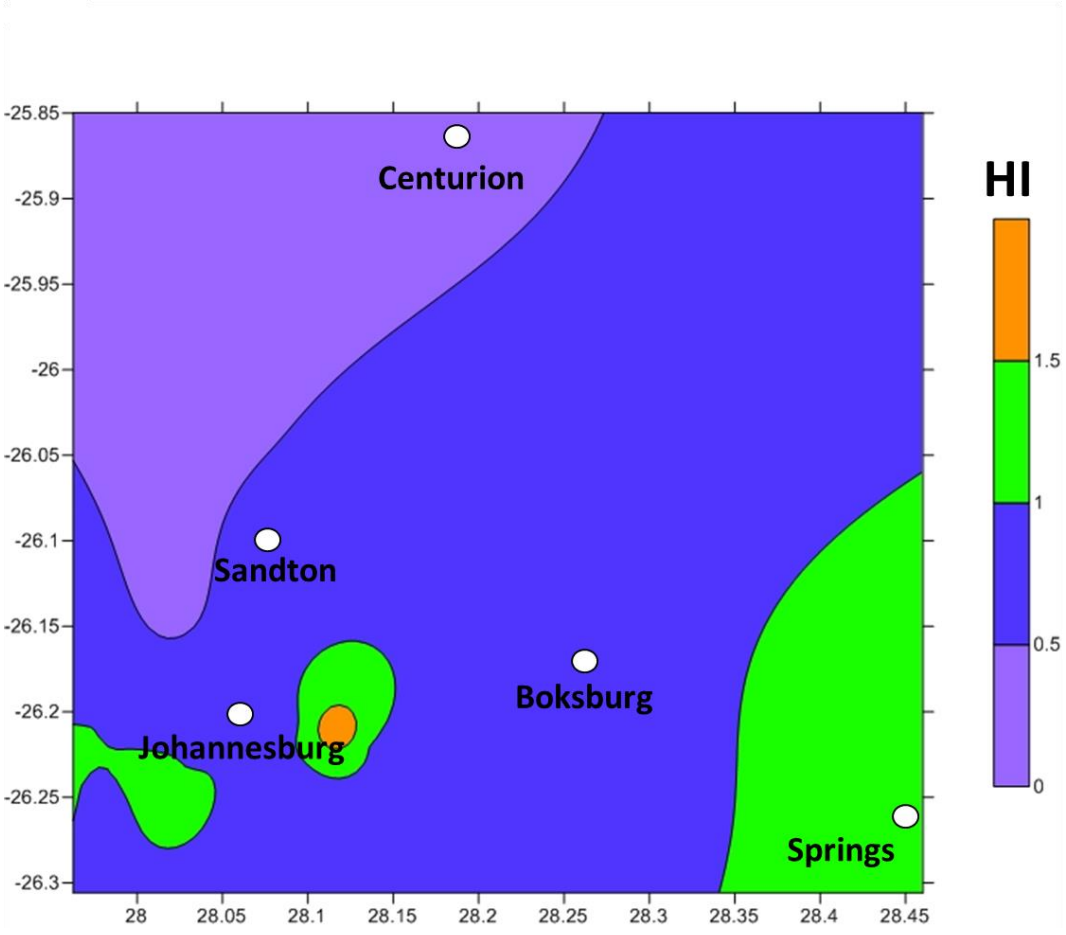

Figure 7.1: Spatial distribution of hazard index (HI) for the children exposed to mercury from Johannesburg street dust.

Pearson correlation studies ($p < 0.05$) showed that the calculated HI value for exposure of children to mercury in dust was dependent on the Hg_{TOT}. It had a correlation coefficient of 1 (Figure 7.2). The sites with the HI values higher than the threshold value of 1, also had high Hg_{TOT} concentration in the dust, i.e. the lower the HI values the lower the concentration of Hg_{TOT}, the reverse was true.

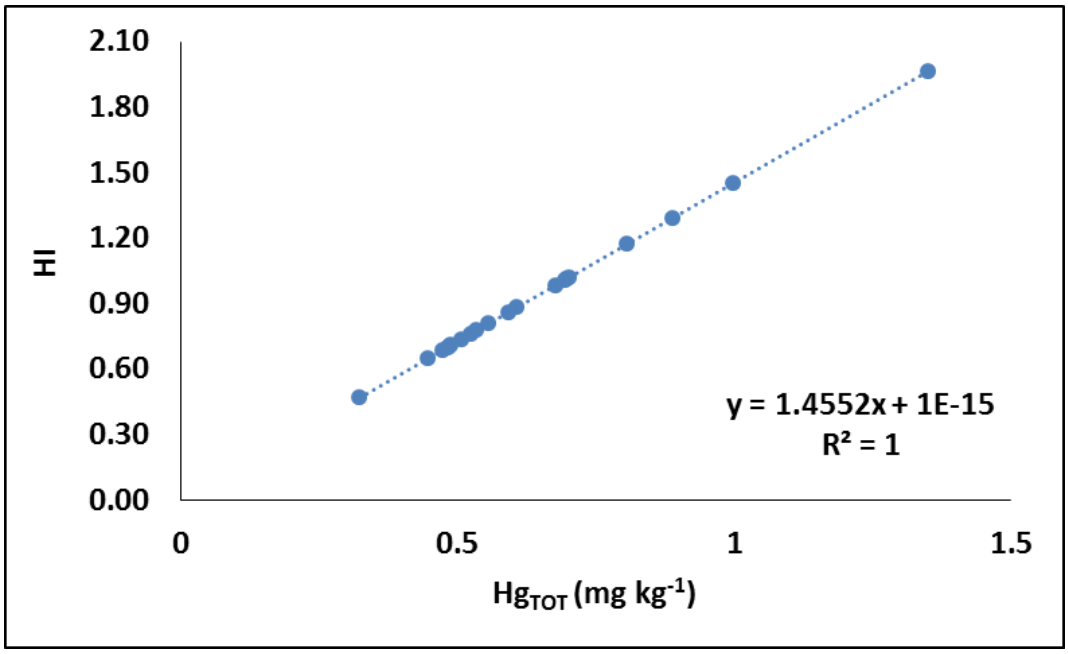

Figure 7.2: Correlation between Hg_{TOT} concentration and HI values for the non-cancer health risk exposure of children to mercury in street dust.

The non-carcinogenic health risk to adults from exposure to mercury in street dust via different pathways are shown in Table 7.2. The HQ values for each of the pathways used in the model for the exposure of adults to mercury in dust were as follows: 9.81E-02 to 1.13E-01 for exposure by vapour inhalation; 9.71E-03 to 1.08E-02 for exposure by ingestion; 8.40E-04 to 1.76E-03 for dermal contact; and 9.06E-07 to 3.00E-07 for exposure by inhalation of dust and suspended soil particles, respectively. It exhibited the same trend as observed by the children. However, the non-cancer health risk for adults was lower than that of children and the HI values were lower than the threshold value of 1. This indicated that adults had little adverse health risk due to exposure of mercury in the street dust.

Table 7.2: Non carcinogenic risk, chronic daily intake (CDI), Hazard quotient (HQ), and Hazard index (HI) for mercury in dust (PM_{25}) via ingestion, inhalation, dermal, and vapour exposure pathways for adults.

SAMPLE SITES	$[Hg_{TOT}]$ mg kg^{-1}	mg kg^{-1} day^{-1}				HQ_{ing}	HQ_{inh}	HQ_{dermal}	HQ_{vapour}	$HI = \Sigma HQ_i$
		CDI_{ing}	CDI_{inh}	CDI_{dermal}	CDI_{vapour}					
Sandton	0.32	4.42E-07	6.50E-11	1.76E-08	1.35E-05	5.16E-03	2.17E-07	8.40E-04	4.51E-02	0.05
Diepkloof	0.69	9.50E-07	1.40E-10	3.79E-08	2.91E-05	1.11E-02	4.66E-07	1.80E-03	9.69E-02	0.11
Riverlea	0.70	9.54E-07	1.40E-10	3.81E-08	2.92E-05	1.11E-02	4.68E-07	1.81E-03	9.73E-02	0.11
Boksburg 1	0.48	6.61E-07	9.72E-11	2.64E-08	2.02E-05	7.71E-03	3.24E-07	1.26E-03	6.74E-02	0.08
Boksburg 2	0.45	6.12E-07	9.00E-11	2.44E-08	1.87E-05	7.14E-03	3.00E-07	1.16E-03	6.24E-02	0.07
Alberton 1	0.51	6.96E-07	1.02E-10	2.78E-08	2.13E-05	8.12E-03	3.41E-07	1.32E-03	7.10E-02	0.08
Alberton 2	0.47	6.47E-07	9.51E-11	2.58E-08	1.98E-05	7.55E-03	3.17E-07	1.23E-03	6.60E-02	0.07
Alberton 3	0.49	6.70E-07	9.85E-11	2.67E-08	2.05E-05	7.81E-03	3.28E-07	1.27E-03	6.83E-02	0.08
CBD 1	0.53	7.32E-07	1.08E-10	2.92E-08	2.24E-05	8.54E-03	3.59E-07	1.39E-03	7.47E-02	0.08
CBD 2	0.61	8.32E-07	1.22E-10	3.32E-08	2.55E-05	9.71E-03	4.08E-07	1.58E-03	8.49E-02	0.10
CBD 3	0.49	6.66E-07	9.79E-11	2.66E-08	2.04E-05	7.77E-03	3.26E-07	1.27E-03	6.79E-02	0.08
CBD 4	0.53	7.18E-07	1.06E-10	2.87E-08	2.20E-05	8.38E-03	3.52E-07	1.37E-03	7.33E-02	0.08
Cemetery	0.70	9.62E-07	1.41E-10	3.84E-08	2.94E-05	1.12E-02	4.72E-07	1.83E-03	9.81E-02	0.11
Soccer City	0.81	1.10E-06	1.62E-10	4.40E-08	3.38E-05	1.29E-02	5.41E-07	2.10E-03	1.13E-01	0.13
Ophirton	0.59	8.10E-07	1.19E-10	3.23E-08	2.48E-05	9.45E-03	3.97E-07	1.54E-03	8.26E-02	0.09
Selby 1	0.56	7.62E-07	1.12E-10	3.04E-08	2.33E-05	8.89E-03	3.73E-07	1.45E-03	7.77E-02	0.09
City Deep	0.68	9.28E-07	1.36E-10	3.70E-08	2.84E-05	1.08E-02	4.55E-07	1.76E-03	9.47E-02	0.11
Crownwood	1.00	1.37E-06	2.01E-10	5.46E-08	4.18E-05	1.60E-02	6.70E-07	2.60E-03	1.39E-01	0.16
Heriotdale	1.35	1.85E-06	2.72E-10	7.37E-08	5.66E-05	2.16E-02	9.06E-07	3.51E-03	1.89E-01	0.21
PPC Cement	0.89	1.22E-06	1.79E-10	4.85E-08	3.72E-05	1.42E-02	5.96E-07	2.31E-03	1.24E-01	0.14

The major highlights were that all sample areas showed HI values < 1, indicating that there is a little adverse health risk or no potential risk of toxic pathology resulting from the ingestion or inhalation or dermal contact of Hg in dust.

Non-carcinogenic exposure of Hg for both children and adults exhibited the following order of exposure: vapour ingestion > ingestion > dermal contact > inhalation. Inhalation of soil vapour Hg is significant due to the fact that Hg has a low vapour pressure, and elemental mercury is usually deposited in the surrounding environments from mining and smelting activities (Ordonez *et al*., 2011). Exposure of children to mercury in dust increases with the increase in the frequency of pica behaviour, hand and finger sucking behaviour (Mielke *et al*., 1999; Rasmussen *et al*., 2001), increased playtime outdoors, the proximity to TSFs (e.g. Diepkloof, Soweto residence, where they are surrounded by TSFs and occasionally experience dust storms leading to tailings materials being distributed over a wide area and affecting even the playgrounds), poor hygiene, and serving food outdoors in areas highly affected by dust storms.

Mercury risk factor characterization in different cities and urban areas has showed that ingestion is the major exposure pathway, followed by inhalation and lastly dermal (James *et al*., 2012). In one study, mercury source was identified as vehicular traffic on unpaved roads (James *et al*., 2012), paving these roads resulted in a large reduction of the amount of soil particles resuspended into the atmosphere, ranging from 13 to 50% (James *et al*., 2012). On other hand, some studies have shown that dermal absorption is the main exposure pathway (Li *et al*., 2014). They further showed that mining activities pose potentially high non-carcinogenic risk to the public, especially children. Children and infants were shown to be highly susceptible to exposure to environmental contaminants per unit body weight due to behavioural and physiological characteristics (hand to mouth activities for soils-pica behaviour, deficient hygienic habits, higher respiration rates per unit body weight, and increased gastrointestinal absorption of some substances) (Qu *et al*., 2012; Zota *et al*., 2011; Man *et al*., 2010; Madrid *et al*., 2008; Ljung *et al*., 2007). Generally, children's exposure to toxic metals was one order of magnitude higher

than for adults. The following order of exposure to Hg from dust was observed: ingestion > dermal contact > inhalation (Ordonez *et al*., 2011; Shi *et al*., 2011). These sites exhibited HI greater than 1 as compared to other regions (Li *et al*., 2012; Zhang *et al*., 2012; Ordonez *et al.,* 2011).

Comparison of the impact of mining was carried out by compiling data from countries with an active mining fraternity such as China, India, Iran, South Korea, Spain, and Vietnam (Table 7.3). Of interest, is the fact that the environment surrounding the mining areas is grossly polluted by heavy metals dispersed from mining operations.

Table 7.3: Comparison of trace elements (mg kg^{-1}) observed in this study with those found in other metal soil studies.

Site	As	Cd	Cr	Cu	Ni	Pb	Zn	Hg	References
Johannesburg, South Africa	**280.00**	**35.00**	**790.00**	**260.00**				**0.60**	**This study**
China (72 examined mines)	195.50	11.00	84.28	211.90	106.60	641.30	1163	3.82	Li *et al*., 2014
Iran (3 examined mines)	146.20	1.49		88.40		1002	363.40	3.13	Dayani and Mohammadi, 2010; Rafiei *et al*., 2010; Rahimsouri *et al*., 2011
Spain (16 examined)	191.90	6.59	63.20	120.80	28.35	881.80	465.80	52.90	Lambrechts *et al*., 2011; Oyarzun *et al*., 2011
South Korea (70 examined)	70.08	1.99		79.09	22.00	111.10	183.20	1.12	Chon *et al*., 2011; Jung, 2008; Kim *et al*., 2008; 2005; Ko *et al*., 2010; Lee *et al*., 2005; Lim *et al*., 2008
Vietnam (3 examined mines)	3144	135	1501	271.40	2254	30635	41094		Chu Ngoc *et al*., 2009; Ha *et al*., 2011; Kien *et al*., 2010
India (5 examined mines	18.62	3.82	1509	63.49	1069	304.70	338.80		Anju and Banerjee, 2012; Das and Chakrapani, 2011; Krishna *et al*., 2010; Ladwani *et al*., 2012;
China 21 urban soils	15.00	0.88	76.80	99.20	99.60	61.30	133.00	0.35	Luo *et al*., 2012
China (12 Agricultural soils	10.18	0.43	58.87	31.71	27.53	37.55	117.70	0.24	Wei and Yang, 2010

For examples, in the northern and southern regions of Spain, the surrounding soils are heavily contaminated by heavy metals (Ordonez *et al*., 2011); in South Korea, agricultural land surrounding mines is heavily polluted with heavy metals (Kim *et al*., 2005); in Vietnam, heavy metal pollution flows into low streams and farmland due to collapse of dykes constructed around the mines in the rainy season (Ha *et al*., 2011; Kien *et al*., 2010); and lastly in China, small scale coal, gold and mercury mining is responsible for emitting large amounts of mercury annually into the environment (Li *et al*., 2008; Gunson and Veiga, 2004; Li and Jiang, 2004). China is currently facing a difficult task of effectively balancing mineral resource development and usage with implementation of environmental protection laws. This is worsened by the use of obsolete technology and inefficient mining operations, poor mine waste management, weak enforcement of relevant laws and regulations (Li, 2006; Zhong, 1997).

In South Africa, the number of tailings dams left unattended and not rehabilitated are in excess of 270. Therefore, the dust generated from the mine tailings finds its way to the surrounding communities and neighbouring environments, and due to the high levels of trace metal pollutants, it poses a high potential health risk to human beings inhabiting the environment and the surrounding ecosystems. This was evident in this study as high levels of Hg concentration were experienced in the areas surrounded by or in close proximity to the mine tailings or gold ore processing plant. As the distance increased away from the mine tailings, the Hg concentration decreased, indicating that the anthropogenic source of Hg were mine tailings from the gold mining activity. The health risk assessment model also confirmed the findings by showing some sampling sites from industrial and residential areas next to the tailings had a hazard index (HI) greater than 1, which was above the safe level of 1 (HI = 1).

The non-cancer Hg exposure results showed that exposure pathway which resulted in the highest levels of risk for human exposed to road dust was vapour inhalation of elemental Hg emitted from dust/soils followed by ingestion of this dust, which was followed by dermal contact, lastly inhalation of dust particles and resuspended

soil particles. Children were highly susceptible to non-cancer effects of Hg and if they were exposed to large doses, it would trigger neurological and developmental disorders (Ferreira-Baptista and De Miguel, 2005). The atmospheric deposition of dust (particulate matter) due to windblown dust from the mine tailings, is the main source of Hg pollution in the urban street dust, whilst vehicular emissions and population weigh in with a small contribution of heavy metals pollution.

7.1.2 Cancer risk

The carcinogenic risk was calculated based on the estimated lifetime exposure of an individual developing cancer as a result of exposure to the carcinogen. The carcinogenic risk results due to ingestion exposure to As, Cd, and Cr for children and adults are summarised in Table 7.4. For children, the carcinogenic risk levels ranged from 1.46E-04 to 5.75E-04; 1.82E-04 to 2.61E-04; and 1.12E-02 to 9.31E-03 for As, Cd, and Cr, respectively. For adults, the carcinogenic risk levels ranged from 1.02E-04 to 8.99E-05; 1.00E-04 to 9.50E-05; and 1.03E-02 to 9.30E-04 for As, Cd, and Cr, respectively. The total carcinogenic risk values for ingestion exposure for both children and adults to these elements in dust were slightly higher than the internationally acceptable precautionary criterion value (10^{-4} and 10^{-6}) (Corzine and Mauriello, 2009; Granero and Domingo, 2002, Kelly, 1991; U.S. Environmental Protection Agency, 1991b), which indicates that the carcinogenic risk for all elements due to street dusts exposure is cause for concern in Johannesburg. In both cases, the highest cancer risk was calculated to be from exposure to Cr, while exposure to both As and Cd produced similar risk. Cr contributed 91% to the total cancer risk (i.e., $CR_{As} + CR_{Cd} + CR_{Cr}$) from ingestion exposure to As, Cd and Cr (VI) in the street dust for both children and adults.

Table 7.4: Carcinogenic risk for children and adults via ingestion exposure to As, Cd, and Cr in Johannesburg street dust.

SAMPLE	Cr_{As}		CR_{Cd}		CR_{Cr}		Total *CR*	
SITES	**Children**	**Adults**	**Children**	**Adults**	**Children**	**Adults**	**Children**	**Adults**
Sandton	4.66E-04	2.00E-4	2.42E-04	1.04E-04	3.97E-03	1.70E-03	4.68E-03	2.00E-03
Diepkloof	3.87E-04	1.66E-4	2.55E-04	1.09E-04	2.18E-03	9.34E-04	2.82E-03	1.21E-03
Riverlea	1.89E-04	8.10E-5	2.34E-04	1.00E-04	2.08E-03	8.91E-04	2.50E-03	1.07E-03
Boksburg 1	3.48E-04	1.49E-4	2.48E-04	1.06E-04	1.96E-03	8.42E-04	2.56E-03	1.10E-03
Boksburg 2	5.15E-04	2.21E-4	2.42E-04	1.04E-04	3.10E-03	1.33E-03	3.86E-03	1.66E-02
Alberton 1	2.91E-04	1.25E-4	2.39E-04	1.02E-04	1.12E-02	4.81E-03	1.18E-02	5.04E-03
Alberton 2	5.75E-04	2.46E-4	2.56E-04	1.96E-04	1.65E-02	7.07E-03	1.73E-02	7.43E-03
Alberton 3	5.50E-04	2.36E-4	2.52E-04	1.98E-04	2.40E-02	1.02E-02	2.48E-02	1.06E-03
CBD 1	3.01E-04	1.29E-4	2.22E-04	9.50E-05	4.11E-03	1.76E-03	4.64E-03	1.99E-03
CBD 2	4.64E-04	1.89E-4	2.36E-04	1.01E-04	3.94E-03	1.69E-03	4.64E-03	1.99E-03
CBD 3	3.55E-04	1.52E-5	2.33E-04	1.00E-04	5.59E-03	2.40E-03	6.18E-03	2.65E-03
CBD 4	3.46E-04	1.48E-4	2.15E-04	9.22E-05	4.97E-03	2.13E-03	5.53E-03	2.37E-03
Cemetery	2.07E-04	8.99E-5	2.38E-04	1.02E-04	1.12E-02	4.80E-03	1.17E-02	4.99E-03
Soccer City	3.48E-04	1.49E-4	2.40E-04	1.03E-04	2.46E-03	1.05E-03	3.05E-03	1.31E-03
Ophirton	1.75E-04	7.57E-5	2.61E-04	1.12E-04	4.12E-03	1.77E-03	4.56E-03	1.95E-03
Selby 1	1.46E-04	6.30E-5	2.60E-04	1.12E-04	6.67E-03	2.86E-03	7.08E-03	3.03E-03
City Deep	4.43E-04	1.90E-4	2.37E-04	1.01E-04	2.62E-02	1.12E-02	2.69E-02	1.15E-02
Crownwood	4.06E-04	1.72E-4	2.47E-04	1.06E-04	8.56E-03	3.67E-03	9.21E-03	3.95E-03
Heriotdale	2.37E-04	1.02E-4	1.82E-04	7.80E-05	4.36E-03	1.87E-03	4.77E-03	2.05E-03
PPC Cement	4.03E-04	1.73E-4	0	0	9.31E-03	3.99E-03	9.71E-03	4.16E-03

The carcinogenic risk from inhalation exposure to As, Cd and Cr (VI) in the street dust by humans (children and adults) was summarised in Table 7.5. For children, the carcinogenic risk levels ranged from 1.17E-11 to 4.13E-11; 3.38E-11 to 4.86E-11; and 1.23E-08 to 9.76E-10 for As, Cd, and Cr, respectively. For adults, the carcinogenic risk levels ranged from 1.04E-11 to 9.94E-11; 1.01E-11 to 9.95E-12; and 1.18E-08 to 9.85E-09 for As, Cd, and Cr, respectively. In both cases, the inhalation exposure of both children and adults to dust, Cr (VI) is the highest contributor to the overall cancer risk followed by As, and lastly the Cd. Cr (VI) is two orders of magnitudes higher than the As and Cd elements. However, these results are lower than the cancer safety limit of 10^{-6}. Therefore the risk of developing cancer following inhalation exposure to As, Cd, and Cr from urban street dusts is almost negligible and exposure to these elements from the street dust would not cause serious health impacts, i.e., are too low for inhalation cancer risk.

The total cancer risk for As, Cd, and Cr via ingestion and inhalation exposure over a period of a lifetime (25550 days) are presented in Table 7.6. The contribution from inhalation exposure for both children and adults is almost negligible and the overall cancer risk is almost entirely due ingestion exposure of dust containing As, Cd, and Cr elements. It is believed that Cr is enriched in the road dust and body tissue can accumulate considerable amounts before pathological changes can be seen. Studies have shown that excessive build-up of the Cr in human bodies may trigger lung cancer and stomach cancer. As could be accumulated in the body, as a carcinogen which can cause lung and skin cancer. According to its concentration and enrichment factors, both Cr and As are of more concern than other heavy metals (e.g., Cu) (Zheng *et al* 2010a, b).

Basically, total risk for all elements via ingestion and inhalation exposure showed that 1 in 100 to 1 in 1000 for children while 1 in 100 to 1 in 1000 for adults could develop cancer. In other studies similar results have been reported, whereby an increased risk of cancer due to the inhalation of Cr in resuspended urban soils was observed (Nadal *et al*., 2004, 2005; Schuhmacher *et al*., 2009).

Table 7.5: Carcinogenic risk for children and adults via inhalation to As, Cd, and Cr in Johannesburg street dust.

SAMPLE	Cr_{As}		CR_{Cd}		CR_{Cr}		Total *CR*	
SITES	**Children**	**Adults**	**Children**	**Adults**	**Children**	**Adults**	**Children**	**Adults**
Sandton	3.74E-11	8.43E-11	4.50E-12	1.01E-11	1.86E-09	4.20E-09	2.97E-09	4.29E-09
Diepkloof	3.10E-11	6.99E-11	4.75E-12	1.07E-11	1.02E-09	2.31E-09	2.18E-09	2.39E-09
Riverlea	1.51E-11	3.41E-11	4.36E-12	9.83E-12	9.76E-10	2.20E-10	2.03E-10	2.24E-10
Boksburg 1	2.79E-11	6.30E-11	4.62E-12	1.04E-11	9.22E-10	2.08E-10	2.05E-10	2.15E-10
Boksburg 2	4.13E-11	9.30E-11	4.51E-12	1.02E-11	1.45E-09	3.29E-09	2.57E-09	3.39E-09
Alberton 1	2.33E-11	5.26E-11	4.45E-12	1.00E-11	5.27E-09	1.19E-09	6.35E-09	1.20E-09
Alberton 2	4.61E-11	1.074-11	4.59E-12	1.04E-11	7.75E-09	1.75E-09	8.89E-09	1.76E-09
Alberton 3	4.41E-11	9.94E-11	4.69E-12	1.06E-11	1.13E-08	2.54E-08	1.24E-08	2.55E-08
CBD 1	2.41E-11	5.44E-11	4.13E-12	9.31E-12	1.93E-09	4.36E-09	2.94E-09	4.42E-09
CBD 2	3.71E-11	8.38E-11	4.40E-12	9.92E-12	1.85E-09	4.18E-09	2.94E-09	4.27E-09
CBD 3	2.84E-11	6.41E-11	4.35E-12	9.81E-12	2.62E-09	5.92E-09	3.69E-09	5.99E-09
CBD 4	2.77E-11	6.25E-11	4.00E-12	9.02E-12	2.33E-09	5.26E-09	3.31E-09	5.33E-09
Cemetery	1.66E-11	3.73E-11	4.42E-12	9.98E-12	5.26E-09	1.18E-09	6.32E-09	1.19E-09
Soccer City	2.79E-11	6.28E-11	4.48E-12	1.01E-11	1.15E-09	2.60E-09	2.24E-09	2.68E-09
Ophirton	1.41E-11	3.16E-11	4.86E-12	1.10E-11	1.93E-09	4.36E-09	3.11E-09	4.41E-09
Selby 1	1.17E-11	2.65E-11	4.85E-12	1.09E-11	3.13E-09	7.06E-09	4.30E-09	7.10E-09
City Deep	3.54E-11	8.00E-11	4.41E-12	9.95E-12	1.23E-08	2.78E-08	1.34E-08	2.78E-08
Crownwood	3.21E-11	7.23E-11	4.60E-12	1.04E-11	4.02E-09	9.07E-09	5.15E-09	9.15E-09
Heriotdale	1.90E-11	4.28E-11	3.38E-12	7.63E-12	2.04E-09	4.61E-09	2.87E-09	4.66E-09
PPC Cement	3.23E-11	7.28E-11	0	0	4.37E-09	9.85E-09	4.40E-09	9.93E-09

Table 7.6: Comparison of concentration, enrichment factor and total risk of As, Cd, and Cr in Johannesburg street dust.

Sample sites	Concentration (mg kg^{-1})			Enrichment Factor			Total *CR*	
	As	Cd	Cr	As	Cd	Cr	Children	Adults
Sandton	283.7	35.0	724.0	285.8	317.4	14.4	4.68E-03	2.00E-03
Diepkloof	235.2	36.9	397.9	147.6	208.42	4.5	2.82E-03	1.21E-03
Riverlea	114.9	33.9	379.3	85.5	227.1	5.1	2.50E-03	1.07E-03
Boksburg 1	212.0	35.9	358.6	118.5	180.6	3.6	2.56E-03	1.10E-03
Boksburg 2	313.3	35.1	566.6	259.4	261.5	8.4	3.86E-03	1.66E-03
Alberton 1	177.1	34.6	2049.5	158.8	279.2	33.1	1.18E-02	5.04E-02
Alberton 2	349.8	35.7	3011.9	336.5	309.0	52.1	1.73E-02	7.43E-02
Alberton 3	334.6	36.5	4379.3	314.4	308.7	74.1	2.48E-02	1.06E-02
CBD 1	183.1	32.1	750.7	183.5	289.5	13.5	4.64E-03	1.99E-03
CBD 2	282.1	34.2	719.7	227.2	247.9	10.4	4.64E-03	1.99E-03
CBD 3	215.7	33.8	1020.2	197.5	278.6	16.8	6.18E-03	2.65E-03
CBD 4	210.4	31.1	906.2	171.2	227.8	13.8	5.53E-03	2.37E-03
Cemetery	125.7	34.4	2044.2	109.1	268.8	31.9	1.17E-02	4.99E-02
Soccer City	211.6	34.8	448.6	184.5	273.1	7.0	3.05E-03	1.31E-03
Ophirton	106.7	37.8	752.0	98.5	314.2	12.5	4.56E-03	1.95E-03
Selby 1	89.1	37.7	1217.7	76.1	289.8	18.7	7.08E-03	3.03E-03
City Deep	269.2	34.3	4784.0	237.9	272.8	76.1	2.69E-02	1.15E-03
Crownwood	243.6	35.8	1563.0	210.9	278.1	24.3	9.21E-03	3.95E-03
Heriotdale	144.2	26.3	794.9	112.9	185.4	11.2	4.77E-03	2.05E-03
PPC Cement	245.2	0	1698.4	241.7	0	30.1	371.3-03	4.16E-03

Chapter 8

Conclusions and recommendations

The novel findings associated with exposure to street dust, and risk faced by Johannesburg community were presented. Conclusions were drawn based on the results obtained and recommendation were made to advance the health risk assessment model for toxic metals.

8.1 General conclusions

The Hg_{TOT} concentration reported in the PM_{25} size fraction was the highest, followed by PM_{50}, and PM_{100} size fractions. This was attributed to the high specific surface area where toxic heavy metals adsorb and are enriched. In the PM_{25} size fraction, mercury exhibited the following decreasing order of Hg_{TOT}: industrial area > CBD > residential area. This order shows that the Hg_{TOT} concentration in the street dust decreased with increased distance from the TSFs. The highlight was that the highest Hg_{TOT} was reported in industrial areas next to the TSFs, tailings reprocessing areas, and tailings footprints. Furthermore, in residential areas grossly affected by TSFs and tailings reprocessing, they reported high Hg_{TOT} values similar to those reported for industrial samples. These results indicated that the source of the anthropogenic mercury is majorly TSFs although traffic emissions, crematorium, industrial waste also contributed to a certain extent. In addition, climatic conditions play a key role in the distribution and spread of environmental mercury.

Based on particle size distribution analysis, the results demonstrated that the greater the fraction of finer material, the greater the Hg_{TOT} concentration. Correlation studies reported similar and consistent results as the particle size analysis. Significant high levels of mercury are observed in certain fractions of dust with lower diameters.

Mineralogy and elemental analysis on the dust and the TFSs were done to determine which components represent the hazardous materials and identify the source of the dust in relation to the TSFs. Quartz was reported as the most dominant mineral component in the dust and TSFs with averages of 88.0, and 72 wt.%. The dust had a higher quartz content as compared to the TSF, mainly due to the large volume of small particle size fractions, which tended to trap and enrich chemical compounds and elements alike. The minor mineral components determined were as follows: chloritoid, chlorite, K-feldspar, jarosite, mica, muscovite, pyrite, and pyrophyllite, and were all below 10 wt. %. The geochemical profile of the dust is predominantly quartz intertwined with alumina-silicates coated or binding trace elements such as:

Al, As, Ca, Co, Cr, Cu, Fe, Hg, Mg, Mn, Ni, Pb, S, U, and Zn. Al, Ca, Fe, Mn and Si elements are enriched in the dust, however, they are of geologic nature. These results, when compared to those of tailings from the Witwatersrand past studies, exhibited similar and consistent chemical composition and elemental concentrations, indicating that the source of the dust was largely due to the wind erosion of the tailings dams.

The pH of the street dust varied from slightly acidic to alkaline (pH 5.4 to 10.1). Samples located near the mining sites had slightly acidic pH, an indication of acid mine drainage formation. The neutral to alkaline pH values were an influence from the dolomitic background and the liming effect during the processing of the gold ore, resulting in the dumping of tailings material that is alkaline.

Contamination assessment factor was carried out to classify the pollution levels and indicate whether they are from natural or anthropogenic sources. Based on the EF, C_f, and I_{geo}, 70, 82, and 84% of the street dust samples were classified as heavily enriched, very highly contaminated, and strongly polluted by mercury, respectively.

The bioaccessible Hg extracted by lung fluid (up to 3% of Hg_{TOT}) was higher than that of gastric fluid (up to 1% of Hg_{TOT}) and was related to the mobile pool of Hg in dust. This suggests that human exposure to Hg in dust via inhalation is greater than that via the gastric tract. Basically, areas affected by windy and dusty conditions (e.g. Soweto, which experience periodic dust storms resulting in windblown dust from the tailings) where exposure to Hg is through inhalation are at a greater risk of suffering mercury related illnesses as compared to areas with similar conditions but where exposure to Hg is through ingestion for similar Hg levels in the dust.

The developed human health risk model was useful in identifying the areas of health risks from exposure to mercury pollution. Spatial HQ patterns related to land use were employed to assess the human health risk assessment in this study. The spatial patterns of the HQ and Hg_{TOT} concentration in dust are similar, and the HQ for Hg

is greater than 1.0 in industrial areas affected by TSFs, tailings reprocessing and on the tailings footprints. It was concluded that Hg is the major pollutant contributing to human health risk in the study area. The results shows that children faced greater harmful health risk due to street dust mercury than adults. The exposure pathways which resulted in the highest levels of risk for humans exposed to road dust mercury showed the following order: ingestion > dermal contact > inhalation dust particles. For non-cancer risk in children, Hg exhibited a Hazard Index (HI) greater than 1, above the benchmark value of 1 for dust samples from industrial areas (Heriotdale, PPC Cement, Crownwood, Soccer City, and Cemetery), and residential areas (Diepkloof and Riverlea). This is because these areas have a substantial high Hg_{TOT} concentration and are in close proximity to the TSFs. The overall risk of non-cancer in industrial area was greater than those in the CBD and residential areas.

To conclude, this study showed that risks of human Hg exposure and absorption are not related to the total concentration of Hg in dust but actual intake depends on exposure pathways (i.e. dust intake vs. inhalation of dust particles vs. diet) which is related to land use and history of the land itself (source of Hg, soil geochemistry, atmospheric particulate matter emissions). Currently, there are different analytical tools to quantify the levels of the potential exposure for each of these pathways. It is recommended that site specific methods should be used in order to give a more realistic estimation of the health risk posed by mercury contamination. Risk assessment has proven to be a very useful tool to identify the contaminants and exposure pathways of metals in the dust from mining and TSF sites.

8.2 Recommendations

Arising from the findings of this study, the following recommendations are made

- There is a need for performing controlled regularised monitoring programs, mainly for (i) assessment of the toxic trace elements within the TSFs areas, (ii) adherence to set environmental standards (Department of environmental affairs) and regulations, and (iii) development of remediation methodology based on the levels of pollution experienced.

- Due to large population in a residential area, there is a higher chance of adverse human health effects occurring. Therefore, epidemiology studies should be carried out, on the population affected by these periodic dust storms, to determine the impact of toxic heavy metals such as As, Cd, Co, Cr, Cu, Hg, Mn, Ni, U, and Zn.. Studies have shown that during these storms, ambient particulate matter (PM_{10}, PM_5) concentration levels as high as 2160 µg m^{-3} were experienced at the TSF sites (i.e. DRD tailings dams in Soweto), and these values were above the South African air quality limit (120 µg m^{-3}). This demonstrates that pollution is occurring unabated and its impact has not been ascertained. Once conclusive figures are available, remediation can be implemented, medical interventions given to the affected residents, and the responsible parties will be prosecuted.

References

Adachi, K.; Tainosho, Y. (2004). Characterization of heavy metal particles embedded in tire dust. *Environment International*, **30**, 1009-1017.

Ahlqwist, M., Bengtsson, C., Lapidus, L., Gergdahl, I. A., Schütz, A. (1999) Serum mercury concentration in relation to survival, symptoms, and diseases: results from the prospective population study of women in Gothenburg, Sweden. *Acta Odontol Scand*; **57** (3): 168-174.

Ajmone-Marsan, F.; Biasioli, M.; Kralj, T.; Grčman, H.; Davidson, C. M.; Hursthouse, A. S.; Madrid, L.; Rodrigues, S. (2008**).** Metals in particle-size fractions of the soils of five European cities. *Environ. Pollut.* **152**, 73-81.

Akagi, H. & Naganuma, A. (2000). Human exposure to Mercury and the accumulation of methylmercury that is associated with gold mining in the Amazon Basin, Brazil. *Journal of Health Science, v*ol. 46, no. 5, pp. 323-328.

Al-Khashman, O.A. (2007). The investigation of metal concentrations in street dust samples in Aqaba city, Jordan. *Environmental Geochemistry and Health* **29**, 197–207.

Alvarez, R., Clemente, C., Gomez-Limon, D. (1997). Reduction of thermal coals environmental impact by nitric pre-combustion desulfurization. *Environmental Science and Technology*, **31**, 3148–3153.

Alvim-Ferraz, M. C. M., Afonso, S. A. V. (2003). Incineration of Different Types of Medical Wastes: Emission Factors for Particulate Matter and Heavy Metals. *Environmental Science & Technology,* **37**, (14), 3152-3157.

Amato, F.; Pandolfi, M.; Moreno, T.; Furger, M.; Pey, J.; Alastuey, A.; Bukowiecki, N.; Prevot, A. S. H.; Baltensperger, U.; Querol, X.; (2011a). Sources and variability of inhalable road dust particles in three European cities. *Atmospheric Environment,* **45** (37), 6777-6787.

Amato, F., Viana, M., Richard, A., Furger, M., Prévôt, A.S.H., Nava, S., Lucarelli, F.; Bukowiecki, N.; Alastuey, A.; Reche, C.; Moreno, T.; Pandolfi, M.; Pey, J.; Querol, X. (2011b). Size and time-resolved roadside enrichment of atmospheric particulate pollutants. *Atmospheric Chemistry and Physics*, **11** (6), 2917-2931.

Amato, F.; Pandolfi, M. Viana, M.; Querol, X.; Alastuey, A.; Moreno, T. (2009). Spatial and chemical patterns of PM10 in road dust deposited in urban environment. *Atmospheric Environment*, **43**, 1650–1659.

Amey Earle B. (2002) *United States Geological Survey minerals yearbook*, U.S. Geological Survey, Reston, Virginia.

Amyot, M., Southworth G., Lindberg S. E., Hintelmann H., Lalonde J. D., Ogrinc N., Poulain A. J., Sandilands K. A. (2004). Formation and evasion of dissolved gaseous mercury in large enclosures amended with ($HgCl_2$)-Hg-200. *Atmospheric Environment,* **38**, 4279–4289. Amyot M., Southworth G., Lindberg S. E., Hintelmann H., Lalonde J. D., Ogrinc N., Poulain A. J., Sandilands K. A. (2004). Formation and evasion of dissolved gaseous mercury in large enclosures amended with ($HgCl_2$)-Hg-200. *Atmospheric Environment,* **38**, 4279–4289.

Annegarn Environmental Research (2007). Crown Gold Recoveries Quarterly Dust Monitoring Report for DRD (July – September 2007). Rand burg: Annegarn Environmental Research (Pty) Ltd (now SGS Environmental).

Annegarn, H. J. (2006). Implications of the new Air Quality Act for the residential built environment. *Environ. Manage.* **1** (3), 18–21.

Annegarn, H. J.; Surridge, A. D.; Hlapolosa, H. S. P.; Swanepoei, D. J. D. V.; and Horne, A. R. (1991). A review of 10 years of environmental dust monitoring at Crown Mines. *Journal of the Mine Ventilation Society of South Africa*, vol. **44**, no. 3, p. 46.

Anju, **M.**; Banerjee, D. K. (2012). Multivariate statistical analysis of heavy metals in soils of a Pb–Zn mining area, India. *Environmental Monitoring and Assessment*; **184**, 4191-4206.

Ariya, **P.**; Peterson, K.; Snider, G.; Amyot, M. (2009). Mercury chemical transformations in the gas, aqueous and heterogeneous phases: state-of-the-art science and uncertainties. In: Mason, R., Pirrone, N. (Eds.), Mercury Fate and Transport in the Global Atmosphere. Springer, US, pp. 459–501.

Ariya P. A., Skov H., Grage M. L. & Goodsite M. E. (2008). Gaseous elemental mercury in the ambient atmosphere: review of the application of theoretical calculations and experimental studies for determination of reaction coefficients and mechanisms with halogens and other reactants. *Advances in Quantum Chemistry,* **55**, 43–54.

Atgin, **R. S.**; El-Agha, O.; Zararsız, A.; Kocabas, A.; Parlak, H.; Tuncel, G. (2000). *Spectrochim. Acta B* **55**, 1151–1164.

ATSDR (1999) Toxicological profile for mercury (update). Atlanta, GA, US Department of Health and Human Services, Public Health Service, Agency for Toxic Substances and Disease Registry, March.

Aucamp, P & van Schalkwyk, A. (2003) Trace element pollution of soils by abandoned gold mine tailings, near Potchefstroom, South Africa", *Bulletin of Engineering Geology and the Environment*, vol. 62, pp. 123–134.

Bailey, E. A., Gray, J. E., Theodorakos, P. M. (2002). Mercury in vegetation and soils at abandoned mercury mines in south western Alaska, USA. *Geochemistry: Exploration, Environment, Analysis,* **2**, 275–285.

Bailey, E. A., Gray, J. E. (1997). Mercury in the Terrestrial Environment, Kuskokwim Mountains Region, South western Alaska. In: Dumoulin, J. A. & Gray, J. E. (eds) Geologic Studies in Alaska by the US Geological Survey, 1995. US Geological Survey Professional Paper, **1574**, 41–56.

Banerjee, A. D. K. (2003). Heavy metal levels and solid phase speciation in street dusts of Delhi, India. *Environmental Pollution,* **123**, 95–105.

Barkay, T.; Kroer, N.; Poulain, A. J. (2011). Some like it cold: microbial transformations of mercury in Polar Regions. *Polar Research*, **30**, 1-15.

Barnett, M. O.; Turner, R. R. (2001)**.** Bioaccessibility of mercury in soils. *Soil Sediment. Contam.* **10**, 301–316.

Beckwith, P. R.; Ellis, J. B.; Revitt, D. M.; Oldfield, F. (1986). Heavy metal and magnetic relationships for urban source sediments. *Phys. Earth Planet. Inter.,* **42**, 67-75.

Beldowski, J.; Pempkowiak, J. (2007). Mercury transformations in marine coastal sediments as derived from mercury concentration and speciation changes along source/sink transport pathway (Southern Baltic). *Estuarine Coastal Shelf Sci.* **72,** (1–2), 370–378.

Benoit, J. M., Gilmour, C. C., Mason, R. P., Heyes, A. (1999). Sulfide Controls on Mercury Speciation and Bioavailability to Methylating Bacteria in Sediment Pore Waters. *Environmental Science & Technology*,**33**(6), 951-957.

Bergh, J.P., Falcon, R.M.S., Falcon, L.M. (2011). Trace element concentration reduction by beneficiation of Witbank Coalfield no 4 seam. *Fuel Processing Technology,* **92**, 812–816.

Biester, H.; Bindler, R.; Martinez-Cortizas, A.; Engstrom, D. R. (2007). Modelling the past atmospheric deposition of mercury using natural archives. *Environmental Science & Technology*, **41**, (14), 4851−4860.

Biester, H.; Muller, G.; Scholer, H. F. (2002a). Estimating distribution and retention of mercury in three different soils contaminated by emissions from chlor-alkali plants: part I. *Sci. Total Environ.* **284**, 177–189.

Biester, H.; Muller, G.; Scholer, H. F. (2002b). Binding and mobility of mercury in soils contaminated by emissions from chlor-alkali plants. *Sci. Total Environ.* **284**, 191-203.

Biester, H.; Gosar, M.; Covelli, S. (2000). Mercury speciation in speciation in sediments affected by dumped mining residues in the drainage area of the Idrija mercury mine, Slovenia. *Environ. Sci. Technol*., **34** (16), 3330-3336.

Biester, H.; Gosar, M.; Muller, G. (1999). Mercury speciation in tailings of the Idrija mercury mine. *J. Geochem. Explor*. **65**, 195-204.

Biester, H.; Scholz, C. (1997). Determination of mercury binding forms in contaminated soils: mercury pyrolysis versus sequential extractions. *Environ. Sci. Technol.* **31**, 233–239.

Blight, G. E. (2007). Wind erosion of tailings dams and mitigation of the dust nuisance. *The Journal of the Southern African Institute of Mining and Metallurgy*, **107**, 99-108.

Blight, G. E. (1989). Erosion losses from the surfaces of gold tailings dam. *J. S. Afr. Inst. Min. Metall.* **89** (1), 23–29.

Blight, G. E.; Caldwell, J. A. (1984). The abatement of pollution from abandoned gold residue dams. *J. S. Afr. Inst. Min. Metall.* **84** (12), 1–9.

Bloom, N.S., Preus, E., Katon, J. & Hiltner, M. (2003). Selective extractions to assess the biogeochemically relevant fractionation of inorganic mercury in sediments and soils. *Anal. Chim. Acta* **479** (2), 233-248.

Bloom, N.S.; Katon, J. In: Assessing and managing mercury from historic and current mining activities. U.S. EPA conf. 28–30 November 2000, online pdf report with file name ‘EPA Mines’

Boening, D. W. (2000). Ecological effects, transport, and fate of mercury: a general review. *Chemosphere* **40**/12, 1335-1351.

Bose-O'Reilly, S., Lettmeier, B., Matteucci Gothe, R., Beinhoff, C., Siebert, U. & Drasch, G. (2008). Mercury as a serious health hazard for children in gold mining areas. *Environmental Research,* **107**, (1), pp. 89-97.

Bose-O'Reilly, S., Drasch, G., Beinhoff, C., Rodrigues-Filho, S., Roider, G., Lettmeier, B., Maydl, A., Maydl, S. & Siebert, U. (2010). Health assessment of artisanal gold miners in Indonesia. *Science of The Total Environment,* **408**(4), 713-725.

Boszke, L.; Kowalski, A.; Astel, A.; Barański, A.; Gworek, B. and Siepak, J. (2008) Mercury mobility and bioavailability in soil from contaminated area. *Environmental Geology*, **55**(5): 1075-1087.

Boszke, L., Kowalski, A., Szczuciński, W., Rachlewicz, G., Lorenc, S. & Siepak, J. (2006). Assessment of mercury mobility and bioavailability by fractionation method in sediments from coastal zone inundated by the 26 December 2004 tsunami in Thailand. *Environ. Geol*. **51** (4), 527-536.

Boudou, A., Maury-Brachet, R., Coquery, M., Durrieu, G., Cossa, D. (2005). Synergic Effect of Gold Mining and Damming on Mercury Contamination in fish. *Environmental Science & Technology*, **39**, 2448-2454.

Bright, D. A.; Richardson, G. M.; Dodd, M. (2006). Do current standards of practice in Canada measure what is relevant to human exposure at contaminated sites? I: An A discussion of soil particle size and contaminant partitioning in soil. *Human and Ecological Risk Assessment*,

Brooks, S., Saiz-Lopez, A., Skov, H., Lindberg, S., Plane J. M. C., Goodsite M. E. (2006). The mass balance of mercury in the springtime Arctic environment. *Geophysical Research Letters* **33**, L13812, doi: 10.1029/2005GL025525.

Brotons, J. M., Diaz, A. R., Sarria, F. A., Serrato, F. B. (2010). Wind erosion on mining waste in southeast Spain. *Land Degradation Development*, **21**(2), 196 – 209.

Brunekreef, B. & Forsberg, B. (2005). Epidemiological evidence of effects of coarse airborne particles on health. *European Respiratory Journal,* **26**, 309-318.

Brunori, C. L., Galleti, M., Cremisini, C., Morabito, R. (2004). Comparison of three sequential extraction procedures (original and modified 3 steps BCR procedure) applied to sediments of different origin. *Annali di Chimica*, **94**,409–419.

Bullock, S. (2006). Sustainable Development Report. Anglo Platinum Limited, Johannesburg, South Africa.

Bunt, J. R., Waanders, F. B. (2008). Trace element behaviour in the Sasol–Lurgi MK IV FBDB gasifier. Part 1 - The volatiles elements: Hg, As, Se, Cd, and Pb. *Fuel*, **87**, 2374–2387.

Carpi, A, Lindberg, S. E. (1998). Application of a Teflon (TM) dynamic flux chamber for quantifying soil mercury flux: tests and results over background soil. *Atmospheric Environment* **32**:873–82.

Carvalho, J. A., Higuchi, N., Araujo, T., Santos, J. C. (1998). Combustion completeness in a rain forest clearing experiment in Manaus, Brazil. *Journal of Geophysical Research*, **103** (D11): 13195-13200.

Caussy, D., Gochfeld, M., Gurzau, E., Neagu, C., Ruedel, H. (2003). Lessons from case studies of metals: investigating exposure, bioavailability, and risk. *Ecotoxicology and environmental safety*, **56**, 45-51.

Charlesworth, S., De Miguel, E., Ordónez, A. (2011). A review of the distribution of particulate trace elements in urban terrestrial environments and its application to considerations of risk. *Environ Geochemistry & Health*, **33**, 103–123.

Cheng, J. P.; Gao, L. L.; Zhao, W. C.; Liu, X. J.; Sakamoto, M.; Wang, W. H. (2009). Mercury levels in fisherman and their household members in Zhoushan, China: impact of public health. *Sci Total Environ*, **407**, 2625–2630.

Chao, T. T. (1972). Selective dissolution of manganese oxides from soils and sediments with acidified hydroxylamine hydrochloride. *Soil Sci. Soc. Am. Proc*., **36,** 764–76.

Chon, H. T.; Lee, J. S.; Lee, J. U. (2011). Heavy metal contamination of soil, its risk assessment and bioremediation. *Geosystem Engineering*; **14**: 191-206.

Choi, K. H., Lee, H. J., Yang, T. H., Lee, H. P., Yum H. K., Choi S. J. (1999). A case of pulmonary embolism associated with intravenous mercury injection. *Tuberc Respir Dis*; **46** (5): 723-728 (Korean).

Chu Ngoc, K.; Van Nguyen, N.; Nguyen Dinh, B.; Le Thanh, S.; Tanaka, S.; Kang, Y. (2009). Arsenic and heavy metal concentrations in agricultural soils around tin and tungsten mines in the Dai Tu district, N. Vietnam. *Water, Air, & Soil Pollution*; **197**: 75-89.

Christoforidis, A., Stamatis, N. (2009). Heavy metal contamination in street dust and roadside soil along the major national road in Kavala's region, Greece. *Geoderma* **151**, 257–263.

Clarkson, T.W., Vyas, J.B. & Ballatori, N. (2007). Mechanisms of mercury disposition in the body. *American Journal of Industrial Medicine*, **50(**10), 757-764.

Clarkson, T. W., Magos, L. (2006). The toxicology of mercury and its chemical compounds. *Critical Rev Toxicology* **36**: 609-662.

Clarkson, T. W. (2002). The three modern faces of mercury. *Environmental Health Perspectives*, **110**, Supplement 1, 11–23.

Colombo, C.; Monhemius, A. J.; Plant, J. A. (2008). Platinum, palladium and rhodium release from vehicle exhaust catalysts and road dust exposed to simulated lung fluids. *Ecotox. Environ. Safe*, **71**, 722–730.

Compeau, G.C. & Bartha, R. (1985). Sulfate-Reducing Bacteria: Principal Methylators of Mercury in Anoxic Estuarine Sediment. *Applied and Environmental Microbiology*, **50**(2), 498-502.

Corbitt, E. S., Jacob, D. J., Holmes, C. D., Streets, D. Sunderland, E. M. (2011). Global source-receptor relationships for mercury deposition under present-day and 2050 emissions scenarios. *Environmental Science & Technology*, **45**(24), 10477-10484.

Cordy, P., Veiga, M.M., Salih, I., Al-Saadi, S., Console, S., Garcia, O., Mesa, L.A., Velasquez-Lopez, P.C., Roeser, M. (2011). Mercury contamination from artisanal gold mining in Antioquia, Colombia: the world's highest per capita mercury pollution. *Sci. Total Environ.* **410**, 154–160.

Corriveau, M. C., Jamieson, H. E., Parsons, M. B., Campbell, J. L., Lanzirotti, A. (2011). Direct characterization of airborne particles associated with arsenic-rich mine tailings: particle size, mineralogy and texture. *Applied Geochemistry*, vol. **26**, pp. 1639 – 1648.

Costa, M., Liss, P. (1999). Photoreduction of mercury in sea water and its possible implications for Hg^0 air–sea fluxes, *Mar. Chem.*, **68**, 87-95.

Csavina, J., Landázuri, A., Wonaschütz, A., Rine, K., Rheinheimer, P., & Barbaris B. 2011, "Metal and metalloid contaminants in atmospheric aerosols from mining operations", *Water, Air, & Soil Pollution*, vol. 221, pp. 145 – 157.

Csavina, J., Field, J., Taylor, M. P., Gao, S., Landázuri, A., Betterton, E. A., Eduardo Sáez, A. (2012). A review on the importance of metals and metalloids in atmospheric dust and aerosol from mining operations. *Science of the Total Environment,* **433**, 58–73.

Da Pelo, S., Musu, E., Cidu, R., Frau, F., Lattanzi, P. 2009. Release of toxic elements from rocks and mine wastes at the Furtei gold mine (Sardinia, Italy). *Journal of Geochemical Exploration*, 100: 142-152.

Dabrowski, J.M., Ashton, P.J., Murray, K., Leaner, J.J. & Mason, R.P. (2008). Anthropogenic mercury emissions in South Africa: Coal combustion in power plants. *Atmospheric Environment*, 42(27), 6620-6626.

Dart, R. C, Sulliva, J. B. Mercury. In: Dart RC, editor. Medical toxicology. 3rd ed. Philadelphia: Lippincott Williams & Wilkins; 2004, p. 1437-1448**.**

Das, S. K, Chakrapani, G. J. (2011). Assessment of trace metal toxicity in soils of Raniganj Coalfield, India. *Environmental Monitoring and Assessment*, **177**: 63-71.

Davies, T. C. & Mundalamo, H. R. (2010). Environmental health impacts of dispersed mineralisation in South Africa. *Journal of African Earth Science,* vol. **58**, pp. 652–666.

Davis, A.; Bloom, N. S.; Que Hee, S. S. (1997). The environmental geochemistry and bioaccessibility of mercury in soils and sediments: A review. *Risk Anal*., **17,** 557–569.

Dayani, M.; Mohammadi, J. (2010). Geostatistical assessment of Pb, Zn and Cd contamination in near-surface soils of the urban-mining transitional region of Isfahan, Iran. *Pedosphere,* **20**: 568-577.

DEFRA, Department for Environment, Food and Rural Affairs, UK. Mercury emissions from crematoria 2003. Available at: http://www.defra.gov.uk/Environment/ppc/old-consultations/crematoria/consultation.pdf.

De Miguel, D., Llamas, J., Chaco´ n E, Berg, T., Larssen, S., Røyset, O., Vadset, M. (1997). Origin and patterns of distribution of trace elements in street dust: unleaded petrol and urban lead. *Atmospheric Environment,* vol. **31**, no. 17, pp. 2733 – 2740.

De Miguel, E., Iribarren, I., Chacón, E., Ordoñez, A., Charlesworth, S., (2007). Risk based evaluation of the exposure of children to trace elements in playgrounds in Madrid (Spain). *Chemosphere* 66, 505–513.

De Miguel, E.; Llamas, J.F.; Chaco´ n, E.; Mazadiego, L.F. (1999). Sources and pathways of trace elements: a multi-elemental qualitative approach. *Sci. Total Environ.* **235**, 355–357.

Diehl, S.F., Stracher, G.B., Taylor, T.P. (2004). Modes of occurrence of mercury and other trace elements in coals from the Warrior Field, Black Warrior basin, north western Alabama. *International Journal of Coal Geology*, **59**, 193–208.

Di Giulio, R.T.; Ryan, E.A. (1987). Mercury in soils, and clams from a North Carolina peatland. *Water Air Soil Pollut.* **33**, 205– 219.

Driscoll, C. T.; Mason, R. P.; Chan, H. M.; Jacob, D. J.; Pirrone, N. (2013) Mercury as a Global Pollutant: Sources, Pathways, and Effects. *Environmental Science and Technology*, **47**, 4967-4983.

Driscoll, C. T., Yan, C., Schofield, C. L., Munson, R. & Holsapple, J. (1994). The mercury cycle and fish in the Adirondack lakes. *Environmental Science & Technology*, **28**, (3), 136A-143A.

Dreyer, J.C. (2006). An overview of the geology of the Waterberg Coalfield, implications for future exploitation. Presented at the Fossil Fuel Foundation of South Africa Conference: The Waterberg Coalfield 2006 and beyond – quo vadis? Lephalale (previously Ellisras), 22 – 23 August 2006.

Driver, J. H.; Konz, J. J.; Whitmyre, G. K. (1989). Soil adherence to human-skin. Bull Environ Contam Toxicol; 43, 814–20.

Duggan, M.J., Inskip, M.J., (1985). Childhood exposure to lead in surface dust and soil: a community health problem. *Public Health Reviews* **13,** 1–54.

Durnford, D., Dastoor, A., Figueras-Nieto, D., Ryjkov, A. (2010). Long range transport of mercury to the Arctic and across Canada. *Atmospheric Chemistry and Physics* **10**, 6063–6086.

Eastes, W.; Hadley, J. G. (1995). Dissolution of Fibers Inhaled by Rates. *Inhalation Toxicol.*, **7**, 179–196.

Ebinghaus, R.; Jennings, S. G.; Schroeder, W. H.; Berg, T.; Donaghy, T.; Guentzel, J.; Kenny, C.; Kock, H. H.; Kvietkus, K.; Landing, W.; Müleck, T.; **Munthe, J**.; Prestbo, E. M.; Schneeberger, D.; Slemr, F.; Sommar, J.; Urba, A.; Wallschläger, D.; Xiao, Z. (1999). International field intercomparison measurements of atmospheric mercury species at Mace Head, Ireland. *Atmos. Environ.*, **33**(18), 3063−3073.

El Haddad, I.; Marchand, N.; Dron, J.; Temime-Roussel, B.; Quivet, E.; Wortham, H.; Jaffrezo, J. L.; Baduel, C.; Voisin, D.; Besombes, J. L.; Gille, G. (2009).

Comprehensive primary particulate organic characterization of vehicular exhaust emissions in France. *Atmospheric Environment*, **43** (39), 6190-6198.

Engle, M. A., Gustin, M. S., Zhang, H. (2001). Quantifying natural source mercury emissions from the Ivanhoe Mining District, north-central Nevada, and USA. *Atmos. Environ.* **35**, 3987–3997.

Engler, D. E. (2005). Mercury "bleaching" creams. *J Am Acad Dermatol*; **52** (6): 1113-1114.

Engstrom, D. R. (2007). Fish respond when the mercury rises. Proc. Natl. Acad. Sci. USA, **104**, 16394–95.

Erasmus, C.S., Sellchop, J.P.F. & Hallbauer, D.K. (1982). Major amounts of mercury in native gold from Upper Witwatersrand Sediments, Mintek-Council for Mineral Technology, Johannesburg.

ESKOM, (2002). Energy Efficiency. Available from http://www.eskom.co.za/live/content.php?Item_ID=2787&Session_ID=18cb732d547d5c940b025d631c441823 (Accessed May 2013).

European Committee for Standardization & British Standard Institute 1993. Workplace atmospheres—size fraction definitions for measurement of airborne particles, British Standard Institute, Great Britain, BS EN 481:1993/BS 6069-3.5:1993.

Faiz, Y.; Tufail, M.; Javed, M.T.; Chaudhry, M.M.; Siddique, N. (2009). Road dust pollution of Cd Cu, Ni, Pb and Zn along Islamabad Expressway, Pakistan. *Microchemical Journal*, **92**, 186–192.

Fang, F. M.; Wang, H. D., Lin, Y. S. (2011). Spatial distribution, bioavailability, and health risk assessment of soil Hg in Wuhu urban area, China. *Environmental Monitoring and Assessment*, **179**, 255-265.

Feather, C. E., Koen, G. M. (1975). The mineralogy of the Witwatersrand reefs. *Mineral. Sci. Eng*., **7**, 189–224.

Fernandez Espinosa, A. J., Ternero Rodriguez, M., Barragan de la Rosa, F. J., Jimenez Sanchez, J. C. (2001). Size distribution of metals in urban aerosols in Seville (Spain). *Atmospheric Environment* 35, 2595-2601.

Fernandez-Camacho, R., de la Rosa, J., de la Campa, A. M. S., Gonzalez-Castanedo, Y., Alastuey, A., Querol, X., Rodríguez, S. (2010). Geochemical

characterization of Cu-smelter emission plumes with impact in an urban area of SW Spain. *Atmospheric Research*, vol. 96, pp. 590 – 601.

Ferreira-Baptista, L.; De Miguel, E. (2005).Geochemistry and risk assessment of street dust in Luanda, Angola: a tropical urban environment. *Atmospheric Environment*, **39**, 4501–4512.

Ferrara, R.; Maserti, B. E.; Andersson, M.; Edner, H.; Ragnarson, P.; Svanberg, S.; Hernandez, A. (1998). Mercury emissions from the Almaden mercury deposit. *Atmospheric Environment*, **32**, 3897.

Filgueiras, A. V.; Lavilla, I.; Bendicho, C. (2002). Chemical sequential extraction for metal partitioning in environmental solid samples. *Journal of Environmental Monitoring*, **4** (6), 823–857.

Finkelman, R. B. (1994). Modes of occurrence of potentially hazardous elements in coal: level of confidence. *Fuel Process. Technol.* **39**, 21–34.

Fitzgerald, W. F.; Engstrom, D. R.; Mason, R. P.; Nater, E. A. (1998). The case for atmospheric mercury contamination in remote areas. *Environmental Science & Technology*, **32**, 1–7.

Fitzgerald, W. F., Mason, R. P., Vandal, G. M. (1991). Atmospheric cycling and air water exchange of mercury over mid continental lacustrine regions. *Water, Air & Soil Pollution* **56**: 745-767.

Fleming E. J., Mack, E. E., Green, P. G., Nelson, D. C. (2006). Mercury methylation from unexpected sources: Molybdate-inhibited freshwater sediments and an iron-reducing bacterium. *Applied and Environmental Microbiology* **72**, 457–464.

Friberg. L., Mottet N. K. (1989). Accumulation of methylmercury and inorganic mercury in the brain. *Biol Trace Elem Re*s; **21**: 201-206.

Friedli, H. R., Radke, L. F., Lu, J. Y., Banic, C. M., Leaitch, W. R., MacPherson, J. I. (2003). Mercury emissions from burning of biomass from temperate North American forests: Laboratory and airborne measurements. *Atmospheric Environment* **37** (2), 253−267.

Friedli, H.R., Radke, L.R., Lu, J.Y. (2001). Mercury in smoke from biomass fires. *Geophys. Res. Lett.* **28**, 3223–3226.

Friedli, H. R., Arellano, A. F., Cinnirella, S., Pirrone, N. (2009). Mercury emissions from global biomass burning: spatial and temporal distribution. In: Mercury Fate and Transport in the Global Atmosphere: Emissions, Measurements and Models, Pirrone Nicola and Mason Robert (Editors), Springer Dordrecht Heidelberg, New York, pp. 3-49.

Frimmel, H. E., Gartz, V. H. (1997). Witwatersrand gold particle chemistry matches model of metamorphosed, hydrothermally altered placer deposits. *Mineral Deposita*, **32**, 523-530.

Fritsche, J., Obtrist, D., Alewell C. (2008). Evidence of microbial control of Hg^0 emissions from uncontaminated terrestrial soils. *Journal of Plant Nutrition and Soil Science*, **171**, 200-209.

Forstner, U. & Wittmann, G.T.W. 1976, "Metal Accumulations in Acidic Waters from Gold Mines in South Africa", *Geoforum*, vol. 7, pp. 41-49.

Funke J. W. 1990, *The Water Requirements and Pollution Potential of South African Gold and U mines*, Water Research Commission, Pretoria, South Africa.

Gabriel, M. C.; Williamson, D. G. (2004**)** Principal biogeochemical factors affecting the speciation and transport of mercury through the terrestrial environment. *Environ Geochem Health* **26**, 421–434.

Gauderman, W.J., Avol, E., Gilliland, F., Vora, H., Thomas, D., Berhane, K., McConnell, R., Kuenzli, N., Lurmann, F., Rappaport, E., Margolis, H., Bates, D. & and Peters, J. (2004). The Effect of Air Pollution on Lung Development from 10 to 18 Years of Age. *The New England Journal of Medicine*, vol. **351**, no. 11, pp. 1057-1067.

Gao, Y., Nelson, E.D., Field, M.P., Ding, Q., Li, H., Sherrell, R.M., Gigliotti, C. L., Van Ry, D. A., Glenn, T. R., Eisenreich, S. J. (2002). Characterization of Atmospheric trace elements on PM2.5 particulate matter over the New York-New Jersey harbor estuary. *Atmospheric Environment*, **36**, 1077-1086.

GDARD, 2011. Feasibility study on reclamation of mine residue areas for development purposes: Phase II strategy and implementation plan, July 2011, Report 788/06/02/201, Final Draft, Umvoto Africa, to Gauteng department of Agriculture and Rural development.

Gilmour, C.C. & Henry, Elizabeth A. and Mitchell, Ralph (1992) Sulfate stimulation of mercury methylation in freshwater sediments. *Environmental Science & Technology*, **26**, (11), 2281-2287.

Gilmour, C.C. & Henry, E.A. (1991). Mercury methylation in aquatic systems affected by acid deposition", *Environmental Pollution*, **71**, (2-4), 131-169.

Gray, J. E., Plumlee, G. S., Morman, S. A., Higueras, P. L., Crock, J. G., Lowers, H. A., Witten, M. L. (2010). In Vitro Studies Evaluating Leaching of Mercury from Mine Waste Calcine using Simulated Human Body Fluids. *Environmental Science & Technology*, **44**, (12), 4782–4788.

Grigal D. F. (2002). Inputs and outputs of mercury from terrestrial watersheds: a review. *Environ. Rev.* **10**, 1–39.

Granero S, Domingo J. (2002) Levels of metals in soils of Alcalá de Henares, Spain: human health risks. *Environ Int*. **28**, 159–64.

Griffin, D., Kellogg, C., & Shinn, E. 2001, "Dust in the wind: long range transport of dust in the atmosphere and its implications for global public and ecosystem health", *Global Change Human Health*, vol. 2, pp. 20 – 33.

Gietl, J. K.; Lawrence, R.; Thorpe, A. J.; Harrison, R. M.; (2010). Identification of brake wear particles and derivation of a quantitative tracer for brake dust at a major road. *Atmospheric Environment*, **44** (2), 141-146.

Gilbert, R. O. (1987). Statistical methods for environmental pollution monitoring. New York, Van Nostrand Reinhold; 177–85.

Gosar, M.; Šajn, R.; Biester, H. (2006). Binding of mercury in soils and attic dust in the Idrija mercury mine area (Slovenia). *Science of the Total environment*, **369**, 150-162.

Gómez-Ariza, J. L.; Gira´ldez, I.; Sanchez-Rodas, D.; Morales, E. (2000). Comparison of the feasibility of three extraction procedures for trace metal partitioning in sediments from south-west Spain. *The Science of the Total Environment*, **246**, 271–283.

Guney, M.; Welfringer, B.; Repentigny, C. D. (2013). Children's exposure to mercury contaminated soils: Exposure assessment and risk characterization. *Ach. Environ. Contam. Toxicol*. **65**, 345-355.

Gunson, A. J.; Veiga, M. M. (2004). Mercury and artisanal mining in China. *Environ Pract*, **6**, 109–120.

Gustin, M.S., Stamenkovic, J. (2005). Mercury emissions from soils: effect of watering and soil water content. *Biogeochemistry*, 76, 215–232.

Gustin, M. S., Biester, H., Kim, C. S. (2002). Investigation of the light-enhanced emission of mercury from naturally enriched substrates. *Atmospheric Environment*, 36, 3241–54.

Gustin, M. S.; Coolbaugh, M.; Engle, M.; Fitzgerald, B.; Nacht, D.; Zehner, R.; Sladek, C.; Keislar, R; Rytuba, J.; Lindberg, S. E.; Zhang, Z. (2000). Mercury emissions from mine waste: In Assessing and managing mercury from historic and current mining activities. U.S. EPA conf. 28–30 November 2000, online pdf report with file name 'EPA Mines.

Ha, N. T. H.; Sakakibara, M.; Sano, S.; Nhuan, M. T. (2011). Uptake of metals and metalloids by plants growing in a lead–zinc mine area, Northern Vietnam. *Journal of Hazardous Materials*, **186**, 1384–1391.

Han, Y. M., Du, P. X., Cao, J. J.; Posmentier, E. S. (2006). Multivariate analysis of heavy metal contamination in urban dusts of Xi'an, Central China. *Sci Total Environ*, **355**, 176–186.

Haitzer, M., Ryan, J. & Aiken, G.R. (2002). Binding of Mercury (II) to Dissolved Organic Matter: The Role of the Mercury-to-DOM Concentration Ratio. *Environmental Science & Technology*, **36**, (16), 3564–3570.

Hakanson, L. (1980). An ecological risk index for aquatic pollution control. A sedimentalogical approach. *Water Res.* **14**, 975-1001.

Hall, G. E. M.; Gauthier, G.; Pelchat, J. C.; Pelchat, P.; Vaive, J. E. (1996). Application of a sequential extraction scheme to ten geological certified reference materials for the determination of 20 elements. *Canadian Journal of Analytical Atomic Spectrometry*, **11**(9), 787–796.

Hall, B. (1995). The gas phase oxidation of elemental Mercury by Ozone. *Water, Air & Soil Pollution,* **80,** 301-315.

Hallbauer, D. K. & Barton, J. M. 1987, "The fossil gold placers of the Witwatersrand: A Review of their Mineralogy, Geochemistry and Genesis", *Gold Bulletin*, vol. 20, no. 3, pp. 68-70.

Hallbauer, D. K. (1986). The mineralogy and geochemistry of the Witwatersrand pyrite, gold, uraninite and carbonaceous matter. In: Mineral Deposits of Southern Africa, C. R. Anhaeusser and S. Maske (Editors), Geological Society of South Africa, 731–752.

Hallbauer, D. K., EIs, B. G. (1986) A geochemical identification of provenance-controlled gold distribution patterns in the Ventersdorp Contact Reef placer of the Carletonville gold field. Proc Int Conf Gold 100, vol 1: Gold Mining Technology, Johannesburg. South Afr Inst Min Metall, 45-62.

Hallbauer, D. K. & Von Gehlen, K. (1983). The Witwatersrand pyrites and metamorphism. *Mineralogical magazine*, **47**, 473 - 479.

Harada, M. (1996). Characteristics of industrial poisoning and environmental contamination in developing countries. *Environmental Sciences*, **4** (Suppl), 157–169.

Harrison, R.M. & Yin, J. 2000, "Particulate matter in the atmosphere: which particle properties are important for its effects on health?", *The Science of the Total Environment,* vol. 249, pp. 85-101.

Hartnady, C. J. H. (2009). South Africa's gold production and reserves. *South African Journal of Science,* **105(**9 & 10), 328 – 329.

Hayes, S., Webb, S. M., Bargar, J., O'Day, P. A., Maier, R. M., Chorover, J. 2012, "Geochemical weathering increases lead bioaccessibility in semi-arid mine tailings", *Environmental Science & Technology,* vol. 46, pp. 5834 – 5841.

Hayward, C.L., Reimold, W.U., Gibson, R.L. & and Robb, L.T. 2005, "Gold mineralization within the Witwatersrand Basin, South Africa: evidence for a modified placer origin and the role of the Vredefort impact event" in *Mineral deposits and earth Evolution: Issue 248 of Geological Society Special Publication,* ed. McDonald Iain (Dr.), Geological Society, London, pp. 31 - 58.

Health and Safety Executive, (1997). Dust: General principles of protection, *Health and Safety Executive,* UK, EH 44.

Hedgecock, I.M., Pirrone, N. (2001). Mercury and photochemistry in the marine boundary layer – modelling studies suggest the in situ production of reactive gas phase mercury. *Atmospheric Environment,* **35**, 3055-3062.

Heimburger, L.E. (2010). Methyl mercury distributions in relation to the presence of nano- and picophytoplankton in an oceanic water column (Ligurian Sea, North-Western Mediterranean). *Geochim. Cosmochimica. Acta,* **74**, 5549–5559.

Hemphill, C. P., Ruby, M. P., Beck, B. D., Davis, A. 1991, "The bioavailability of lead in mining wastes: physical/chemical considerations", *Chemical Speciation and Bioavailability,* vol. 3, pp. 135 – 148.

Henriksson, J., Tjälve, H. (1998). Uptake of inorganic mercury in the olfactory bulbs via olfactory pathways in rats. *Environ Res*; **77** (2), 130-140.

Heyes, A., Miller, C., Mason, R. P. (2004). Mercury and methylmercury in Hudson River sediment: impact of tidal re-suspension on partitioning and methylation. *Marine Chemistry*, **90**, (1-4), 75-89.

Hilson, G., Pardie, S. (2006). Mercury: an agent of poverty in Ghana's small-scale gold-mining sector? *Resour. Policy*, **31**, 106–116.

Hintelmann, H., Harris, R., Heyes, A., Hurley, J.P., Kelly, C.A., Krabbenhoft, D.P., Lindberg, S.E., Rudd, J.W.M., Scott, K.J. & St. Louis, V.L. (2002). Reactivity and Mobility of New and Old Mercury Deposition in a Boreal Forest Ecosystem during the First Year of the METAALICUS Study. *Environmental Science & Technology*, **36**, (23), 5034-5040.

Hintelmann, H., Wilken, R. (1995). Levels of total mercury and methylmercury compounds in sediments of the polluted Elbe River: influence of seasonally and spatially varying environmental factors. *Science of the Total Environment*, **166**(1-3), 1-10.

Hnizdo, E. (1995). Risk of silicosis in relation to fraction of respirable quartz. American Journal of Industrial Medicine, 27, 619-622.

Hnizdo, E. (1994). Risk of silicosis: Comparison of South African and Canadian Miners. American Journal of Industrial Medecine, 25, 771-772.

Hnizdo, E.; Sluis-Cremer, G.; Thomas, G. K. (1993). Correctional between radiological and pathological diagnosis of silicosis: An autopsy population based study. American Journal of Industrial Medecine, 24, 427-445.

Hu, X.; Zhang, Y.; Luo, J., Wang, T.; Lian, H. (2011)**.** Bioaccessibility and health risk of arsenic, mercury and other metals in urban street dusts from a mega-city, Nanjing, China. *Environ. Pollut.* **159**, 1215-1221.

Huang, M., Wang, W., Chan CY, Cheung, K. C., Man, Y. B., Wang, X., Wong M. H. (2014). Contamination and risk assessment (based on bioaccessibility via ingestion and inhalation) of metal(loid)s in outdoor and indoor particles from urban centers of Guangzhou, China. *Science of the Total Environment*, **81**:27–35.

Huang, X., Olmez, I., Aras, N. K. and Gordon, G. E. (1994). Emissions of Trace Elements from Motor Vehicles: Potential Marker Elements and Source Composition Profile. *Atmospheric Environment*, 28(8), 1385–1391.

Hursh J. B., Clarkson TW, Nowak TV, Pabico RC, McKenna BA, Miles E. (1985). Prediction of kidney mercury content by isotope techniques. *Kidney Int*, **27** (6), 898-907.

Issaro, N., Abi-Ghanem, C., Bermond, A. (2009). Fractionation studies of mercury in soils and sediments: a review of the chemical reagents used for mercury extraction. *Anal Chim Acta*, **631**, 1–12.

Iverfeldt, A., Lindqvist, O. (1986). Atmospheric oxidation of elemental mercury by ozone in the aqueous phase. *Atmospheric Environment* **20**, 1567-1573.

Janisch, P. R. (1986). Gold in South Africa. *Journal of the South African Institute of Mining and Metallurgy*., vol. 86, no. 8, pp. 273-316.

Janssen, N.A.H., Van Mansom, D.F.M., Van Der Jagt, K., Harssema, H., Hoek, G. (1997). Mass concentration and elemental composition of airborne particulate matter at street and background locations. *Atmospheric Environment* **31**, 1185-1193.

Jay, J.A.; Morel, F. M. M.; Hormand, H. F. (2000). *Environ. Sci. Technol.* **34**, 2196.

Jiang, J., Hao, J., Wu, Y., Streets, D.G., Duan, L., Tian, H., (2005). Development of mercury emission inventory from coal combustion in China. *Environ. Sci.* **26**, 34–43. (Chinese).

Johansson, K. and Iverfeldt, A. (Ed) 1994, Mercury pollution - Integration and synthesis, Lewis Publishers.

Johansson, K., Aastrup, M., Andersson, A., Bringmark, L. & Iverfeldt, A. 1991, *Water, Air, & Soil Pollution*, vol. 56, pp. 267–281.

Joksic, A. S., Katz, S. A., Horvat, M., Milacic, R. (2005). Comparison of single and sequential extraction procedures for assessing metal leaching from dredged coastal sediments. *Water, Air and Soil Pollution*, **162**, 265–283.

Jones, G. A.; Brierly, S. E.; Geldenhuis, S. J. J.; Howard, J. R. (1988). Research on the Contribution of Mine Dumps to the Mineral Pollution Load at the Vaal Barrage. Water Research Commission Report No. 136/1/89. Water Research Commission, Pretoria.

Jung, Y. S., Sakong, J., An, S.Y., Lee, Y. E., Song, K. B., Choi, Y. H. (2012). The relationship between dental amalgam fillings and urinary mercury concentration among elementary school children in a metropolitan area. *J Dent Hyg Sci*; **12** (3), 253-258 (Korean).

Jung, M. C. (2008). Heavy metal concentrations in soils and factors affecting metal uptake by plants in the vicinity of a Korean Cu-W mine. *Sensors*, **8**: 2413-2423.

Jurinski, J. B.; Rimstidt, J. D. (2001). Biodurability of talc. *American Mineralogist*, ***86*,** 392–399.

Kabata-Pendias, A. and Mukherjee, A.B. (Ed) 2007, Trace elements from soil to human, Springer-Verlag, Berlin Heidelberg.

Keeler, G.J., Glinsorn, G., Pirrone, N. (1995). Particulate mercury in the atmosphere: Its significance, transport, transformation and sources. *Water, Air, & Soil Pollution* 80: 159-168.

Kennedy, V. H.; Sanchez, A. L.; Oughton, D. H.; Rowland, A. P. (1997). Use of single and sequential chemical extractants to assess radionuclide and heavy metal availability from soils for root uptake. *Analyst*, **122** (8), 89R–100R.

Kerin, E. J.; Gilmour, C. C.; Roden, E.; Suzuki, M. T.; Coates, J. D.; Mason, R. P. 2006. Mercury methylation by dissimilatory iron-reducing bacteria. *Appl. Environ. Microbial*, 72(12), 7919−7921.

Kerper, L.E., Ballatori, N., Clarkson, T.W. (1992). Methylmercury transport across the blood–brain barrier by an amino acid carrier. *American Journal of Physiology*, vol. **262**, pp. R761 –R765.

Khwaja, A., Bloom, P.R., Brezonik, P.L. (2006). Binding constants of divalent Mercury (Hg^{2+}) in soil humic acids and soil organic matter. *Environ. Sci. Technol.* **40**, 844–849.

Kien, C. N.; Noi, N. V.; Son, L. T.; Ngoc, H. M.; Tanaka, S.; Nishina, T. (2010). Heavy metal contamination of agricultural soils around a chromite mine in Vietnam. *Soil Science & Plant Nutrition*, **56**, 344–356.

Kim, S.; Kwon, H. J.; Cheong, H. K.; Choi, K.; Jang, J. Y.; Jeong, W.C. (2008). Investigation on health effects of an abandoned metal mine. *Journal of Korean medical science*; **23**: 452-458.

Kim, J. Y.; Kim, K. W.; Ahn, J. S.; Ko, I.; Lee, C. H. (2005). Investigation and risk assessment modelling of As and other heavy metals contamination around five abandoned metal mines in Korea. *Environmental geochemistry and health*, **27**, 193–203.

Kim, C. S.; Brown Jr. G. E.; Rytuba, J. J. (2000). Characterization and speciation of mercury bearing mine wastes using X-ray absorption spectroscopy. *Sci. Total Environ.* **261**, 157–168.

Kim, K. H., Hansom, P. J., Barnett, M.O. & and Lindberg, S. (1997). Biogeochemistry of mercury in the air-soil-plant system: In Metal Ions in Biological Systems, Sigel, A. and Sigel, H., Marcel Dekker (editors), Inc, New York, Basel, Hong Kong.

Kim, K. H., Lindberg, S. E., Meyers, T.P. (1995). Micrometeorological measurements of mercury vapour fluxes over background forest soils in eastern Tennessee. *Atmospheric Environment* **29**: 267-282.

Kingman, A., Albertini, T., Brown, L. J. (1998). Mercury concentrations in urine and whole blood associated with amalgam exposure in a US military population. *J Dent Res*; **77**(3): 461-471.

Kocman, D.; Horvat, M.; Kotnik, J. (2004). Mercury fractionation in contaminated soils from the Idrija mercury mine region. *Journal of Environmental Monitoring*, **6**, 696-703.

Koekkoek, B. (2013). Measuring Global Progress towards a Transition Away from Mercury Use in Artisanal and Small-Scale Gold Mining. M.A. Royal Roads University, Victoria, Canada. p.74. http://dspace.royalroads.ca/docs/bitstream/handle/10170/567/Koekkoek_brenda.pdf?sequence=1 (accessed 10.12.13).

Kolluru, R. V.; Bartell, S. M.; Pitblado, R. M.; Stricoff, R. S. (1996). Risk Assessment and Management Handbook. New York: McGraw-Hill.

Kolker, A., Tewalt, S.J., and Finkelman, R. (2011). Summary of USGS coal quality data for mercury and chlorine in South African coal. VIII MEC Workshop, May 18–20, in Kruger Park, South Africa.

Kong, S.; Lu, B.; Ji, Y.; Zhao, X.; Chen, L.; Li, Z.; Han, B.; Bai, Z. (2011). Levels, risk assessment and sources of PM_{10} fraction heavy metals in four types dust from a coal-based city. *Microchemical Journal*, **98**, 280-290.

Kostyniak, P. J. (1998). Mercury as a potential hazard for the dental practitioner. *N Y State Dent J*; **64**(4):40-43.

Kot, F. S., Matyushkina, L.A., Nikorych V.N. & Polivichenko V.G. (2002). Mercury in chemical and thermal fractions of soils of Eastern Ukrainian Polissya. *Soil Sci.* **3**, 94-101.

Kot, F. S.; Matyushkina, L. A. (2002). Distribution of mercury in chemical fractions of contaminated urban soils of middle Amur, Russia. *J. Environ. Monitor*. **4**, 803-808.

Klock, P. R.; Czamanske, G. K.; Foose, M.; Pesek, J. (1986). Selective chemical dissolution of sulfides: An evaluation of six methods applicable to assaying sulfide-bound nickel. *Chemical Geology*, **54**(1–2), 157–163.

Krabbenhoft, D. P., Branfireun, B. A., Heyes, A. (2005). Mineralogical Association of Canada Short Course 34. 1369-156.

Krishna, A. K.; Mohan, K. R.; Murthy, N. N. (2010). Heavy metal pollution in soils around the abandoned mine sites of Nuggihalli Schist Belt, Karnataka, India. *Geochimica Et Cosmochimica Acta*, **74**: A30-A30.

Krishnamurti, G. S. R., Naidu, R. (2003). Solid-solution equilibria of cadmium in soils. *Geoderma*, **113**, 17 – 30.

Krombach, F., Munzing, S., Allmeling, A. M., Gerlach, J. T., Behr, J., Dorger, M. (1997). Cell size of alveolar macrophages: an interspecies comparison. *Environmental Health Perspectives,* **105**, 1261 – 1263.

Kumar, A., Jain, S. K., Bansal, N. K. (2003). Disseminating energy-efficient technologies: a case study of compact fluorescent lamps in India. *Energy Policy* **31**, 259-272.

Kwon, E. E.; Castaldi, M Kříbek, B.; Majer, V.; Pašava, J.; Kamona, F.; Mapani, B.; Keder, J.; Ettler, V. (2014). Contamination of soils with dust fallout from the tailings dam at the Rosh Pinah area, Namibia: Regional assessment, dust dispersion modeling and environmental consequences. *Journal of Geochemical Exploration*, 144, 391-408

Lacerda, L. D. (2003). Updating global Hg emissions from small-scale gold mining and assessing its environmental impacts. *Environmental Geology*, vol. **43**, 308-314.

Lacerda, L. D. (1997**).** Global mercury emissions from gold and silver mining. *Water Air Soil Pollution***, 97**, 209–21.

Ladwani, K. D.; Ladwani, K. D.; Manik, V. S.; Ramteke, D. S. (2012). Assessment of heavy metal contaminated soil near coal mining area in Gujarat by toxicity characteristics leaching procedure. *International Journal of Life Sciences Biotechnology and Pharma Research*, **1**, 73-80.

Lambrechts, T.; Couder, E.; Bernal, M. P.; Faz, Á.; Iserentant, A.; Lutts, S. (2011). Assessment of heavy metal bioavailability in contaminated soils from a former mining area (La Union, Spain) using a rhizospheric test. *Water, Air, & Soil Pollution*, **217**, 333-346.

Laperdina, T. G., Melnikova, M. V., Khvostova T. E. (1999). Gold mining in Siberia as a source of mercury contamination of the environment. In: Ebinghaus R, Turner RR, Lacerda LD, Vasiliev O, Salomons W (editors) Mercury contaminated sites: characterization, risk assessment and remediation. Springer, Berlin Heidelberg New York, pp 357–376.

Lechler, P. J.; Miller, J. R.; Hsu, L.C.; Desilets, M. O. (1997). Mercury mobility at the Carson River Superfund Site, west-central Nevada, USA: interpretation of mercury speciation data in mill tailings, soils, and sediments. *J. Geochem. Explor*. **58,** 259-267.

Leaner, J. J.; Dabrowski, J. M.; Mason, R. P.; Resane, T.; Richardson, M.; Ginster, M.; Gericke, G.; Petersen, C. R.; Masekoameng, E.; Ashton, P.J.; Murray, K.

(2009). Mercury emissions from point sources in South Africa: In Mercury Fate and Transport in the Global Atmosphere: Emissions, Measurements and Models, Pirrone Nicola and Mason Robert, (editors). Springer Dordrecht Heidelberg, New York, pp. 113 -131.

Lee, P.-K.; Touray, J.-C.; Baillif, P.; Ildefonse, J.-P. (1997). *Sci. Total Environ.* **201**, 1–15.

Lee, J. A., Allen, B. L. Peterson, R. E. Gregory, J. M. and Moffett, K. E. (1994). Environmental controls on blowing dust direction at Lubbock, Texas, USA. *Earth Surface Processes & Landforms*, **19**(5), 437–449, 1994.

Leermakers, M.; Baeyens, W.; Quevauviller, P.; Horvat, M. (2005). Mercury in environmental samples: speciation, artifacts and validation. *Trends Anal. Chem.* **24** (5), 383–393.

Lim, H.S., Lee, J.S., Chon, H.T., Sager, M., (2008). Heavy metal contamination and health risk assessment in the vicinity of the abandoned Songcheon Au-Ag mine in Korea. *J. Geochem. Explor.* **96**, 223–230.

Li J. (2009). Use of the BCR sequential extraction procedure for the study of metal availability to plants. *Journal of Environmental Monitoring*, **12**, 466-471.

Li, P. Feng, X. B.; Shang, L. H.; Qiu, G. L.; Meng, B.; Liang, P. (2008). Mercury pollution from artisanal mercury mining in Tongren, Guizhou, China. *Appl. Geochem,* **23**, 2055–2064

Li, Z.; Ma, Z.; van der Kuijp, T. J.; Yuan, Z.; Huang, L. (2014). A review of soil heavy metal pollution from mines in China: Pollution and health assessment. *Science of the Total Environment*, **468-469**, 843-853.

Lin, C.-J., Pongprueksa, P., Lindberg, S. E., Pehkonen, S. O., Byun, D., and Jang, C. (2006). Scientific uncertainties in atmospheric mercury models I: Model science evaluation, *Atmospheric Environment* **40**, 2911–2928.

Lin, Che-Jen and Pehkonen, Simo O. (1999a). The chemistry of atmospheric mercury: a review. *Atmospheric Environment*, **33**(13), 2067-2079.

Lin, Che-Jen and Pehkonen, Simo O. (1999b). Aqueous phase reactions of mercury with free radicals and chlorine: Implications for atmospheric mercury chemistry. *Chemosphere*, **38**(6), 1253-1263.

Lin, Chen-Jen and Pehkonen, Simo O. (1998). Oxidation of elemental mercury by aqueous chlorine: implications for tropospheric mercury chemistry. *Journal of Geophysical Research*, **103**, 28093-28102.

Lin, C. J., Pehkonen, S.O. (1997). Aqueous free radical chemistry of mercury in the presence of iron oxides and ambient aerosol. *Atmospheric Environment* **31**, 4125-4137.

Lin, Y., Guo, M. and Gan, W. (1997). Mercury pollution from small gold mines in China. *Water, Air, Soil pollution*, **97** (3-4), 233-239.

Lin, Z. X., Harsbo, K., Ahlgren, M., & Qvarfort, U. (1998). The source and fate of lead in contaminated soils at the urban area of Falun in Central Sweden. ", *Science of the Total Environment*, vol. 209, pp. 47–58.

Lindberg, S.E., Bullock, R., Ebinghaus, R., Engstrom, D., Feng, X., Fitzgerald, W., Pirrone, N., Prestbo, E., Seigneur, C. (2007). A Synthesis of Progress and Uncertainties in Attributing the Sources of Mercury in Deposition. *Ambio* **36**, 19-32.

Lindberg, S. E., Southworth, G., Prestbo, E. M., Wallschläger, A., Bogle, M. A., Price, J. (2005). Gaseous methyl-and inorganic mercury in landfill gas from Florida, Minnesota, Delaware and California. *Atmospheric Environment*, **34**, 249-258.

Lindberg, S. E., Lin, C. J., Scott, K. J., Landis, M. S., Stevens, R. K., Goodsite, M., Richter, A. (2002). Dynamic Oxidation of Gaseous Mercury in the Arctic Troposphere at Polar Sunrise. *Environmental Science & Technology*, **36**(6), 1245-1256.

Lindberg, S. E. & Stratton, W. J. (1998). Atmospheric Mercury Speciation: Concentrations and Behaviour of Reactive Gaseous Mercury in Ambient Air. *Environmental Science & Technology*, **32**(1), 49-57.

Lindberg S. E, Kim K. H, Meyers T. P, Owens J. G. (1995). Micrometeorological gradient approach for quantifying air/surface exchange of mercury-vapour: tests over contaminated soils. *Environmental Science & Technology* **29**, 126–35.

Lindberg, S.E., Meyers, T.P., Taylor, G.E., Turner, R.R. & Schroeder, W.H. (1992). Atmosphere/surface exchange of mercury in a forest: Results of modelling and gradient approaches. *Journal of Geophysical Research*, vol. 97, pp. 2519-2528.

Lindqvist, O. & Rodhe, H. (1985). Atmospheric mercury-a review. *Tellu*s B, vol. 37B, no. 3, pp. 136-159.

Liu G. Q.; Liang, C. H.; Du, L. Y.; Chen, X. Z.; Wang, F. (2006). Primary study of heavy metal contamination of soil in the area of Hongtou Mountains. *Chin Agric Sci Bull*, **22**, 364–7. [In Chinese with English abstract].

Liu, Q. T., Diamond, M. E., Gingrich, S. E., Ondov, J. M., Maciejczyk, P., Stern, G.A. (2003). Accumulation of metals, trace elements and semi-volatile organic compounds on exterior windows surfaces in Baltimore. *Environmental Pollution*, **122**, 51–61.

Liu, G.; Cabrera, J.; Allen, M. and Cai, Y. (2006) Mercury characterization in a soil sample collected nearby the DOE Oak Ridge Reservation utilizing sequential extraction and thermal desorption method. *Science of the Total Environment*, **369**(1-3): 384-392.

Liu J., Goyer, R. A, Waalkes, M. P. Toxic effects of metals. In: Casarett LJ, Doull J, Klaassen CD, editors. Casarett and Doull's toxicology: the basic science of poisons. 7th Ed. New York: McGraw-Hill; 2008. p. 931-979.

Li, Y. G.; Jiang, G. M. (2004). Ecological restoration of mining wasteland in both China and abroad: an over review. *Acta Ecol Sin*, **24,** 95–100. [In Chinese with English abstract].

Lodenius, M., Tulisalo, E., Soltanpour-Gargar, A. (2003). Exchange of mercury between atmosphere and vegetation under contaminated conditions. *The Science of the Total Environment*, **304**(1-3), 169-174.

Lodenius M, Malm O. (1998). Mercury in the Amazon. *Rev Environ Contam Toxicol*; **157,** 25-52.

Londonio, A.; Fujiwara, F.; Rebagliati, R. J.; Gomez, D.; Smichowski, P. (2012). Determination of mercury in size fractionated road dust samples by flow injection-cold vapor-atomic absorption spectrometry. *Microchemical Journal*, **105**, 77-82.

Lourie, B. (2003). Mercury in the environment: A primer, In: Pollution Probe, (Ed) Ogilvie, K., 1-82

Loska, K., Wiechula, D., Korus, I. (2004). Metal contamination of farming soils affected by industry. *Environ. Int.* **30**, 159-165.

Lu, X. W.; Li, L. Y.; Wang, L. J.; Lei, K.; Huang, J.; Zhai, Y. X. (2009). Contamination assessment of mercury and arsenic in roadway dust from Baoji, China, *Atmospheric Environment*, **43**, 2489–2496.

Luo, X. S.; Yu, S.; Li, X. D. (2011). Distribution, availability, and sources of trace metals in different particle size fractions of urban soils in Hong Kong: Implications for assessing the risk to human health. *Environmental pollution*, **159**(5) 1317-1326.

MacDonald, D. D.; Ingersoll, C. G.; Berger, T. A. (2000)**.** Development and evaluation of consensus-based sediment quality guidelines for freshwater ecosystems. *Arch. Environ. Contam. Toxicol*. **39**, 20–31.

Madrid F.; Biasioli, M.; Ajmone-Marsan, F. (2008) Availability and bioaccessibility of metals in fine particles of some urban soils. *Arch Environ Contam Toxicol*, **55**, 21–32.

Madrid, L., Díaz-Barrientos, E., Madrid, F., (2002). Distribution of heavy metal contents of urban soils in parks of Seville. *Chemosphere*, vol. 49, pp. 1301 – 1308.

Maloney, S. R.; Phillips, C. A.; Mills, A. (1998). Mercury in the hair of crematoria workers. *Lancet*, **352**, 1602.

Man, Y. B.; Sun, X. L.; Zhao, Y. G.; Lopez, B. N.; Chung, S. S.; Wu, S. C. (2010). Health risk assessment of abandoned agricultural soils based on heavy metal contents in Hong Kong, the world's most populated city. *Environ Int*, **36**, 570–576.

Manta D. S.; Angelone, M.; Bellanca, A.; Neri, R.; Sprovieri, M. (2002). Heavy metals in urban soils: a case study from the city of Palermo (Sicily), Italy. *Science of the Total Environment*, **300**: 229–243.

Maponga O. (1997**)** Small scale mining and the environment in Zimbabwe: The case of alluvial gold panning and chromite mining. In: Ghose AK, editor. Mining on a small and medium scale: a global perspective. London: IT Publications.

Marsden, D. D. (1987). The vegetating of mine-residue deposits on the Witwatersrand. *Journal of the South African Institute of Mining and Metallurgy*, **87** (6), 189-194.

Marsden, D. D., (1986). The current limited impact of Witwatersrand goldmine residues on water pollution in the Vaal river system. *Journal of the South African Institute of Mining and Metallurgy,* **86**, 481–504.

Martuzevicius, D.; Grinshpun, S. A.; Reponen, T.; Gorny, R. L., Shukla, R.; Lockey, J.; Hu, S.; McDonald, R.; Biswas, P.; Kliucininkas, L.; LeMasters, G. (2004). Spatial and temporal variations of PM2.5 concentration and composition

throughout an urban area with high freeway density-the Greater Cincinnati study. *Atmospheric Environment*, **38**, 1091-1105.

Mason, R. P.; Choi, A. L.; Fitzgerald, W. E.; Hammerschmidt, C. R.; Lamborg, C. H.; Soerensen A. L.; Sunderland E. M. (2012). Mercury biogeochemical cycling in the ocean and policy implications. *Environmental Research*, **119**, 101-117.

Mason, R. P. (2009) Mercury Emissions from Natural sources and their Importance in the Global Mercury Cycle. In: Mercury Fate and Transport in the Global Atmosphere: Measurements, models and policy implications, Pirrone, N. and Mason, R (Eds.), Springer, Dordrecht Heidelberg, London, New York, doi: 10.1007/978-0-387-93958-2.

Mason, R.P. and Benoit, J.M. (2003). Organomercury Compounds in the Environment, In: Organometallic Compounds in the Environment, chapter2, Second Edition, Craig, P.J. (Ed), John Wiley and Sons Ltd, Chichester, UK, doi:10.1002/0470867868.

Mason, R.P., Sheu, G.R., (2002). Role of the ocean in the global mercury cycle. *Global Biogeochemical Cycles* **16**, 401–414.

Mason, R.P., Lawson, N.M., Sheu, G.R., (2001). Mercury in the Atlantic Ocean: factors controlling air-sea exchange of mercury and its distribution in the upper waters. *Deep-Sea Res.* II **48**, 2829–2853.

Mason, R.P., Morel, F.M.M. & Hemond, H.F. (1995). The role of microorganisms in elemental mercury formation in natural waters. *Water, Air, & Soil Pollution*, **80**(1-4), 775-787.

Mason, R.P., Fitzgerald, W.F. & Morel, F.M.M. (1994). The biogeochemical cycling of elemental mercury: Anthropogenic influences. *Geochimica et Cosmochimica Acta*, **58**(15), 3191-3198.

Mast, M. A.; Manthorne, D. J.; Roth, D. A. (2010). Historical deposition of mercury and selected trace elements to high-elevation National Parks in the western U.S. inferred from lake-sediment cores. *Atmospheric Environment*, **44**, 2577–2586.
Mattson, S. M. (1994). Glass Fibers in Simulated Lung Fluid: *Dissolution Behaviour and Analytical Requirements. Ann. Occup. Hyg.* **38**, 857–877.

McCarthy, T. S. & Venter, J. S. (2006). Increasing pollution levels on the Witwatersrand recorded in the peat deposits of the Klip river wetland. *South African Journal of Science*, vol. **102**, pp. 27 – 35.

Melchart, D., Wühr, E., Weidenhammer, W., Kremers, L. (1998). A multicenter survey of amalgam fillings and subjective complaints in non-selected patients in the dental practice. *Eur J Oral Sci*; **106**(3), 770-777.

Meza-Figueroa, D.; De la O-Villanueva, M.; De la Parra, M. L. (2007). Heavy metal distribution in dust from elementary schools in Hermosillo, Sonora, México. *Atmospheric Environment,* **41**, 276–288.

Meza-Figueroa, D., Maier, R. M., de la O-Villanueva, M., Gomez-Alvarez, A., Moreno-Zazueta, A., Rivera, J. (2009). The impact of unconfined mine tailings in residential areas from a mining town in a semi-arid environment: Nacozari, Sonora, Mexico. *Chemosphere,* vol. **77**, pp. 140 –147.

Mielke H, Gonzales C, Smith M, Mielke P. (1999). The urban environment and children's health: soils as an integrator of lead, zinc, and cadmium in New Orleans, Louisiana, USA. *Environ Res*; **81**, 117–29.

Mineral resources, South Africa year book 2012/13 www.gcis.gov.za/files/docs/resourcecentre/yearbook/2012/16%20Mineral%20Resources_0.pdf. (Accessed 23 March 2014)

Moreno, T.; Oldroyd, A.; McDonald, I.; Gibbons, W. (2007). Preferential fractionation of trace metals–metalloids into PM10 re-suspended from contaminated gold mine tailings at Rodalquilar, Spain. *Water Air Soil Pollut*, **179**, 93-105.

Moreno, T.; Higueras, P.; Jones, T.; McDonald, I.; Gibbons, W. (2005**).** Size fractionation in mercury-bearing airborne particles (HgPM10) at Almaden, Spain: Implications for inhalation hazards around old mines. *Atmospheric Environment*, **39**, 6409–6419.

Morisset, T.; Ramirez-Martinez, A.; Wesolek, N.; Roudot, A. C. (2013). Probabilistic mercury multimedia exposure assessment in small children and risk assessment. *Environment International,* **59**, 431-441.

Mossop, K. F., Davidson, C. M. (2003). Comparison of original and modified BCR sequential extraction procedures for the fractionation of copper, iron, lead, manganese and zinc in soils and sediments. *Analytica Chimica Acta,* **478**,111–118.

Moszczyński P. (1999). Immunological disorders in men exposed to metallic mercury vapour. A review. *Central European Journal of Public Health,* **7** (1), 10-14.

Mphephu, N. F. (2001). Rehabilitation of tailings dams on the Central Rand, Johannesburg. www.techtransfer.osme.gov (Accessed 17 June 2012).

Mukherjee, A. B.; Zevenhoven, R.; Bhattacharya, P.; Sajwan, k. S.; Kikuchi, R. (2008). Mercury flow via coal and coal utilization by-products: A global perspective. *Resources, Conservation and Recycling*, **42**(2), 155-182.

Muller, G. (1969). Index of geo-accumulation in sediments of the Rhine River. *Geojournal,* **2** 108–118.

Muniz, P., Venturini, N., Gómez-Erache, N. (2004). Spatial distribution of chromium and lead in the benthic environmental coastal areas of the Río de la Plata estuary (Montevideo, Uruguay). *Braz. J. Biol.* **64** (1), 103–116.

Munthe, J.; Bodaly, R. A.; Branfireun, B. A.; Driscoll, C. T.; Gilmour, C. C.; Harris, R.; Horvat, M.; Lucotte, M.; Malm, O. (2007). Recovery of mercury-contaminated fisheries. *AMBIO: A Journal of the Human Environment*, **36** (1), 33−44.

Munthe, J. (1992). The aqueous oxidation of elemental mercury by ozone. *Atmospheric Environment,* **26A**, 1461:1468.

Munthe, J., McElroy, W. (1992). Some aqueous reactions of potential importance in the atmospheric chemistry of mercury. *Atmospheric Environment,* **26A**, 553-557.

Naicker, K.; Cukrowska, E.; McCarthy, T. S. (2003). Acid mine drainage arising from gold mining activity in Johannesburg, South and environs. *Environmental Pollution*, **122**, 29-40.

Nadal M, Schuhmacher M, Domingo JL. (2004). Metal pollution of soils and vegetation in an area with petrochemical industry. *Sci Total Environ,* **321,** 59–69.

Nadal M, Bocio A, Schuhmacher M, Domingo JL. (2005). Trends in the levels of metals in soils and vegetation samples collected near a hazardous waste incinerator. *Arch Environ Contam Toxicol,***49**, 290–8.

Ndasi, M. B. (2007). The accumulation of heavy metals in Sedimentary deposits in the Fleurhof and Russel stream dams of the Central rand, Johannesburg. Masters of Science Report, University of the Witwatersrand.

Neculita, C.; Zagury, J. G.; Deschênes, L. (2005). Mercury speciation in highly contaminated soils from chlor-alkali plants using chemical extractions. *Journal of Environmental Quality*, **34,** 255.

Nemmar, A.; Hoet, P.H. M.; Vanquickenborne, B.; Dinsdale, D.; Thomer, M.; Hoylaerts, M. F.; Vanbilloen, H.; Mortelmans, L.; Nemery, B. (2002). Passage of inhaled particles into the blood circulation in humans. *Journal of the American Heart Association*, 105, 411-414.

Neuman, C. M.; Boulton, J. W.; Sanderson, S. (2009**).** Wind tunnel simulation of environmental controls on fugitive dust emissions from mine tailings. *Atmospheric Environment*, **43**, 520–529.

NERSA (National Energy Regulator of South Africa), (2005). Electricity Supply

Statistics for South Africa. NERSA, Pretoria, South Africa.

Nguyen, H. T., Ki-Hyun, K., Min-Yooung, K., Zang-Ho, S. (2008). Exchange pattern of gaseous elemental mercury in an active urban landfill facility. *Chemosphere*, **70**: 821-832.

Nhlengetwa, K., Hein, K. A. A. (2014). Zama-Zama mining in the Durban Deep/Roodepoort area of Johannesburg, South Africa: An invasive or alternative livelihood? *Extr. Ind. Soc*. http://dx.doi.org/10.1016/j.exis.2014.07.003.

Nieschmidt, A. K. and Kim, N. D. (1997). Effects of mercury release from amalgam dental restorations during cremation on soil mercury levels of three New Zealand crematoria. *Bulletin of Environmental Contamination and Toxicology*, **58**(5), 744-751.

Nordberg GF, Brune D, Gerhardsson L, Grandjean P, Vesterberg O, Wester P. O. (1992). The ICOH and IUPAC international programme for establishing reference values of metals. *The Science of the Total Environment*, **120**(1–2): 17–21.

Nriagu, J. and Becker, C. (2003). Volcanic emissions of mercury to the atmosphere: global and regional inventories. *The Science of the Total Environment*, **304**, 3-12.

Nriagu, J. O. (1989). A global assessment of natural sources of atmospheric trace metals. *N Obrist D. (2007). Atmospheric mercury pollution due to losses of terrestrial carbon pools? Biogeochemistry, **85,** 119–23.*

Nriagu, J. O.; Pacyna, J. M. (1988). Quantitative assessment of worldwide contamination of air, water and soils by trace metals. *Nature*, **333**, 134–139.

Obrist D. (2007). Atmospheric mercury pollution due to losses of terrestrial carbon pools? *Biogeochemistry*, **85,** 119–23.

Oguntoke, O.; Ojelede, M. E.; Annegarn, H. J. (2013). Frequency of Mine Dust Episode sand the Influence of Meteorological Parameters on the Witwatersrand Area, South Africa. *International Journal of Atmospheric Science*,

Oguntoke, O.; Ojelede, M. E.; Annegarn, H. J. (2013). Frequency of mine dust episodes and the influence of meteorological parameters on the Witwatersrand area, South Africa. *International Journal of Atmospheric Sciences*, Article ID 128463, 10 pages http://dx.doi.org/10.1155/2013/128463.

Ordóñez, A.; Álvarez, R.; Charlesworth, S.; De Miguel, E.; Loredo, J. (2011). Risk assessment of soils contaminated by mercury mining, Northern Spain. *J Environ Monit*; **13,** 128–136.

Ojelede, M. E.; Annegarn, H. J.; Kneen, M. A (2012). Evaluation of aeolian emissions from gold mine tailings on the Witwatersrand. *Aeolian Research*, **3** (4), 477-486.

Oliveira, C.; Martins, N.; Tavares, J.; Pio, C.; Cerqueira, M.; Matos, M.; Silva, H.; Oliviera, S.; Camoes, F. (2011). Size distribution of polycyclic aromatic hydrocarbons in a roadway tunnel in Lisbon, Portugal. *Chemosphere*, **83** (11), 1588-1596.

Omar, N.; Abas, M.; Rahman, N.; Tahir, N.; Rushdi, A.; Simoneit, B. (2007). Levels and distributions of organic source tracers in air and roadside dust particles of Kuala Lumpur, Malaysia. *Environmental Geology*, **52**, 1485‑1500.

Omstedt, G.; Bringfelt, B.; Johansson, C. (2005). A model for vehicle-induced non-tail pipe emissions of particles along Swedish roads. *Atmospheric Environment*, **39**, 6088-6097.

Oomen, A. G., Rompelberg, C. J. M., Bruil, M. A., Dobbe, C. J. G., Pereboom, D. P. K. H., Sips, A. J. A. M. (2003). Development of an in vitro digestion model for estimation of bioaccessibility of soil contaminants. *Archives of Environmental Contamination and Toxicology*, **44**, 281–287.

Oyarzun, R.; Lillo, J.; López-García, J. A.; Esbrí, J. M.; Cubas, P.; Llanos, W. (2011). The Mazarrón Pb–(Ag)–Zn mining district (SE Spain) as a source of heavy metal contamination in a semiarid realm: Geochemical data from mine wastes, soils, and stream sediments. *Journal of Geochemical Exploration*; **109**: 113-124.

Pacyna, E. G., Pacyna J. M., Sundseth, K., Munthe, J., Kindbom, K., Wilson, S., Steenhuisen, F., and Maxson, P. (2010). Global emission of mercury to the atmosphere from anthropogenic sources in 2005 and projections to 2020. *Atmospheric Environment*, **44**, 2487-2499.

Pacyna, E.G., Pacyna, J.M., Steenhuisen, F. & Wilson, S. (2006). Global anthropogenic mercury emission inventory for 2000. *Atmospheric Environment*, **40**, (22), 4048-4063.

Pacyna, E.G. & Pacyna, J.M. (2002). Global emission of mercury from anthropogenic sources in 1995. *Water, Air, and Soil Pollution,* **137**, 149-162.

Pacyna, J. M. (1998). Source Inventories for Atmospheric Trace Metals. In: Harrison, R.M., van Grieken, R.E. (Eds.), Atmospheric Particles, IUPAC Series on

Analytical and Physical Chemistry of Environmental Systems, Vol. 5. Wiley, Chichester, UK, pp. 385-423.

Park, J. D., Zheng, W. (2012). Human exposure and health effects of Inorganic and Elemental mercury. *Journal of Preventive Medicine and Public Health*, **45**, 344-352.

Park, S. S. & Wexler, A. S. (2008). Size-dependent deposition of particles in the human lung at steady-state breathing. *Journal of Aerosol Science,* 39, 266 – 276.

Paustenbach, D. J. (2002). Human and Ecological Risk Assessment: Theory and Practice. New York: Wiley.

Paustenbach, D. J., Bruce, G. M., Chrostowski, P. (1997). Current views on the oral bioavailability of inorganic mercury in soil: Implications for health risk assessment. *Risk Analysis*, **17**(5):533–544.

Pehkonen, S. O., Lin, C. J. (1998). Aqueous photochemistry of mercury with organic acids. *Journal of the Air & Waste Management Association,* **48,** 144-150.

Petavratzi, E., Kingman, S., Lowndes, I. (2005). Particulates from mining operations: A review of sources, effects and regulations. *Minerals Engineering,* **18**, 1183-1199.

Petersen, G, Munthe, J., Pleijel, L., Bloxam, R., Kumar, V.A. (1998). A comprehensive eulerian modelling framework for airborne mercury species: Development and testing of the tropospheric chemistry module (TCM). *Atmospheric Environment,* **32,** 829-843.

Pfeiffer, W. C., Lacerda, L. D. (1988). Mercury inputs into the Amazon region, Brazil. *Environ Technol Lett*, **9,** 325–330.

Piani, R.; Covelli, S.; Biester, H. (2005). Mercury contamination in Marano Lagoon (Northern Adriatic sea, Italy): source identification by analyses of Hg phases. *Appl. Geochem.* **20**, 1546–1559.

Pinheiro, H. J. (Ed.), (2000). Bulletin 113: A techno-economic and historical review of the South African Coal Industry in the 19th and 20th Centuries, and Analyses of Coal product samples of South African Collieries 1998–1999. South African Bureau of Standards.

Pirrone, N., Cinnirella, S., Feng, X., Finkelman, R. B., Friedli, H. R., Leaner, J., Mason, R., Mukherjee, A.B., Stracher, G.B., Streets, D. G. and Telmer, K. (2010). Global mercury emissions to the atmosphere from anthropogenic and natural sources. *Atmospheric Chemistry and Physics*, **10**, 4719–4752.

Pirrone, N., Cinnirella, S., Feng, X., Finkelman, R.B., Friedli, H.R., Leaner, J., Mason, R., Mukherjee, A.B., Stracher, G.B. & Streets, D. G. and Telmer, K. (2009), "Global mercury emissions to the atmosphere from anthropogenic and natural sources" in Mercury fate and transport in the Global Atmosphere: Emissions, Measurements and Models, ed. Pirrone Nicola and Mason Robert, Springer Dordrecht Heidelberg, New York, pp. 3-49.

Pirrone, N., Hedgecock, I., Forlano, L. (2000). The Role of the Ambient Aerosol in the Atmospheric Processing of Semi-Volatile Contaminants: A Parameterised Numerical Model (GASPAR). *Journal of Geophysical Research*, **105**, (D8), 9773-9790.

Pirrone, N.; Allegrini, I.; Keeler, G. J.; Nriagu, O.; Rossmann, R.; Robbins, J. A. (1998). Historical Atmospheric Mercury Emissions and depositions in North America compared to mercury accumulations in Sedimentary records. *Atmospheric Environment*, **32**, 929-940.

Pirrone N.; Keeler, G.J.; Nriagu, O. (1996). Regional differences in worldwide emissions of mercury to the atmosphere. *Atmospheric Environment*, **30**, (17): 2981-2987.

Pleijel, K., Munthe, J. (1995). Modelling the Atmospheric Mercury Cycle – Chemistry in Fog Droplets. *Atmospheric Environment*, **29**, 1441-1457.

Plumlee, G. S.; Ziegler, T. L. (2006). The Medical Geochemistry of dust, Soils, and other Earth Materials. In: Treatise on Geochemistry. Volume 9. Lollar BS (ed) Elsevier Denver CO: US geological Survey. Plumlee GS, Ziegler TL (2006) The medical geochemistry of dusts, soils, and other earth materials, online version, http://www.sciencedirect.com/science/referenceworks/0080437516.

Pope III, C. A.; Burnett, R. T.; Thurston, G. D.; Thun, M. J.; Calle, E. E.; Krewski, D.; Godleski, J. J. (2004). Cardiovascular mortality and long-term exposure to particulate air pollution: epidemiological evidence of general pathophysiological pathways of disease. *J. Am. Heart Assoc.* **109**, 71–77.

Pope, P., Van Eeckhout, E., & Rofer, C. (1996). Waste site characterization through digital analysis of historical aerial photographs. *Photogrammetry* and *Remote Sensing*, **62**, 1387 – 1394.

Put, G. V., van Broeder, L., Penris, M., Abbing, E. W. R. (2001). Experience with HIA at national policy level in the Netherlands: a case study. Brussels: European centre for health Policy, World health Organisation. EUR/00/5019128/4. http://www.who.dk/hs/ECHP/index.htm (Accessed 26 March 2014).

Qu, C. S.; Sun, K.; Wang, S. R.; Huang, L.; Bi, J. (2012). Monte Carlo simulation based health risk assessment of heavy metal pollution: a case study in Qixia mining area, China. *Hum Ecol. Risk Assess*, **18**, 733–750.

Querol X, Alastuey A, Lopez-Soler A, Plana F. (2000). Levels and chemistry of atmospheric particulates induced by a spill of heavy metal mining wastes in the Donana area, Southwest Spain. *Atmospheric Environment*, **34**, 239–53.

Rafiei, B.; Khodaei, A. S.; Khodabakhsh, S.; Hashemi, M.; Nejad, M. B (2010). Contamination Assessment of Lead, Zinc, Copper, Cadmium, Arsenic and, Antimony in Ahangaran Mine Soils, Malayer, West of Iran. Soil and Sediment Contamination: *An International Journal*; **19,** 15.

Rahimsouri, Y.; Yaghubpur, A.; Modabberi, S.; Alipour, S. (2011). Environmental impacts of natural contaminants and mining activities on the surface and agricultural soils in the Aq-Darreh river watershed, Takab, West Azerbaijan Province, NW Iran. *Iranian Journal of Science & Technology*, **2**, 101-111.

Ramirez Requelme, M. E.; Ramos, J. F. F.; Angelica, R. S.; Brabo, E. S. (2003). Assessment of mercury-contamination in soils and stream sediments in the mineral district of Nambija, Ecuadorian Amazon (example of an impacted are affects by artisanal gold mining). *Applied Geochemistry*, **18**, 371–381.

Rashed, M. N. (2008). Total and extractable heavy metals indoor, outdoor and street dust from Aswan city, Egypt. *Clean*, **36** (10–11), 850–857.

Rasmussen, P. E., Beauchemin, S., Nugent, M., Dugandzic, R., Lanouette, M., Che´nier, M. (2008). Influence of matrix composition on the bioaccessibility of Copper, Zinc, and Nickel in urban residential dust and soil. *Human and Ecological Risk Assessment,* **14**, 351–371.

Rasmussen, P. E., Subramanian, K. S., & Jessiman, B. J. (2001). A multi-element profile of house dusts in relation to exterior dust and soils in the city of Ottawa, Canada. *Science* of the *Total Environment*, vol. **267**, pp. 125 – 40.

Rasmussen, P.E., Edwards, G.C., Kemp, J.R., Fitzgerald-Hubble, C.R., Schroeder, W.H. (1998). Towards an improved natural sources inventory for mercury. In: Skeaff, J. (Ed.), Proc. Canadian Institute of Mining Internat. Symp. On the Metals in the Environment, pp. 74–82.

Rasmussen, P. E. (1994). Current methods for estimating atmospheric mercury fluxes in remote areas. *Environ. Sci. Tech*., **28**, 2233-2241.

Rauret, G.; Lopez-Sanchez, J. F.; Sahuquillo, A.; Rubio, R.; Davidson, C.; Ure, A.; Quevauviller, P. H. (1999). Improvement of the BCR three step sequential extraction procedure prior to the certification of new sediment and soil reference materials. *J. Environ. Monit.* **1**, 57-61.

Ravi, S., D'Odorico, P., Breshears, D. D., Field, J. P., Goudie, A., Huxman, T. E., Li, J., Okin, G. S., Swap, R. J., Thomas, A. D., Van Pelt, S., Whicker, J. J., & Zobeck, T. M. 2011, "Aeolian processes and the biosphere: interactions and feedback loops", *Reviews of Geophysics*, vol. 49, no. 3, pp. 1 – 49.

Ravichandran, M. (2004). Interactions between mercury and dissolved organic matter—a review. *Chemosphere* **55**/3, 319–331.

Ravichandran, M.; Aiken, G.R.; Reddy, M. M.; Ryan, J. N. (1998). *Environ. Sci. Technol.* **32**, 3305.

Rea, A. W., Lindberg, S. E., Scherbatskoy, T., Keeler, G. J. (2002). Mercury accumulation in foilage over time in two northern mixed-hardwood forests", *Water, Air and soil pollution*, **133**(1-4), 49-67.

Rendell, E. G.; McGinty, K. A, (2007) Collegeville Area Air Monitoring Report, Commonwealth of Pennsylvania Department of Environmental Protection, Collegeville Area Air Toxics Study.
www.dep.state.pa.us (Accessed 3 December 2014).

Renwick, L. C.: Donaldson, K.; Clouter, A. (2001). Impairment of alveolar macrophage phagocytosis by ultrafine particles. *Toxicology and Applied Pharmacology*, **172**, 119-127.

Research Triangle Institute; Agency for Toxic Substances and Disease Registry. Toxicological profile for mercury. Atlanta: US Department of Health and Human Services; 1999.

Revis, N. W., Osborne, T. R., Holdsworth, G., Hadden, C. (1989). Distribution of mercury species in soil from a mercury-contaminated site. *Water, Air, & Soil Pollution*, **45**, (1-2), 105-113.

Risher, J. F. Elemental mercury and inorganic mercury compounds: Human health aspects: Concise international chemical assessment document 50, World Health Organization, 2003

Robb, L. J. & Robb, V. M. (1998). Gold in the Witwatersrand Basin. In: *The Mineral Resources of South Africa: Handbook Volume 16*, ed. Wilson M. G. C. and

Anhaeusser C. R., 6th ed., Council for Geosciences, Pretoria, South Africa, pp. 294–349.

Rodrigues, S. M., Coelho, C., Cruz, N., Monteiro, R.J.R., Henriques, B., Duarte, A. C., Römkens, P.F.A.M., Pereira, E. (2014). Oral bioaccessibility and human exposure to anthropogenic and geogenic mercury in urban, industrial and mining areas. *Science of the Total Environment*, **496**, 649-661.

Rodrigues, S.; Pereira, M. E.; Duarte, A. C.; Ajmone-Marsan, F.; Davidson, C. M.; Grčman, H., Hossack, I., Hursthouse, A. S., Ljung, K., Martini, C., Otabbong, E., Reinoso, R., Ruiz-Cortés, E., Urquhart, G. J., Vrščaj, B. (2006). Mercury in urban soils: A comparison of local spatial variability in six European cities. *Science of the Total Environment*, **368**: 926–936.

Roemer, W., Hoek, G., Brunekreef, B., Clench-Aas, J., Forsberg, B., Pekkanen, J. & Schutz, A. (2000). PM10 elemental composition and acute respiratory health effects in European children (PEACE project)", *European Respiratory Journal*, vol. 15, pp. 553-559.

Roulet, M., Lucotte, M., Farella, N., Serique, G., Coelho, H., Sousa Passos, C. J., De Jesus da Silva, E., Scavone de Andrade, P., Mergler, D., Guimaraes, J. R. D., Amorium, M. (1999). Effects of recent human colonization on the presence of mercury in Amazonian ecosystems. *Water, Air, and soil pollution*, **112**: 297-313.

Rösner, T., Boer, R., Reyneke, R., Aucamp, P., Vermaark, J. (2001). A preliminary assessment of pollution contained in the unsaturated and saturated zone beneath reclaimed gold-mine residue deposits. Water Research Commission Report No. 797/1/01. www.wrc.org.za (accessed 20 March 2012).

Rösner T. & Van Schalkwyk, A. (2000). The environmental impact of gold mine tailings footprints in the Johannesburg region, South Africa. *Bulletin of Engineering Geology and the Environment*, vol. **59**, pp. 137–148.

Rösner, T. (1999). The environmental impact of seepage from gold mine tailings dams near Johannesburg, South Africa.

Rösner, T., Boer, R., Reyneke, R., Aucamp, P., & Vermaak, J. (1998). A preliminary assessment of pollution contained in the unsaturated and saturated zone beneath gold mine residue deposits. Rep K5/797/0/1. Water Research Commission of South Africa, Pretoria.

Ruby, M. V., Schoof, R., Brattin, W., Goldade, M., Post, G., Harnois, M., Mosby, D. E., Casteel, S. W., Berti, W., Carpenter, M., Edwards, D., Cragin, D., and

Chappell, W. (1999) Advances in evaluating the oral bioavailability of inorganics in soil for use in human health risk assessment. *Environmental Science & Technology*, **33**, 3697–3705.

Ruby, M. V., Davis, A., Schoof, R., Eberle, S., and Sellstone, C. M. (1996) Estimation of lead and arsenic bioavailability using a physiologically based extraction test. *Environmental Science & Technology,* **30**, 422-430.

Ruby, M. V., Davis, A., Link, T. E., Schoof, R., Chaney, R. L., Freeman, G. B., and Bergstrom, P. (1993). Development of an in vitro screening test to evaluate the in vivo bioaccessibility of ingested mine-waste lead. *Environmental Science & Technology* **27**, 2870–2877.

Rudd, J. M. W. (1995) Sources of methyl mercury to fresh water ecosystem: A review. *Water, Air, & Soil Pollution*, **80**, (1-4), 697-713.

Rytuba, J. J. (2005) Geogenic sources of mercury to the environment. In Mercury: Sources, Measurements, Cycles, and Effects, Parsons, M. B. And Percival, J. B. (eds.), Mineral. Assoc. Canada, Short Course, 34, 21-41.

Rytuba, J. J. (2003) Mercury from mineral deposits and potential environmental impact. *Environmental Geology*, **43**, 326–338.

Sahuquillo, A.; Lopez-Sanchez, J. F.; Rubio, R.; Rauret, G.; Thomas, R. P.; Davidson, C. M. (1999). Use of a certified reference material for extractable trace metals to assess sources of uncertainty in the BCR three-stage sequential extraction procedure. *Analytica Chimica Acta*, **382**(3), 317–327

Sánchez, de la Campa, A. M., de la Rosa, J., Fernández-Caliani, J.C, González-Castanedo, Y. "Impact of abandoned mine waste on atmospheric respirable particulate matter in the historic mining district of Rio Tinto (Iberian Pyrite Belt)". *Environmental Research,* vol. **111**, pp. 1018 – 1023.

Sánchez, D. M.; Quejido, A. J.; Fernandez, M.; Hernández, C.; Schmid, T.; Milan, R. (2005). Mercury and trace element fractionation in Almaden soils by application of different sequential extraction procedures. *Analytical and Bioanalytical Chemistry*, **381**, 1507–1513.

Sandborgh-Englund, G., Elinder, C. G., Langworth, S., Schütz, A., Ekstrand, J. (1998). Mercury in biological fluids after amalgam removal. *J Dent Res*, **77** (4): 615-624.

Sasol, 2008. Annual Report 2008: Sasol Annual Review and Summarised Financial Information Available from. http://www.sasol.com/sasol_internet/downloads/ Sasol_AR_2008_1223884814646.pdf (accessed October 2008)

Sax, I. N. & Lewis, R. J. 1984, Dangerous properties of industrial materials, 7th Edn. Vol. I, Van Nostrand Publication, New York, USA.

Schroder, H. H. E., Van der Linde, A. & Strydom, N.B. (1982). The emission of mercury from gold-reduction works in South Africa. *Journal of the South African institute of mining and metallurgy*, 193-199.

Schroeder, W. H. & Munthe, J. (1998) Atmospheric mercury—an overview. *Atmospheric Environment*, **32**, no. 5, pp. 809-822

Schuhmacher, M., Nadal M, Domingo JL. (2009). Environmental monitoring of PCDD/Fs and metals in the vicinity of a cement plant after using sewage sludge as a secondary fuel. *Chemosphere*, **74**, 1502–8.

Schuster, P. F.; Krabbenhoft, D. P.; Naftz, D. L.; Cecil, L. D.; Olson, M. L.; Dewild, J. F.; Susong, D. D.; Green, J. R.; Abbott, M. L. (2002). Atmospheric mercury deposition during the last 270 years: A glacial ice core record of natural and anthropogenic sources. *Environmental Science & Technology*, **36**, 2303–2310.

Schuster, E. (1991). The behavior of mercury in the soil with special emphasis on complexation and adsorption processes—a review of the literature. *Water Air Soil Pollut.* **56**, 667–680.

Scorgie, Y. (2006). Air quality assessment of the Durban Roodepoort (DRD). West Rand Consolidated (WRC) and Princess Tailings complexes and review of environmental management measures and programmes. Report NO. APP/05/LRC-01 Rev.1.0, Johannesburg: Legal resource Center.

Seccatore, J. (2012). An Estimation of the Artisanal Small-Scale Production of Gold in the World. Report for World Gold Council. Codex Engineering Services, Lungomare, Italy, pp. 19 (unpublished).

Seigneur, C., Wrobel, J. & Constantinou, E. (1994) A Chemical Kinetic Mechanism for Atmospheric Inorganic Mercury. *Environmental Science & Technology*, **28**, 1589-1597.

Semple, K.T.; Doick, J. K.; Jones, K. C.; Bureauel, P.; Craven, A.; Harms, H. (2004). Defining bioavailability and bioaccessibility of contaminated soil and sediments is complicated. *Environmental Science & Technology*, **2**, 229A–231A.

Sheppard, S.C.; Evenden, W.G. (1994). Contaminant enrichment and properties of soil adhering to skin. *Journal of Environmental Quality*, **23**, 604‑613.

Shuman, L. M. (1982). Separating soil iron- and manganese oxide fractions for microelement analysis. *Soil Science Society of America Journal*, **46**(5), 1099–1102.

Siciliano, S. D.; James, K.; Zhang, G. Y. Schafer, A. N. Peak, J. D. (2009). Adhesion and enrichment of metals on human hands from contaminated soil at an Arctic urban brownfield. *Environmental Science and Technology*, **43**, 6385‑6390.

Singh, M.; Jaques, P. A.; Sioutas, C. (2002). Size distribution and diurnal characteristics of particle-bound metals in source and receptor sites of the Los Angeles Basin. *Atmospheric Environment* **36**, 1675-1689.

Škrbić, B., Mladenovic, N. Đ. (2010). Chemometric interpretation of heavy metal patterns in soils worldwide. *Chemosphere,* **80**, 1360–1369.

Skyllberg, U., Bloom, P.R., Qian, J., Lin, C.-M., Bleam, W.F. (2006). Complexation of Mercury (II) in soil organic matter: EXAFS evidence for linear two-coordination with reduced sulfur groups. *Environ. Sci. Technol.* **40** (13), 4174–4180.

Skyllberg, U., Xia, K., Bloom, P.R., Nater, E.A., Bleam, W.F. (2000). Binding of mercury (II) to reduced sulfur in soil organic matter along upland-p eat soil transects. *J. Environ. Qual.* **29**, 855– 865.

Slemr, F.; Brunke, E. G.; Ebinghaus, R.; Kuss, J. Worldwide trend of atmospheric mercury since 1995. *Atmos. Chem. Phys.* 2011, 11, 4479−4787.

Slemr, F., Schuster, G., and Seiler, W. 1985. Distribution, speciation, and budget of atmospheric mercury, *Journal of Atmospheric Chemistry*, **3**, 407–434.

Slemr, F., Seiler, W., Schuster, G.J. (1981): Latitudinal distribution of mercury over the Atlantic Ocean. *Journal of Geophysical Research: Oceans,* **86**, 1159-1166.

Smith, J and Lee, K. (2003). Soil as a source of dust and implications for human health. *Advances in Agronomy*, **80**, pp. 1–32.

Smith-Downey, N. V.; Sunderland, E. M.; Jacob, D. J. (2010). Anthropogenic impacts on global storage and emissions of mercury from terrestrial soils: Insights from a new global model. *Journal of Geophysical Research: Biogeosciences.* 115

Soerensen, A. L.; Sunderland, E. M.; Holmes, C. D.; Jacob, D. J.; Yantosca, R. M.; Skov, H.; Christensen, J. H.; Strode, S. A.; Mason, R. P. (2010). An improved global model for air-sea exchange of mercury: High concentrations over the North Atlantic. *Environmental Science & Technology.*, **44**, 8574–8580.

Sommar, J., Gårdfeldt, K., Strömberg, D., Feng, X. (2001). A kinetic study of the gas phase reaction between hydroxyl radical and atomic mercury. *Atmospheric Environment,* **35**, 3049-3054.

Sommar, J., Hallquist, M., Ljungström, EL, Lindqvist, O. 1997. On the gaseous reaction between volatile biogenic mercury species and the nitrate radical. *J. Atmos. Chem.* 27: 233-247.

Sorensen, J., Glass, G.E., Schmidt, K.W. & Huber, James K. and Rapp Jr., George R. 1990, "Airborne mercury deposition and watershed characteristics in relation to mercury concentrations in water, sediments, plankton, and fish of eighty northern Minnesota lakes", *Environmental Science & Technology*, vol. 24, no. 11, pp. 1716-1727.

Spear, T. M., Svee, W., Vincent, J. H., & Stanisich, N. (1998). Chemical speciation of lead dust associated with primary lead smelting. *Environmental Health Perspectives,* **106**, 565 – 571.

Spencer, A. J. (2000). Dental amalgam and mercury in dentistry. *Aust Dent J*; 45(4), 224-234.

Spiegel, S. J., Veiga, M.M., (2010). International guidelines on mercury management in small-scale gold mining. *J. Clean. Prod.* 18 (4), 375–385.

Sprovieri, F., Pirrone, N., Ebinghaus, R., Kock, H., Dommergue, A., 2010. A review of worldwide atmospheric mercury measurements. *Atmospheric Chemistry and Physics* 10 (17), 8245-8265.

Stafilov, T., Sajn, R., Pancevski, Z., Boev, B., Frontasyeva, M. V., Strelkova, L. P. (2010). Heavy metal contamination of top soils around a lead and zinc smelter in the Republic of Macedonia. *Journal of Hazardous Materials,* **175**, 896 – 914.

State of the Air Report in South Africa (2005). A report on the state of air in South Africa. Department of Environmental Affairs, ISBN 978-0-621-38724-7 Pretoria, South Africa.

Steffen A., Douglas T., Amyot M., Ariya P., Aspmo K., Berg T., Bottenheim J., Brooks S., Cobbett F., Dastoor A., Dommergue A., Ebinghaus R., Ferrari C., Gardfeldt K., Goodsite M.E., Lean D., Poulain A., Scherz C., Skov H., Sommar J. & Temme T. (2007). A synthesis of atmospheric mercury depletion event chemistry linking atmosphere, snow and water. *Atmospheric Chemistry and Physics Discussions, **7**,* 10837–10931.

Stein, E. D., Cohen, Y., Winer, A. M. (1996). Environmental distribution and transformation of mercury compounds. *Critical reviews in Environ. Sci. Technol.* **26**(1): 1-43.

Stopford, W.; Turner, J.; Cappellini, D.; Brock, T. (2003). Bioaccessibility testing of cobalt compounds. *J. Environ. Monit.* **5**, 6675-680.

Stramma, L., Johnson, G.C., Sprintall, J., Mohrholz, V., 2008. Expanding oxygen minimum zones in the tropical oceans. *Science* 320 (5876), 655–658.

Streets, D.G., Devane, M.K., Lu, Z., Bond, T.C., Sunderland, E.M., Jacob, D.J., 2011. All time releases of mercury to the atmosphere from human activities. *Environmental Science & Technology* 45 (24), 10485-10491.

Streets, D. G., Zhang, Q., and Wu, Y. 2009. "Projections of Global mercury emissions in 2050". *Environmental Science & Technology*, 43, 2983-2988.

Streets, D. G.; Hao, J.; Wu, Y.; Jiang, J.; Chan, M.; Tian, H.; Feng, X. 2005. Anthropogenic mercury emissions in China. *Atmospheric Environment*, 39, 7789–7806.

Sterckeman, T., Douay, F., Proix, N., Fourrier, H. 2000, "Vertical distribution of Cd, Pb and Zn in soils near smelters in the North of France". *Environmental Pollution*, vol. 107, pp. 377 – 389.

Sternbeck, J.; Sjodin, A. A.; Andreasson, K. (2002). Metal emissions from road traffic and the influence of resuspension-results from two tunnel studies. *Atmospheric Environment*, **36**, 4735-4744.

Sun, G.; Li, Z.; Bi, X.; Chen, Y.; Lu, S.; Yuan, X. (2013). Distribution, sources and health risk assessment of mercury in kindergarten dust. *Atmospheric Environment*, **73**, 169-176.

Sunderland, E.M., Dalziel, J., Heyes, A., Branfireun, B.A., Krabbenhoft, D.P., Gobas, F., (2010). Response of a macrotidal estuary to changes in anthropogenic mercury loading between 1850 and 2000. *Environmental Science & Technology* 44 (5), 1698–1704.

Sunderland, E.M., Krabbenhoft, D. P., Moreau, J. W., Strode, S. A., Landing, W. M. (2009). Mercury sources, distribution, and bioavailability in the North Pacific Ocean: insights from data and models. *Global Biogeochemical Cycles*, **23**, GB2010.

Sunderland, E. M., Mason, R. P., (2007). Human impacts on open ocean mercury concentrations. *Global Biogeochemical Cycles* **21**, GB4022. doi: 4010.1029/ 2006GB002876.

Sutton, M. W. (2008). Use of remote sensing and GIS in a risk assessment of gold deposits and identification of vulnerable land use. MSc Research Report: University of Witwatersrand.

Sutton, M. W., Weiersbye, I. M., Galpin, J. S., Heller, D. (2006). A GIS-based history of gold mining residue deposits and risk assessment of post-mining land

uses on the Witwatersrand basin, South Africa. In: A. B. Fourie and M. Tibbett (editors). *Proceedings of the 1st International Seminar on Mine Closure*, Perth: Australian Centre for Geomechanics, pp 667-678.

Swain, E.B., Jakus, P.M., Rice, G., Lupi, F., Maxson, P.A., Pacyna, J.M., Penn, A. & Spiegel, Samuel J. and Veiga, Marcello M. (2007). Socioeconomic Consequences of Mercury Use and Pollution", *AMBIO: A Journal of the Human Environment,* **36**(1), 45-61.

Swaine, D. J. (1994). Trace elements in coal and their dispersal during combustion. *Fuel Processing Technology* **39**, 121–137.

Takaoka, M.; Oshita, K.; Takeda, N.; Morisawa, S. (2010). Mercury emission from crematories in Japan. *Atmos. Chem. Phys.* **10**, 3665-3671.

Tanner, P.A., Ma, H.L., Yu, P.K.N. (2008). Fingerprinting metals in urban street dust of Beijing, Shanghai, and Hong Kong. *Environ. Sci. Technol*. **42**, 7111–7117.

Tang H. L, Chu, K. H., Mak, Y. F., Lee, W., Cheuk, A., Yim, K. F. (2006). Minimal change disease following exposure to mercury-containing skin lightening cream. *Hong Kong Med J*. **12** (4):316-318.

Taylor, M. P., Mackay, A. K., Hudson-Edwards, K. A., Holz, E. (2010). Soil Cd, Cu, Pb and Zn contaminants around Mount Isa city, Queensland, Australia: potential sources and risks to human health", *Applied Geochemistry*, vol. 25, pp. 841 – 855.

Telmer Kevin, H. and Veiga Marcello M. (2009). World Emissions of Mercury from Artisanal and Small Scale Gold Mining, In: Mercury fate and transport in the Global Atmosphere: Emissions, Measurements and Models, ed. Pirrone Nicola and Mason Robert, Springer Dordrecht Heidelberg, New York, pp. 131-172.

Telmer, K., Costa, M., Angelica, R. S., Araujo, E. S., Maurice, Y. (2006). The source and fate of sediment and mercury in the Tapajos River, Para, Brazilian Amazon: Ground and space-based evidence. *Journal of Environmental Management*, **81**, 101-113.

Tlacuilo-Parra A., Guevara-Gutiérrez, E., Luna-Encinas, J. A. (2001). Percutaneous mercury poisoning with a beauty cream in Mexico. *J Am Acad Dermatol*; **45**(6):966-967.

Tlowana, S; Coetzee, H.; Makgae, M. (2013). Realistic simulation of acid mine drainage generation in the gold mines of the Witwatersrand, South Africa, In: Wolkersdorfer, Brown & Figueroa. Ed. International Mine Water, Reliable Mine Water Technology, Golden CO, USA, 475-480.

Tokalıoğlu, S.; Kartal, S.; Birol, G. (2003). *J. Environ. Monitor*. **5** 468–476.

Tokos, J. J., Hall, B., Calhoun, J.A., Prestbo, E.M. (1998). *Atmos. Environ.* **32**, 823-827.

Toole-O'Neil, B., Tewalt, S.J., Finkelman, R.B., Akers, D.J., 1999. Mercury concentration in coal – unravelling the puzzle. *Fuel* **78**, 47–54.

Trade Union Congress. 2001, Hazards at work—TUC guide to health and safety, Trade Union Congress, UK.

Trivedi, P.; Axe, L. (2001). Ni and Zn sorption to amorphous versus crystalline iron oxides: macroscopic studies. *J. Colloid Interface Sci.* **244**, 221 – 229.

Tutu, H.; McCarthy, T. S.; Cukrowska, E. (2008). The chemical characteristics of acid mine drainage with particular reference to sources, distribution and remediation: The Witwatersrand Basin, South Africa as a case study. *Applied Geochemistry*, **23**, 3666-3684.

Tutu, H.; Cukrowska, E. M.; Dohnal, V.; Havel, J. (2005). Application of artificial neural networks for classification of uranium distribution in the Central Rand goldfield, South Africa. *Environmental Modelling and Assessment*, **10**, 143-152.

United Nations Environment Programme, (2013). Global Mercury Assessment 2013: Sources, Emissions, Releases and Environmental Transport. Geneva, Switzerland. UNEP – United Nations Environment Programme, 2013. Global Mercury Assessment 2013: Sources, Emissions, Releases and Environmental Transport. Division of Technology, Industry and Economics (DTIE), Geneva, pp. 44. http://www.unep.org/PDF/PressReleases/GlobalMercuryAssessment2013.pdf (Accessed 04.09.13).

United Nations Environment Programme, (2008). Mercury in products and wastes; [cited 2012 August 20]. Available from: http://www.unep.org/hazardoussubstances/Portals/9/Mercury/AwarenessPack/English/UNEP_Mod1_UK_Web.pdf.

United States Environmental Protection Agency (2011). National Ambient Air Quality Standards (NAAQS). www.epa.gov/ttn/naaqs/standards/pm/s-pm (Access on 30 March 2012).

United States Environmental Protection Agency, (US EPA), 1989. Risk assessment guidance for superfund, Vol.1: Human Health Evaluation Manual. EPA/540/1-89/002. Ishington. D.C: Office of Soild Iste and Emergency Response.

United States Environmental Protection Agency, (US EPA), 2001. Risk Assessment Guidance for Superfund: Volume III –Part A, Process for Conducting Probabilistic Risk Assessment. US Environmental Protection Agency, Ishington, D.C. EPA 540-R-02-002.

United States Environmental Protection Agency, (1991c). Role of the baseline risk assessment in superfund remedy selection decisions. April 22 – Memorandum. Office of solid waste and emergency response. OSWER Directive 9355.0-30. (Accessed on 25 March 2014).

United States Environmental Protection Agency, (1989a). Exposure factors handbook. EPA 600/8-89/043. US. Environmental Protection Agency, Washington D. C. (Accessed 25 March 2014).

United States Environmental Protection Agency, (1989b). Risk Assessment guidance for superfund. Volume i: Human health evaluation manual. Interim final. OSWER Directive 9285.7-01a. U. S. environmental Protection Agency, Washington, D.C. http://www.epa.gov/pswer/riskassessment/ragsa/pdf/rags_a.pdf (Accessed 25 March 2014).

United States Geological Survey, *Mineral commodity summaries 2013*, U. S. Geological Survey, Reston, VA.

United States Environmental Protection Agency, (2001). Supplemental Guidance for Developing Soil Screening Level for Superfund Sites. OSWER 9355.4-24.Office of Solid Waste and Emergency
Response, Washington.

United States Environmental Protection Agency, (1993). Reference dose (RfD): description and use in health risk assessments. Background Document 1A. Integrated risk information system (IRIS).

United States Environmental Protection Agency, (1986). Superfund Public Health Evaluation Manual EPA/540/1-86.

United States Environmental Protection Agency: Fourth External Review Draft of Air Quality Criteria for Particulate Matter (June 2003). EPA/400/3-91/003Ad, United States Environmental Protection Agency, research triangle 20 park A.C, 2003.

Valiulis, D., Sakalys, J., Plauskaite, K. (2008). Heavy metal penetration into the human respiratory tract in Vilnius. *Lithuanian Journal of Physics,* **48**, 349 – 355.

van Alphen, M. (1999). Atmospheric heavy metal deposition plumes adjacent to a primary lead–zinc smelter", *Science* of the *Total Environment,* **236**, 119 – 134.

van Dyk, J. C., Keyser, M. J., Coetzee, M. (2006). Syngas production from South African coal sources using Sasol-Lurgi gasifiers. *International Journal of Coal Geology,* **65**, 243-253.

van Gehlen, K. (1983). Silver and mercury in single gold grains from the Witwatersrand and Barberton, South Africa. *Mineral Deposita,* **18**.

van Straaten P. (2000). Mercury contamination associated with small-scale gold mining in Tanzania and Zimbabwe. *The Science of the Total Environment*, **259**:105-113.

Valente, R. J., Shea, C., Humes, K. L., Tanner, R. L. *Atmos. Environ.* **41** (2007) 1861.

Veiga, M. M., Angeloci-Santos, G., Meech, J. A. Review of barriers to reduce mercury use in artisanal gold mining. *Extractive Industries and Society* (2014), Http://dx.doi.org/10.1016/j.exis.2014.03.004.

Veiga, M. M., Nunes, D., Klein, B., Shandro, J. A., Velasquez-Lopez, P.C., Sousa, R.N. (2009). Mill leaching: a viable substitute for mercury amalgamation in the artisanal gold mining sector? *J. Clean. Prod.* **15**, 1373–1381.

Veiga, M. M., Maxson, P. A., Hylander, L.D. (2006). Origin and consumption of mercury in small-scale gold mining. *Journal of Cleaner Production*, 14, 436-447.

Veiga, M. M.; Bermudez, D.; Pacheco-Ferreira, H.; Pedroso, R.L.R.M.; Gunson, A.J.; Berrios, G.; Vos, L.; Huidobro, P.; Roeser, M. Mercury pollution from artisanal gold mining in block B, El Callao, Bolivar State, Venezuela. In *Dynamics of Mercury Pollution on Regional and Global Scales; Pirrone, N., Mahaffey, K., Editors; Springer, NY, 2005, 421–450.*

Veiga, M. M., Hinton, J. J. (2002). Abandoned artisanal gold mines in the Brazilian Amazon: a legacy of mercury pollution. *Nat. Res. Forum (Genova)* **26** (1), 15–26.

Veiga, M. M., Meech, J. A. & Onante, N. (1994). Mercury pollution from deforestation. *Nature*, **368**, 816-817.

Vermette, S. J., Irvine, K. N., & Drake, J. J. (1991). Temporal variability of the elemental composition in urban street dust", *Environmental Monitoring and Assessment,* **18**, pp. 69–77.

Viljoen, M. (2009). The life, death and revival of the central Rand Goldfield, In: World Gold Conference, *The South African Institute of Mining and Metallurgy* 2009.

Viljoen, M. J., Reimold, W. U. (1999). An introduction to South Africa's geological and mining heritage, Geological Society of South Africa and Mintec, 37-39.

Von Burg R. (1995). Inorganic mercury. *J Appl Toxicol*; **15** (6): 483-493.

Wade, P.; Coetzee, H. (2008). Risk assessment of uranium in the selected gold mining areas in South Africa. In: B. J. Merkel and A. Hashe-Berger (editors). Uranium, Mining and Hydrogeology. Berlin Springer.

Wagner, N. J. & Hlatshwayo, B. (2005). The occurrence of potentially hazardous trace elements in five Highveld coals, South Africa. *International Journal of Coal Geology,* **63**(3–4), 228-246.

Wagner, N. J., Tlotleng, M. T. (2012). Distribution of selected trace elements in density fractionated Waterberg coals from South Africa. *International Journal of Coal Geology*, **94**, 225–237.

Wagner, N. J., Hlatshwayo, T.B., Ginster, M. A (2008). Source apportioned mercury mass balance across a coal-based petrochemical complex. *Fuel Process. Technol.* **89**, 1351–1357.

Wallschläger, D., Desai, M.V.M., Spengler, M. & Wilken, R.-D. (1998a). Mercury speciation in floodplain soils and sediments along a contaminated river transect. *Journal of Environmental Quality*, **27**(5), 1034-1044.

Wallschläger, D., Desai, M.V.M., Spengler, M., Windmöler, C.C. & Wilken, R.D. (1998b). How humic substances dominate mercury geochemistry in contaminated floodplain soils and sediments. *Journal of Environmental Quality,* 27(5), 1044-1054.

Whalin, L., Kim, E.-H., Mason, R.P. (2007). Factors influencing the oxidation, reduction, methylation and demethylation of mercury species in coastal waters. *Mar. Chem.* **107**, 278–294.

Wahlin, P.; Berkowicz, R.; Palmgren, F. (2006). Characterisation of traffic-generated particulate matter in Copenhagen. *Atmospheric Environment,* **40** (12), 2151-2159.

Wang, X.; Qin, Y. (2007**).** Relationships between heavy metals and iron oxides, fulvic acids, particle size fractions in urban roadside soils. *Environ. Geol.*, **52**, 63–69.

Wang, X., Qin, Y., & Chen, Y. (2006). Heavy meals in urban roadside soils, part 1: effect of particle size fractions on heavy metals partitioning. *Environmental Geology*, **50**, 1061 – 1066.

Wang, D.; Shi, X.; Wei, S. (2003). .Accumulation and transformation of atmospheric mercury in soil. *Sci. Total Environ.* **304**, 209–214.

Watling, R. J., Watling, H. R., (1982). Metal Concentrations in some South African coals. *South African Journal of Science* **78**, 166 – 264.

Watras, C. J., Bloom, N. S., Claas, S. A., Morrison, K. A., Gilmour, C. C. & Craig, S. R. (1995). Methylmercury production in the anoxic hypolimnion of a Dimictic Seepage Lake. *Water, Air, & Soil Pollution*, **80**(1-4), 735-745.

Wei, B. G.; Yang, L. S. (2010). A review of heavy metal contaminations in urban soils, urban road dusts and agricultural soils from China. *Microchemical Journal*, **94**, 99-107.

Wei, B.G.; Jiang, F. Q.; Li, X. M.; Mu, S. Y. (2009). Spatial distribution and contamination assessment of heavy metals in urban road dusts from Urumqi, NW China. *Microchemical Journal*, **93,** 147–152.

Whicker, C. L., Hayes, W. J., Khoo, C. S., Athol, B. H. (1997). Heavy metals in ceiling dust of some Sydney houses, New South Wales, Australia. *Journal of Proceedings of the Royal Society NSW*, **130**, 65–78.

Wieringa, M. H., Weyler, J. J., Van Bastelaer, F. J., Nelen V. J., Van Sprundel, M. P., & Vermeire, P. A. 1997, "Higher asthma occurrence in an urban than a suburban area: role of house dust mite skin allergy", *European Respiratory Journal*, vol. 10, pp. 1460–1466.

Wittsiepe, J.; Schrey, P.; Hack, A.; Selenka, Wilhelm, M. (2001). Comparison of different digestive tract models for estimating bioaccessibility of polychlorinated dibenzo-p-dioxins and dibenzofurans (PCDD/F) from red slag 'Kieselrot' *International Journal of Hygiene and Environmental Health*, **203**, 263-273.

Wilhelm, S. M. (2001). Mercury in Petroleum and Natural Gas: Estimation of Emissions from Production, Processing, and Combustion. (EPA/600/R-01/ 066). Research Triangle Park, NC: National Risk Management Research Laboratory.

Wilhelm, S. M, Bloom, N. (2000). Mercury in petroleum. *Fuel Process Technol.*, **63**:1–27.

Winfrey, M. R. & Rudd, J. W. M. (1990). Environmental factors affecting the formation of methylmercury in low pH lakes. *Environmental Toxicology and Chemistry*, **9**(7), 853-869.

World Health Organization (2005). Air quality guidelines for particulate matter, ozone, nitrogen dioxide and sulphur dioxide. Global update 2005. Summary of risk assessment Geneva. http://www.World HealthOrganization.int/watersanitation_health/dwq/guidelines2/en/ (Accessed on 30 April 2012).

World Health Organisation (2000). Evaluation and use of epidemiological evidence for environmental health risk assessment. Guideline document e68940, Copenhagen: Who. www.euro,who,int/document/pdf. (Accessed 26 march 2014).

World Health Organization, (1999). Hazard Prevention and Control in the Work Environment: Airborne Dust, *World Health Organization*, Switzerland, WHO/SDE/OEH/99.14.

World Health Organization (1991); International Program on Chemical Safety. Inorganic mercury: environmental health criteria 118. Geneva: World Health Organization.

Xiao, Z. F., Munthe, J., Stromberg, D., Lindqvist, O. (1994). Photochemical behaviour of inorganic Hg compounds in aqueous solution. In: Mercury as a Global Pollutant –Integration and Synthesis; Watras, C.J., Huckabee, J.W. (Eds.). Lewis Publishers, pp. 581-592.

Yamamoto, N.; Takahashi, Y.; Yoshinaga, J.; Tanaka, A.; Shibata, Y. (2006). Size distributions of soil particles adhered to children's hands. *Archives of Environmental Contamination and Toxicology*, **51**, 157‑163.

Ye, X. B.; Qian, H. J.; Xu, P. C.; Zhu, L.; Longnecker, M.; Fu, H. (2009). Nephrotoxicity, neurotoxicity, and mercury exposure among children with and without dental amalgam fillings. *Int J. Hyg Environ Health*, **212**, 378–386.

Yoshida, M.; Kishomoto, T.; Yamamura, Y.; Tabuse, M.; Akama, Y.; Satoh, H. (1994). Amount of mercury from dental amalgam filling released into the atmosphere by cremation. *Japanese Journal of Public Health*, **41**, (7), 618-624.

Yu, X.; Li, H.; Pan, K.; Yan, Y.; Wang, W. X. (2012). Mercury distribution, speciation and bioavailability in sediments from the Pearl River Estuary, southern China. *Mar. Pollut. Bull.* **64**, 1699-1704.

Yudovich, Y. E. & Ketris, M. P. 2005, "Mercury in coal: a review: Part 1. Geochemistry", *International Journal of coal Geology*, vol. 62, no.3, pp. 107-134.

Zagury, G. J., Bedeaux, C., Welfringer, B. (2009) Influence of mercury speciation and fractionation on bioaccessibility in soils. *Arch Environ Contam Toxicol* **56**:371–379.

Zehner, R. E., Gustin, M. S. Estimation of mercury vapour flux from natural substrate in Nevada. *Environmental Science & Technology*, **36**: 4039-4045.

Zhang, D.; Pan, X.; Lee, D. J. (2014). Potentially harmful metals and metalloids in the urban street dusts of Taipei City. *Journal of the Taiwan Institute of Chemical Engineers*, 45, 1727-1732.

Zhang, X. W.; Yang, L. S.; Li, Y. H.; Li, H. R.; Wang, W. Y.; Ye, B. X. (2012). Impacts of lead/zinc mining and smelting on the environment and human health in China. *Environ Monit Assess,* **184**, 2261–73.

Zhang, M. K., Wang, H. (2009a). Concentrations and chemical forms of potentially toxic metals in road-deposited sediments from different zones of Hangzhou, China. *J Environ Sci*, **21**, 625–631.

Zhang, L.; Wright, L. P.; Blanchard, P. (2009b). A review of current knowledge concerning dry deposition of atmospheric mercury. *Atmos. Environ.*, **43**, 5853−5864.

Zhang, X. M.; Luo, K. L.; Sun, X. Z.; Tan, J. A.; Lu, Y. L. (2006). Mercury in the topsoil and dust of Beijing City. *Science of the Total Environment,* **368**, 713-722.

Zhang, J., Ren, D., Zhu, Y., Chou, C.-L., Zeng, R., Zheng, B. (2004). Mineral matter and potentially hazardous trace elements in coals from Qianxi Fault Depression Area in south-western Guizhou, China. *International Journal of Coal Geology,* **57**, 49 – 61.

Zhao, H.; Li, X.; Wang, X. (2011). Heavy metal contents of road-deposited sediment along the urban-rural gradient around Beijing and its potential contribution to runoff pollution. *Environmental Science and Technology*, **45**, 7120-7127.

Zhao, H., Li, X., Wang, X., Tian, D. (2010a). Grain size distribution of road-deposited sediment and its contribution to heavy metal pollution in urban in urban runoff in Beijing, China. *Journal of Hazardous Materials*, **183**, 203–210.

Zhao, P., Feng, Y., Zhu, T., & Wu, J. (2006). Characterizations of resuspended dust in six cities of North China", *Atmospheric Environment*, vol. **40**, pp. 5807 – 5814.

Zheng, N., Liu, J.S., Wang, Q.C., Liang, Z.Z. (2010a). Health risk assessment of heavy metal exposure to street dust in the zinc smelting district, Northeast of China. *Sci. Total Environ.* **408**, 726–733.

Zheng, N., Liu, J.S., Wang, Q.C., Liang, Z.Z., (2010b). Heavy metals exposure of children from stairway and sidewalk dust in the smelting district, northeast of China. *Atmos. Environ.* **44**, 3239–3245.

Zvěřina, O.; Coufalík, P.; Josef Komárek, J.; Gadas, P.; Sysalová, J. (2014**).** Mercury associated with size-fractionated urban particulate matter: three years of sampling in Prague, Czech Republic. *Chemical Papers***, 68**, 197–202.

Appendix

Appendix A

Table A.1: Comparison of mean Hg_{TOT} (µg kg^{-1}) in three different particle size fractions in dust samples (Mean ± standard deviation) collected in the month of September 2014.

Site No.	Sampling sites	PM_{100}	PM_{50}	PM_{25}	pH
1	Res. Alberton 1	122.33 ± 6	205.05 ± 9	**507.90 ± 33**	7.77
2	Res. Alberton 2	117.05 ± 5	224.80 ± 15	**472.14 ± 36**	7.75
3	Res. Alberton 3	124.71 ± 6	201.67 ± 15	**488.79 ± 24**	7.74
4	Res. Boksburg 1	192.63 ± 14	247.51 ± 16	**482.45 ± 23**	7.61
5	Res. Boksburg 2	148.73 ± 24	229.22 ± 23	**446.60 ± 24**	7.78
6	Res. Centurion	80.32 ± 12	121.51 ± 23	**269.84 ± 22**	7.11
7	Res. Diepkloof	172.02 ± 17	389.41 ± 41	**693.43 ± 36**	7.60
8	Res. Germiston	118.85 ± 28	171.26 ± 7	**418.73 ± 07**	8.01
9	Res. Greenside	89.20 ± 9	132.56 ± 29	**289.37 ± 30**	7.21
10	Res. Riverlea	184.81 ± 14	356.33 ± 14	**696.58 ± 14**	7.67
11	Res. Sandton	107.19 ± 9	211.97 ± 5	**322.83 ± 13**	7.33
12	CBD 1	143.78 ± 16	215.89 ± 20	**534.40 ± 12**	7.84
13	CBD 2	163.57 ± 22	332.59 ± 33	**607.59 ± 12**	7.89
14	CBD 3	142.33 ± 19	240.63 ± 27	**486.07 ± 12**	7.90
15	CBD 4	187.68 ± 26	271.82 ± 21	**524.54 ± 41**	7.86
16	CBD 5	156.03 ± 6	255.72 ± 10	**505.44 ± 10**	8.18
17	CBD 6	191.73 ± 9	246.18 ± 13	**473.01 ± 46**	7.59
18	CBD Cemetery	137.64 ± 12	349.56 ± 7	**702.26 ± 13**	7.10
19	Crown North 1	109.90 ± 17	193.89 ± 10	**491.81 ± 09**	7.36
20	Crown North 2	111.57 ± 4	198.01 ± 8	**473.04 ± 07**	7.52
21	Crown South 1	136.57 ± 9	255.18 ± 22	**483.80 ± 53**	7.90
22	Crown South 2	155.56 ± 13	257.82 ± 11	**494.98 ± 11**	8.11
23	Ophirton	136.30 ± 7	267.02 ± 26	**591.18 ± 40**	7.45
24	Cross	170.92 ± 12	250.34 ± 15	**570.00 ± 19**	10.06
25	Selby 1	155.68 ± 11	267.02 ± 5	**556.20 ± 52**	6.93
26	Selby 2	118.29 ± 22	316.65 ± 34	**607.38 ± 41**	7.48
27	Loveday	199.50 ± 2	316.29 ± 5	**690.05 ± 45**	8.53
28	Booysen	128.89 ± 24	360.28 ± 24	**769.82 ± 38**	7.61
29	Crownwood	121.96 ± 31	415.24 ± 29	**998.08 ± 45**	7.55
30	Soccer City	122.04 ± 12	498.98 ± 41	**805.56 ± 23**	6.76
31	Aeroton 1	125.47 ± 8	248.11 ± 18	**583.80 ± 18**	6.93
32	Aeroton 2	142.99 ± 6	222.35 ± 18	**560.52 ± 18**	7.20
33	Aeroton 3	114.77 ± 17	205.56 ± 14	**595.68 ± 14**	7.33
34	Steeldale 1	139.14 ± 12	248.49 ± 16	**549.19 ± 37**	7.25
35	Steeldale 2	127.14 ± 14	266.96 ± 15	**509.57 ± 16**	7.27
36	Steeldale 3	123.71 ± 17	239.31 ± 16	**500.67 ± 27**	7.22
37	City deep 1	153.10 ± 11	363.05 ± 11	**677.44 ± 19**	7.87

38	City deep 2	188.13 ± 15	336.04 ± 32	**619.25 ± 38**	8.73
39	City deep 3	224.04 ± 13	394.62 ± 39	**701.92 ± 16**	8.86
40	Benrose 1	114.77 ± 17	345.55 ± 11	**502.73 ± 13**	7.55
41	Benrose 2	203.57 ± 27	333.67 ± 11	**537.34 ± 66**	7.73
42	Benrose 3	209.14 ± 25	383.11 ± 29	**624.97 ± 11**	7.64
43	Heriotdale	139.74 ± 3	419.13 ± 20	**1348.63 ± 4**	8.01
44	PPC Cement	149.21 ± 11	406.37 ± 26	**887.36 ± 17**	7.64
45	Germiston 1	136.53 ± 6	240.81 ± 15	**541.65 ± 43**	8.15
46	Germiston 2	153.60 ± 5	247.91 ± 31	**531.46 ± 22**	8.06
47	Germiston 3	242.78 ± 9	336.95 ± 35	**719.25 ± 61**	7.68
48	Springs 1	189.51 ± 21	445.10 ± 43	**840.25 ± 144**	7.80
49	Springs 2	203.36 ± 22	431.33 ± 27	**956.72 ± 106**	7.85
50	Springs 3	209.07 ± 28	420.98 ± 35	**854.18 ± 152**	8.60
51	VR 1			**541.31 ± 05**	5.32
52	VR 2			**500.01 ± 04**	5.40
53	West Wits dust			**479.66 ± 43**	5.36
	MDL (µg L^{-1})	**0.6139**	**0.1269**	**0.1310**	

Table A.2: Contamination assessment factors for selected PM_{25} dust samples from Johannesburg.

Site No.	Sampling sites	Enrichment Factor (EF)	Contamination Factor (C_f)	Geoaccumulation index (I_{geo})
1	**Res. Alberton 1**	13.79	6.35	7.77
2	**Res. Alberton 2**	13.09	5.90	7.75
3	**Res. Alberton 3**	7.33	6.11	7.74
4	**Res. Boksburg 1**	9.33	6.03	7.61
5	**Res. Boksburg 2**	8.42	5.58	7.78
6	**Res. Centurion**		8.67	7.11
7	**Res. Diepkloof**	9.92	8.67	7.60
8	**Res. Germiston**		5.23	8.01
9	**Res. Greenside**		3.62	7.21
10	**Res. Riverlea**	11.81	8.71	7.67
11	**Res. Sandton**		4.04	7.33
12	**CBD 1**	10.23	6.68	7.84
13	**CBD 2**	10.46	7.59	7.89
14	**CBD 3**	7.3	6.08	7.9
15	**CBD 4**	10.44	6.56	7.86
16	**CBD 5**		6.32	8.18
17	**CBD 6**		5.91	7.59
18	**CBD Cemetery**	8.95	8.78	7.1
19	**Crown North 1**		6.15	7.36
20	**Crown North 2**		5.91	7.52
21	**Crown South 1**		6.05	7.9
22	**Crown South 2**		4.94	8.11
23	**Ophirton**	13.21	7.39	7.45
24	**Cross**		7.13	10.26
25	**Selby 1**	11.34	6.95	6.93
26	**Selby 2**		7.59	7.48
27	**Loveday**		8.63	8.53
28	**Booysen**		9.62	7.61
29	**Crownwood**	11.33	12.48	7.55
30	**Soccer City**	23.28	10.07	6.76
31	**Aeroton 1**		7.3	6.93
32	**Aeroton 2**		7.01	7.2
33	**Aeroton 3**		7.45	7.33
34	**Steeldale 1**		6.86	7.25
35	**Steeldale 2**		6.37	7.27
36	**Steeldale 3**		6.26	7.22
37	**City deep 1**	19.65	8.47	7.87
38	**City deep 2**		7.74	8.73

39	**City deep 3**		8.77	8.86
40	**Benrose 1**		6.28	7.55
41	**Benrose 2**		6.72	7.73
42	**Benrose 3**		7.81	7.64
43	**Heriotdale**	29.40	16.86	8.01
44	**PPC Cement**	19.21	11.09	7.64
45	**Germiston 1**		6.77	8.15
46	**Germiston 2**		6.64	8.06
47	**Germiston 3**		8.99	7.68
48	**Springs 1**		10.5	7.8
49	**Springs 2**		11.96	7.85
50	**Springs 3**		10.68	8.6

APPENDIX B

Table B.1: Mercury concentration (µg kg^{1}) extracted by simulated gastric solutions.

SAMPLE SITES	Oral Leachates						Hg_{TOT}
	Artificial gastric juice		Dil. HCl		Conc. HCl		
	Mean ± SD	%	Mean ± SD	%	Mean ± SD	%	
Sandton	1.35 ± 0.01	0.39	5.47 ± 0.34	1.56	50.87 ± 0.33	14.78	344.08
Boksburg 1	1.40 ± 0.01	0.39	7.26 ± 0.56	2.03	68.95 ± 3.53	19.33	356.78
Boksburg 2	1.27 ± 0.01	0.35	8.33 ± 0.41	2.31	76.85 ± 5.53	21.35	359.97
Alberton 1	1.59 ± 0.01	0.38	8.49 ± 0.65	2.02	78.75 ± 5.89	18.76	419.69
Alberton 2	1.56 ± 0.01	0.48	7.64 ± 0.66	2.34	68.75 ± 3.89	21.03	326.95
Alberton 3	1.68 ± 0.01	0.38	8.02 ± 0.57	1.83	93.84 ± 8.04	21.44	437.61
Diepkloof	2.23 ± 0.01	0.49	6.00 ± 0.35	1.31	63.74 ± 4.98	13.95	456.75
Riverlea	3.56 ± 0.02	0.67	9.71 ± 0.71	1.81	92.17 ± 7.33	17.15	537.40
CBD 1	3.25 ± 0.02	0.60	13.85 ± 0.91	2.57	135.66 ± 9.98	25.18	538.82
CBD 2	3.08 ± 0.02	0.49	11.41 ± 0.81	1.82	120.63 ± 10.9	19.24	627.14
CBD 3	3.07 ± 0.02	0.62	11.85 ± 1.01	2.40	116.46 ± 9.78	23.63	492.78
CBD 4	2.13 ± 0.01	0.42	16.12 ± 1.29	3.18	159.69 ± 11.6	31.54	506.32
Cemetery	2.83 ± 0.01	0.33	15.10 ± 1.33	1.77	144.37 ± 11.9	16.97	850.78
Soccer City	5.08 ± 0.03	0.49	26.36 ± 1.82	2.52	235.55 ± 18.5	22.55	1044.55
Crownwood	5.32 ± 0.04	0.57	27.78 ± 2.22	2.99	298.88 ± 23.8	32.13	930.13
Ophirton	5.30 ± 0.05	0.93	12.49 ± 1.41	2.19	123.82 ± 9.21	21.67	571.29
Selby 1	3.01 ± 0.02	0.64	12.18 ± 1.21	2.58	127.85 ± 10.3	27.06	472.49
City Deep	4.41 ± 0.03	0.82	12.13 ± 0.97	2.25	137.50 ± 10.5	25.53	538.67
Heriotdale	6.22 ± 0.05	0.40	65.57 ± 0.33	4.26	505.22 ± 36.7	30.27	1669.18
PPC Cement	3.17 ± 0.02	0.40	25.52 ± 0.18	3.21	301.43 ± 15.6	37.91	795.14

Table B.2: Mercury concentration (µg kg ^{1}) extracted by simulated lung fluids.

SAMPLE SITES	Lung Leachates						Hg_{TOT}
	Artificial lung fluid		Grays' solution		Gamble's solution		
	Mean ± SD	%	Mean ± SD	%	Mean ± SD	%	
Sandton	4.22 ± 0.21	1.23	0.48 ± 0.02	0.14	0.17 ± 0.01	0.0	344.08
Boksburg 1	4.69 ± 0.28	1.32	0.46 ± 0.02	0.13	0.13 ± 0.01	0.0	356.78
Boksburg 2	4.55 ± 0.27	1.26	0.42 ± 0.02	0.12	0.11 ± 0.01	0.0	359.97
Alberton 1	6.35 ± 0.37	1.58	0.61 ± 0.03	0.15	0.12 ± 0.01	0.0	419.69
Alberton 2	6.68 ± 0.21	1.55	0.64 ± 0.04	0.15	0.09 ± 0.01	0.0	326.95
Alberton 3	6.85 ± 0.48	1.41	0.59 ± 0.04	0.12	0.26 ± 0.01	0.0	437.61
Diepkloof	6.38 ± 0.51	1.57	0.72 ± 0.05	0.18	0.31 ± 0.02	0.0	537.25
Riverlea	8.11 ± 0.67	1.58	0.81 ± 0.06	0.16	0.40 ± 0.02	0.0	593.94
CBD 1	10.78 ± 0.92	1.72	0.99 ± 0.07	0.16	0.17 ± 0.01	0.0	538.82
CBD 2	10.52 ± 0.81	1.68	0.94 ± 0.08	0.15	0.18 ± 0.01	0.0	627.14
CBD 3	6.67 ± 0.32	1.37	0.60 ± 0.04	0.12	0.17 ± 0.01	0.0	492.78
CBD 4	8.35 ± 0.41	1.59	0.83 ± 0.07	0.16	0.33 ± 0.02	0.0	506.32
Cemetery	15.67 ± 1.20	2.09	1.44 ± 0.11	0.19	0.82 ± 0.04	0.0	850.78
Soccer City	24.60 ± 1.89	2.27	2.48 ± 0.21	0.23	0.72 ± 0.04	0.0	1044.55
Crownwood	16.51 ± 1.43	1.86	1.19 ± 0.09	0.13	0.88 ± 0.06	0.0	930.13
Ophirton	12.36 ± 1.01	1.99	1.11 ± 0.10	0.18	0.29 ± 0.01	0.0	571.29
Selby 1	8.29 ± 0.69	1.55	0.83 ± 0.06	0.15	0.49 ± 0.03	0.0	472.49
City Deep	11.79 ± 0.93	1.85	1.52 ± 0.11	0.24	0.39 ± 0.02	0.0	538.67
Heriotdale	34.40 ± 2.48	2.68	3.59 ± 0.23	0.28	0.61 ± 0.03	0.0	1669.18
PPC Cement	14.78 ± 1.36	2.06	1.42 ± 0.12	0.20	0.53 ± 0.03	0.0	795.14

APPENDIX C

Table C.1: Mercury concentration (µg kg^{-1}) extracted by n-SEP (Neculita *et al*., 2005).

SAMPLE SITES	Fractions								Total[a]	Hg_{TOT}	% Recovery[b]
	F1		F2		F3		Residual				
	Mean ± SD	%	Mean ± SD	%	Mean ± SD	%	Mean ± SD	%			
Sandton	2.87 ± 0.10	1.08	25.73 ± 1.87	9.67	3.75 ± 1.23	1.41	233.71 ± 15.5	87.82	266.06	266.14	99.97
Boksburg 1	4.85 ± 0.23	1.35	31.36 ± 1.06	8.71	1.25 ± 0.11	0.35	321.25 ± 21.7	89.24	358.71	359.97	99.65
Boksburg 2	5.12 ± 0.39	1.43	29.83 ± 2.11	8.36	1.38 ± 0.07	0.39	321.07 ± 17.3	89.99	357.39	356.78	100.17
Alberton 1	8.33 ± 0.13	2.07	30.33 ± 1.33	7.54	43.62 ± 2.33	10.84	320.93 ± 23.7	79.73	403.20	402.50	100.17
Alberton 2	5.19 ± 0.09	0.29	37.06 ± 2.03	8.62	15.33 ± 1.09	3.57	375.24 ± 30.7	87.30	432.81	429.84	100.69
Alberton 3	1.61 ± 0.07	0.94	30.65 ± 0.17	6.30	29.39 ± 2.51	6.04	422.81 ± 18.3	86.95	487.43	486.24	100.24
Diepkloof	6.92 ± 0.48	1.38	48.81 ± 2.43	9.71	7.66 ± 0.43	1.52	436.74 ± 13.8	86.87	500.13	502.74	99.48
Riverlea	4.94 ± 0.32	0.86	41.18 ± 1.78	7.14	6.16 ± 0.37	1.07	528.22 ± 22.4	91.62	580.50	576.50	100.69
CBD 1	4.52 ± 0.44	0.72	50.70 ± 2.52	8.08	2.08 ± 0.17	0.33	570.67 ± 33.7	90.99	627.96	627.21	100.12
CBD 2	6.72 ± 1.03	1.07	79.65 ± 4.59	12.73	0.62 ± 0.05	0.10	543.06 ± 42.8	86.78	630.05	625.79	100.68
CBD 3	1.25 ± 0.11	0.26	30.92 ± 2.42	6.35	0.26 ± 0.01	0.05	457.41 ± 23.7	93.91	489.84	487.06	100.57
CBD 4	0.65 ± 0.04	0.12	51.19 ± 3.13	9.77	1.56 ± 0.08	0.30	471.84 ± 10.1	90.03	525.24	524.11	100.22
Cemetery	17.90 ± 1.07	2.35	72.89 ± 5.01	9.59	2.97 ± 0.19	0.39	672.76 ± 19.7	88.47	766.52	760.44	100.80
Soccer City	10.03 ± 0.10	1.16	76.88 ± 3.16	8.90	2.29 ± 0.11	0.27	772.42 ± 39.9	89.45	861.63	863.52	99.78
Crownwood	26.15 ± 0.14	2.95	61.89 ± 1.04	6.98	0.35 ± 0.01	0.04	804.84 ± 67.9	90.73	893.23	887.05	100.70
Ophirton	2.77 ± 0.11	0.45	25.62 ± 1.73	4.12	1.62 ± 0.01	0.26	596.09 ± 29.3	95.95	626.10	621.28	100.78
Selby 1	1.04 ± 0.08	0.20	27.11 ± 1.24	5.08	1.73 ± 0.01	0.31	501.21 ± 28.9	93.92	531.08	533.63	99.52
City Deep	0.80 ± 0.06	0.12	56.28 ± 3.63	8.82	1.42 ± 0.01	0.22	587.08 ± 3.19	91.98	645.58	638.26	101.15
Heriotdale	7.25 ± 0.36	0.56	123.26 ± 9.73	9.61	3.13 ± 0.02	0.24	1149.25 ± 42.4	89.57	1282.88	1283.00	99.99
PPC Cement	6.75 ± 0.31	0.94	70.20 ± 5.46	9.78	2.26 ± 0.02	0.32	647.12 ± 36.7	90.13	726.33	718.00	101.16

[a]***Fraction Total = F1 + F2 + F3 + $F_{residual}$***

[b]***Recovery = (F1 + F2 + F3 + $F_{residual}$)/Hg_{TOT}***

Table C.2: Mercury concentration (µg kg ^{1}) extracted by modified BCR SEP (Rauret *et al*., 1999).

SAMPLE SITES	Fractions								Fraction Total[a]	Hg_{TOT}	% Recovery[b]
	F1		F2		F3		Residual				
	Mean ± SD	%	Mean ± SD	%	Mean ± SD	%	Mean ± SD	%			
Sandton	2.48 ± 0.1	0.72	1.23 ± 1.07	0.36	10.18 ± 0.63	2.96	333.41 ± 15.1	96.90	347.30	344.08	100.94
Boksburg 1	0.95 ± 0.03	0.27	2.04 ± 0.06	0.57	11.85 ± 1.53	3.32	342.02 ± 3.18	95.86	356.85	356.78	100.02
Boksburg 2	1.17 ± 0.09	0.33	1.95 ± 0.11	0.54	13.81 ± 1.17	3.84	34505 ± 10.1	95.85	361.98	359.97	100.56
Alberton 1	1.79 ± 0.13	0.37	2.00 ± 0.17	0.41	15.69 ± 1.23	3.23	466.31 ± 24.3	95.90	485.79	486.24	99.91
Alberton 2	1.17 ± 0.09	0.29	2.17 ± 0.12	0.54	13.46 ± 0.89	3.34	389.13 ± 2.49	96.68	405.93	402.50	100.85
Alberton 3	1.61 ± 0.07	0.37	2.44 ± 0.17	0.57	15.62 ± 1.07	3.63	410.74 ± 33.5	95.56	430.40	429.84	100.13
Diepkloof	10.08 ± 0.08	2.49	7.52 ± 0.33	1.86	10.03 ± 0.83	2.47	377.62 ± 27.4	93.13	405.25	405.47	99.94
Riverlea	10.27 ± 0.82	2.00	4.34 ± 0.23	0.84	9.30 ± 0.63	1.81	488.67 ± 17.5	95.00	512.58	514.41	99.64
CBD 1	10.58 ± 0.64	1.69	2.51 ± 0.22	0.40	13.92 ± 0.97	2.22	604.34 ± 5.13	96.35	631.34	627.21	100.66
CBD 2	14.86 ± 1.03	2.37	5.38 ± 0.41	0.86	16.24 ± 1.18	2.59	587.34 ± 38.6	93.86	624.89	625.79	99.64
CBD 3	4.22 ± 0.23	0.87	3.25 ± 0.21	0.67	17.34 ± 1.18	3.56	460.96 ± 31.5	94.64	623.82	487.06	99.69
CBD 4	1.03 ± 0.08	0.20	2.71 ± 0.13	0.52	13.88 ± 0.53	2.65	504.98 ± 40.9	96.35	522.59	524.11	99.71
Cemetery	1.13 ± 0.07	0.09	13.95 ± 0.11	1.15	37.53 ± 2.73	3.10	1169.45 ± 96.6	96.55	1222.06	1211.26	100.89
Soccer City	2.56 ± 0.23	0.24	3.22 ± 0.23	0.30	74.05 ± 4.60	6.82	986.02 ± 59.3	90.81	1065.85	1085.85	98.16
Crownwood	2.26 ± 0.14	0.25	28.77 ± 1.04	3.24	101.26 ± 7.14	11.42	777.37 ± 57.3	87.64	935.73	887.05	100.60
Ophirton	7.23 ± 0.61	1.16	2.89 ± 0.20	0.46	26.90 ± 1.13	4.33	586.08 ± 24.8	94.33	569.19	621.28	99.63
Selby 1	1.38 ± 0.08	0.26	3.02 ± 0.24	0.57	16.86 ± 0.94	3.16	516.02 ± 5.74	96.70	468.56	533.63	99.17
City Deep	1.06 ± 0.09	0.17	2.63 ± 0.18	0.41	13.65 ± 1.03	2.14	504.11 ± 6.79	97.70	535.27	638.26	100.42
Heriotdale	8.24 ± 0.06	0.49	17.35 ± 0.3	1.04	57.22 ± 4.63	3.43	1559.40 ± 42.4	93.42	1642.21	1669.18	98.38
PPC Cement	13.88 ± 0.11	1.93	7.16 ± 0.61	1.00	37.66 ± 0.23	5.24	666.29 ± 28.2	92.80	724.99	718.00	100.97

[a]*Fraction Total = F1 + F2 + F3 + $F_{residual}$*

[b]*Recovery = (F1 + F2 + F3 + $F_{residual}$)/Hg_{TOT}*

Table C.3: Mercury concentration (µg kg^{-1}) extracted by SSE (Bloom *et al.*, 2003).

SAMPLE SITES	Fractions										Fraction Total[a]	% Recovery[b]
	F1		F2		F3		F4		Residual			
	Mean ± SD	%	Mean ± SD	%	Mean ± SD	%	Mean ± SD	%	Mean ± SD	%		
Sandton	9.43 ± 0.57	2.92	25.73 ± 1.27	7.97	13.35 ± 1.07	4.13	1.32 ± 0.01	0.41	271.91 ± 13.9	84.25	321.80	99.68
Boksburg 1	14.88 ± 1.13	308	30.01 ± 1.51	6.22	18.78 ± 1.33	3.89	57.89 ± 2.33	12.00	359.12 ± 21.7	74.44	480.67	99.63
Boksburg 2	13.77 ± 0.89	3.08	33.86 ± 2.01	7.58	18.60 ± 1.07	4.17	38.69 ± 1.43	8.66	340.12 ± 16.8	76.16	445.05	99.65
Alberton 1	2.83 ± 0.01	0.56	16.99 ± 1.17	3.34	17.25 ± 0.83	3.40	45.98 ± 2.23	9.05	420.86 ± 21.4	82.86	503.90	99.21
Alberton 2	21.18 ± 1.19	4.49	31.31 ± 2.02	6.63	20.78 ± 1.89	4.40	75.70 ± 4.49	16.03	320.17 ± 16.2	67.81	469.14	99.36
Alberton 3	23.10 ± 1.32	4.73	22.60 ± 1.13	4.62	11.91 ± 0.97	2.44	80.75 ± 3.55	16.52	350.40 ± 17.5	71.69	488.76	99.99
Diepkloof	15.29 ± 0.98	2.20	29.51 ± 1.63	4.26	48.00 ± 3.83	6.92	79.71 ± 5.74	11.50	519.92 ± 10.5	74.98	692.43	99.86
Riverlea	1.61 ± 0.01	0.23	16.02 ± 0.93	2.30	20.68 ± 1.03	2.97	57.41 ± 1.75	8.24	598.85 ± 30.6	85.97	694.58	99.71
CBD 1	4.54 ± 0.23	0.85	17.09 ± 1.08	3.20	18.87 ± 0.97	3.53	70.68 ± 3.15	13.23	424.22 ± 21.8	79.38	535.40	100.19
CBD 2	2.26 ± 1.49	0.37	19.26 ± 0.81	3.17	11.86 ± 0.58	1.95	58.58 ± 3.77	9.64	518.64 ± 43.7	85.36	610.59	100.49
CBD 3	7.68 ± 0.57	1.58	12.89 ± 0.61	2.65	22.45 ± 1.18	4.62	43.32 ± 1.98	8.91	398.74 ± 19.3	82.03	485.07	99.80
CBD 4	6.78 ± 0.38	1.29	10.70 ± 0.50	2.04	25.81 ± 1.25	4.92	117.28 ± 9.56	22.36	366.97 ± 12.6	69.69	527.54	100.57
Cemetery	18.64 ± 1.23	2.65	73.88 ± 3.61	10.52	53.30 ± 2.93	7.59	125.74 ± 8.72	17.90	429.70 ± 34.2	61.19	701.26	99.86
Soccer City	15.41 ± 0.77	1.91	44.46 ± 2.22	5.52	47.01 ± 3.60	5.84	117.07 ± 9.89	14.78	578.61 ± 28.1	71.83	804.56	99.88
Crownwood	31.58 ± 1.98	3.16	47.67 ± 1.84	4.78	76.55 ± 4.97	7.67	45.33 ± 1.19	4.54	792.95 ± 59.7	79.45	994.08	99.60
Ophirton	13.33 ± 0.93	2.26	47.08 ± 2.40	7.96	23.05 ± 1.15	3.90	51.61 ± 3.58	8.73	452.11 ± 39.8	76.48	587.18	99.32
Selby 1	14.98 ± 0.86	2.69	30.86 ± 1.50	5.55	19.93 ± 1.04	3.58	87.69 ± 4.78	15.77	405.73 ± 9.78	72.95	559.20	100.54
City Deep	3.87 ± 0.17	0.57	47.20 ± 3.67	6.97	38.96 ± 2.17	5.75	105.70 ± 5.89	15.60	480.72 ± 36.2	70.96	676.46	99.86
Heriotdale	24.85 ± 1.24	1.84	38.49 ± 2.49	2.85	29.35 ± 2.73	2.18	83.95 ± 4.59	6.22	1169.99 ± 83.7	86.75	1346.63	99.85
PPC Cement	26.12 ± 1.31	2.94	37.73 ± 2.61	4.25	51.93 ± 3.33	5.85	59.85 ± 3.09	6.74	713.73 ± 69.9	80.43	889.36	100.23

[a]***Fraction Total = F1 + F2 + F3 + F4 + $F_{residual}$***

[b]***Recovery = (F1 + F2 + F3 + F4 + $F_{residual}$)/Hg_{TOT}***